Investigating the Influence of Tropical Urban Climates on Vegetation Phenology

A thesis submitted to The University of Manchester for the degree of

Doctor of Philosophy in the Faculty of Humanities

2019

Peter Kabano

School of Environment Education and Development

‘Blank page’

Contents

LIST OF TABLES 8

LIST OF FIGURES 10

LIST OF FIGURES IN APPENDIX 12

ABSTRACT 15

DECLARATION 17

COPYRIGHT STATEMENT 18

ACKNOWLEDGEMENTS 19

GLOSSARY OF ABBREVIATIONS 20

CHAPTER 1. RESEARCH IN CONTEXT 22

1.1 Landcover change and climate feedback 22

1.1.1 Urbanisation and urban climate 23

1.2 Factors influencing tropical urban climate 25

1.2.1 Morphology of cities 25

1.2.2 Importance of vegetation in Tropical African cities 25

1.2.3 Importance of water availability in tropical urban climate 25

1.3 Vegetation phenology in tropical urban environments 26

1.3.1 Deciduous nature of trees in tropical cities 27

1.3.2 Landscape phenology in tropical cities 28

1.4 Thesis Aims and Contributions 28

1.5 Research methodology 30

1.6 Thesis structure 31

CHAPTER 2. LITERATURE REVIEW 33

2.1 Urban climate 33

2.1.1 The Urban Heat Island (UHI) effect 33

2.1.2 Quantifying UHI 37

2.1.3 Factors affecting Urban Heat islands 43

2.1.4 Urban Heat Islands in the tropics 47
2.1.5 Urban dryness Island effect 57
2.2 Vegetation Phenology 60
2.2.1 Quantifying vegetation phenology 61
2.2.2 Remote sensing phenology 62
2.2.3 Drivers of vegetation phenology 65
2.3 Phenology in urban environments 68
2.3.1 Phenology in tropical urban environments 69
2.3.2 Conclusion 71
CHAPTER 3. METHODOLOGY 74
3.1 Study area 74
3.1.1 Criteria for Choice of study area 74
3.1.2 Description of study area 75
3.2 Local scale climate and landscape phenological processes 78
3.2.1 Urban form characterisation 78
3.2.2 Landscape phenology characterisation 86
3.2.3 Land surface temperature 90
3.3 Phenological processes of individual tree species 90
3.3.1 Select tree species 91
3.3.2 Phenology sampling sites 92
3.3.3 Characterisation of surface cover and structure at each site 94
3.3.4 Phenology data collection 95
3.3.5 Urban climate characterisation 96
3.4 Data Processing and Analysis 98
3.4.1 Local scale climate and phenological processes 98
3.4.2 Micro scale climate and phenological processes 102
3.4.3 Analysis 105

CHAPTER 4. EVIDENCE OF URBAN HEAT ISLAND IMPACTS ON LANDSCAPE PHENOLOGY IN A TROPICAL CITY107

4.1 Abstract 107

4.2 Introduction 108

4.3 Materials and methods 111

4.3.1 Study area 111

4.3.2 Data 112

4.3.3 Data analysis 117

4.4 Results 118

4.4.1 Surface and structural differences between urban form (LCZ) types 118

4.4.2 Phenology 119

4.4.3 Land surface temperature 120

4.4.4 Relationship between LST and Phenology 120

4.5 Discussion 123

4.6 Conclusion 125

CHAPTER 5. SPATIOTEMPORAL DYNAMICS OF URBAN CLIMATE DURING THE WET-DRY SEASON TRANSITION IN A TROPICAL AFRICAN CITY 127

5.1 Abstract 127

5.2 Introduction 128

5.3 Methods 131

5.3.1 Study area 131

5.3.2 Data analysis 135

5.4 Results 137

5.4.1 Temporal change in urban climate with relation to proportion of man-made surface 137

5.4.2 Influence of land cover on urban climate 140

5.5 Discussion 143

5.6 Conclusions 146

CHAPTER 6. SENSITIVITY OF CANOPY PHENOLOGY TO LOCAL URBAN ENVIRONMENTAL CHARACTERISTICS IN A TROPICAL CITY 147

6.1 Abstract 147

6.2 Introduction 148

6.3 Methods 150

6.3.1 Study area 150

6.3.2 Selected tree species 152

6.3.3 Individual tree and phenology site selection 153

6.3.4 Phenology data 154

6.3.5 Phenology data processing 155

6.3.6 Urban climate 156

6.3.7 Data analysis 157

6.4 Results 158

6.4.1 Temporal changes in canopy cover 158

6.4.2 Rate of change of tree canopy cover under varying urbanisation intensity 159

6.4.3 Species Influence on total percentage of tree canopy cover 159

6.4.4 Species Influence on net leaf loss 160

6.4.5 Influence of land cover 162

6.4.6 Influence of urban climate 162

6.5 Discussion 165

6.5.1 Conclusion 167

CHAPTER 7. CONCLUSIONS 169

7.1 Introduction 169

7.2 Summary of research findings 169

7.2.1 Effect of the urban heat island on landscape phenological processes 169

7.2.2 Spatiotemporal dynamics of urban climate during the wet-dry season transiton 171

7.2.3 The sensitivity of canopy phenology to local environmental settings 172

7.3 Significance of the findings of the research 173
7.3.1 Tropical urban climate 173
7.3.2 Phenology in tropical cities 174
7.3.3 Climate change science 176
7.3.4 Implications for urban development 176
7.4 Strength and limitations 179
7.4.1 Strengths 179
7.4.2 Limitations 180
7.5 Research recommendations 180
BIBLIOGRAPHY 184
APPENDIX I 207
APPENDIX II 211
APPENDIX III 217
APPENDIX IV 220
APPENDIX V 227

Word Count: 46,924

LIST OF TABLES

TABLE 1-1: SUMMARY OF THE FOUR MAIN MOIST TROPICAL CLIMATE TYPES. TROPICAL CLIMATE UNDER THE KOPPEN CLASSIFICATION CONSISTS OF 4 MAIN TROPICAL CLIMATE TYPES (SOURCE: KOTTEK *ET AL.*, 2006; PEEL *ET AL.*, 2007).26
TABLE 2-1: SUMMARY OF TROPICAL CLIMATE TYPES. TROPICAL CLIMATE UNDER THE KOPPEN CLASSIFICATION CONSISTS OF 4 MAIN TROPICAL CLIMATE TYPES. 49
TABLE 2-2: SUMMARY OF RECENT TROPICAL URBAN CLIMATE STUDIES. STUDIES ON ATMOSPHERIC UHI AND SURFACE UHI STUDIES ARE PRESENTED SEPARATELY UNDER SPECIFIC CLIMATE TYPES....51
TABLE 2-3 SUMMARISES SOME OF THE PHENOLOGY PARAMETERS THAT ARE RECORDED FOR GIVEN PHENOEVENTS (FENNER, 1998) 61
TABLE 2-4 LANDSCAPE PHENOLOGICAL METRICS DERIVED FROM REMOTE SENSING (SOURCE: EKLUNDH AND JÖNSSON, 2015, 2016) 63
TABLE 2-5 SHOWING THE MERITS AND DEMERITS FOR DIFFERENT METHODS FOR UNDERTAKING LANDSCAPE PHENOLOGY OBSERVATIONS (SOURCE: SCHWARTZ, 2003) 64
TABLE 2-6 SUMMARISING THE KNOWLEDGE GAPS IDENTIFIED FROM THE LITERATURE REVIEW AND THE AND SPECIFIC HYPOTHESES THAT THIS STUDY AIMS TO INVESTIGATE....73
TABLE 3-1: SURFACE AREA AND PROPORTION OF RESULTING LCZ CLASSES WITHIN 20 KM FROM THE CITY CENTRE (COMPACT MIDRISE AND COMPACT LOW RISE) 83
TABLE 3-2: SHOWS THE DEFINITION OF PHENOLOGY METRICS IN LAND SURFACE PHENOLOGY (SOURCE: EKLUNDH AND JÖNSSON, 2015, 2016) 88
TABLE 3-3: SUMMARY TABLE OF SETTINGS APPLIED IN TIMESAT 3.2 FOR SMOOTHING THE IMAGE TIME SERIES AND EXTRACTION OF THE SEASONAL PARAMETERS 89
TABLE 3-4 SHOWING THE CHARACTERISTICS OF *TABEBUIA ROSEA* AND *JACARANDA MIMOSIFOLIA* 91
TABLE 3-5: SHOWING THE NUMBER OF TREES AT EACH PHENOLOGY SITE. 92
TABLE 3-6: SURFACE COVER AND STRUCTURAL CHARACTERISTICS (PERCENTAGE OF IMPERVIOUS SURFACES, PAVED SURFACES, BUILDINGS, TREES AND PERVIOUS SURFACES) OF THE TWENTY TWO URBAN CLIMATE STATIONS. THE LOCATIONS ARE GROUPED ROW-RISE WITH RELATION TO PROPORTION OF MAN-MADE IMPERVIOUS SURFACES. PHENOLOGY SITES ARE INDICATED IN BOLD AND UNDERLINED. 103
TABLE 3-7: CHARACTERISTICS OF THE NINE PHENOLOGY SITES, THEIR ASSOCIATED URBAN FORM (PERCENTAGE COVER OF PERVIOUS SURFACES, PAVED SURFACES AND BUILDINGS) AND NUMBER OF INDIVIDUAL TREES (PER SPECIES) SAMPLED AT EACH PHENOLOGY SITE. THE LAST ROW INDICATES THE URBANISATION INTENSITY CATEGORY ASSIGNED TO EACH PHENOLOGY SITE 104
TABLE 4-1 SHOWS THE AREA COVERED BY THE SELECTED LCZ TYPES. IN TOTAL THIS REPRESENTED APPROXIMATELY 87% OF THE STUDY AREA 114
TABLE 4-2 SHOWING MIXED MODEL ASSESSING THE EFFECT OF URBAN FORM (LCZ) AND DISTANCE FROM THE CITY CENTRE ON PHENOLOGY.... 119
TABLE 5-1 SHOWING THE URBAN INTENSITY GROUPS AND PROPOTION OF DIFFERENT LAND COVER TYPES (IMPERVIOUS SURFACES, PAVED SURFACES, BUILDINGS, TREES AND PERVIOUS SURFACES) AT EACH LOCATION. LOCATION USED FOR OBSERVATION ON VOLUMETRIC SOIL MOISTURE CONTENT ARE IN BOLD AND UNDERLINED 134
TABLE 5-2: AICC STATISTICS FOR MODELS FOR RELATIVE HUMIDITY AND NIGHTTIME TEMPERATURE WITH RELATION TO LAND COVER FOR THE WET AND DRY SEASON. AICC = AIC CORRECTED FOR SMALL SAMPLE SIZE, DF = DEGREES OF FREEDOM, R^2 = ADJUSTED REGRESSION COEFFICIENT, P = P-VALUE, ΔAICC = DIFFERENCE BETWEEN THE TOP MODEL AND GIVEN MODEL AICC, WI = MODEL WEIGHT. ONLY MODELS WITH ΔAICC < 2 ARE SHOWN.... 141
TABLE 5-3: RELATIVE IMPORTANCE VALUES (RIV) OF PREDICTOR VARIABLES FOR MODELS RELATING LAND COVER WITH TEMPERATURE AND RELATIVE HUMIDITY DURING BOTH THE WET AND DRY SEASON 142
TABLE 6-1: CHARACTERISTICS OF THE NINE PHENOLOGY SITES, THEIR ASSOCIATED URBAN FORM (PERCENTAGE COVER OF PERVIOUS SURFACES, PAVED SURFACES AND BUILDINGS) AND THE NUMBER OF INDIVIDUAL TREES (PER SPECIES) SAMPLED AT EACH PHENOLOGY SITE. THE LAST ROW INDICATES THE URBANIZATION INTENSITY CATEGORY ASSIGNED TO EACH PHENOLOGY SITE. 154

TABLE 6-2: ESTIMATED REGRESSION PARAMETERS, STANDARD ERRORS (IN BRACKETS) AND SIGNIFICANCE LEVELS FOR THE RELATIONSHIP BETWEEN URBANISATION INTENSITY AND CANOPY COVER DECLINE. NB: *P<0.1; **P<0.05; ***P<0.01 160
TABLE 6-3: ESTIMATED REGRESSION PARAMETERS, STANDARD ERRORS (IN BRACKETS) AND SIGNIFICANCE LEVELS FOR THE EFFECTS OF SPECIES ON THE RELATIONSHIP BETWEEN URBANISATION INTENSITY AND (1) NET LEAF LOSS (2) TOTAL PERCENTAGE CANOPY COVER. NB: *P<0.1; **P<0.05; ***P<0.01 161
TABLE 6-4: AICC STATISTICS FOR MODELS FOR TOTAL PERCENTAGE CANOPY COVER AND NET LEAF LOSS RELATIONSHIPS WITH LAND COVER AND URBAN CLIMATE FOR EACH SPECIES SEPARATELY. AICC = AIC CORRECTED FOR SMALL SAMPLE SIZE, DF = DEGREES OF FREEDOM, R^2 = ADJUSTED REGRESSION COEFFICIENT, P = MODEL P-VALUE, ΔAICC = DIFFERENCE BETWEEN THE TOP MODEL AND GIVEN MODEL AICC, WI = MODEL WEIGHT. ONLY MODELS WITH ΔAICC < 2 ARE SHOWN. 163
TABLE 6-5: RELATIVE IMPORTANCE VALUES (RIV) OF PREDICTOR VARIABLES FOR MODELS PREDICTING TOTAL PERCENTAGE CANOPY COVER AND NET LEAF LOSS FOR EACH SPECIES SEPARATELY BASED ON LAND COVER AND URBAN CLIMATE 164

LIST OF FIGURES

FIGURE 1-1: AN OUTLINE OF THE THESIS STRUCTURE 31
FIGURE 2-1: TYPICAL SKETCH OF AN URBAN HEAT ISLAND PROFILE (OKE, 1987) 34
FIGURE 2-2: TEMPERATURE GAINS AND LOSSES AS A CONSEQUENCE OF DIFFERENCES IN SURFACE COVER AND STRUCTURE BETWEEN URBAN AND RURAL AREAS THAT RESULT IN FORMATION OF THE URBAN HEAT ISLAND. LATENT HEAT IS THE HEAT REQUIRED TO CONVERT A SOLID OR LIQUID TO VAPOUR WITHOUT CHANGE IN TEMPERATURE. SENSIBLE HEAT IS THE HEAT EXCHANGED BY A THERMODYNAMIC SYSTEM IN WHICH THE EXCHANGE OF HEAT CHANGES THE TEMPERATURE OF THE SYSTEM (ADAPTED FROM: GORSE *ET AL.*, 2019) 34
FIGURE 2-3: SCALES FOR ASSESSING URBAN CLIMATE AND THE VERTICAL LAYERS WITHIN EACH SCALE (URBAN CANOPY LAYER (UCL), URBAN BOUNDARY LAYER (UBL), RURAL BOUNDARY LAYER (RBL), PLANETARY BOUNDARY LAYER PBL). THE BROAD ARROWS REPRESENT PREVAILING ATMOSPHERIC FLOW WHEREAS SMALL ARROWS REPRESENT SMALL SCALE ATMOSPHERIC FLOW (MODIFIED FROM OKE, 1997). 38
FIGURE 2-4: TYPES OF UHI ON THE BASIS OF SCALE OF URBAN CLIMATE (ADAPTED FROM: ROTH, 2012; KOTHARKAR AND SURAWAR, 2016).....39
FIGURE 2-5: SIMILARITY BETWEEN SURFACE AND AIR TEMPERATURE DURING NIGHT TIME WHEN THE UHI IS STRONGEST (VOOGT, 2000; EPA, 2008) 39
FIGURE 2-6: MEASUREMENT APPROACHES FOR DIFFERENT TYPES OF UHI (VOOGT, 2007) 41
FIGURE 2-7: FACTORS AFFECTING UHI INTENSITY OF A CITY CAN BE CLASSED INTO THE ANTHROPOGENIC CAUSES AND NATURAL CAUSES. NATURAL CAUSES ARE DEPENDENT ON GEOGRAPHICAL LOCATION (SOURCE: VOOGT, 2007).....44
FIGURE 2-8 SHOWING DAY LENGTH VARIATION AT DIFFERENT TIME OF THE YEAR FOR DIFFERENT LATITUDES (SOURCE: PIDWIRNY, 2006).....46
FIGURE 2-9: DISTRIBUTION OF CLIMATE ZONES BASED ON KÖPPEN-GEIGER CLIMATE CLASSIFICATION. THE CLIMATE ZONES ARE DERIVED FROM PATTERNS OF AVERAGE PRECIPITATION, TEMPERATURE AND NATURAL VEGETATION (ARNFIELD, 2020). 50
FIGURE 2-10 ILLUSTRATING DIFFERENCES IN WATER INFILTRATION AND EVAPORATION WITH RELATION TO PROPORTION OF IMPERVIOUS SURFACES (SOURCE: FEDERAL INTERAGENCY STREAM RESTORATION WORKING GROUP, 2001) 58
FIGURE 2-11 TEMPORAL CHANGES IN VEGETATION WITHIN A GIVEN GROWING SEASON FROM A REMOTE SENSING PERSPECTIVE (ADAPTED FROM: EKLUNDH AND JÖNSSON, 2015, 2016) 63
FIGURE 3-1: SHOWS CLIMATE RECORDS OF KAMPALA OVER A PERIOD OF 30 YEARS (ADAPTED FROM: WMO, 2016) 76
FIGURE 3-2: LAND USE AND LAND COVER TYPES IN KAMPALA (30 M SPATIAL RESOLUTION).....77
FIGURE 3-3 SHOWING A WORKFLOW FOR LCZ CLASSIFICATION USING SAGA-GIS AND GOOGLE EARTH (GREY FILL POLYGONS) (ADAPTED FROM: BECHTEL *ET AL.*, 2019) 79
FIGURE 3-4 STRUCTURAL CHARACTERISTICS OF LOCAL CLIMATES ZONES (ADOPTED FROM STEWART AND OKE, 2012) 80
FIGURE 3-5: AN LCZ MAP OF KAMPALA (100 M RESOLUTION). THE CENTRAL BUSINESS DISTRICT IS COMPRISED OF COMPACT MIDRISE AND COMPACT LOW RISE LCZ TYPES WHEREAS LESS BUILT LCZ TYPES EXTEND OUT OF THE CITY. THE BLUE CIRCLE REPRESENTS THE REGION OF INTEREST THAT WAS THE MAIN FOCUS OF SUBSEQUENT ANALYSIS WITHIN 20 KM OF CITY CENTRE (I.E. COMPACT MIDRISE AND COMPACT LOWRISE).....82
FIGURE 3-6: MAP SHOWING VEGETATION ABUNDANCE FROM THE MOD13Q1 ENHANCED VEGETATION INDEX (250 M RESOLUTION). THE RANGE OF VALUES FOR THE EVI IS -1 TO 1, WHERE VALUES ABOVE 0.2 ARE INDICATIVE OF INCREASING VEGETATION BIOMASS (SEE APPENDIX I FOR MORE DETAILS OF SPATIAL PATTERNS). THE BLUE CIRCLE SHOWS THE REGION OF INTEREST USING IN THE ANALYSIS 85
FIGURE 3-7: ALGORITHM THEORETIC BASIS OF FOR PERFORMING TIME SERIES ANALYSIS AND EXTRACTING SEASONALITY PARAMETERS IN TIMESAT (SOURCE: EKLUNDH AND JÖNSSON, 2015, 2016). THE BLUE LINE DEPICTS THE ACTUAL VEGETATION INDEX DATA VALUE FOR A GIVE PIXEL AT DIFFERENT POINTS IN TIME, WHEREAS THE RED LINE SHOWS THE FITTED VEGETATION INDEX DATA. A SUMMARY OF EACH PHENOLOGY PARAMETER (REPRESENTED BY LETTERS "A"-"I" OF THE ALPHABET) IS PRESENTED IN TABLE 3-2.....88

Figure 3-8 showing surface cover differences of sites used for microscale climate and phenology processes. Locations 1, 2, 6, 7, 8, 13, 16, 22B, 23B were used for phenology (see 3.4.2.2). NDVI (30 m) was scaled to show the extent of differences in vegetation cover and impervious surfaces. 93
Figure 3-9: Workflow of Worldview images classification using OBIA 95
Figure 3-10: (a) An i-button (model DS1923) and HOBO (U23-001) displayed side by side; (b) Radiation shield (L: 15 cm*W: 15 cm* H: 15 cm) used to house the sensors (c) Sensor housed in a radiation shield at one of the sites 97
Figure 3-11: Characteristics of the candidate LCZ classes used in this study (Adapted from: Stewart and Oke, 2012) 99
Figure 3-12 showing aerial imagery acquired from Google Earth representing the candidate LCZ classes used in the analysis. A yellow line stretching 1 km has been added as a reference for the scale 100
Figure 3-13 showing box plots depicting the denoting the extent and significance of differences in vegetation cover (EVI) across all LCZ types and between pairs of LCZs 101
Figure 3-14: shows a summary of data attributes for each MODIS EVI pixel as a unit of the analysis 102
Figure 3-15: Conceptual diagram showing tree canopy change across time and traits of canopy cover change (total percentage canopy cover and net leaf loss) that were extracted from the time series as indicators of leaf production and leaf loss 105
Figure 4-1: Monthly maximum and minimum air temperature across the study site in the 2013, 2015 and 2015 (Source: WorldWeatherOnline, 2019) 111
Figure 4-2 shows the workflow of the data processing steps and analysis used in this study 112
Figure 4-3: An LCZ map of Kampala showing the location of the study site and Region of Interest (within ~20 km of the city centre) that was the basis of the analysis. 113
Figure 4-4: Characteristics of the candidate LCZ classes used in this study (Adapted from Stewart and Oke, 2012) 115
Figure 4-5 shows a summary of data attributes for each MODIS EVI pixel as a unit of the analysis 117
Figure 4-6 showing box plots depicting the denoting the extent and significance of differences in vegetation cover (EVI) across all LCZ types and between pairs of LCZs 118
Figure 4-7: Effect plots showing the influence of urban form and distance from the city centre on Start (a & b), End (c & d) and Length (e & f) of season and day (g & h). LCZ classification: B-Scattered trees; Nine-sparsely Built, Six-Open lowrise; Three_F-Compact low rise_Bare soil 122
Figure 5-1: Location (numbered) of the urban climate monitoring sites and volumetric soil moisture content (crossed) with relation to proportion of man-made features (and vegetation cover, as indicated by higher values of the NDVI (normalised difference vegetation index)) 132
Figure 5-2: Kampala's climate between February and September 2017, depicting monthly rainfall and number of days with more than 1mm of rain 132
Figure 5-3: Temporal change in Volumetric moisture content that was used to demarcate the dry down period from the rainy season. Dry indicate the transition for the wet season show the transition time of the end of the rains and start of the dry down period (DOY=130) 135
Figure 5-4: Spatiotemporal differences in night time air temperature and relative humidity with relation to proportion of man-made features 139
Figure 5-5: Spatiotemporal differences in temperature (a) and relative humidity (c) during the dry season. (b) Relationship between spatial differences in temperature and mean soil moisture. (c) Relationship between spatial differences in relative humidity and mean soil moisture 140
Figure 6-1: Locations of *Jacaranda* (red) and *Tabebuia* (turquoise) trees within each phenology site (black ring). Each phenology site (radius=100 m) represents the coverage of the sensor measurements (air temperature and relative humidity). Tree sample sizes, land cover, and urban form characteristics are summarised in Table 6-1 151
Figure 6-2: Kampala's climate between February and September 2017, (a) monthly rainfall and number of days with more than 1mm of rain and (b) Monthly night time air temperature and relative humidity.

Error bars represent the standard deviation and show the monthly variation of nighttime temperature and relative humidity across the phenology sites. 152
Figure 6-3: (a) *Jacaranda* and (b) *Tabebuia* are ornamental trees commonly found throughout Kampala .. 153
Figure 6-4: Conceptual diagram showing tree canopy change across time and traits of canopy cover change (total percentage canopy cover and net leaf loss) that were extracted from the time series as indicators of leaf production and leaf loss 156
Figure 6-5: Temporal changes in canopy cover for all trees for each species of trees with relation to changes in volumetric soil moisture content. Soil moisture data after DOY=212 were removed prior to analysis due to equipment malfunction 159
Figure 6-6: Interaction effect of species and urbanisation intensity on (a) Total percentage canopy cover and (b) Net leaf loss. 161
Figure 6-7: Effect plots showing the influence of land cover and urban climate on total percentage canopy cover and net leaf loss 163

LIST OF FIGURES IN APPENDIX

Figure AI 1: EVI scores in the select LCZ types used for the analysis depicting surface cover differences across LCZs (EVI> 0.2 depicts vegetation cover and EVI<0.2 represents vegetated surfaces. 207
Figure AI 2 shows surface cover differences along the urban rural gradient depicted by EVI. Each unit of Distance (Dist_250) is equivalent to 250 m with mean SE bars 207
Figure AI 3: Land Surface Temperature differences (°C) between LCZ across different years with mean SE bars 208
Figure AI 4: Land Surface Temperature differences (°C) between LCZ in 2015 that had the weakest differences between years with SE bars 208
Figure AI 5 shows Land Surface Temperature differences (°C) along the urban rural gradient across three years used in the analysis. Each unit of Distance (Dist_250) is equivalent to 250 m with mean SE bars209
Figure AI 6 shows differences in the Length of season between the LCZ across different years with mean SE bars..... 209
Figure AI 7 shows differences in the timing of start of season between the LCZ across different years with mean SE bars 210
Figure AI 8 shows differences in the timing of end of season between the LCZ across different years with mean SE bars 210

Figure AII 1: Approach used in the classification of urban form around all 22 sites (including 9 sites for phenology) used for spatial temporal characterisation of urban climate at a microscale 211
Figure AII 2: Proportion of man-made features (Buildings and paved surface) at Locations 1-6. The sensors location is represented by a red place mark. The locations with a green background (on the location name) were used for phenology of trees. *Jacaranda* and *Tabebuia* tree locations are represented by green and pink points on the map 212
Figure AII 3: Proportion of man-made features (Buildings and paved surface) at Locations 7-12. The sensors location is represented by a red place mark. The locations with a green background (on the location name) were used for phenology of trees. *Jacaranda* and *Tabebuia* tree locations are represented by green and pink points on the map 213
Figure AII 4: Proportion of man-made features (Buildings and paved surface) at Locations 13-18. The sensors location is represented by a red place mark. The locations with a green background (on the location name) were used for phenology of trees. *Jacaranda* locations are represented by green points on the map 214

Figure AII 5: Proportion of man-made features (Buildings and paved surface) at Locations 19, 22, 22B, 23 & 23B. The sensors location is represented by a red place mark. The locations with a green background (on the location name) were used for phenology of trees. *Jacaranda* and *Tabebuia* tree locations are represented by green and pink points on the map 215
Figure AII 6: Dendogram showing clustering of the phenology sites based on urban form data. The location names have a prefix ("L"). Local Climate Zones were assigned to the 216

Figure AIII 1: Images of *Jacaranda mimosifolia*. The tree has compound bi-pinnate leaves, purple flowers and green seen that explodes and turns brown as it matures 217
Figure AIII 2: Images of *Tabebuia rosea* (common name: Pink Trumpet tree). The tree has got digitate leaves and pink "tumpet-like" flowers 218
Figure AIII 3: Histograms showing Diameter at Breast Height (cm) of trees at each of the nine locations... 219

Figure AIV 1: Temporal change (March to September 2017) of canopy cover (%) of *Tabebuia* and *Jacaranda* trees pooled across all phenology locations in Kampala using a loess model. The yellow band to the left shows the main rain season (March-May), whereas the second band (to the right) highlights a mild rain season. See 221 for a detailed image of rainfall ditribution 220
Figure AIV 2: Rainfall distribution and number of rainfall days in each month in Kampala. The yellow band represent the rain seasons 221
Figure AIV 3: Differences in temporal change of *Jacaranda* trees between heavily built and lightly built locations using a loess model. The AUCs (Area Under the Curve - indicator of leaf loss) of individual trees had a negative and significant correlation (green) with impervious surfaces, suggesting that trees in heavily built neighbourhoods experienced high leaf loss. 222
Figure AIV 4: Differences in temporal change of *Tabebuia* trees between heavily built and lightly built locations using a loess model. The AUCs (Area Under the Curve - indicator of leaf loss) of individual trees had a negative correlation with impervious surfaces, suggesting that trees in heavily built neighbourhoods experienced high leaf loss. 223
Figure AIV 5: Temporal change of canopy cover at each one of the phenology locations..... 224
Figure AIV 6: Cluster analysis of temporal change of canopy cover of *Jacaranda* trees showed that the most built up locations (One, Two and Thirteen) had relatively similar time series..... 225
Figure AIV 7: Cluster analysis of temporal change of canopy cover of *Tabebuia* tree showed that the most built up locations (One, Two and Thirteen) had relatively similar time series..... 226

Figure AV 1: Temporal change of surface moisture at the phenology sites. Red and green lines have been added for reference to points indicating maximum and minimum surface moisture..... 227
Figure AV 2: Daily maximum night time temperature at 22 urban climates sites across a 50 day period. NDVI score is used to represent the site characteristics, with the highest NDVI scores indicating high vegetation cover in a given location. Green and red vertical lines represent the highest (32°C) and lowest (18°C) mode temperatures at locations fifteen and Eighteen respectively. The black line is the mode across all sites. The nine phenology sites are encircled 228
Figure AV 3: Daily average night time temperature at 22 urban climates sites across a 50 day period. NDVI score is used to represent the site characteristics, with the highest NDVI scores indicating high vegetation cover in a given location. Green and red vertical lines represent the highest (23°C) and lowest (21°C) mode temperatures at locations fifteen and nineteen respectively. The blackline is mode across all sites. The nine phenology sites are encircled 229
Figure AV 4: Daily average relative humidity at 22 urban climates sites across a 50 day period. NDVI score is used to represent the site characteristics, with the highest NDVI scores indicating high vegetation cover

IN A GIVEN LOCATION. GREEN AND RED VERTICAL LINES REPRESENT THE HIGHEST (77%) AND LOWEST (67%) MODE RELATIVE HUMIDITY AT LOCATIONS NINETEEN AND FOUR RESPECTIVELY. THE BLACK LINE REPRESENTS THE MODE ACROSS ALL SITES. THE NINE PHENOLOGY SITES ARE ENCIRCLED. 230

ABSTRACT

Urbanisation poses a major challenge for global sustainability because urban areas drive environmental change and the global population of urban dwellers is expected to continue to grow rapidly. Vegetation phenology, which is the study of the timing and duration of plant development phases, is important for monitoring the effects of urbanisation and the spatial variability of urban vegetation ecosystem and provisioning functions. Moreover, studies on the impact of the urban heat island effect on phenology can be a useful way for understanding the impacts of climate change. However, although the drivers of phenology in cities in temperate climates are well understood, vegetation phenology in the tropical city context is less studied and poorly resolved. Phenology in tropical cities would particularly be useful because urban residents rely strongly on vegetation for ecosystem and provisioning functions such as urban agriculture and regulation of all year round high temperatures. Linked to this is the fact that tropical cities are expected to have a high risk of exposure to the impacts of climate change which vegetation cover could minimise. However, tropical developing cities are experiencing the fastest rates of urbanisation around the world characterised by high losses of vegetation cover. This creates an urgent need for empirical studies on vegetation dynamics in tropical cities that cover a wide range of tropical climate types and urbanisation practices, including sub-Saharan Africa that is largely underrepresented in the urban ecology literature.

This study quantifies the effects of urbanisation and urban climate on vegetation phenology in the tropical city of Kampala, Uganda (sub-Saharan African) using a wholly empirical approach that assesses phenology at the landscape and tree species levels. The specific objectives of the study include the following: (1) examining the influence of the urban heat island effect on landscape phenology; (2) investigating the spatiotemporal dynamics of urban climate during the wet-dry season transition; (3) investigating the sensitivity of canopy phenology to local environmental settings.

This study showed that increase in surface temperature associated with the Urban Heat Island (UHI) resulted in shorter vegetation growing seasons at the landscape scale. Also, the magnitude of spatial variability in the UHI and Urban Dryness Island (UDI) was dependent on moisture availability and increased with the advancement of the dry season. Therefore, the influence of land cover composition on the UHI and UDI varied between seasons and was greatest during the dry season. With regard to the phenology of individual trees, a stronger UHI resulted in high leaf loss which equates to shorter growing seasons observed at the landscape scale. Moreover, the dynamics of canopy cover change varied between species.

These findings about the effect of the UHI in tropical cities contrasts with the established knowledge in temperate cities were stronger UHIs lead to longer growing season lengths. Therefore, urban planning policies geared towards lengthening the vegetation growing season by minimising the UHI and UDI intensity ought to be adopted to maximise the benefits of vegetation for the attainment of sustainable urban development.

DECLARATION

No portion of the work referred to in the thesis has been submitted in support of an application for another degree or qualification of this or any other university or other institute of learning.

COPYRIGHT STATEMENT

i. The author of this thesis (including any appendices and/or schedules to this thesis) owns certain copyright or related rights in it (the "Copyright") and s/he has given The University of Manchester certain rights to use such Copyright, including for administrative purposes.

ii. Copies of this thesis, either in full or in extracts and whether in hard or electronic copy, may be made only in accordance with the Copyright, Designs and Patents Act 1988 (as amended) and regulations issued under it or, where appropriate, in accordance Presentation of Theses Policy You are required to submit your thesis electronically Page 11 of 25 with licensing agreements which the University has from time to time. This page must form part of any such copies made.

iii. The ownership of certain Copyright, patents, designs, trademarks and other intellectual property (the "Intellectual Property") and any reproductions of copyright works in the thesis, for example graphs and tables ("Reproductions"), which may be described in this thesis, may not be owned by the author and may be owned by third parties. Such Intellectual Property and Reproductions cannot and must not be made available for use without the prior written permission of the owner(s) of the relevant Intellectual Property and/or Reproductions.

iv. Further information on the conditions under which disclosure, publication and commercialisation of this thesis, the Copyright and any Intellectual Property and/or Reproductions described in it may take place is available in the University IP Policy (see http://documents.manchester.ac.uk/DocuInfo.aspx?DocID=2442 0), in any relevant Thesis restriction declarations deposited in the University Library, The University Library's regulations (see http://www.library.manchester.ac.uk/about/regulations/) and in The University's policy on Presentation of Theses

ACKNOWLEDGEMENTS

First, I would like to thank my supervisors, Sarah Lindley and Angela Harris, for their countless contributions and support throughout the PhD process.

This work was funded by the Commonwealth Secretariat and the Prince Albert II of Monaco Foundation through the Intergovernmental Panel for Climate Change PhD scholarship programme.

Thanks to the Geography Laboratory staff for all the assistance with the field equipment. I am greatly indebted to all those who assisted with the fieldwork: Daniel Kanamara, Grace Namugalu and Harriet Kyakyo.

A special thanks go to the Kampala Capital City Authority, Uganda National Council for Science and Technology and Kampala Metropolitan Police for the permission to undertake this research.

I am greatly indebted to all the properties in Kampala that accepted me to conduct the field data collection in their premises. These include Kampala Capital City Authority, Hormisdallen PS, Kamwokya Mosque PS, Kitante PS, Makerere University PS, Kololo SS, Lubiri SS, Bahá'í House of Worship, Hotel Africana, Kampala Golf Club, Mukwano Coffee Marketing Board, Nsambya Hospital and Phoenix Logistics/ Fine Spinners Limited.

Thank you to all my fellow PhD students in Geography and wider School of Environment Education and Development (past and present) for the camaraderie and inspiration.

There is an endless list of friends that I would like to thank for keeping me energised throughout the PhD. For fear of forgetting some, I will skip the list, but trust that you'll know you are one of them if you read the thesis this far. Thank you to my family for always believing in me and other half's family for the encouragement during the PhD process.

I wish to thank my other half Jana and our dear daughter Nala who have been by my side throughout this PhD. Thank you for your encouragement, sacrifice, love and unwavering selflessness.

GLOSSARY OF ABBREVIATIONS

2-D	Two Dimensional
3-D	Three Dimensional
AT	Air Temperature
AUC	Area under the Curve
AUHI	Atmospheric Urban Heat Island
BLUHI	Boundary Layer Urban Heat Island
CBD	Central Business District
CLUHI	Canopy Layer Urban Heat Island
CM	Centimetre
DBH	Diameter at Breast Height
EOS	End of Season
EPA	Environment Protection Agency
EVI	Enhanced Vegetation Index
FAO	Food and Agriculture Organization
GI	Green Infrastructure
GIS	Geographical Information Systems
GSL	Growing Season Length
IPCC	Intergovernmental Panel on Climate Change
KCCA	Kampala Capital City Authority
LCZ	Local Climate Zone
LMM	Linear Mixed Model
LST	Land Surface Temperature
NDVI	Normalized Differences Vegetation Index
NIR	Near-Infrared

OBIA	Object Based Image Analysis
PBL	Planetary Boundary Layer
RBL	Rural Boundary Layer
RF	Random Forest
RH	Relative Humidity
SAGA	System for Automated Geoscientific Analysis
SE	Standard Error
SEB	Surface Energy Balance
SFT	Space For Time
SOS	Start of Season
SSA	Sub-Saharan Africa
SUHI	Surface Urban Heat Island
UBL	Urban Boundary Layer
UCL	Urban Canopy Layer
UDI	Urban Dryness Island
UHI	Urban Heat Island
UMT	Urban Morphology Type
US	United States
VI	Vegetation Index
VMC	Volumetric soil moisture content

CHAPTER 1. **RESEARCH IN CONTEXT**

1.1 Landcover change and climate feedback

The flow and exchange of energy and materials such as trace gases, nutrients and water between the atmosphere and biosphere is bidirectional (Hungate and Koch, 2015; Suni *et al*., 2015). This interaction occurs at different temporal and spatial scales with different implications at each scale (Field *et al*., 2007). Understanding the consequences of the changes to the dynamics of energy and material flow between the terrestrial biospere and atmosphere is crucial for enacting environmentally sustainable land use practices.

The rapid growth of the human global population and increase in demand for energy, water, food, fibre and shelter has profoundly changed the earth's surface (Vitousek *et al.*, 1997; Foley *et al.*, 2005). Over exploitation of natural resources through the increase of agricultural and urban areas have been accompanied by increase in consumption of water and energy (Vitousek *et al.*, 1997; Foley *et al.*, 2005). In turn, partitioning of energy between the atmosphere and biosphere and biological production and consumption of trace gases has been altered. The main agents of this change include: biodiversity loss, species invasion, land use and land cover change, climate change, rising atmopsheric CO_2, acid rain and increased nitrogen deposition (Hungate and Koch, 2015).

The conversion of natural forests and savannas into grassland and farm lands in the tropics has led to increase in temperature, wind speed and decline in rainfall and relative humidity (Hoffman and Jackson, 2000; Hoffman, Schroeder and Jackson, 2002; Duveiller, Hooker and Cescatti, 2018). Moreover, these conditions have led to an increase in fire frequency which in turn further reduces cloud formation and precipitation and enhances further losses of tree cover density (Hoffman and Jackson, 2000; Field *et al*., 2007). Hoffman, Schroeder and Jackson, (2002) observed significant increases in the frequency of dry periods within wet periods and a 10% decline in precipitation in tropical Africa. These changes were observed to damage shallow rooted plants and to affect albedo and roughness length (duration of season)

triggering an increase in air temperature by 0.5°C. Using global data, Duveiller, Hooker and Cescatti, (2018) observed increases in local surface temperature of up to 0.23°C resulting from recent conversions of natural vegetation cover to agricultural land use between 2000 and 2015. The loss of deeper rooted plants diminishes latent heat flux and increases sensible heat (Hoffman, Schroeder and Jackson, 2002). However, changes in land cover and land use through urbanisation represent an even more extreme form of land cover and land used change.

1.1.1 Urbanisation and urban climate

Urbanisation ranks highly among the primary drivers of environmental change at local, regional and global scales (McDonnell and Pickett, 1990; Grimm *et al.*, 2008; McCarthy, Best and Betts, 2010; Pickett *et al.*, 2011; Wu, 2014). Urban areas and the global population living in cities is expected to increase to 60% in 2030 from current estimates of 55% (United Nations, 2018). This should in turn exacerbate the environmental change attributed to cities. Moreover, greater margins of growth in size of cities and number of urban dwellers is expected to occur in Asia and Africa (United Nations, 2018) where change in land cover and land use has already caused detrimental effects on the environment (Hoffman and Jackson, 2000; Hoffman, Schroeder and Jackson, 2002; Duveiller, Hooker and Cescatti, 2018).

Urban areas are renowned for the Urban Heat Island (UHI) effect where urban areas experience significantly higher temperatures than their rural surroundings (Heisler and Brazel, 2010; Roth, 2012). This phenomenon results from contrasts in the release of anthropogenic heat; the capture and storage of incoming solar radiation; and less radiative cooling in urban areas (Landsberg, 1981; Oke, 1987). Impervious surfaces and a high density of buildings strongly absorb and retain heat and slowly release stored heat. Rural areas, on the other hand, have a low thermal admittance and high heat loss through evapotranspiration due to high vegetation and pervious surface cover (Roth, 2007).

Tied to the notion of the UHI, is the Urban Dryness Island Effect (UDI) which shows that urban areas have drier atmospheres (less humid) than their rural surrounding (Hage 1975; Ackerman 1978). The UDI is important for understanding moisture and

energy transfer dynamics in the near surface atmosphere with implications for vegetation development and thermal comfort (Jochner *et al*., 2013; Hass *et al*., 2017). In tropical cities where urban residents heavily depend upon vegetation for urban ecosystem services (Lindley *et al*., 2018) and vegetation growth and development is dependent on water availability (de Camargo *et al*., 2018), studies about the UDI are necessary. However, the UDI effect to date remains less studied than the UHI effect (Hao *et al*., 2018, Luo and Lau, 2019).

All cities that exhibit differences in surface cover and structure between urban and rural areas produce a city microclimate. Urban climate research is fast evolving to account for the connectivity of local urban features to acknowledge the combined effect of both surface and structural characteristics across space (i.e. the combined effect of vegetation, buildings and impervious combined) as opposed to quantifying the influence of individual land cover types (Stewart and Oke, 2012). This enables systematic studies to be done across multiple cities for cross comparison and also to understand the implications of different urbanisation practices around the world (Stewart and Oke, 2012).

Urban climate is connected to the regional climate (Roth, 2007) necessitating differentiating urban climate by region. Unlike temperate regions that have extreme seasonal changes in temperature, tropical regions experience warmer year-round temperatures. As of 2007, only 20% of urban climate research focussed on tropical cities (Roth, 2007) and, although the past decade has seen a significant upward trend in tropical urban climate research (Giridharan and Emmanuel, 2018), very few studies have been undertaken in tropical Sub-Saharan Africa (SSA). Therefore, there is a strong impetus for empirical investigations that exemplify the variety of tropical climate types and urbanisation practices, including sub-Saharan Africa which is underrepresented in the tropical urban ecology literature (Haaland and van den Bosch, 2015; Giridharan and Emmanuel, 2018).

1.2 Factors influencing tropical urban climate

1.2.1 Morphology of cities

Sub-Saharan Africa (SSA) is rapidly urbanising, and its urban population is expected to grow threefold from 400 million to 1.26 billion by 2050 (United Nations, 2014). In some African cities, polarised and spontaneous informal developments and heterogeneous urban morphology have resulted from resource constrained urban planning structures that are unable to cope with the overwhelming growth in human population and pressure for infrastructure (Antos *et al.*, 2016; Pérez-Molina *et al.*, 2017; Lindley *et al.*, 2018). In the context of this study, urban morphology refers to the spatial integration and linkage between human activities and natural processes (Pauleit *et al.*, 2015). Although some research has been done examining the climate of some African cities (e.g. Cavan *et al.*, 2014; Scott *et al.*, 2017), the number of cities studied remains low in comparison the number of African cities which differ in terms of urbanisation practices and morphology (Cavan *et al.*, 2014; Antos *et al.*, 2016). Consequently, urban climate studies that cover the extensive range of urban morphology and climate types of Africa are needed to fill the current knowledge gap.

1.2.2 Importance of vegetation in Tropical African cities

Vegetation in cities plays a vital role in regulating thermal comfort through radiative cooling (Taha, 1997; Dimoudi and Nikolopoulou, 2003; Cavan *et al.*, 2014; Feyisa, Dons and Meilby, 2014), and it is posited to improve urban liveability in tropical African cities where temperatures are high all year round (du Toit *et al.*, 2018). However, vegetation cover is being lost at an unprecedented rate in much of urban Africa (Yao *et al.*, 2019), without a clear understanding of how this loss may affect the regulatory functions of vegetation (Cilliers *et al.*, 2013; du Toit *et al.*, 2018).

1.2.3 Importance of water availability in tropical urban climate

Tropical urban heat islands are weaker during the rainy season than the dry season indicating the role surface moisture plays in altering albedo (Chow and Roth, 2006). However, the wet-dry season dichotomy is simplistic and overlooks the continuum of subtle temporal changes in water availability from the wet season through to dry down. Moreover temporal change in moisture ought to vary among the tropical climate types which are distinguished by the amount of precipitation and moisture

availability (Roth, 2007; Giridharan and Emmanuel, 2018). Therefore, urban climate in tropical cities can ideally be represented according to the Köppen classification (Table 1-1) to fully understand how dynamics of surface energy balance and UHI-induced plant water deficits (Zipper *et al.*, 2017) vary within the tropics. Further discussions into the different moist tropical climates are presented under section 2.1.4.2.

Table 1-1: Summary of the four main moist tropical climate types. Tropical climate under the Koppen classification consists of 4 main tropical climate types (Source: Kottek *et al.*, 2006; Peel *et al.*, 2007).

Tropical climate type	Description	Example cities
Tropical rainforest climate (*Af*)	-High rainfall all year round (average rainfall of 60 mm each month) -Climates occur within 10° latitude of the equator -Lack of differences in day light hours and mean monthly temperature	Kampala (Uganda), Singapore (Singapore), Surabaya (Indonesia) and Kuala Lumpur (Malaysia)
Tropical savanna climate; grouped into *Aw* and *As* types	- *Aw*: the dry season occurs during winter -*Aw* exhibit pronounced dry seasons with the driest month experiencing less than 60 mm precipitation	Cancun (Mexico), Bangkok (Thailand), Mumbai (India) and Lagos (West Africa)
	-*As*: The dry season occurs during summer (when the days are longer)	Mombassa (Kenya), Cali (Colombia), Chennai (India), Abidjan (Ivory Coast)
, Tropical monsoon climate (*Am*)	-Climate occurs mainly in the outer margins of the tropical zone greater than 10° latitude, but lower than the mid-20s latitude -Largely controlled by monsoon winds and a period of dryness that occurs after the winter solstice	Monrovia (West Africa) and Jakarta (Indonesia), Kochi (India), Miami (USA)

1.3 Vegetation phenology in tropical urban environments

Vegetation phenology refers to the study of the seasonal timing of the different stages of plant growth and development (e.g. leafing and flowering), their magnitude and drivers (Fenner, 1998). Phenology is widely considered to be useful for environmental monitoring with applications ranging from monitoring terrestrial responses to climate variation (Abernethy *et al.*, 2018), assessing variability in terrestrial productivity (Badeck *et al.*, 2004); and evaluating the effects of land-use change (Zhang, Friedl, Schaaf, Strahler, *et al.*, 2004).

In temperate regions where phenology is sensitive to photoperiod and temperature after wintertime dormancy (Menzel *et al.*, 2006; Zhang, Friedl and Schaaf, 2006), the UHI induces earlier starts of the vegetation growing season and results in longer seasons in urban than rural areas (Neil and Wu, 2006; Jochner and Menzel, 2015).

Other than temperature, the variability of other abiotic factors such as water availability have been observed to be strongly related to urban-rural (and intra-urban) phenological differences (e.g. Jochner *et al.*, 2011; Buyantuyev and Wu, 2012; Walker, de Beurs and Henebry, 2015).

In addition to there being a limited understanding of phenological processes in the tropics, the existing knowledge on tropical urban phenological processes is very limited (Jochner and Menzel, 2015) and emerges from two known studies (Gazal *et al.*, 2008; Jochner, Alves-Eigenheer, *et al.*, 2013). These studies compared the UHI effect on the timing of start of the vegetation growing season for select tree species between tropical and temperate cities (Gazal *et al.*, 2008; Jochner, Alves-Eigenheer, *et al.*, 2013). Results from both studies suggest that the UHI effect has a more significant impact in temperate than tropical climates, and this might have resulted from differences in UHI intensities that are known to be weaker in tropical than temperate cities (Roth, 2007). However, relative humidity was observed to be an essential predictor of a few of the studied species (Gazal *et al.*, 2008; Jochner *et al.*, 2013). There is a need for more research into the sensitivity of other species not studied yet, and empirical studies that examine the mechanisms of relative humidity. Furthermore, given the strong importance of precipitation as a factor that triggers leaf flush and production (Williams *et al.*, 1997; Clinton *et al.*, 2014; de Camargo *et al.*, 2018), studies that quantify the effect of the UHI ought to control for the effect of moisture availability. Moreover, the UHI is associated with increased evaporation and plant water requirements in temperate cities (Zipper *et al.*, 2017). However, the combined effect of the UHI and soil moisture has not been studied yet in tropical cities.

1.3.1 Deciduous nature of trees in tropical cities

In natural environments, canopies of deciduous tropical trees undergo gradual leaf loss as moisture diminishes during the dry season (e.g. Williams *et al.*, 1997; Condit *et al.*, 2000; Valdez-Hernandez *et al.*, 2010; Dalmolin *et al.*, 2015; de Camargo *et al.*, 2018). The extent of canopy cover change varies with respect to trees species and the nature of the environment. In extremely stressed environmental conditions, the extent of canopy cover loss might impact upon the productivity of vegetation in successive growing seasons (Singh and Kushwaha, 2016) with consequences for the ecosystem

and climate feedback. Despite there being evidence that urban climate is heterogeneous within cities and that canopy cover is critical for climate regulation (Feyisa, Dons and Meilby, 2014), there is a limited understanding of spatial variability of canopy cover in tropical cities. The existing knowledge on the effect of urbanisation on phenology of tropical cities is derived from studies that have focused on the timing of start of budding season alone (e.g. Gazal *et al.*, 2008; Susanne Jochner *et al.*, 2013). The wide range of parameters for quantifying phenology including: start of season, the magnitude and intensity of an event (Fenner, 1998; Denny *et al.*, 2014) ought to be exploited to gain an understanding of the sensitivity of trees to urbanisation and urban climate in the tropics. More about vegetation phenology and its drivers is discussed under section 2.2.

1.3.2 Landscape phenology in tropical cities

The collective response of vegetation to seasonal changes in local environmental settings demonstrated by changes in vegetation greenness is commonly referred to as landscape phenology (Liang and Schwartz, 2009; Morisette *et al.*, 2009). Landscape phenology is inherently different from the phenology of individual species, and a holistic understanding of vegetation phenology necessitates the use of both approaches (Badeck *et al.*, 2004; Jochner and Menzel, 2015).

In cities experiencing cool temperate climates, the duration of the vegetation growing season declines along the urban-rural gradient, and is significantly long in heavily built-up locations as a result of the UHI (White *et al.*, 2002; Zhang, Friedl, Schaaf, Strahler, *et al.*, 2004; Han and Xu, 2013; Dallimer *et al.*, 2016; Zhou *et al.*, 2016; Zipper *et al.*, 2016; Melaas *et al.*, 2016; Gervais, Buyantuev and Gao, 2017; Yao *et al.*, 2017; Krehbiel, Zhang and Henebry, 2017; Li *et al.*, 2017; Qiu, Song and Li, 2017; Parece and Campbell, 2018; Ren *et al.*, 2018). Equivalent understanding of these processes in the tropical context is unknown. There remains very little evidence of the impacts of urban form and the UHI effect on phenology in the tropics at both species and landscape scales.

1.4 Thesis Aims and Contributions

The overarching aim of this study is to identify and quantify the impacts of urbanisation and urban climate on vegetation phenology in Kampala Uganda, a tropical

city located in SSA. Kampala is an excellent case study city because it has a tropical equatorial climate and a wide range of urban form types from densely built-up to highly vegetated that typify several cities in tropical Africa and developing countries in general.

This study examines vegetation phenology at both the landscape and species level. At the landscape, phenology is assessed with relation to variations in urban form types using the local climate zone classification (Stewart and Oke, 2012) and along an urban-rural distance gradient and the associated differences in Land Surface Temperature (LST). At the species level, canopy phenology of two trees species (i.e. *Jacaranda mimosifolia* and *Tabebuia rosea*) is analysed with relation to urbanisation intensity, land cover composition and urban climate. The tree species were selected because they are sensitive to variation in local environmental settings in their natural habitats and were widely distributed across Kampala. Therefore, the thesis aims and objectives are as follows:

- To examine the influence of the urban heat island effect on landscape phenology
    - To determine the vegetation phenological response resulting from increased distance from the city centre, and differences in local climate zone class
    - To assess the influence of increased distance from the city centre and local climate zone class on LST
    - To quantify the effect of temperature on the start, end and length of the vegetation growing season
- To investigate the spatiotemporal dynamics of urban climate during the wet-dry season transition
    - To determine the relationship between spatial differences in urban climate (air temperature and relative humidity) and fine temporal change in surface moisture from the wet season through to dry down
    - To assess the influence of land cover composition on urban climate between the wet and dry season

- To investigate the sensitivity of canopy phenology to local environmental settings
    - To assess the effect of urbanisation intensity on canopy cover change for *Tabebuia* and *Jacaranda* trees during senescence
    - To compare the sensitivity of the canopy phenology of *Jacaranda* and *Tabebuia* to urbanisation intensity
    - To quantify the influence of land cover and urban climate on the canopy phenology of *Jacaranda* and *Tabebuia*

1.5 Research methodology

The study involved a wholly empirical approach that combined remote sensing and ground monitoring. The details of the methods adopted in this study are in a comprehensive methodology chapter and precede each of the three main research outputs results presented in chapters four, five and six. A general overview of the methodology is summarised below.

Firstly, a desk-based pilot survey and analysis using freely available satellite data was undertaken to characterise urban form and how it relates with LST and vegetation phenology. Phenology and LST data was derived for a limited period (i.e. 2013-2015) to minimise the effects of rapid land use and land cover change. The next step applied the knowledge gained on the relationships between urban form types, urban climate and phenology to design field monitoring of the local urban climate and the phenology of *Jacaranda* and *Tabebuia* trees from the wet to dry season between March and September 2017. This stage involved the selection of locations that typify the diverse range of urban structural differences from lightly to densely built-up areas. The investigation of urban climate with relation to land cover was treated separately from the assessment of the influence of land cover composition and urban climate on tree canopy phenology. The relationship between dependent and independent variables under each research objective were determined using regression analyses (i.e. mixed modelling, multivariate and univariate regression) and Information-Theoretic analysis.

1.6 Thesis structure

This thesis is structured in the 'alternative thesis format' and consists of three chapters (4-6) that are presented in the journal format (see Figure 1-1). It is the intention to submit the results chapter as papers for publication in the autumn of 2019. A summary of the articles and intended journal for publication is as follows:

Chapter 3/ Paper 1 Kabano, P., Lindley, S.J, and Harris, A. (2019). "Evidence of Urban Heat Island impacts on landscape phenology in a tropical city"
Intended journal: Science of the Total Environment

Chapter 4/ Paper 2 Kabano, P., Harris, A., and Lindley, S.J. (2019). "Spatiotemporal dynamics of urban climate during the wet-dry season transition in a Tropical African City"
Intended journal: Landscape and urban planning

Chapter 5/ Paper 3 Kabano, P., Harris, A., and Lindley, S.J. (2019). "Sensitivity of tree canopy phenology to local environmental settings in a tropical city"
Intended journal: Urban forestry and urban greening

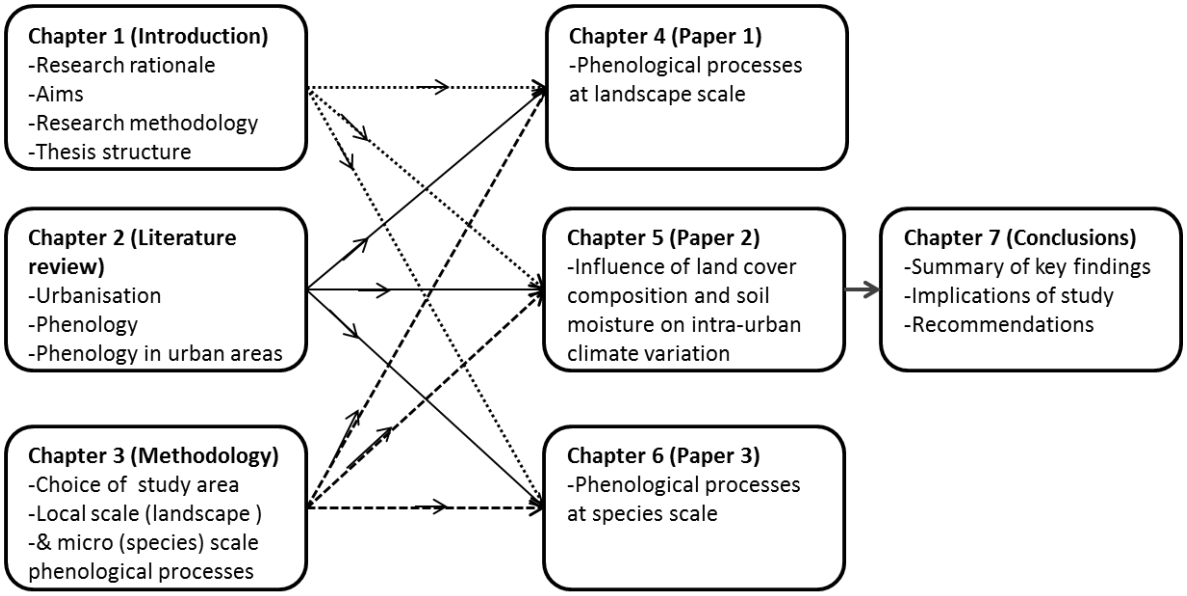

Figure 1-1: An outline of the thesis structure

Chapter 1 has summarised the background, justification, overarching aim and objectives of this study.

Chapter 2 will provide a detailed review of the current knowledge on urban climate and vegetation phenology. The first part of this chapter will give a general overview of urban climatology and contextualise it to the tropics, by including pertinent and recent urban climate research in tropical cities. Further into this assessment will be a general overview of urbanisation in SSA and why it makes for a unique case for research into the dynamics of tropical urban climate. The second part will present a general overview of phenology and its differences between temperate and tropical climates leading to an evaluation of the current body of literature in the context of urban environments and prognosis of phenological processes in tropical cities. Given the striking lack of empirical studies on phenology in tropical urban environments, the broader literature on temperate urban phenology studies forms a great deal of the conceptual set-up for the final part of chapter 2.

Chapter 3 provides the criteria for the choice of the study area, an outline and justification of the methodological approach used. This chapter includes details of the data acquisition techniques using remote sensing and field sampling and analysis used in this study.

Chapter 4 investigates the spatial patterns of LST and how they influence the length of the growing season using satellite remote sensing

Chapter 5 examines the spatiotemporal trends of urban climate and their main drivers using field monitoring techniques

Chapter 6 assesses the sensitivity of canopy phenology of *Tabebuia rosea* and *Jacaranda mimosifolia* to land cover composition, air temperature, surface moisture and relative humidity

Chapter 7 summarises the findings of the research and their broader significance. The chapter also presents suggestions for improving the study and recommendations for future research.

CHAPTER 2. **LITERATURE REVIEW**

The overarching aim of this chapter is to explore the fundamental theory of urban climate (i.e. Urban Heat Island and Urban Dryness Island) and phenology and to situate this discussion in a tropical context where urban phenological research is strikingly lacking with only two known studies (Gazal *et al.*, 2008; Jochner *et al.*, 2013). The knowledge gaps emerging at the end of the review form the basis and justification for the overarching aim and research objectives of this thesis.

2.1 Urban climate

The climate of cities is distinguished from the climate of the surrounding less urbanised rural areas by differences of air temperature, humidity, amount of precipitation and wind speed and direction (Kuttler 2008). Most notable of the urban-rural climate differences is the urban heat island, where urban areas experience elevated near-surface air temperature in comparison to the cooler rural surrounding (Landsberg, 1981; Voogt and Oke, 2003; Heisler and Brazel, 2010; Kleerekoper, Van Esch and Salcedo, 2012; Zhou *et al.*, 2015; Melaas *et al.*, 2016).

2.1.1 The Urban Heat Island (UHI) effect

The Urban Heat Island (UHI) effect has a long history and the term was first coined in the 1940s (e.g. Balchin and Pye, 1947). The phenomenon itself was established much earlier in the early 19th century, by Luke Howard (Stewart, 2011). He was motivated to undertake meteorological observations due to a lack of advancement of the discipline in comparison to other well established disciplines of the time. Howard observed an "artificial excess heat" in London compared to its rural surrounding. Since Howard's study, heat island studies have been published in hundreds of cities worldwide making it the most studied of climate effects of cities (Stewart, 2011).

Voogt (2007) estimates that a large sized city of approximately 10 million inhabitants may experience an annual temperature that is 1°–2°C warmer than its rural surrounding, and up to 12°C warmer on clear and calm nights (Voogt, 2007). More generally most cities are between 5-6 °C warmer than their rural surrounding (Oke, 2012). The spatial distribution of temperature across the urban and neighbouring rural

areas forms island-shaped patterns of isotherms similar to elevation contours of an island on a map (Roth, 2012; Voogt, 2007). The UHI effect is characterised by a peak that is associated with the city centre, a large gradient at the city periphery ("cliff"), and lower values associated with less urbanised rural surroundings (Oke, 1982) as depicted in Figure 2-1.

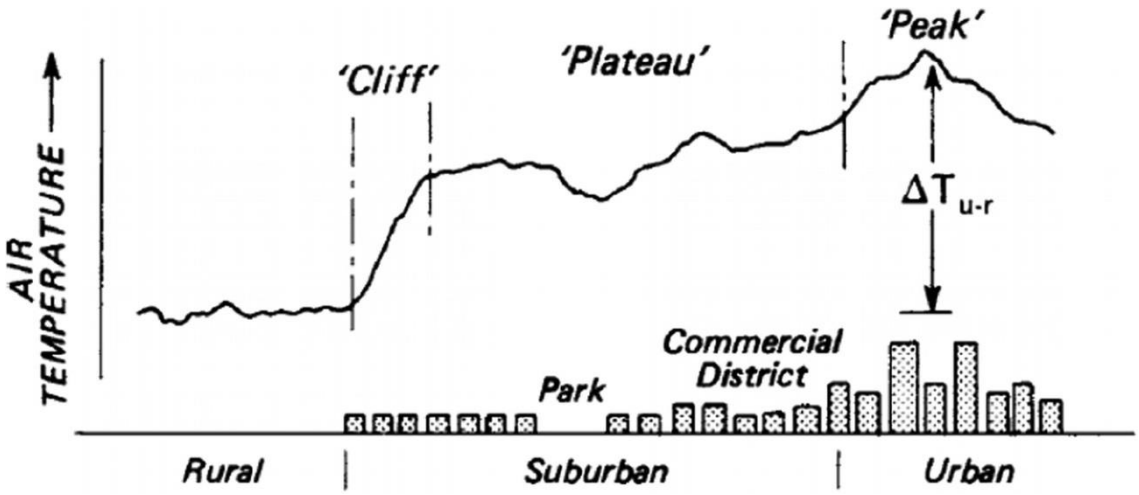

Figure 2-1: Typical sketch of an urban heat island profile (Oke, 1987)

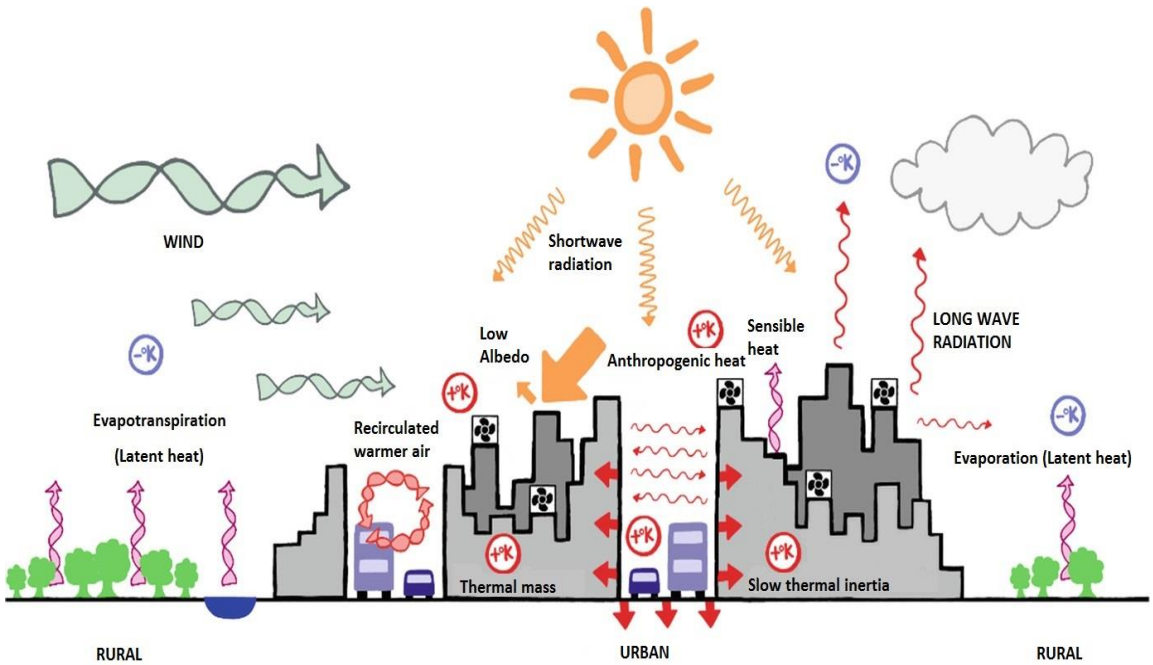

Figure 2-2: Temperature gains and losses as a consequence of differences in surface cover and structure between urban and rural areas that result in formation of the urban heat island. LATENT HEAT is the heat required to convert a solid or liquid to vapour without change in temperature. SENSIBLE HEAT is the heat exchanged by a thermodynamic system in which the exchange of heat changes the temperature of the system (Adapted from: Gorse *et al*., 2019)

The UHI effect mainly results from the differences in thermal admittance, and cooling between urban and rural areas and within urban areas (i.e. intra-urban) (Landsberg, 1981; Voogt and Oke, 2003; Heisler and Brazel, 2010; Kleerekoper, Van Esch and Salcedo, 2012; Zhou *et al.*, 2015; Melaas *et al.*, 2016). The replacement of natural land cover with buildings and impervious surface layers and the intensification of human activity (such as heavy traffic) through urbanisation alter the cycling of materials and energy (Figure 2-2) in the atmosphere and near-surface (Grimm *et al.*, 2008; McCarthy, Best and Betts, 2010; Pataki *et al.*, 2011; Pickett *et al.*, 2011; Wu, 2014). Urban areas are composed of artificial surfaces (e.g. concrete, asphalt and metal) and a design (i.e. high building density, tall buildings, and narrow streets) that lowers albedo (Sailor, 1995; Taha, 1997), promotes the transformation of short wave radiation into heat and inhibits radiative cooling (Landsberg, 1981; Oke, 1987; Voogt and Oke, 2003) as depcited in Figure 2-2. Different surfaces exhibit differences in thermal behaviour as a result of differences in density, heat capacity, thermal conductivity, thermal diffusivity and thermal admittance coefficients (Kuttler 2008). Furthermore, the heat released from intensified fossil fuel combustion in cities and by-products of energy consumption that are emitted as moisture and sensible heat are retained by the atmosphere of the city (Sailor, 2011). The UHI intensity has been observed to be strongest in the city centre (i.e. Central Business District/CBD), due to the presence of high rise buildings and a high density of buildings (Oke 1982; Oke, 1987). High rise buildings have been linked to the urban canyon effect (Schwarz and Manceur, 2014) which results in high thermal admittance and storage, and slow release of stored heat (Roth, 2007; Giridharan and Emmanuel, 2018).

In contrast, rural areas are highly pervious and vegetated and exhibit higher evapotranspiration than urban areas resulting in higher fluxes of latent heat and less release of sensible heat (Taha, 1997; Dimoudi and Nikolopoulou, 2003; Pataki *et al.*, 2011; Kleerekoper, Van Esch and Salcedo, 2012; Cavan *et al.*, 2014; Feyisa, Dons and Meilby, 2014; Duarte *et al.*, 2015; Lindley *et al.*, 2015). The net result of these differences in moisture, radiative, thermal, aerodynamic properties and the cycling of energy and materials between urban and rural areas is an urban climate and that is distinct from rural areas and the UHI effect. Therefore, vegetation in cities enhances

thermal comfort through evapotranspiration and provision of shade (Li, Ratti and Seiferling, 2018) and maintenance of its cover has been strongly advocated for as a means for mitigating the UHI intensity (Pataki *et al.*, 2011; Kabisch *et al.*, 2017).

2.1.1.1 **Importance of UHI studies**

The UHI effect is critical for human health and wellbeing mainly due to the increased exposure to heat and associated risks including: thermal stress, heat cramps and exhaustion, non-fatal heat strokes, and heat mortalities. Moreover the associated risks of heat exposure are exacerbated by heat wave events (Heaviside, Macintyre and Vardoulakis, 2017). To counter the UHI effect, air conditioning is used, but this is also without challenges.

Electricity demand for cooling to compensate the UHI effect has been estimated to account for 5-10% of community wide demand for electricity (Hashem and Akbari 2005; Akbari *et al.,* 2001). Skelhorn *et al* (2016) estimated between 9-12% increase in air conditioning due to the summer UHI effect, whereas by *Li el at* (2019) estimated increases in building cooling energy consumption of upto 19%. Although the amount of energy consumed varies in regard to the nature of UHI, there is a general tendency towards increased energy consumption for cooling due to the UHI effect which leads to higher spending on energy and increased release of carbon dioxide, as a by-product of energy production (Kolotroni *et al*., 2012). Moreover, increased carbondioxide resulting from energy production affects infra-red properties of the atmosphere (Kuttler 2008).

The UHI effect enhances the reaction of combustion gases in the atmosphere (Kondo and Kikegawa 2003) and formation of ground-level ozone commonly referred to as urban smog (Akbari *et al*., 2001) which reduces air quality. Moreover the spatial distribution and temporal evolution of air pollutants in cities is driven by thermodynamic and dynamic processes of the cities, including enhanced turbulence that significantly modifies the availability of ozone and nitrogen dioxide (Sarrat *et al*., 2005).

The UHI phenomena has received considerable critical attention because of its direct effects on human health, but its effects on ecosystems that are depended upon for

wellbeing remain far less studied (Yang *et al*., 2016). For example, there is evidence that the urban heat island affects seasonality of vegetation in urban areas (discussed under section 2.3). This is significant because urban ecosystem functions such as climate regulation and urban agriculture might be dependent upon seasonal growth and development of vegetation.

2.1.2 Quantifying UHI

2.1.2.1 **Influence of scale**

Interactions between the terrestrial system and atmosphere occur at different spatial and temporal scales (Hungate and Koch, 2015; Suni *et al.*, 2015). Therefore, scale is an important factor to consider in the spatial representation of not only the UHI intensity, but also urban climate in general (Roth, 2012). The three scales for undertaking observations on urban climate include: (1) microscale (one to hundreds of metres); (2) mesoscale (tens of kilometres); (3) and local scale (more than one kilometre, but less than ten kilometres) (Oke, 2008) as shown in Figure 2-3.

Microclimates typify the climate emanating from individual surfaces, objects and features in the landscape such as courtyards, gardens, roads, trees, and individual buildings that are located within the canopy layer (Oke, 2008; Heisler and Brazel, 2010; Roth, 2012; Kotharkar and Surawar, 2016) as shown in Figure 2-3(c). The canopy layer (Figure 2-3) is the area between the ground and the average height of the main roughness elements such as trees and buildings (Oke, 2008; Heisler and Brazel, 2010).

The urban climate at the mesoscale (Figure 2-3(a)) is different from the regional climate and results from the presence of a city at the surface. The climate at the mesoscale embodies climate of the urban boundary layer (UBL), which is above the urban canopy layer and extends to the planetary boundary layer zone where urban landscapes have no influence on the atmosphere (Figure 2-3). The mesoscale climate represents exchanges at the lower surface of the UBL, which is the interface located at roof level with generalised roughness, thermal and radiative characteristics (Oke, 2008).

Local-scale climate (Figure 2-3(b)) incorporates the effect of landscape features, urban form and function (e.g. surface cover, size and spacing of buildings and human

activity). The local-scale climate emerges from the integration of microclimates over large areas and is representative of uniform hourly turbulence of sensible, latent, and storage heat fluxes (Grimmond and Oke, 2002). The local climate combines the climatic aspects of both micro and mesoscale processes and local weather.

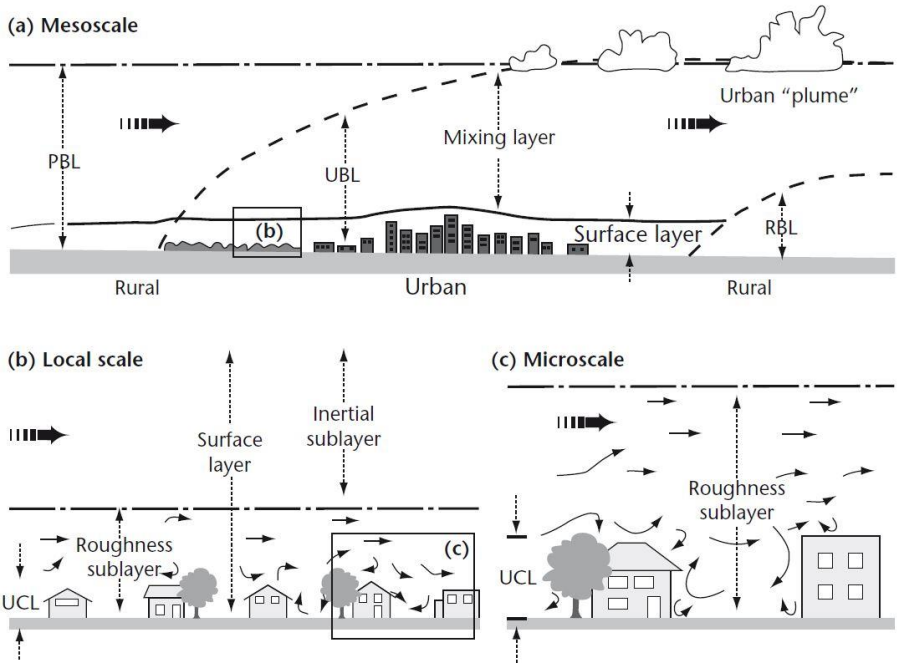

Figure 2-3: Scales for assessing urban climate and the vertical layers within each scale (Urban Canopy Layer (UCL), Urban Boundary Layer (UBL), Rural Boundary Layer (RBL), Planetary Boundary Layer PBL). The broad arrows represent prevailing atmospheric flow whereas small arrows represent small scale atmospheric flow (modified from Oke, 1997).

2.1.2.2 **Types of UHIs**

The Urban Heat Island is broadly categorised into the Surface UHI (SUHI) and Atmospheric UHI (AUHI) (Kotharkarand Surawar, 2016), illustrated in Figure 2-4 and Figure 2-5. The spatial distribution of air and surface temperature are connected and similar (Voogt, 2000; Ayanlade, 2016) because surface temperature regulates the air temperature of the lowest layers of the urban atmosphere and moderates energy balance of the surface (Voogt, 2003). Nevertheless the establishment of SUHI and AUHI are distinct processes and their quantification differs (Figure 2-6).

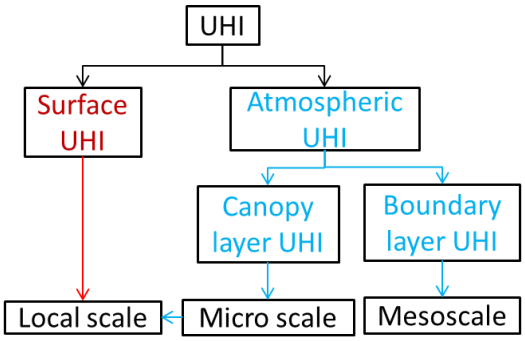

Figure 2-4: Types of UHI on the basis of scale of urban climate (Adapted from: Roth, 2012; Kotharkar and Surawar, 2016)

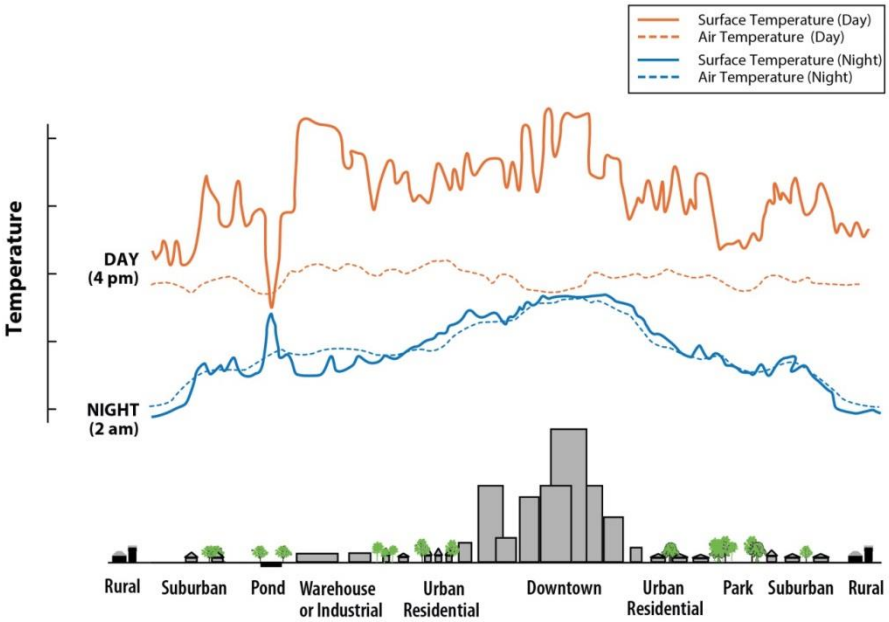

Figure 2-5: similarity between surface and air temperature during night time when the UHI is strongest (Voogt, 2000; EPA, 2008)

The AUHI is divided into nocturnal canopy layer UHI, and the Boundary Layer UHI (Oke, 2008). The canopy layer UHI is a microscale climate phenomenon whereas the boundary layer UHI is a mesoscale climate phenomenon (Figure 2-4). Sensible heat transfer from the surface (near-surface air temperature) and atmospheric exchange with layers above the near-surface (i.e. interface between the canopy and boundary layer) result in the canopy layer UHI (Figure 2-2). Urban-rural air temperature differences within the canopy layer during the day time are considerably lower, but increase after sunset and reach a peak at night (Figure 2-5) arising from reduced cooling rates in urban areas (Roth, 2012). The vertical mixing of air is highest during the day and declines during the night (Heisler and Brazel, 2010; Roth, 2012). Therefore, the

UHI effect is observed to be strongest at night and under clear sky conditions when there is higher exposure to incoming solar radiation (Heisler and Brazel, 2010; Voogt and Oke 2003).

The surface UHI (SUHI) is a local scale climate phenomena (Figure 2-5) and encompasses the temperature of the surface extending over the entire 3-D envelope of urban features, highlighting the variations of thermal (e.g., heat capacity, thermal admittance) and radiative (e.g., reflectivity or albedo) properties of urban surfaces (Heisler and Brazel, 2010; Roth, 2012; Kotharkar and Surawar, 2016). The magnitude of the SUHI is most substantial during day time (Figure 2-5) due to variability in the effect of solar heating between rural areas that are highly pervious and vegetated and impervious urban surfaces (Roth, 2012). At night however, the distribution of the SUHI is closely similar with the AUHI (Figure 2-5).

Urban boundary and canopy layer UHI are quantified using air temperature measurements. In-situ sensors at screen height at fixed weather stations or mounted on automobile objects can be used to measure the urban canopy layer UHI (Figure 2-6). On the other hand, boundary layer UHI is measured using fixed (tower), traverse (e.g. aircraft or balloon) and sodar remote sensors (Figure 2-6).

Measurements of surface temperature are derived insitu from thermocouples or thermistors. Alternatively, space and airborne remote sensors can estimate apparent surface temperature based upon radiance using infra-red radiometry (Voogt and Oke 1997; Voogt and Oke 2003). Other than the use of direct measurements, UHIs can be quantified using numerical models. Exemplar studies using the different methods of quantifying the UHI are presented under section 2.1.4.

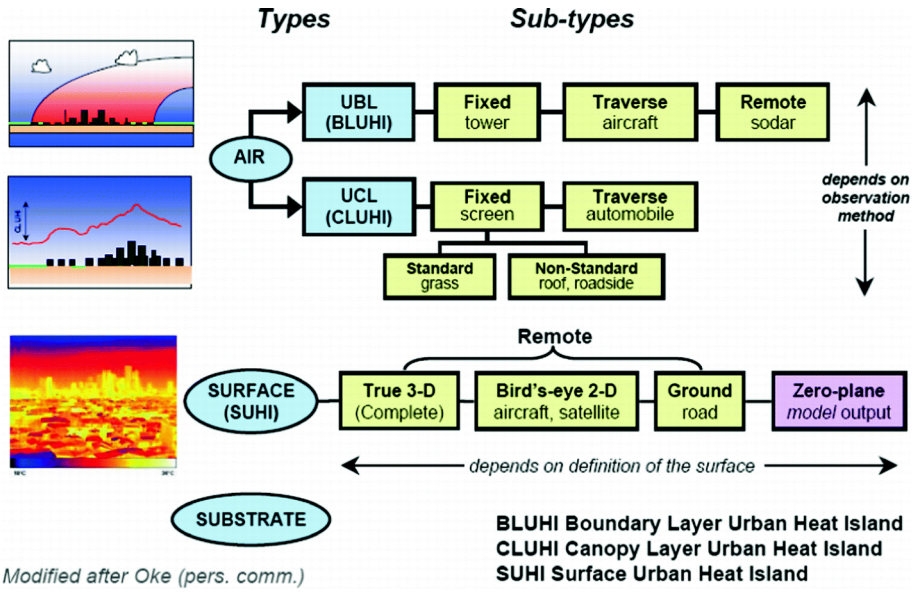

Figure 2-6: Measurement Approaches for different types of UHI (Voogt, 2007)

2.1.2.3 Characterisation of urban areas for urban climate studies

The characterisation of surface cover and structure across cities with respect to the effect of spatial scale is an essential component of quantifying urban climate. This in itself is a discipline that has been continually evolving with the advancement of urban climate research. A brief discussion thus follows into the evolution of spatial representation of urban areas for urban climate studies.

Traditionally, two weather stations (one urban and the other rural) were used to distinguish the climate of the city from the regional climate in what is classically referred to the urban-rural dichotomy (Stewart and Oke, 2012). However standard climate stations are designed to measure climate at a micro scale (see Influence of scale under section 2.1.2.1), and a single urban station only goes as far as measuring the climate of its nearby surrounding and not the entire city (Oke, 2008; Stewart and Oke, 2012). Refinements have been made to the urban-rural dichotomy highlighting the transition from urban to rural areas. Comber and Brundson, (2015) used a qualitative approach for describing land use that consisted of suburban, urban, built-up areas and gardens in England and Wales. Mimet *et al.*, (2009) used three levels to describe the extent of urbanisation in Rennes that included: inner ring (urban core), suburban ring and the peri-urban ring. Urban Morphology framework that connects urban form, social, cultural and biophysical processes into Urban Morphology Types (UMT) has been used in the UK (Gill *et al.*, 2008) and in Africa (Lindley *et al.*, 2015; Cavan *et al.*,

2014). Vizzari and Sigura, (2015) produced a gradient of landscape modifications highlighting the differences in landscape structure in Italy. Another approach has been the assessment of ecological approaches on a distance gradient from the urban core to the city centre (Zhang *et al*., 2004; Zhou *et al*., 2015) on the basis that the extent of urban development and its ecological forcing function diminish along the urban-rural gradient (McDonnell and Pickett, 1990). Although these finer qualitative measures of urbanisation offer an improvement to the urban-rural dichotomy, the main criticism that they are faced with is the lack of quantitative metadata describing urban form (surface cover and structure). Moreover, qualitative qualifiers of the extent of urbanisation are often subjective and vary from one region to another. This hinders their transferability and application to other cities with different urbanisation practises.

In a review of heat island literature, up to three-quarters of the studies were inadequate in providing quantitative metadata of meteorological sites (Stewart, 2011). There is an impetus to attribute urban climate at micro and local scales to quantitative measures of the bio-physical, structural and cover aspects of urban areas (Stewart and Oke, 2012). Quantitative aspects of the physical nature of cities provide a nuanced and scientifically relevant means for measuring urbanisation and its impacts.

Urban climate has been observed to have an unequivocal association with surface cover; precisely proportion of impervious man-made features including buildings or the percentage of pervious surfaces (i.e. open spaces and vegetation) (Yuan and Bauer, 2007; Gazal *et al.*, 2008; Xu, Lin and Tang, 2013; Feyisa, Dons and Meilby, 2014; Kurniati and Nitivattananon, 2016; Zipper *et al.*, 2016; Chibuike *et al.*, 2018; Giridharan and Emmanuel, 2018). However, this approach only serves to account for the effect of individual components of surface cover and not the combined effects of different structural features.

The use of zones to designate areas that have uniform composition of surface cover and structure (urban form) takes into account the connectivity of urban features (as opposed to individual features) and their collective influence on micro and local scale climate processes. Using data from North, America, Europe and Asia, Loridan and

Grimmond (2011) developed Urban Zones for purposes of atmospheric modelling to distinguish urban areas and characterise energy partitioning on the basis of incoming radiation. Threshold values for the active (engaged in energy exchange) built surface and vegetative fractions are used for the designation of the four main zones. Oke (2004) proposed urban climate zones for urban areas which were later modified to local climate zones to incorporate rural areas (Stewart and OKe, 2012). The zones are distinguished by their fabric (materials), surface cover, urban structure, metabolism (human activity) and capacity to modify local climate.

These zoning approaches however have limitations because their application is constrained to measuring a specific scale of urban climate. For example, the local climate zone has a minimum threshold area of radius 200 m within which urban form needs to be uniform for attribution of local scale climate to urban form. In cities where urban form is highly heterogeneous within areas smaller than the minimum set thresholds, application of these frameworks becomes quite limited. Therefore, the choice of method for characterisation of urban form and its attribution to urban climate should be tailored to the city context (e.g. extent of heterogeneity) and adjustments done accordingly.

2.1.3 Factors affecting Urban Heat islands

2.1.3.1 **Human factors**

The processes driving the urban climate of different cities around the world are quite similar (see 2.1). However, the intensity and nature of the urban heat island can be quite varied across cities (Cheung 2011; Yang *et al*., 2016; Debbage and Shepherd 2015) due to local context regarding the urban area, urban form, urban function and geographical location of the city (Kuttler 2008) as summarised in Figure 2-7. The combined effect of differences in urban form, urban function and geographical location (driving regional climate) makes each city unique with regards to urban climate. Therefore, empirical studies that aim to study the UHI intensity of individual cities are very relevant for adopting climate resilient strategies that are tailored to each individual city especially for cities that are small and projected to grow.

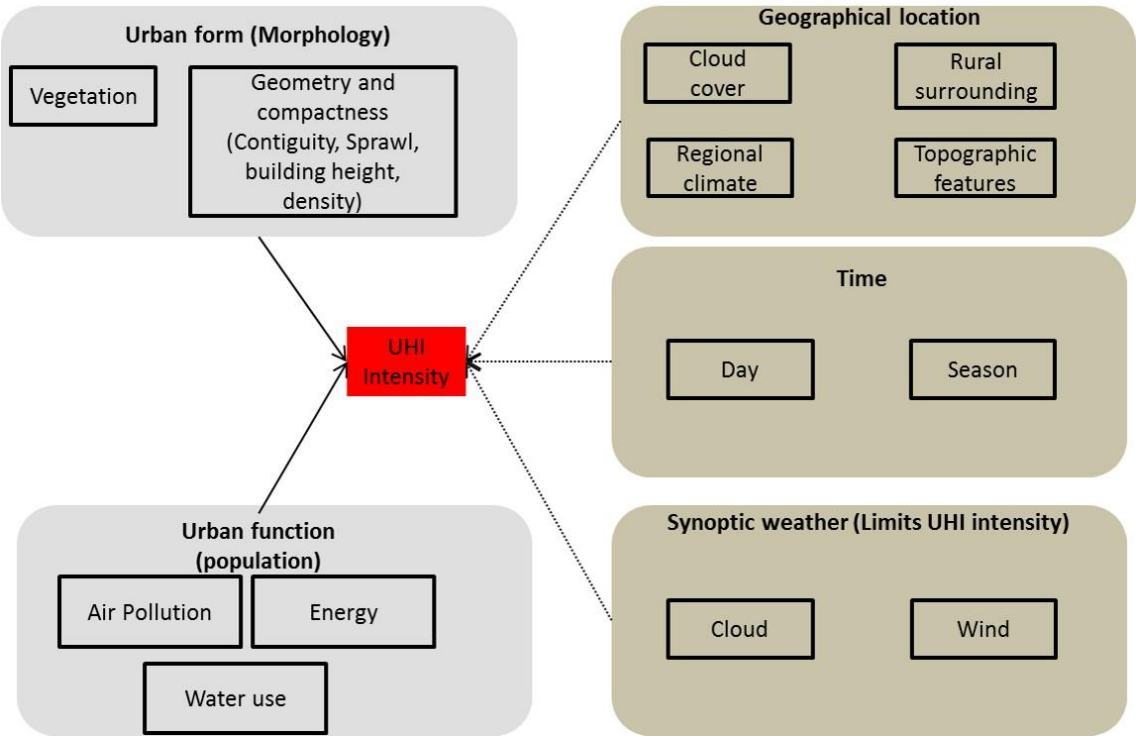

Figure 2-7: Factors affecting UHI intensity of a city can be classed into the anthropogenic causes and natural causes. Natural causes are dependent on geographical location (Source: Voogt, 2007).

Urban morphological differences are a key determinant of differences in UHI intensity with highly compact cities (i.e. high building density) exhibiting stronger UHI intensities (Zhou *et al*., 2017). A global study of the major determines of the urban heat island intensity by Clinton and Gong (2013) observed that in addition to development intensity (extent of compactness), vegetation amount and the size of the urban area are critical for prediction of heat differentials. Cities that are highly vegetated show weak UHI intensities (Clinton and Gong 2013) due to enhanced evapotranspiration and latent heat flux (Taha, 1997; Dimoudi and Nikolopoulou, 2003; Pataki *et al.*, 2011; Kleerekoper, Van Esch and Salcedo, 2012; Cavan *et al.*, 2014; Feyisa, Dons and Meilby, 2014; Duarte *et al.*, 2015; Lindley *et al.*, 2015). Moreover, differences in vegetation type, the canopy structure and cover, tree species; park shape, and park size have been observed to result in differences in thermal regulation and UHI intensity (Feyisa, Dons and Meilby, 2014; Gioia *et al*., 2014).

The configuration of rapidly sprawling cities enhances high UHI intensities (Stone 2012; Debbage and Shepherd 2015). Sprawl which is defined as low density leapfrog urban growth that consists of isolated land uses and widespread commercial strip

development (Debbage and Shepherd 2015) intensifies the UHI through land clearance, increased impervious areas and excess heat release per capita in comparison to higher density developments (Stone 2012). Moreover, a warm urban periphery, limits the cooling influence of UHI circulation (Stone 2012). As with the effect of urban sprawl, higher UHI intensities are associated with more spatially contiguous cities (Debbage and shepherd 2015), cities that exhibit high fractality (unsystematic urban development) and high anisometry (Zhou 2017).

The size and population of the city are key indicators of the functioning of a city, with larger sized and highly populous cities exhibiting high UHI intensity (Kuttler 2008). City size is also used as a convenient proxy for urban geometry (Roth 2007) which has a relationship with UHI intensity. Linked to the population of a city is its energy consumption and energy consumption is directly proportional to population density (Sailor 2011). Population density is a key factor that drives anthropogenic heating from human metabolism. In the US, daytime population densities are upto 5000 people per square kilometre with a corresponding heat flux of about 1 w/m2 and stronger UHI intensities are experienced with higher population densities (Sailor 2011).

Large city sizes have also been associated with increased atmospheric pollution (Lamsal *et al*., 2013) and whilst stronger UHI intensities further intensify air pollution (see Importance of UHI studies under 2.1.1.1), the UHI intensity is also affected by the air pollution. Cao *et al*., (2016) observed stronger UHI intensities linked to the enhanced haze pollution. Contrary to this, UHI intensities have been observed to be weakened by higher concentration of fine particles (Wu *et al*., 2017; Meier *et al*., 2018).

In addition to city size, geographical location is a critical factor influencing UHI intensity. Cities with a mid-latitude climate have been shown to exhibit a strong relationship between the size of the city and atmospheric UHI (Oke 1973) and surface UHI (Clinton and Gong 2013; Zhou *et* al., 2017). This is an important indicator of the influence of geographical location on UHI intensity.

2.1.3.2 **Natural factors**

Although an urban climate is a characteristic feature of every city that has artificial surface and structural features that are distinguished from the rural surrounding, the

underlying regional climate results in urban-rural climate differences among regions (e.g. Gazal *et al.*, 2008; Jochner, Alves-Eigenheer, *et al.*, 2013; Dallimer *et al.*, 2016; Zhou *et al.*, 2016). Insolation which defines the cumulative energy at a given location over a given period plays a vital role in determining regional climate and varies according to latitude (Figure 2-8). Insolation in temperate regions (i.e. higher latitudes) undergoes substantial seasonal changes each year which in turn result in extreme temperature changes. In the tropics however, temperature changes are relatively the same (and high) across the year due to uniform distribution of insolation across the year (Figure 2-8).

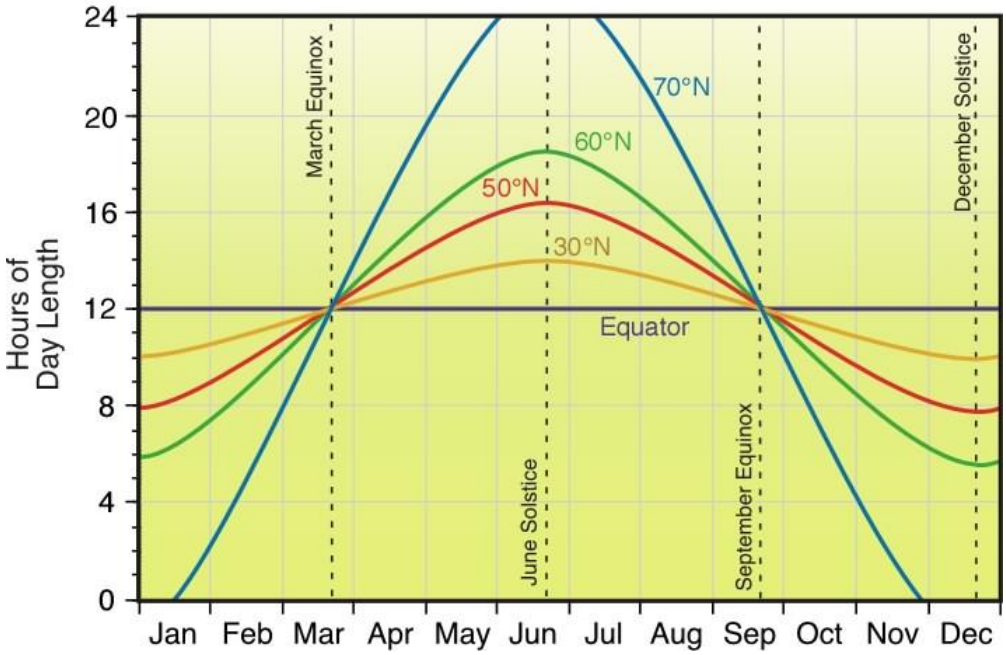

Figure 2-8 showing day length variation at different time of the year for different latitudes (Source: Pidwirny, 2006)

A strong relationship exists between latitude and urban-rural climate differences such that the more northern a city is located, the stronger the UHI intensity (Kuttler 2008; Dallimer *et al*., 2016; Zhou *et al*., 2016). Moreover, UHI intensities are much stronger in higher latitude cities than tropical cities attributable to differences in anthropogenic heat release and surface energy balance (Roth, 2007). However, this does not negate the value of undertaking UHI studies in tropical regions as the UHI effect would exacerbate effects associated with high temperature all year round.

2.1.4 Urban Heat Islands in the tropics

2.1.4.1 **Recent trends and patterns of emerging literature**

Two of the most recent and critical articles about tropical urban climate (Roth, 2007; Giridharan and Emmanuel, 2018) have collectively reviewed literature from the tropics (23.5 °N and 23.5° S) and subtropics (up to 30° N and 30°S). Although the tropics and subtropics share similarities in urban climate, Roth (2007) and Giridharan and Emmanuel, (2018) stress the need for a wider range of studies that cover different tropical climate types and regions. This would account for regional climate differences (precipitation and temperature) in gaining a concise understanding of urban climate differences and similarities within and between the tropical and subtropical regions.

The past decade has seen a significant upward trend in the proportion of UHI studies emanating from the tropics, from a lowly estimate of 20% in 2007 (Roth, 2007). Some recent studies since Roth's review (2007) are provided in Table 2-2. The existing studies show that there is a strong relationship between surface cover (mainly absence of vegetation cover) and the magnitude of the UHI intensities, which is in agreement with previous discussions on factors determining UHI intensities (see section 2.1.1 and 2.1.3). However, studies about the collective and combined effect of the different and connected urban features across the urbanscape (i.e. pervious surfaces, impervious, buildings and vegetation cover) are still lacking. Also, as noted by Voogt and Oke, (2003) and Roth, (2012), Surface Urban Heat Island (SUHI) still remains far less studied than Atmospheric Urban Heat Islands (AUHI). There also appears to be far more studies in subtropics than the moist tropical climate types (see Table 2-1). In the moist tropical climate that have seen an increase in exemplar studies in recent years, there remains a disparity in the number of representative studies per geographic region. For example, most of the recent studies in tropical rainforest climate are from Asia, while none are known in Africa.

2.1.4.2 **Surface moisture and Tropical moist climate types**

One common feature across the studies that have assessed the seasonality of the UHI (see Table 2-2) is the role that surface moisture plays in determining the intensity of the UHIs. Tropical regions undergo seasonal changes in surface moisture despite having limited temperature ranges (Kottek *et al*., 2006; Peel *et al*., 2007) and tropical UHI

intensity is greater in the dry than the wet season. Roth (2007) suggested that the surface temperature range is smaller (UHI) during the wet season with increased thermal admittance of wet soil and decreased cooling in rural areas. The influence of water availability as the basis for the seasonality of UHI intensity in the tropics is still poorly understood because UHI seasonality is based on the wet-dry season dichotomy (Roth, 2007; Giridharan and Emmanuel, 2018 and references therein). The simplistic wet-dry season dichotomy does not sufficiently account for the continuum of soil moisture changes across the wet to dry season temporal gradient which might offer insights into the mechanisms of UHI seasonality. Such an approach could help in understanding the coupling between soil moisture and temperature.

Surface moisture availability is critical for land surface atmospheric interactions specifically surface temperature and energy balance (Lakshmi, Jackson and Zehrfuhs, 2003; Pablos *et al.*, 2016). Surface moisture determines the proportion of rainfall partitioned into runoff, surface storage, and infiltration and the partitioning of solar and longwave radiation into outgoing longwave radiation, latent, sensible and ground heat flux (Lakshmi, Jackson and Zehrfuhs, 2003). Wet soils exhibit smaller changes in temperature due to the thermal inertia of water and drier soils exhibit higher temperatures (Lakshmi, Jackson and Zehrfuhs, 2003). Surface temperature in turn affects surface moisture and the relationship between surface moisture and surface temperature is seasonal (Lakshmi, Jackson and Zehrfuhs, 2003; Pablos *et al.*, 2016). However, surface moisture changes vary across different moist tropical climate types (Table 2-1) and UHI intensity ought to be modified accordingly and different across different tropical climate types (Roth 2007; Giridharan 2018).

Moist Tropical Climates are diverse in terms of precipitation with four main types (Table 2-1; Figure 2-9) according to the Köppen climate classification framework (Kottek *et al*., 2006; Peel *et al*., 2007). This arises from differences in changes in water availability that are triggered by movement of the Hadley cells and the Inter-Tropical Convergence Zone, linked to solar altitude and the movement of low pressure (and seasonal rainfall) (Kottek *et al*., 2006; Peel *et al*., 2007). The differences in surface moisture driven arising among the different tropical climate type ought to be

accounted for to gain a fuller understanding of the seasonality of UHIs in the tropics (Roth 2007; Giridharan and Emmanuel, 2018).

Table 2-1: Summary of tropical climate types. Tropical climate under the Koppen classification consists of 4 main tropical climate types.

Tropical climate type	Description	Example cities
Tropical rainforest climate (*Af*)	-High rainfall all year round (average rainfall of 60 mm each month) -Climates occur within 10° latitude of the equator -Lack of differences in day light hours and mean monthly temperature	Kampala (Uganda), Singapore (Singapore), Surabaya (Indonesia) and Kuala Lumpur (Malaysia)
Tropical savanna climate; grouped into *Aw* and *As* types	- *Aw*: the dry season occurs during winter -*Aw* exhibit pronounced dry seasons with the driest month experiencing less than 60 mm precipitation	Cancun (Mexico), Bangkok (Thailand), Mumbai (India) and Lagos (West Africa)
	-*As*: The dry season occurs during summer (when the days are longer)	Mombassa (Kenya), Cali (Colombia), Chennai (India), Abidjan (Ivory Coast)
, Tropical monsoon climate (*Am*)	-Climate occurs mainly in the outer margins of the tropical zone greater than 10° latitude, but lower than the mid-20s latitude -Largely controlled by monsoon winds and a period of dryness that occurs after the winter solstice	Monrovia (West Africa) and Jakarta (Indonesia), Kochi (India), Miami (USA)

Regimes of water availability and temperature also vary strongly among moist tropical climate types. For example, although both Singapore (1°17'N 103°50'E) and Kampala (00°18'49"N 32°34'52"E) are classified as tropical rain forest climate types, they show different climate patterns (see WMO, 2016). Singapore receives almost twice as much rainfall as Kampala (i.e. 2166 mm vs 1264 mm) with no distinct seasons (i.e. rains all year round). Kampala, on the other hand, has two rain seasons (March-May & September-November) and two dry seasons (June–August & December-February). Also, temperature is quite distinct between the two cities with temperatures in Singapore 4°C higher than in Kampala. Kampala has an average low, and an average high of 17.6°C and 27.8°C (i.e. average 22.7°) respectively whereas Singapore has an average low and average high of 24.7°C and 31.5°C (i.e. average 27.5°). Such differences highlight the need for a wide range of exemplar studies even within the same tropical climate type.

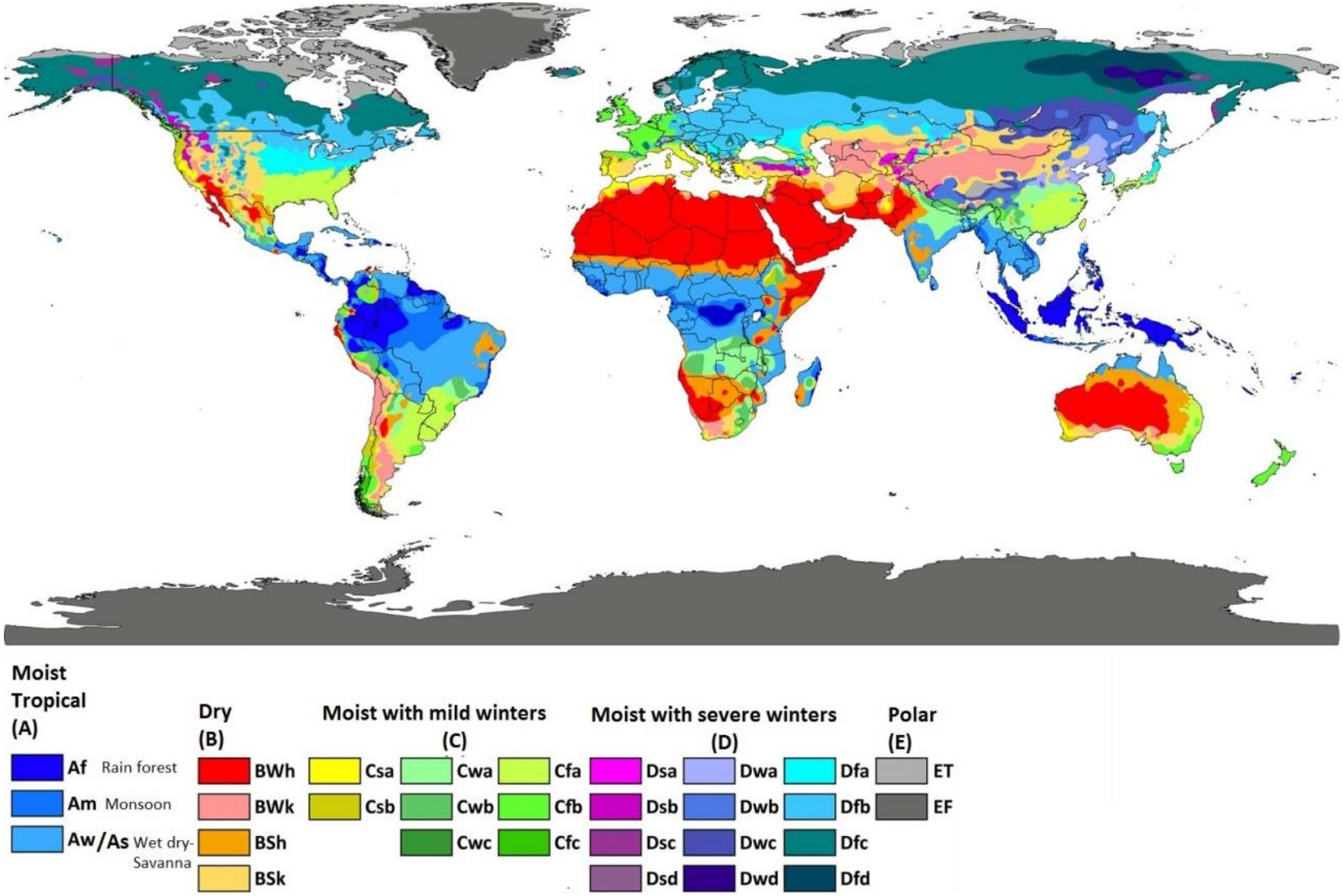

Figure 2-9: Distribution of climate zones based on Köppen-Geiger climate classification. The climate zones are derived from patterns of average precipitation, temperature and natural vegetation (Arnfield, 2020).

Table 2-2: Summary of recent tropical urban climate studies. Studies on Atmospheric UHI and Surface UHI studies are presented separately under specific climate types

STUDY CONTEXT	STUDY SITE {and climate type}	KEY FINDINGS	AUHTOR(S) AND PUBLICATION YEAR
		ATMOSPHERIC URBAN HEAT ISLAND (AUHI) STUDIES	
		AUHI studies in tropical rainforest climates	
City wide modelling of urban climate-Atmospheric Urban Heat Island (AUHI) with relation to land cover	Kuala Lumpur, Malaysia {tropical rain forest}	Model accurately represented spatial patterns of UHI, validating use of land cover (i.e. paved surface, buildings, vegetation and water)	(Wang et al., 2019)
Influence of urban morphology parameters on AUHI	Singapore {tropical rain forest}	Land cover specifically green area was the only significant predictor for night time temperature	(Jin et al., 2018)
Air temperature modelling with relations to changes in the seasons	Kuala Lumpur, Malaysia { tropical rain forest }	UHI intensity is greatest at night. Vegetated surfaces and areas of low density housing cool down at a faster rate than high density urban housing areas.	(Ooi et al., 2017)
Heat exposure (AUHI) in different green spaces	Singapore, Singapore {tropical rain forest}	Vegetation canopy characteristics are important for assessing heat exposure	(Chow et al., 2016)
Cooling potential (AUHI) of different tree species	Penang, Malaysia { tropical rain forest}	Climate regulation varies between species mainly due to Leaf Area Index. *Tabebuia rosea* is an example species noted for high cooling potential	(Tukiran, Ariffin and Ghani, 2016)
AUHI modelling	Singapore { tropical rain forest}	Effect of land use cover and type greatest at night	(Li et al., 2013)
Temporal and spatial dynamics of AUHI	Singapore, Singapore { tropical rain forest}	Differences in urban-rural cooling were influenced by seasonal changes in precipitation. Precipitation decreased the UHI intensity. Urban geometry had an unclear relationship with UHI intensity whereas intra-urban differences in temperature had a strong relationship with presence of green space and anthropogenic heat.	(Chow and Roth, 2006)
		AUHI studies in tropical savanna (wet and dry) climates	
AUHI with relation to LCZs	Nagpur, India {tropical savanna}	Most densely built compact low rise LCZ type was the warmest and the UHI impact varied between seasons (summer and winter)	(Kotharkar and Bagade, 2018)
Impact of land use/land cover, and population density	Nagpur, India {tropical	Strong UHI effect in high building density and populated areas; Low vegetation cover increased the UHI effect	(Kotharkar and Surawar, 2016)

on AUHI	savanna}		
Temporal change of AUHI effect	Lagos, Nigeria {tropical savanna}	UHI effect strongest at night and during the dry season	(Ojeh, Balogun and Okhimamhe, 2016)
Drivers of AUHI and its temporal variability	Akure, Nigeria {tropical savanna}	UHI intensity greatest during the dry season	(Balogun and Balogun, 2014)
AUHI with relation to the LCZs	Kochi, India {tropical monsoon}	High UHI effect observed during winter (dry time of the year) and at predawn; Compact midrise (city) showed the highest UHI effect; Sparsely built LCZ types showed consistently cooler climates throughout all seasons; Fastest cooling rates are in sparsely built up areas whereas slower cooling rates are observed in heavily built up areas;	(Thomas et al., 2014)
		AUHI studies in humid sub-tropical climates	
Local variation of outdoor thermal comfort (AUHI) in different urban green spaces	Guangzhou, China {humid sub-tropical}	Grove (small group of trees) yield cooler temperatures, but higher humidity than grasslands	(Wang et al., 2018)
AUHI comparisons between a temperate and a tropical city	Presidente Prudente, Brazil {humid sub-tropical}	UHI greatest at night and during the dry season for the tropical city. UHI greater for the tropical than temperate city	(Amorim and Dubreuil, 2017)
Influence of species types and compaction of vegetation on microclimate (AUHI)	Campinas, Brazil {humid subtropical}	Species types (i.e. canopy structural differences) and density of vegetation influence microclimate	(de Abreu-Harbicha, Labakia and Matzarakis, 2015)
Microscale cooling effect of vegetation (AUHI)	Sao Paolo, Brazil {humid sub-tropical}	The effect of trees is more pronounced during the summer period when temperature is high	(Duarte et al., 2015)
		AUHI studies in sub-tropical highland climates	
AUHI in informal settlements	Nairobi, Kenya {sub-tropical highland}	Informal settlements experience high temperature and thermal heat stress and this is strongly and negatively related to vegetation cover	(Scott et al., 2017)
Influence of vegetation (species type and park structure) on SUHI and AUHI	Addis Ababa, Ethiopia {sub-tropical highland}	Vegetation cooling effect is dependent on canopy cover and species type; Equally, park size, shape and vegetation density (NDVI) have a strong influence on local climate. Park cooling can reach distances of upto 240 m; cooling effect and differences greatest at mid-day which coincides with high solar radiation	(Feyisa, Dons and Meilby, 2014)
Seasonal variations	Mexico	SUHI was high at night and during the dry	(Cui and De

and drivers of SUHI and AUHI	City, Mexico {subtropical highland}	season; The day time SUHI was low throughout and sometimes exhibited a cool island effect, but was higher during the wet season. AUHI was similar to the night time SUHI and the day time AUHI was fairly constant throughout the entire year; day time SUHI was driven by Vegetation fraction. Night time SUHI was greatest on calm nights. Increased vegetation cover decreased both SUHI and AUHI	Foy, 2012)
		AUHI studies in ARID climates	
Spatio-temporal variation of the AUHI	Muscat, Oman {arid}	Strong UHI was observed during the night time and the summer (dry period); Urban density (or spare nature of the buildings) had a strong relationship with the UHI	(Charabi and Bakhit, 2011)
		SURFACE URBAN HEAT ISLAND (SUHI) STUDIES	
		SUHI studies in tropical savanna (wet and dry) climates	
Changes in SUHI with relation to changes in land use	Nakhon, Thailand {tropical savanna}	Areas of blue and green infrastructure experience increases in temperature over time highlighting a potential effect of local scale urban climate associated with urbanization	(Chotchaiwong and Wijitkosum, 2019)
Spatial and temporal (multiyear and between wet & dry season) variation of SUHI	San Salvador, El Salvador {tropical wet and dry}	The UHI effect increased with urban growth; UHI differed between the wet and the dry season and was related to the amount of vegetation cover.	(Acero and Gonzalez-Asensio, 2018)
Influence of differences in landcover on SUHI	Lagos, Nigeria {tropical savanna}	LST values highest during the dry season; Building density and vegetation cover are main drivers of LST differences	(Ayanlade, 2016)
Comparing the SUHI intensities of two tropical cities	Sao Paolo {humid subtropical} & Rio de Janerio {tropical savanna}	Vegetation cover explains the differences in the UHI intensities of the two cities	(Flores, Pereira Filho and Karam, 2016)
Temperature (SUHI) regulation with relation to urban morphology (i.e. local scale) and green infrastructure	Dares Salaam – Tanzania {tropical wet and dry} & Addis Ababa - Ethiopia {subtropical highland}	Proportion of manmade features (i.e. building mass) significantly raise LST. Presence of vegetation in informal settlements substantially lowers SUHI	(Cavan et al., 2014)
Changes in SUHI with relation to the extent of urbanization	Colombo, Sri Lanka {tropical	(1) Urban density showed a positive relationship with LST (2) Urbanised areas showed the highest increase in LST. Water	(Fonseka et al., 2019)

	monsoon}	and vegetation experienced smaller increases in temperature highlighting a potential local scale climate effect resulting from urbanization	
Multitemporal change in SUHI	Noida, India {tropical monsoon}	Impervious surface area was the main driver of increase in the UHI	(Kikon et al., 2016)
LST (SUHI) with relation to land cover	Colombo, Sri Lanka {tropical monsoon}	Paved surface that are made of asphalt (low albedo) contribute significantly to the UHI effect; Highly vegetated areas had lower surface temperature	(Senanayake, Welivitiya and Nadeeka, 2013)
Influence of impervious surface, water and vegetation on SUHI	Xiamen, China {monsoon al humid subtropical }	LST increased with increase in impervious surface area and declined with increase in vegetation and water; The influence of impervious surface on LST was six times greater than the influence of vegetation and water combined; 10% decrease in impervious surface area and 20 % increase in water or vegetation could decrease LST by up to 2.5 or 2.9 °C, respectively	(Xu, Lin and Tang, 2013)
		SUHI in humid subtropical climates	
Impact of urban growth and loss of vegetation cover on the Atmospheric Urban Heat Island (SUHI)	Brisbane, Australia {humid subtropical }	Increased temperature was linked with Increased urban density and vegetation loss. Vegetation cover had stronger impacts than building height and height/width ratio on temperatures. UHI effect was stronger at night and was seasonal	(Chapman et al., 2018)
Influence of different land cover types on SUHI	Lucknow, India {humid subtropical }	Densely built city centres experience high LST whereas low LST is associated with vegetation (NDVI) and water	(Singh, Kikon and Verma, 2017)
Influence of land cover (i.e. vegetation & impervious surfaces) on SUHI	Nanchang, China {humid subtropical }	Increase in pervious surface and decrease in vegetation cover result in increase in LST	(Zhang, Estoque and Murayama, 2017)
Seasonal influence of Impervious Surface Area (ISA) on SUHI	Chandigar h, India {humid subtropical }	Relationship between SUHI and %ISA changes between seasons. Stronger SUHI (effect of ISA) observed during the winter (drier period)	(Mathew, Khandelwal and Kaul, 2016)
Comparing the SUHI intensities of two tropical cities	Sao Paolo {humid subtropical } & Rio de Janerio {tropical savanna}	Vegetation cover explains the differences in the UHI intensities of the two cities	(Flores, Pereira Filho and Karam, 2016)
		SUHI studies in subtropical highland climates	
SUHI characterisation based on Land surface Temperature (LST) for different	Harare, Zimbabwe {subtropic al	Local Climate Zones (LCZs) representing high building density and low vegetation proportion had the highest LST; Sparsely built up vegetated areas were up to 1°C	(Mushore et al., 2019)

types of Local Climate Zones (LCZ)	highland}	cooler than the "hot" LCZ categories	
Influence of vegetation (species type and park structure) on SUHI and AUHI	Addis Ababa, Ethiopia {sub-tropical highland}	Vegetation cooling effect is dependent on canopy cover and species type; Equally, park size, shape and vegetation density (NDVI) have a strongly influence on local climate. Park cooling can reach distances of upto 240 m; cooling effect and differences greatest at mid-day which coincides with high solar radiation	(Feyisa, Dons and Meilby, 2014)
Temperature (SUHI) regulation with relation to urban morphology (i.e. local scale) and green infrastructure	Dares Salaam – Tanzania {tropical wet and dry} & Addis Ababa - Ethiopia {subtropical highland}	Proportion of manmade features (i.e. building mass) significantly raise LST. Presence of vegetation in informal settlements substantially lowers SUHI	(Cavan et al., 2014)
Seasonal variations and drivers of SUHI and AUHI	Mexico City, Mexico {subtropical highland}	SUHI was high at night and during the dry season; The day time SUHI was low throughout and sometimes exhibited a cool island effect, but was higher during the wet season. AUHI was similar to the night time SUHI and the day time AUHI was fairly constant throughout the entire year; day time SUHI was driven by Vegetation fraction. Night time SUHI was greatest on calm nights. Increased vegetation cover decreased both SUHI and AUHI	(Cui and De Foy, 2012)

2.1.4.3 **Urbanisation and urban climate in Africa**

The vast majority of recent tropical UHI studies emanate from Far East Asia, South Asia and South America with far fewer studies known in Africa (Giridharan and Emmanuel 2018). To estimate the proportion of urban heat island studies emanating from tropical Africa, we compared the results of different searches of the peer-reviewed literature in Web of Knowledge (http://www.webofknowledge.com) and Scopus databases. The search terms in the first search contained the keywords “urban heat island” and generated over 7032 documents for web of Knowledge and 7046 documents for Scopus. In the second search with the word “Africa” added to the search terms, Web of Knowledge and Scopus generated 44 (of 7032) and 47 (of 7046) documents respectively. This highlights the fact that Africa makes up as little as 1% of the known studies on UHI phenomena.

Africa is rapidly urbanising and its urban population is expected to grow three times and reach 1.26 billion by 2050 from current estimates of 400 million inhabitants (United Nations, 2014). Vegetation which is strongly depended upon for provision of urban ecosystem functions like mitigation of all year round urban excess heat (Haaland and van den Bosch, 2015; du Toit *et al.*, 2018; Lindley *et al.*, 2018) is being lost at very high rates (Yao *et al.*, 2019). However, there is a lack of sufficent knowledge about the urbanisation practices in Africa that crosscut densification and urban green space represenetd by a very low estimate of only 1 % of the known studies (Haaland and van den Bosch, 2015).

Urbanisation practices and urban morphology vary strongly across African cities (Cavan *et al.*, 2014; Pauleit *et al.*, 2015; Antos *et al.*, 2016; Taubenböck, Kraff and Wurm, 2018) and informal and polarised development is one of the many forms of urbanisation transpiring from rapid population growth (Pérez-Molina *et al.*, 2017; Lindley *et al.*, 2018). Although this form of urbanisation is known to increase the risk of exposure to UHI (Scott *et al.*, 2017), more emprical studies are needed that quantify the combined effect of both pervious and impervious man-made features on the spatial temporal patterns of urban climate. Furthermore, such studies ought to be undertaken in a wide range of tropical climate types.

A vast majority of urban climate studies in Africa and in the tropics in general have focussed on the urban heat island effect because of its role on public health and wellbeing (Heaviside, Macintyre and Vardoulakis, 2017). Much less attention has been given to other urban climatic parameters that are important for ecological processes like vegetation development that are depended upon for ecosystem functions. Vegetation development and growth phases are vital for provision of ecosystem services (Dj, 1996; Badeck *et al.*, 2004) and surface moisture and humidity are important indicators of vegetation development in the tropics (Archibald and Scholes, 2007; Jochner, Alves-Eigenheer, *et al.*, 2013; de Camargo *et al.*, 2018). The spatiotemporal patterns of surface moisture and humidity ought to be investigated with relation to urban surface and structural differences.

2.1.5 Urban dryness Island effect

The phenomenon that describes urban areas as having drier atmospheres than their less urbanised rural surrounding is commonly known as the "Urban Dryness Island (UDI)" effect (Hage 1975; Ackerman 1978). The UDI is derived by calculating the difference in humidity between urban and rural areas (Yang, Ren and Hou, 2017; Luo and Lau, 2019). Despite of the fact that humidity is an important meteorological variable for determining moisture and energy transfer in the atmosphere, it has generally been less studied than the UHI effect (Hao *et* al., 2018; Luo and Lau, 2019).

The UDI phenomena is attributed to early studies by Ackerman (1971) and Hage (1975) that observed a drier atmosphere (using relative and absolute humidity) in Chicago (a latitude city with a humid continental climate) relative to its less urbanised surrounding. Since then, there have been a number of studies that have observed the UDI effect in different climate types including (but not limited to): tropical wet and dry climate (Adebayo, 1991); subtropical highland climate (Jauregui, 1997); humid subtropical (Hass *et* al., 2016; Chhetri, Fujimori and Moriwaki, 2017; Yang, Ren and Hou, 2017); Monsoon subtropical (Hao *et* al., 2018; Luo and Lau, 2019). Adebayo (1991) assessed the day-time UDI effect using relative humidity and vapour pressure taken from urban and rural meteorological stations in the tropical savanna city of Ibadan. The UDI effect in Mexico city has been studied using observations of specific humidity in urban and rural areas (Jauregui and Tejeda, 1997). Yang, Ren and Hou, (2017) examined diurnal, annual and seasonal differences in relative humidity between urban and rural areas in Beijing. Hao *et al*. (2018) examined the temporal change in UDI intensity using relative humidity and vapour pressure deficit observation in urban and rural meteorological stations. Luo and Lau, (2019) quantified the UDI using a wide range of atmospheric humidity measures including: relative humidity atmospheric water vapour pressure, specific humidity.

The key drivers of the UDI intensity have been observed be the loss of vegetation through urbanisation and the UHI effect (Hao *et al*., 2018). The UHI effect increases Potential Evapotranspiration (Adebayo, 1991; Zipper *et* al., 2017; Luo and Lau, 2019), whereas impervious surfaces impede the capture and storage of water. Land cover differences between urban and rural areas influence moisture availability by impacting

on water infiltration, ground water recharge and evapotranspiration (Figure 2-10). The high presence of impermeable and paved surfaces in urban areas impedes ground water uptake, resulting in water losses through direct run-off (Barnes, Morgan and Roberge, 2001; Whitford, Ennos and Handley, 2001). Rates of infiltration have been observed to decline significantly even in low impact development areas (McGrane, 2016). In contrast, the surrounding rural areas that are highly vegetated and pervious enhance the capture and retention of rain water (Barnes, Morgan and Roberge, 2001; Whitford, Ennos and Handley, 2001).

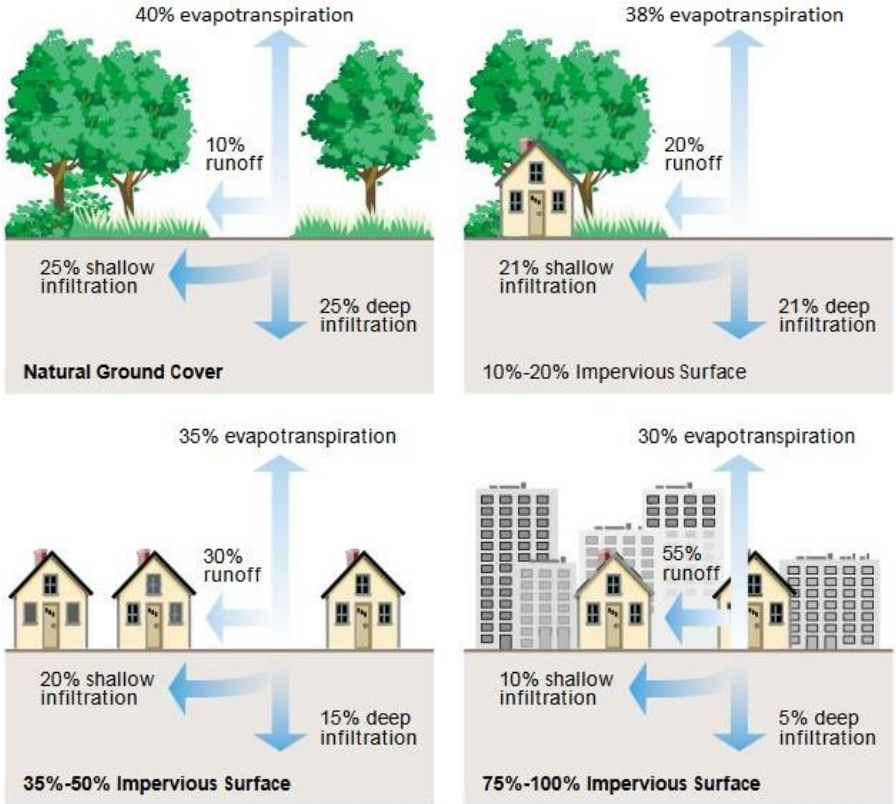

Figure 2-10 illustrating differences in water infiltration and evaporation with relation to proportion of impervious surfaces (Source: Federal Interagency Stream Restoration Working Group, 2001)

Traditionally, urban characteristics on hydrology have focussed on catchment scale dynamics with intent to derive changes to the quantity and quality of water (McGrane, 2016). However, flow pathways and rate of transformation of water during rain events is localised in relation to development types, neighbourhood characteristics and urban structure as demonstrated in Figure 2-10. Therefore dynamics of water availability in urban environments are increasingly accounting for local and microscale effects on the fate of rainfall (McGrane, 2016) and soil moisture (Wiesner, 2016). However, urban

soils can be highly variable within small spatial scales due to heterogeneity in cities with regards to differences in compaction and sealing of natural soils, importation and mixing a variety of synthetic material for construction (Wiesner, 2016). This makes it difficult to determine dynamics of water availability across urban landscapes. However, atmospheric humidity which depicts the exchange of water between the ground and atmosphere can be used for understanding moisture availability (Hao *et al*., 2018).

UDI intensities can be derived using various measures of atmospheric humidity including: relative humidity (Adebayo 1991; Hass 2016; Yang Ren and Hou, 2017; Hao *et al*., 2018; Luo and Lau, 2019); atmospheric vapour pressure (Adebayo, 1991; Hao *et al*., 2018), specific humidity (Jauregui and Tejeda 1997; Hao *et al*., 2018; Luo and Lau, 2019) and vapor pressure deficit (Hao *et al*., 2018; Luo and Lau, 2019). None of the measures of atmospheric humidity is functionally superior over the other (Hao *et al*., 2018). Moreover, different measures of atmospheric humidity have been observed to show similar patterns between. Adebayo (1991) observed that atmospheric vapour pressure and relative humidity were affected in a similar way by urbanisation. Luo and Lau, (2019) and Hao *et al*., (2018) observed a declining trend for relative humidity, specific humidity and an increase in vapor pressure deficit. This highlights the usefulness of using different measures of atmospheric humidity to advance our understanding of the much less studied concept of UDI intensity.

The use of relative humidity alone was previously critiqued by Adebayo (1991) because relative humidity is sensitive to temperature. However, recent studies (Yang, Ren and Hou, 2017; Hao *et al*., 2018) have shown that relative humidity is a reliable measure for estimating the UDI effect and that relative humidity is not affected by temperature alone. The other variables that are posited to play a critical role in relative humidity are moisture flux and evaporation. Hao *et al*. (2018) and Yang, Ren and Hou, (2017) identified differences in the temporal change between temperature and relative humidity, which resulted in weak and insignificant relationships between the two variables. Moreover, temperature and relative humidity have been observed to exert varying influences on the spatial patterns of tree leaf phenophase in tropical (Jochner *et al*., 2013) indicating inherent differences between the two variables.

As with the UHI, the intensity of the UDI effect undergoes temporal change (Hage 1975; Ackerman 1978). Yang Ren and Hou, (2017) observed stronger UDI effects in autumn and summer than in winter and spring in Beijing (humid continental climate). Contrary to this, Luo and Lau, (2019) observed stronger UHI intensities in spring and hot wet summers in the Yangtze River Delta Region (Monsoon subtropical). In the tropics, the intensity of the UDI was observed to be greatest during the dry season (Adebayo, 1991) in Ibadan, a city with a tropical wet and dry savanna. The wet-dry season dichotomy as the basis for quantifying seasonal changes in UDI intensity overlooks the gradual changes in water availability, potential evapotranspiration and evapotranspiration which are known to be affected by the UHI intensity (Zipper *et al*., 2017). The sensitivity of the UDI to UHI (Zipper *et* al., 2017; Luo and Lau, 2019) necessitates inclusion of factors that influence UHI intensity such as urban form (intra-urban urban climate variability), regional climate, and influence of scale discussed in section 2.1.2.1. Jochner *et* al., (2013) and Hass *et al*., (2017) observed that humidity differed in neighbourhoods of varying proportion of vegetation cover and impervious surfaces. However, intra-urban UDI intensity is still much less researched about and several recent studies use the urban rural dichotomy (e.g. Yang, Ren and Hou, 2017; Hao *et* al., 2018; Luo and Lau, 2019). Local and microscale neighbourhood characteristics (e.g. density of housing and vegetation cover) are a key factor that influence water availability (Figure 2-10) and future research ought to account for these differences in the characterisation of the UDI effect. Moreover, the combined effect of the factors determining urban climate makes each city unique in its own right in terms of urban climate (section 2.1.3) necessitating a wide range of empirical studies for the UDI phenomena.

2.2 Vegetation Phenology

The word Phenology comes from the Greek word 'phaino', that means to appear or to show, and vegetation phenology describes the study of repeated plant life cycle stages, their timing and the abiotic and biotic factors that trigger them (Fenner, 1998; Schwartz, 2003; Morisette *et al.*, 2009). Knowledge on tropical phenology is very limited and the number of studies and knowledge of phenological processes in tropical urban environments is strikingly limited in comparison to higher latitudes (Jochner and

Menzel, 2015). Therefore, an extensive review of background knowledge on tropical phenology and urban phenology in general is presented to establish the research context and significance of this study.

2.2.1 Quantifying vegetation phenology

Biological processes occur at a multitude of temporal and spatial scales (Suni *et al.*, 2015) which can be represented using the levels of biological organisation. The levels of biological organisation are a reductionist approach depicting the hierarchical structure of biological systems and the relationships between strata based on biologically relevant criteria like composition and scale (Brooks and Eronen, 2018). The levels of organisation include: atom, molecule, cell, tissue, organ, organism, group, population, community, ecosystem, landscape, and biosphere (Brooks and Eronen, 2018). In vegetation phenology studies, observation can be undertaken at different levels of organisation from individuals (e.g. flowers on a single plant) to the ecosystem levels. Each level has various selective forces and constraints (Rathcke and Lacey, 1985; Fenner, 1998; Hudson and Keatley, 2009; Shivanna and Tandon, 2014). Observations of the aggregate response of vegetation to their environmental conditions can be ideally done at the population level and above to understand ecosystem structure and function (Shivanna and Tandon, 2014).

Vegetation development varies across plant functional types (grasses versus trees, aquatic versus terrestrial) and regional climate (winter dormancy versus tropical dry seasons). As such vegetation phenology involves studying of separate life histories commonly known as phenoevents including: leafing, flowering, fruiting, seed dispersal and germination stages (Rathcke and Lacey, 1985; Fenner, 1998). Phenoevents follow a temporal pattern that is quantified using several parameters as summarised in Table 2-3.

Table 2-3 summarises some of the phenology parameters that are recorded for given phenoevents (Fenner, 1998)

Parameter	Description
Frequency	Usually measured on an annual scale (i.e. number of times each year)
Timing	Start date of the earliest individuals, date of peak activity (mid) and end date (last sightings)

Duration	Time lapse between the start and end date
Magnitude	Mean, variability and intensity (amplitude)
Degree of synchrony	Within and between species

The study of vegetation phenology traditionally involves visually observing the structural aspects of vegetation development of individuals or populations for given species (Fenner, 1998; Rathcke and Lacey, 1985). On the other hand, functional aspects relating to the properties of vegetated surfaces (vegetation greenness activity) can be derived from satellite imagery to represent phenology of the landscape and ecosystems as a whole (Liang and Schwartz, 2009; Morisette *et al.*, 2009; Reed, Schwartz and Xiao, 2009; Hanes, Liang and Morisette, 2014). Phenology at the landscape level is inherently different form phenology at the species level (Badeck *et al.*, 2004; Liang and Schwartz, 2009) and both approaches corroborate each other in the understanding of phenological processes.

2.2.2 Remote sensing phenology

Vegetated surfaces contain chlorophyll pigment which reflects Near-infrared and green light, while absorbing parts of the visible light spectrum (blue and red). Vegetation chlorophyll content influences photosynthetic activity and determines the proportion of incoming electromagnetic radiation coming from the sun that is absorbed, transmitted or reflected and detected by optical satellite sensors (Morisette *et al.*, 2009; Reed, Schwartz and Xiao, 2009; Hanes, Liang and Morisette, 2014). Vegetation Indices (e.g. Normalised Difference Vegetation Index and Enhanced Vegetation Index) connoting canopy "greenness," the combined property of leaf chlorophyll content, leaf area, canopy cover and structure are computed from remote sensors (Huete *et al.*, 2011) and their temporal changes (Figure 2-11) used as the basis for landscape phenology (Morisette *et al.*, 2009; Reed, Schwartz and Xiao, 2009; Hanes, Liang and Morisette, 2014). Vegetation temporal or seasonal changes involves growth, establishment and senescence of leaves with each change altering photosynthetic activity. Landscape phenological metrics (Table 2-4) can be derived using time series of vegetation reflectance to depict these changes in vegetation (Eklundh and Jönsson, 2015, 2016).

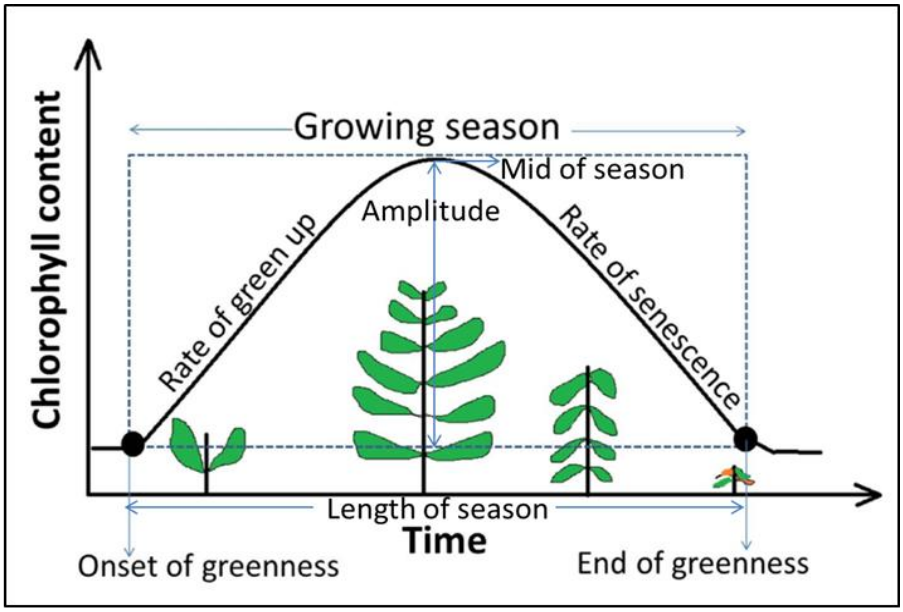

Figure 2-11 Temporal changes in vegetation within a given growing season from a remote sensing perspective (Adapted from: Eklundh and Jönsson, 2015, 2016)

Table 2-4 Landscape phenological metrics derived from remote sensing (Source: Eklundh and Jönsson, 2015, 2016)

Phenology metric	Definition and ecological meaning
Start of Season	Timing (Day of year) of the start of the growing season denoting increment in photosynthetic activity
End of Season	Timing (Day of year) of end of the growing season following a decline in photosynthetic activity
Mid/Peak of season	Timing (Day of year) of peak photosynthetic activity/primary production
Season length	Duration of the growing season (difference between the start and the end of the vegetation growing season)
Amplitude	The change in photosynthetic activity across the growing season and represents the strength of the seasonality (i.e. primary production)
Green-up rate	Represents the rate of increase of leaf flush events
Senescence rate	Denotes the rate of increase of senescence events
Integral over the growing season	Cumulative primary production across the growing season

Although both visual and satellite remote sensing phenology methods are related with biological phenomena, the two approaches are inherently different (Badeck *et al.*, 2004; Morisette *et al.*, 2009; Hanes, Liang and Morisette, 2014; Jochner and Menzel, 2015) and a summary of these differences is presented in Table 2-5. Near surface

remote sensing phenology through the deployment of optical and radiometric sensors above the ground (50 m or less) to quantify changes in the land surface (Richardson, Klosterman and Toomey, 2013; Brown *et al.*, 2016; Alberton *et al.*, 2017) is a novel and promising technique that bridges the understanding between direct visual observations (organism scale) and satellite based phenology (landscape scale) approaches. Near surface remote sensing characterises landscape phenology in a way similar to satellite remote sensors, but at higher spatial and temporal resolution. Although near surface remote sensing has advantages that overcome some of the challenges associated with visual observations (e.g. observer error) and satellite remote sensing, near-surface remote sensing is not without flaws (Table 2-5). Each phenological method has unique attributes that overcome the challenges of another and neither method can wholly override another. This highlights the need for integrated approaches that draw on a combination of methods as a number of studies have shown (e.g. Reed, Schwartz and Xiao, 2009; Liang, Schwartz and Fei, 2011; Hufkens *et al.*, 2012; Jochner and Menzel, 2015; Donnelly and Yu, 2017; Lim *et al.*, 2018; Richardson *et al.*, 2018). The use of combined approaches corroborates an understanding of phenological processes at multiple spatial and temporal scales.

Table 2-5 showing the merits and demerits for different methods for undertaking landscape phenology observations (source: Schwartz, 2003)

	Pros	Cons
Ground Observations	-Enables observation of individual plants and species -Wide range of pheno-phases (e.g. flowering, budburst) can be observed	-Spatial coverage is limited -Temporal resolution often too low and inadequate (weekly) -Observer bias (subjectivity) necessitating the use of a few observer
Remote Sensing	-Measures seasonal greening -Provides spatial integration represented as pixel level data -Large area coverage	-Limited to studying landscape processes -Cloud cover -Possibility of errors in atmospheric correction

Near Surface Remote Sensing	-Allows for quantification of both seasonal greening and specific phenophases -Both spatial integration (pixel data) and specific phenophases of -High temporal coverage -Possibly for both spatial integration and individual observation -Properties of canopy structure (Leaf Area Index) and function (photosynthetic activity) can be separated	-Instrument fragility -Requires specific infrastructure for data management (internet connectivity, data logging equipment and mounting structure like masts) -Limited spatial coverage -Standards for data collection are generally lacking

2.2.3 Drivers of vegetation phenology

An understanding of the main factors driving vegetation phenology is critical for design of phenological studies.

2.2.3.1 **Primary drivers**

The primary drivers of phenology are the natural environmental triggers that determine critical events like the start and end of season. They are categorised into: internal factors which represent the intrinsic attributes of individual plants; and external environmental factors whose effects cuts across all levels of biological organisation (i.e. from organism to biosphere). The main intrinsic properties include: genetic composition, age and species (Schaber and Badeck, 2003; John King, 2011). On the other hand, external factors include variability in abiotic factors that control photosynthetic activity (i.e. light, temperature, soil moisture and nutrients) and biotic factors such as pollinator activity, pathogens and herbivore activity (Rathcke and Lacey, 1985; van Schaik, Terborgh and Wright, 1993; Fenner, 1998). Biotic, abiotic and intrinsic factors might act alone or in combination to influence phenology (Neil and Wu, 2006). Abiotic factors vary geographically largely due to differences in insolation, resulting in regional climatic and biome type differences, which in turn result in geographical differences in phenology (Rathcke and Lacey, 1985; Zhang, Friedl and Schaaf, 2006; J King, 2011).

In temperate and boreal regions where insolation varies strongly across a given year, vegetation phenology is primarily determined by temperature (White, Thornton and

Running, 1997; Menzel *et al.*, 2006; Zhang, Friedl and Schaaf, 2006; Clinton *et al.*, 2014) and photoperiod (Schwartz, 1998; Zhang, Friedl, Schaaf and Strahler, 2004). In the tropics, temperature is fairly stable all year round and the temporal changes in water/rainfall and irradiance are the key drivers of phenological changes for seasonally dry and aseasonal (water is abundant; evergreen vegetation type) biomes respectively (van Schaik, Terborgh and Wright, 1993; Fenner, 1998; Borchert, Rivera and Hagnauer, 2002; Zhang *et al.*, 2005; Zhang, Friedl and Schaaf, 2006; Guan *et al.*, 2013; Clinton *et al.*, 2014; Guan *et al.*, 2014; Abernethy *et al.*, 2018).

2.2.3.2 **Secondary drivers**

Other than the natural primary drivers that initiate vegetation growth, secondary drivers could influence phenology as limiting factors or environmental stressors. In temperate regions, variability in rainfall, humidity, land cover are among the factors that influence phenology (Menzel and Fabian, 1999; Primack *et al.*, 2004). This knowledge comes as a result of long term monitoring. Compared to temperate regions which have records that date back as far as three centuries ago, phenology in the tropics is only as recent as the 1950s (Abernethy *et al.*, 2018). A large proportion of the first tropical phenology studies focused on descriptive work of early naturalists and the reproductive phenological characteristics (i.e. flowering and fruiting) of specific food plants for wildlife (Borchert, 1983). These efforts overlooked the wider diversity of tropical vegetation and phenoevents (Abernethy *et al.*, 2018). Reforms in tropical phenology in the 1990s towards understanding the environmental context and physiology of vegetation has led to an increase in number of tropical phenological studies (Abernethy *et al.*, 2018). However, a vast number of empirical studies on sensitivity of phenology to different abiotic condition are still needed to narrow the knowledge gap of phenology between the tropics and higher latitudes. Moreovoer, this would involve undertaking studies over a wide range of tropical regions and biomes including those located in Africa that remain largely under-researched (IPCC, 2014; Fitchett, Grab and Thompson, 2015; Adole, Dash and Atkinson, 2016; Abernethy *et al.*, 2018).

2.2.3.3 **Effects of temperaure on tropical phenology**

Although phenology is considered to be less sensitive to temperature in the tropics than temperate regions (Zhang *et al.*, 2005; Zhang, Friedl and Schaaf, 2006), predicted increases in temperature due to climate changes make relevant the need for understanding the influence of temperature variability on phenology in the tropics. Given the limited knowledge on temperature-phenology interactions in the tropics, phenological parameters like producition, magnitude and intensity (Fenner, 1998) can be exploited in addition to timing of phenoevents to understand how tropical phenology might be influenced by temperature. This is relevant because vegetation phenology and productivity are mutually constitutive of one another (Asner, Townsend and Braswell, 2000; Yan *et al.*, 2019), in a way that the productivity in a given growing season affects the phenology in the season that comes after (Singh and Kushwaha, 2016).

Optimal temperature is essential for vegetation productivity (Hatfield and Prueger, 2015; Gray and Brady, 2016) and agriculture in tropical regions (Brown, de Beurs and Vrieling, 2010). Temperature has been observed to stress and limit vegetation growth and development in tropics (Workie and Debella, 2018). Experimental manipulations of temperature to sub-optimal levels decreases leaf and canopy gaseous exchange (Doughty and Goulden, 2008) and reduces maximum net photosynthesis (Cunningham and Read, 2002) in climax forest species (Cheesman and Winter, 2013b) and montane plant species (Varhammar *et al.*, 2015) in the tropics. In other experiments, however, increased temperature generally favours growth of pioneer tropical tree species (e.g. *Ficus insipida*, *Ormosia macrocalyx*) (Cheesman and Winter, 2013b). Additionally, elevated night time temperature results in up to a 2-fold biomass accumulation of some tropical tree species' seedlings (Cheesman and Winter, 2013a). This highlights the importance of temperature-dependent night-time processes that are different from photosynthesis directed growth (Cheesman and Winter, 2013a). However, comparisons between experimental warming studies and empirical phenology studies in temperate regions have shown that warming experiments underpredict plant phenological responses to climate change (Wolkovich *et al.*, 2012). Therefore, experimental studies cannot be the sole basis for grasping the impacts of temperature

and climate variability on tropical phenology. This shows a need for empirical field studies on these phenomena in tropical biomes.

2.3 Phenology in urban environments

Phenology is widely considered to be a crucial indicator of environmental change with a wide range of applications for environmental monitoring. These include: monitoring terrestrial responses to climate variation (Schwartz, 1998, 2002; Menzel and Fabian, 1999; Neil and Wu, 2006; Abernethy *et al.*, 2018), assessing variability in terrestrial productivity (Dj, 1996; Badeck *et al.*, 2004); analysing surface and boundary layer climate processes (White *et al.*, 2002); and evaluating the effects of land-use change (e.g. urbanisation) (Zhang, Friedl, Schaaf, Strahler, *et al.*, 2004). Of critical importance for global sustainability is the ability to track the ecological impacts of climate change using phenology, as noted in the IPCC Fourth Assessment Report (Rosenzweig *et al.*, 2007). An understanding of the influence of climate change induced temperature changes on phenology could be acquired using "Space-for-Time" (SFT) (Jochner and Menzel, 2015). This is because SFT assumes that the influence of a given climatic variable on biological processes is comparable between space and time if the continuum of the climate variable of interest is the same across space and time.

Cities are microcosms of the atmospheric changes expected to occur at a global level including climate change-induced increases in temperature and can therefore be used as proxies to investigate the ecological impacts of climate variability (McDonnell and Pickett, 1990; Neil and Wu, 2006; Grimm *et al.*, 2008; Youngstead *et* al., 2015; McPhearson *et al.*, 2016; Kabisch *et al.*, 2017). Moreover phenological studies in cities enable quantification of the effects of urban climate variability (specifically UHI) on phenology (Neil and Wu, 2006; Buyantuyev *et al.*, 2012; Jochner and Menzel, 2015).

Cities in temperate climates experience earlier start of the vegetation growing season and longer durations of the vegetation growing season in comparison to their neighbouring rural surrounding due to the UHI effect (e.g. Neil and Wu, 2006; Jochner and Menzel, 2015). Moreover, the UHI effect has been observed to have a varying impact on species (Jochner and Menzel, 2015). The UHI effect provides optimal temperature conditions for vegetation growth after wintertime dormancy. Also,

vegetation phenology has been observed to be sensitive to local environmental settings such as land cover and urban form that drive the UHI effect (Jochner *et al.*, 2012; Jochner, Alves-Eigenheer, *et al.*, 2013; Zhang *et al.*, 2014; Melaas *et al.*, 2016; Zipper *et al.*, 2016).

Other than the UHI effect, the importance of other abiotic factors (e.g. soil moisture) is increasingly being acknowledged in temperate settings (e.g. Neil and Wu, 2006; Jochner *et al.*, 2011; Buyantuyev and Wu, 2012; Jochner and Menzel, 2015; Walker, de Beurs and Henebry, 2015). However, the influence of the UDI effect and surface moisture on urban phenological processes remains far less studied than the UHI effect.

Traditionally, quantification of the impacts of urbanisation and the UHI effect involved comparing phenological processes between urban and rural areas (e.g. Roetzer *et al.*, 2000; White *et al.*, 2002; Zhang, Friedl, Schaaf, Strahler, *et al.*, 2004; Gazal *et al.*, 2008; Jochner *et al.*, 2011). However, heterogeneity of urban form and structure within cities and along the urban-rural urbanisation intensity gradient creates a myriad of spatially varying ecological forcing functions (e.g. climatic elements of relative humidity and temperature) and processes within cities (McDonnell and Pickett, 1990) which influence phenology on a local scale (Jochner, Alves-Eigenheer, *et al.*, 2013).

2.3.1 Phenology in tropical urban environments

In tropical climates where temperatures are warm all year round, and soil moisture is the primary factor driving vegetation activity, (Borchert, 1983; Clinton *et al.*, 2014; de Camargo *et al.*, 2018), far fewer urban phenological studies have been carried out. The few phenological studies undertaken to date in tropical cities (e.g. Gazal *et al.*, 2008; Jochner, Alves-Eigenheer, *et al.*, 2013) have assessed the effect of the UHI in comparison to temperate cities and found that the effect of UHI on timing of start of the growing season (bud burst) in tropical cities was weaker than in temperate cities. This could be because of milder seasonal temperature changes in the tropics as compared to temperate regions.

Gazal *et al*., (2008), observed that some of tropical cities in their study showed patterns opposite to the temperate classic paradigm of earlier start of season. In this study, temperature data was derived from a single point in time which might not have

been representative of the spatiotemporal differences in temperature as has been about the seasonality of UHI intensity (Roth, 2007). Moreover individual aspects of land cover such as fractional vegetation cover and impervious surface areas as opposed to land cover composition wholly were the basis for examining the influence of urbanisation on phenology. Land cover composition is increasingly being given precedence over individual components of land cover to understand urban climate spatial variability (Stewart and Oke, 2012) and a similar approach ought to be adopted for phenology. Gazal *et al*., (2008) postulated that the observed phenological differences in tropical cities might have been as a result of Vapour Pressure Deficit that has a direct relationship with relative humidity and soil moisture, highlighting the importance of the urban dryness island effect whose effect on tropical urban phenology remains much less studied. Jochner *et al*., (2013) established that relative humidity had a relationship with the leaf unfolding of *Tabebuia chrysotrich* and leaf phenophase of *Tipuana tipu* was sensitive to the UHI effect. These two studies covered a few select species, highlighting the need for other exemplary studies that assess the phenological responses of other tropical trees.

2.3.1.1 **Canopy phenology in tropical urban environments**

The existing literature on tropical urban phenology has almost exclusively focused on the timing of the start of the growing season (e.g. Gazal *et al.*, 2008; Jochner, Alves-Eigenheer, *et al.*, 2013), yet other phenological parameters like the magnitude, intensity and duration (Fenner, 1998; Denny *et al.*, 2014) remain unexplored. There is an established body of literature showing that decrease in moisture and increase in temperature during the dry season drives leaf loss and the extent of canopy cover change varies between species (e.g. Williams *et al.*, 1997; Condit *et al.*, 2000; Valdez-Hernandez *et al.*, 2010; Dalmolin *et al.*, 2015; de Camargo *et al.*, 2018). The study of canopy phenology is increasingly useful for understanding the ecological impacts of climate change (Singh and Kushwaha, 2016; Abernethy *et al.*, 2018) yet it remains much less studied in urban environments.

In tropical cities, trees might experience heavier losses of leaves than they normally would due to the UDI and UHI effect. The significance of this is that heavy loss of leaves in a given period might affect the productivity of vegetation in successive

growing seasons with implications for the provision of regulatory functions (Singh and Kushwaha, 2016) and the extent of shading offered from tree stands in cities.

2.3.1.2 **Landscape phenological processes in tropical urban environments**

Satellite-based remote sensing phenology as a proxy for leaf phenology is increasingly being adopted to understand the drivers and responses of climate variability (Abernethy *et al.*, 2018). Multiple studies have been undertaken in temperate cities (White *et al.*, 2002; Zhang, Friedl, Schaaf, Strahler, *et al.*, 2004; Han and Xu, 2013; Dallimer *et al.*, 2016; Zhou *et al.*, 2016; Zipper *et al.*, 2016; Melaas *et al.*, 2016; Gervais, Buyantuev and Gao, 2017; Li *et al.*, 2017; Qiu, Song and Li, 2017; Yao *et al.*, 2017; Parece and Campbell, 2018; Ren *et al.*, 2018) and shown that the UHI effect creates optimal conditions for vegetation growth resulting in longer vegetation growing seasons in urban than rural areas. Furthermore, the length of the vegetation growing season was observed to be highly localised within cities due to differences in land cover composition (Melaas *et al.*, 2016; Zipper *et al.*, 2016; Parece and Campbell, 2018). Green spaces within cities exhibited season lengths similar to rural areas due to comparably similar cool temperatures (Melaas *et al.*, 2016; Zipper *et al.*, 2016). Equivalent understanding of the effect of differences in urban form and the urban climate effect along the urban-rural gradient (McDonnell and Pickett, 1990) on phenology in tropical cities is lacking. This is intimately tied to the notion of a lack of phenological studies on the leafing characteristics of trees (i.e. duration and magnitude) in tropical cities. Landscape phenology through remote sensing is inherently different from visual observations (Badeck *et al.*, 2004), necessitating studying canopy changes at both species and landscape level in tropical urban environments.

2.3.2 Conclusion

2.3.2.1 **Knowledge gaps**

The flow and exchange of energy and materials such as trace gases, nutrients and water between vegetation and the surrounding environment is bidirectional and varies at different spatial and temporal scales (Field *et* al., 2007; Hungate and Koch, 2015; Suni *et al*., 2015). The continual feedback loop of materials and energy exchange between vegetation and its environment demonstrates that vegetation and its

surrounding are mutually constitutive of one-another and need to be understood together.

Urbanisation is a form of extreme land cover and land use change that alters the flow of energy and materials leading to a unique urban climate. Phenology in cities has been used to gain an understanding of how vegetation growth and development might be affected by variability in urban. However, this research is strikingly lacking in the tropical context. Also, although phenology to a large extent is used to preview the effects of environmental change on vegetation, the extent of vegetation feedback into the climate system would be influenced by phenology. Assessment of phenology in tropical cities at different temporal and spatial scales could therefore benefit the understanding of the relatedness of spatial and temporal variability of phenology and ecosystem services in tropical cities.

A vast majority of urban climate studies have emerged from Asian countries, which do not reflect the inherent physical nature and regional climate of African cities. Therefore, in addition to there being a need for more tropical urban climatic studies in Africa, is the need for urban phenology in Africa and the tropics at large. These studies ought to be undertaken at a variety of spatial and temporal scales including phenology at the landscape and species. Also, the wide range of phenology parameters (e.g. intensity and magnitude) spanning the vegetation growing season should be exploited in addition to the timing of pheno-events. This would benefit the understanding of the influence of secondary drivers and stressors in addition to the established primary drivers of phenology that initiate the start of the growing season. As such the influence of a wide range of spatially varying climate variables (e.g. surface moisture and relative humidity) on phenology can be evaluated.

2.3.2.2 **Research questions**

In view of the knowledge gaps identified from this literature review, three main research questions (Table 2-6) emerge, forming the foundation of this thesis. The literature review also considers the geographic representativeness of the existing tropical urban ecology studies to identify sub-Saharan Africa as a suitable location to empirically test specific hypotheses (Table 2-6).

Table 2-6 summarising the knowledge gaps identified from the literature review and the and specific hypotheses that this study aims to investigate

Research questions	Specific hypotheses
Temperature in tropical moist climate types is above the minimum requirement for plant physiologic activity. Therefore would we expect the UHI to act as a limiting factor (stressor) for the vegetation growing season length?	The magnitude of surface temperature between the most-built up and least built-up urban form types differs across years due to inter-annual climatic differences
	Heavily/intensively built-up locations and locations closest to the city centre exhibit shorter vegetation growing seasons
	Spatial and temporal differences in surface temperature influence the growing season length such that, increased surface temperature shortens the vegetation growing season
What is the combined effect of changes in surface moisture, surface structure and cover on urban climate (i.e. UHI and UDI)?	The magnitude of spatial variability in urban climate is dependent on surface moisture and will increase with the advancement of the dry season
	The influence of specific types of land cover (e.g. proportion of tree cover) on UDI and UHI changes between the wet and the dry season
How do intra-urban differences in surface cover and structure and urban climate influence the canopy phenology of tropical trees?	Trees in heavily built up neighbourhoods would experience higher rates of decline in canopy cover in comparison to less built neighbourhoods
	Differences in tree canopy cover change between heavily and lightly built neighbourhoods differ between tree species
	Leaf production and leaf loss are accounted for by differences in land cover and urban climate

CHAPTER 3. **METHODOLOGY**

This chapter provides a description of the study area and the methods used in this study. This chapter is structured around the empirical approaches used in the current study to quantify urban climate and its impact on vegetation phenology at the landscape (influence of local scale climate), and the tree species levels (influence of microscale climate). The methodology for investigating the spatiotemporal dynamics of urban climate during the wet-dry season is covered under phenological processes of individual trees (3.3). Further details about the methods for each one of the three research aims (1.4) are included in the methodology section of the research results under Chapters four, five and six.

3.1 Study area

Single city studies have successfully been used to investigate phenological processes at the landscape scale (e.g. Melaas *et al.*, 2016; Zipper *et al.*, 2016, 2017; Gervais, Buyantuev and Gao, 2017; Parece and Campbell, 2018) and for individual tree species (e.g. Ziska *et al.*, 2003; Lu *et al.*, 2006; Mimet *et al.*, 2009; Neil, Landrum and Wu, 2010; Jochner, Caffarra and Menzel, 2013). Therefore, a single tropical case study city was deemed feasible for investigating the influence of urban climate on vegetation phenological processes at both landscape and species levels.

3.1.1 Criteria for Choice of study area

To identify a city where the study would be carried out, profiles of different cities were accessed using searches on the internet and each city's physical characteristics explored using Google Earth. The search was constrained to African cities, because of their limited coverage in the body of literature on tropical urban ecology. The first criterion was the size and population of given city highlighting a substantially large city with a wide range of urban form from heavily built to unbuilt (highly vegetated) locations. This would enable sampling to be carried on urban climate and phenological processes across a wide range of neighbourhoods of varying urban form. The second criterion was geographical location within the tropical belt (within 23.5 °N and 23.5° S) and with a "moist" tropical climate type as there are fewer tropical than subtropical

urban climate studies. Cities in arid regions and highland areas (i.e. subtropical highland climate) were subsequently dropped from the selection. The third criterion was ease of organising logistics for undertaking the fieldwork. Existing prior knowledge of the city and ease of establishing networks for data collection were criteria that were highly prioritised given the time constraints of a PhD project. Kampala emerged top of the list because of its large city size, wide range of urban form types and tropical rainforest climate for which too few urban climate studies are documented.

3.1.2 Description of study area

Kampala is the capital city and largest city of Uganda and is located at 00°18'49"N 32°34'52"E. (i.e. less than 0.5° north of the equator; Figure 3-2) with an altitude of roughly 1200 m.a.s.l. Kampala has an area of about 181 Km^2, and a population of over 1.65 million inhabitants (i.e. population density approximately 9000 inhabitants/km^2; from Brinkhoff (2019, http://www.citypopulation.de/).

Kampala is rapidly urbanising each year (Bidandi and Williams, 2017 and references therein) and the city has expanded beyond the central city boundary to incorporate former satellite towns and surrounding rural areas (Vermeiren *et al.*, 2012). The rapid horizontal growth of the city has created an urban surface covering more than 800 km^2 referred to as the Kampala greater metropolitan area (Vermeiren *et al.*, 2012). Like several other cities in sub-Saharan Africa, the urban planning institutions have been unable to cope with the rapidly growing urban population resulting in polarised urban growth and informal development (Bidandi and Williams, 2017; Pérez-Molina *et al.*, 2017) as can be seen by irregular patches of heavily built-up urban areas in Figure 3-2.

Kampala has a tropical rainforest equatorial climate (*Af*) according to the Köppen climate classification, characterised by two rain seasons (March-May and September-November) and annual precipitation of about 1,200 mm based on a thirty years climatic record (data source: WMO, 2016). The March to May rain season is shorter but more intense than the September to November rain season (Figure 3-1). The heaviest rains are typically in April (~169 mm), whereas July represents the driest (roughly 63 mm) month of the year. July is the coolest month of the year, whereas February represents the warmest month. However, the weather conditions have

changed over recent years, characterised by increased temperature and irregular rainfall patterns (Sabiiti *et al.*, 2014; Mubiru *et al.*, 2018).

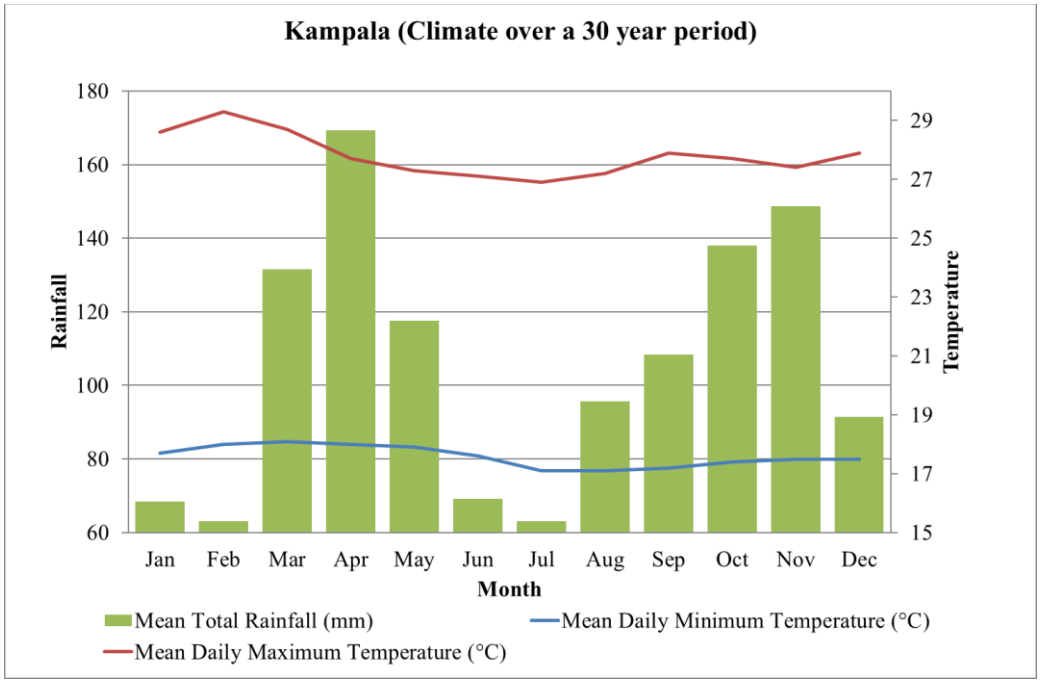

Figure 3-1: shows climate records of Kampala over a period of 30 years (adapted from: WMO, 2016)

Kampala is bordered by Lake Victoria to the south and has an extensive network of wetlands draining into the lake (Figure 3-2). The city lies in the 'forests of the Lake Victoria belt' characterised by short grasses at hilltops, elephant grass thickets with mixed cultivation at the hillsides and forests and swamps in the valleys (FAO, 1981). Under these regimes, climax forests are dominated by the genera *Celtis*, *Chrysophyllum*, *Aningera*, *Piptadenniastrum*, while the succession forests are characterised by the genera *Albizia*, *Antiaris*, *Blighia*, *Canarium schweinfurthii*, *Celtis*, *Entandophragma*, *Fagara*, *Lovoa*, *Majidea* and *Pycanthus*. The understorey of these forest habitats is dominated by the genera *Trichilia*, *Teclea*, *Lycnodiscus*, *Lasiodiscus* and *Acalypha* (FAO, 1981).

A significant proportion of the city's wetland and green areas have been replaced by built-up areas (Schuyt, 2005; Vermeiren *et al.*, 2012, 2013) and indigenous trees species replaced by exotic fast-growing tree species for ornamental purposes or source of fruit. According to an unpublished survey conducted by the Kampala Capital City Authority (KCCA) in 2015, 8 of 9 of the most common species in the central business district (CBD) of Kampala were exotic.

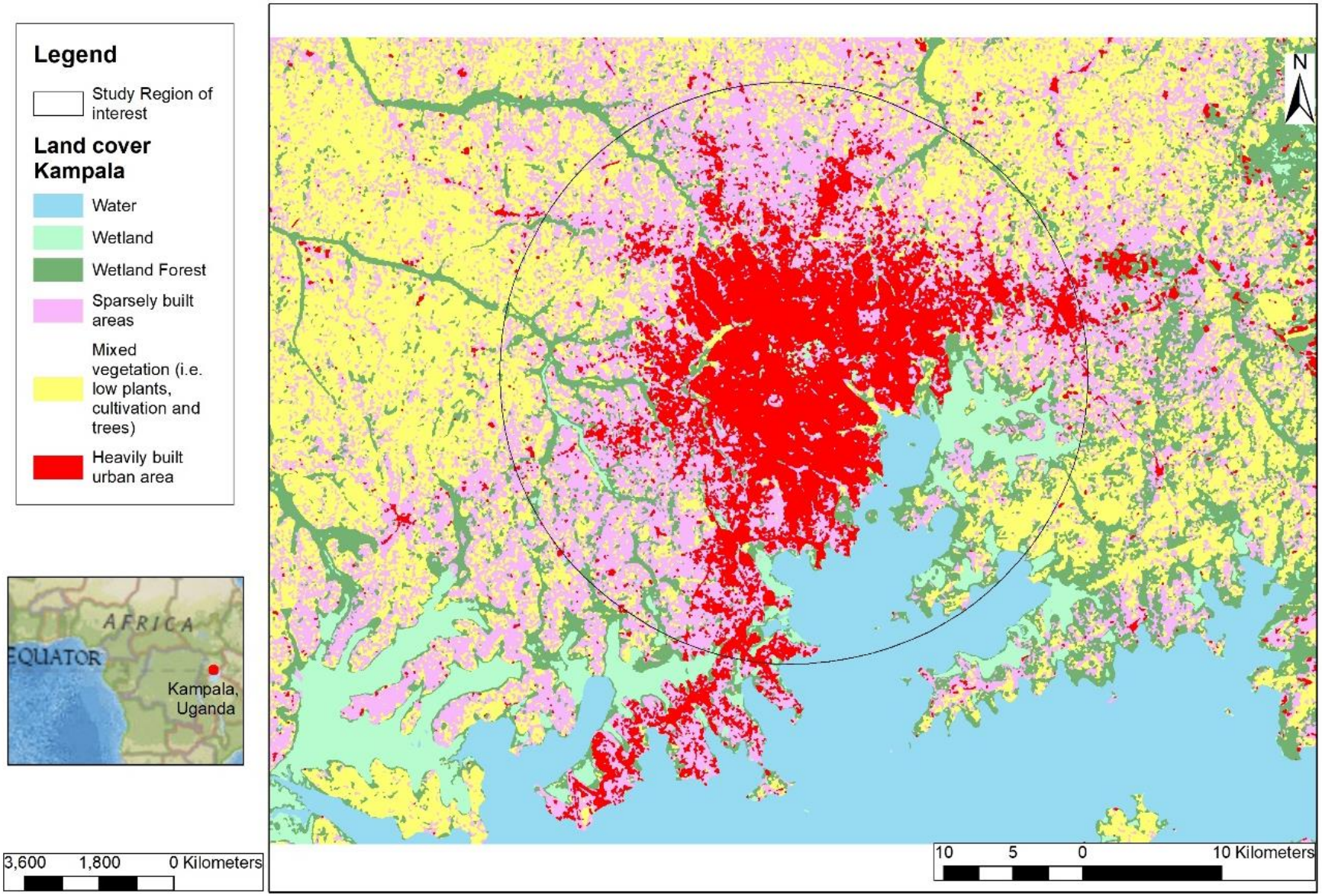

Figure 3-2: Land use and land cover types in Kampala (30 m spatial resolution)

3.2 Local scale climate and landscape phenological processes

This section describes the methods that were used for acquiring and processing data to link landscape phenological processes to local climate. Urban form and function are critical for understanding how local climate impacts on landscape phenology (see section 2.1.1) and an ideal approach for urban form characterisation will concede that urban features have a combined effect on climate within a given space (see section 2.1.2.3). Tied to the notion of urban form is the fact that the effect of diminishing development along the urban-rural gradient on urban climate and ecological processes decays with increased in distance from the CBD (see 2.1.2.3). As such urban form and distance from the CBD are combined as factors that would drive climate and phenology.

3.2.1 Urban form characterisation

Urban form within Kampala was mapped using the Local Climate Zone (LCZ) classification scheme (Stewart and Oke, 2012) as shown in Figure 3-5. The local climate zone (LCZ) scheme enables universal characterisation of cities (Stewart and Oke, 2012) with extensive usage and validation in the discipline of urban climate (Fenner *et al.*, 2014; Ketterer and Matzarakis, 2015; Demuzere *et al.*, 2017; Kotharkar and Bagade, 2018; Perera and Emmanuel, 2018; Brousse *et al.*, 2019; Mushore *et al.*, 2019). Local climate zones represent areas of homogenous land cover composition and climate (minimum area of radius = 200 m). The LCZ scheme has a number of positive attributes including: [1] a wide range of LCZ classes (i.e. up to 17 classes; Figure 3-4) that exemplify the continuum of differences in surface cover and structure from urban to rural areas of most cities in the world (Stewart and Oke, 2012); [2] provision for combining classes or creating new classes (Kotharkar and Bagade, 2018; Brousse *et al.*, 2019); [3] ease of systematic and objective creation of maps covering entire cities and their neighbouring rural areas through the World Urban Database and Access Portals Tools (WUDAPT) (Bechtel *et al.*, 2015, 2019). Therefore, the LCZ scheme is increasingly being integrated in the discipline of urban climatology (Stewart, Oke and Krayenhoff, 2014; Geletič, Lehnert and Dobrovolný, 2016; Kotharkar and Bagade, 2018; Mushore *et al.*, 2019) and the wider field of urban ecology (Perera and Emmanuel, 2018; Verdonck *et al.*, 2018; Brousse *et al.*, 2019; Franco *et al.*, 2019).

The WUDAPT protocol and workflow that classifies local climate zones at a city scale (Figure 3-3) using LANDSAT 8 OLI-TIRS remotely sensed satellite imagery (Bechtel *et al.*, 2015, 2019) was used for generating a map of Kampala's LCZs. This was achieved in a 3-step process involving: (i) acquisition and preprocessing of cloud-free LANDSAT 8 images, (ii) generation of training areas in google earth (iii) classification using supervised machine learning in System for Automated Geoscientific Analysis (SAGA)-GIS (Conrad *et al.*, 2015).

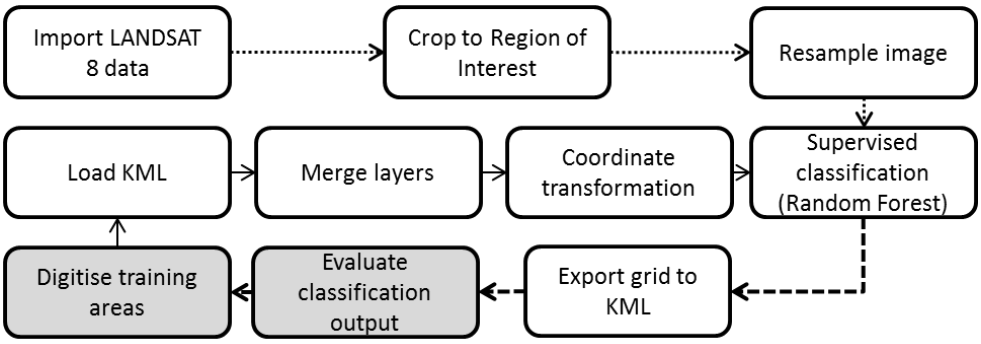

Figure 3-3 showing a workflow for LCZ classification using SAGA-GIS and Google Earth (grey fill polygons) (Adapted from: Bechtel *et al.*, 2019)

Selection of multiple satellite images taken on different dates for the LCZ classification is recommended in order to account for the spectral changes resulting from seasonal changes in vegetation cover (Cai *et al*., 2018; Bechtel *et al*., 2019). However, only two LANDSAT8 OLI-TIRS scenes (taken on 27/02/2015 and 15/03/2015) were available for the classification and were downloaded from the US Geological Survey Earth Explorer (USGS, 2016). Radiometric calibration of the images to Top of Atmosphere Reflectance alone is sufficient for LCZ mapping (Bechtel *et al.*, 2015) and was performed in ENVI5.4. Nine of the 11 LANDSAT 8 bands (i.e. except band 8 – panchromatic band and band 9 – cirrus band) were used in the classification. The images were resampled from 30 to 100 m for attribution of local climate to the combined spectral signal of all urban surface features than individual features (Cai *et al.*, 2018). The training areas were digitised (vectorised kmz files) in GoogleEarth for each LCZ types because of the high spatial resolution which enables clear and accurate delineation of different LCZ types.

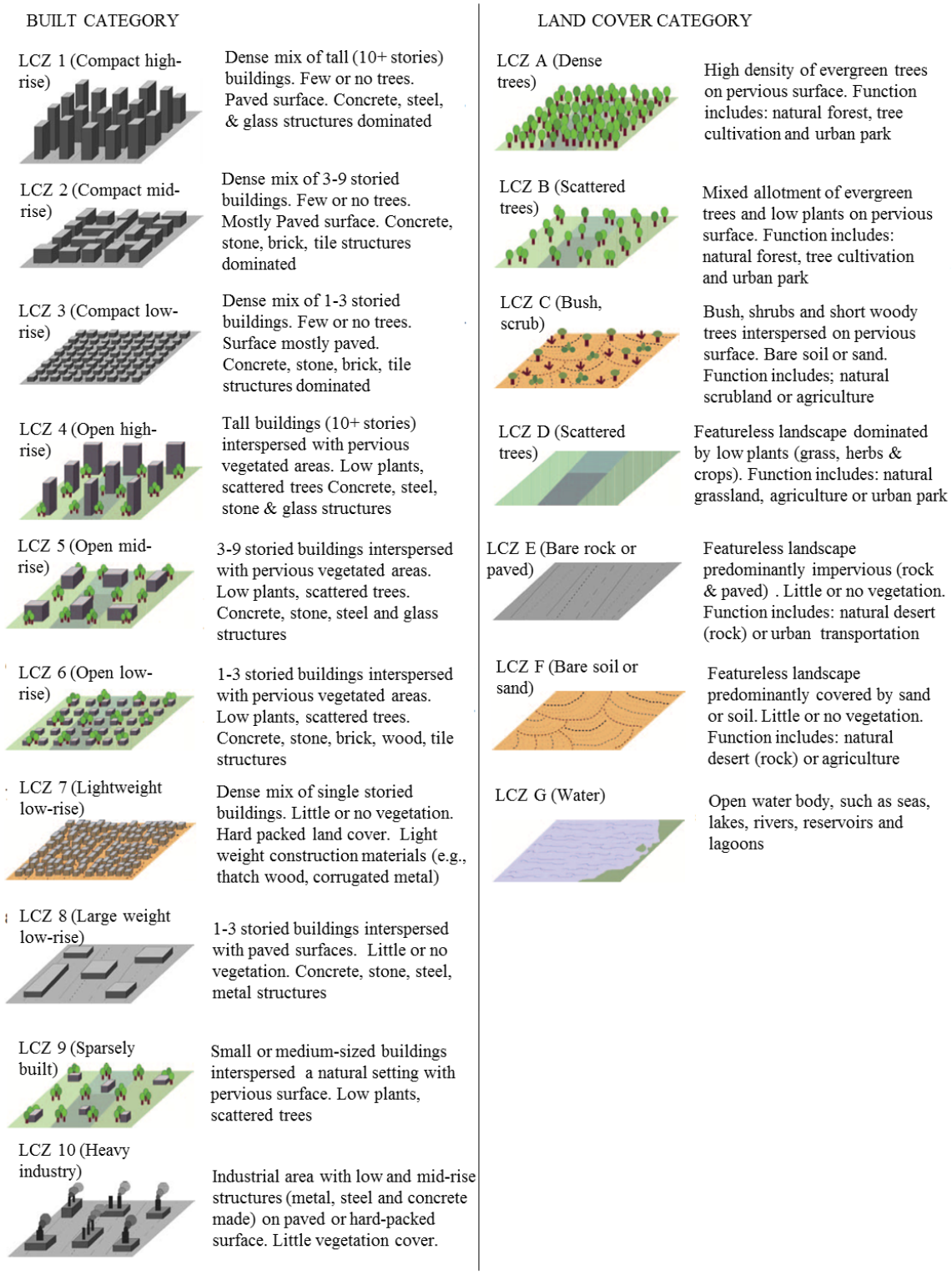

Figure 3-4 structural characteristics of local climates zones (adopted from Stewart and Oke, 2012)

Compact low rise with bare soils (i.e. LCZ3_F) was included in the selection of LCZ-classes as other studies have done (Kotharkar and Bagade, 2018) to highlight this pattern of urban form in Kampala that is absent in the standard set of LCZ classes (Stewart and Oke, 2012). The processed LANDSAT8 images and training areas were used as inputs in SAGA-GIS 2.1.2 to classify the local climate zones of Kampala using random forest classifier (Figure 3-3).

The Random Forest (RF) is a classification and regression algorithm that consists of many individual decision trees that operate as an ensemble (Zhang *et al*., 2019). A classification is achieved using a random sub-sample (from the pool of data), from which a user-specified amount of iterations and the average taken into account to improve accuracy and minimise over-fitting. In other words, RF operates by constructing several decision trees at training and outputting the class that is the mean prediction (regression) or mode of classes (classification) of the individual trees (Zhang *et al*., 2019). RF runs efficiently on large data and input variables and the tree provides unbiased estimates and visual representation of which classes are most important. RF enables computation of differences and similarities between variables and the uncertainty of classification. Random Forest is easily accessible in a number of open source software such as SAGA-GIS which uses RF to assign an LCZ types to each image pixel (Bechtel *et al*., 2019).

Post-classification majority filtering was undertaken as a noise reduction technique to remove isolated pixels from the classification output by setting the search radius to 1 pixel in SAGA-GIS. Assessments of the quality of the LCZ map output (in google earth), resulted in iterative changes to the training areas and image reclassification to improve the representativeness of the mapped LCZs across Kampala. A summary of the proportion of area covered by each LCZ in the final LCZ map (Figure 3-5) is presented in Table 3-1.

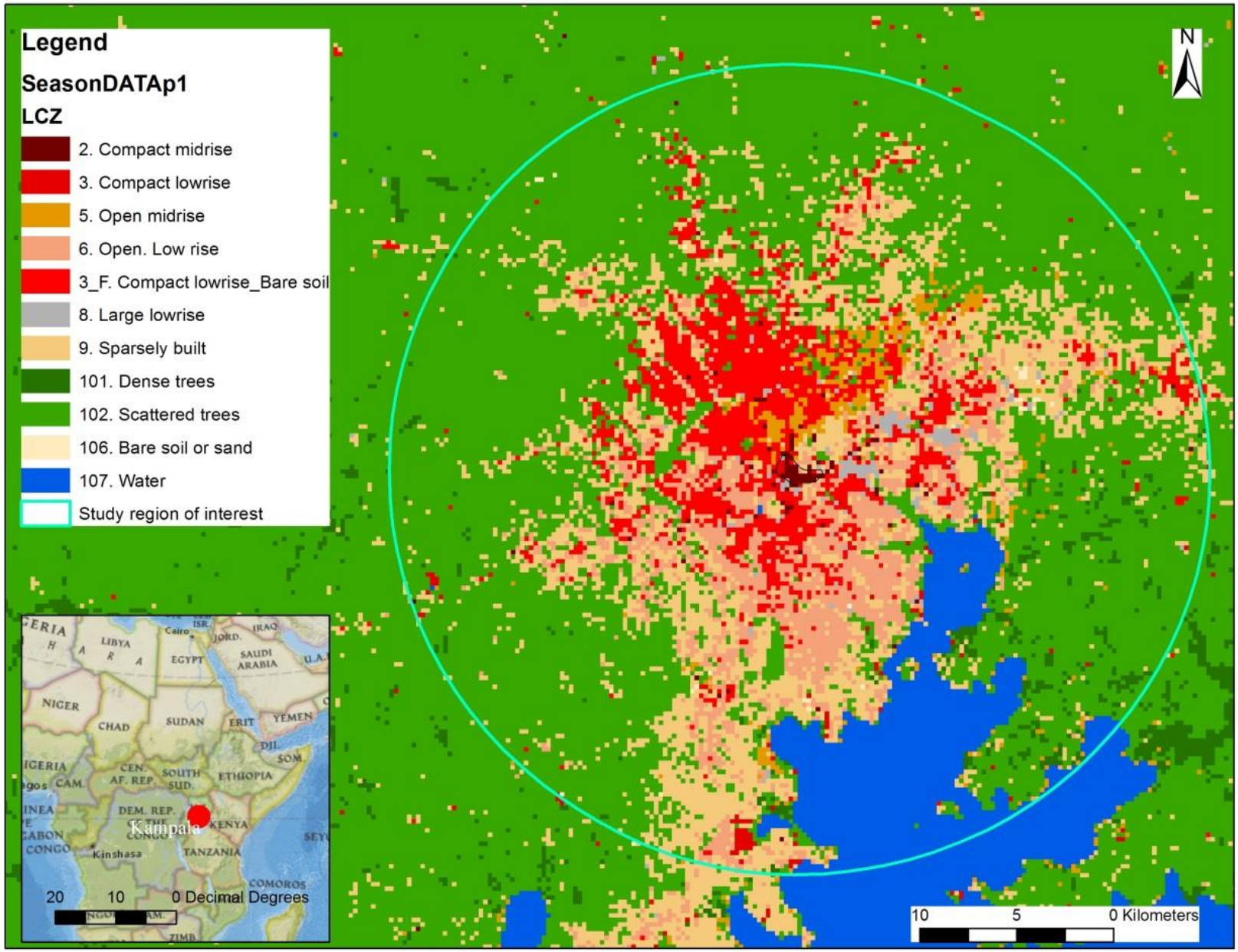

Figure 3-5: An LCZ map of Kampala (100 m resolution). The central business district is comprised of compact midrise and compact low rise LCZ types whereas less built LCZ types extend out of the city. The blue circle represents the region of interest that was the main focus of subsequent analysis within 20 km of city centre (i.e. compact midrise and compact lowrise)

Table 3-1: Surface area and proportion of resulting LCZ classes within 20 km from the city centre (compact midrise and compact low rise)

LCZ class	LCZ name	Surface area (km^2)	Surface area (%)
LCZ 2	Compact midrise	4.6	0.3
LCZ 3	Compact lowrise	8.3	0.5
LCZ3_F	Compact lowrise_Bare soil	134.0	8.3
LCZ 5	Open midrise	28.5	1.8
LCZ 6	Open lowrise	136.6	8.5
LCZ 8	Large lowrise	11.2	0.7
LCZ 9	Sparsely built	277.4	17.2
LCZ A	Dense trees	23.1	1.4
LCZ B	Scattered trees	854.0	53.1
LCZ F	Bare soil or sand	2.3	0.1
LCZ G	Water	128.7	8.0

3.2.1.1 **Vegetation abundance**

Vegetation indices derived from satellite remote sensing are a useful data source for characterising spatial differences in land cover and can be used to depict vegetation abundance (e.g. Weng, Lu and Schubring, 2004; Yuan and Bauer, 2007; Senanayake, Welivitiya and Nadeeka, 2013). Vegetated surfaces contain chlorophyll pigment which reflects Near-infrared and green light, while absorbing parts of the visible light spectrum (blue and red). Vegetation chlorophyll content influences photosynthetic activity and determines the proportion of incoming electromagnetic radiation coming from the sun that is absorbed, transmitted or reflected and detected by optical satellite sensors (Morisette *et al.*, 2009; Reed, Schwartz and Xiao, 2009; Hanes, Liang and Morisette, 2014). Vegetation Indices (e.g. Normalised Difference Vegetation Index and Enhanced Vegetation Index) are proxy measures of canopy "greenness," combining properties of leaf chlorophyll, leaf area, canopy cover and structure (Huete *et al.*, 2011).

Surface cover characteristics across Kampala were derived from the MODIS13Q1 product with a resolution of 250 m to be matched to the respective LCZ units. The MOD13Q1 images for 2013 that represented a typical year unaffected by climate anomalies were downloaded from the Oak Ridge National Laboratory (ORNL), Distributed Active Archive Centre (DAAC), of the National Aeronautics and Space Agency (Daac.ornl.gov, 2016).

The average of the Enhanced Vegetation Index (EVI) was computed in ArcGIS 10.4 for each pixel for all images across 2013 using the raster calculator tool. The MODIS13Q1 product is a 16-day composite image of the Enhanced Vegetation Index (EVI) derived from the Moderate Resolution Imaging Spectroradiometer (MODIS) sensors onboard the Terra and Aqua satellites. EVI was selected because of the following reasons: (1) EVI minimizes canopy background variations and maintains sensitivity over dense vegetation (Huete *et al.*, 2011) making it robust for urban environments; (2) EVI images acquired on a daily basis enable the acquisition of representative measures of vegetation abundance across a given year, in comparison to satellite sensors (e.g. LANDSAT) that have a longer revisit time and have few usable images each year.

Equation 3-1: Retrieval of the Enhanced Vegetation Index from the Red, Near Infrared and Blue bands. ρ is reflectance; L is the canopy background adjustment factor, C_1 and C_2 are aerosol resistance weights. The coefficients are L=1; C_1=6 and C_2=7.5

$$EVI=2.5(\rho_{NIR}-\rho_{RED})/(L+\rho_{NIR}+C_1\rho_{RED}-C_2\rho_{BLUE})$$

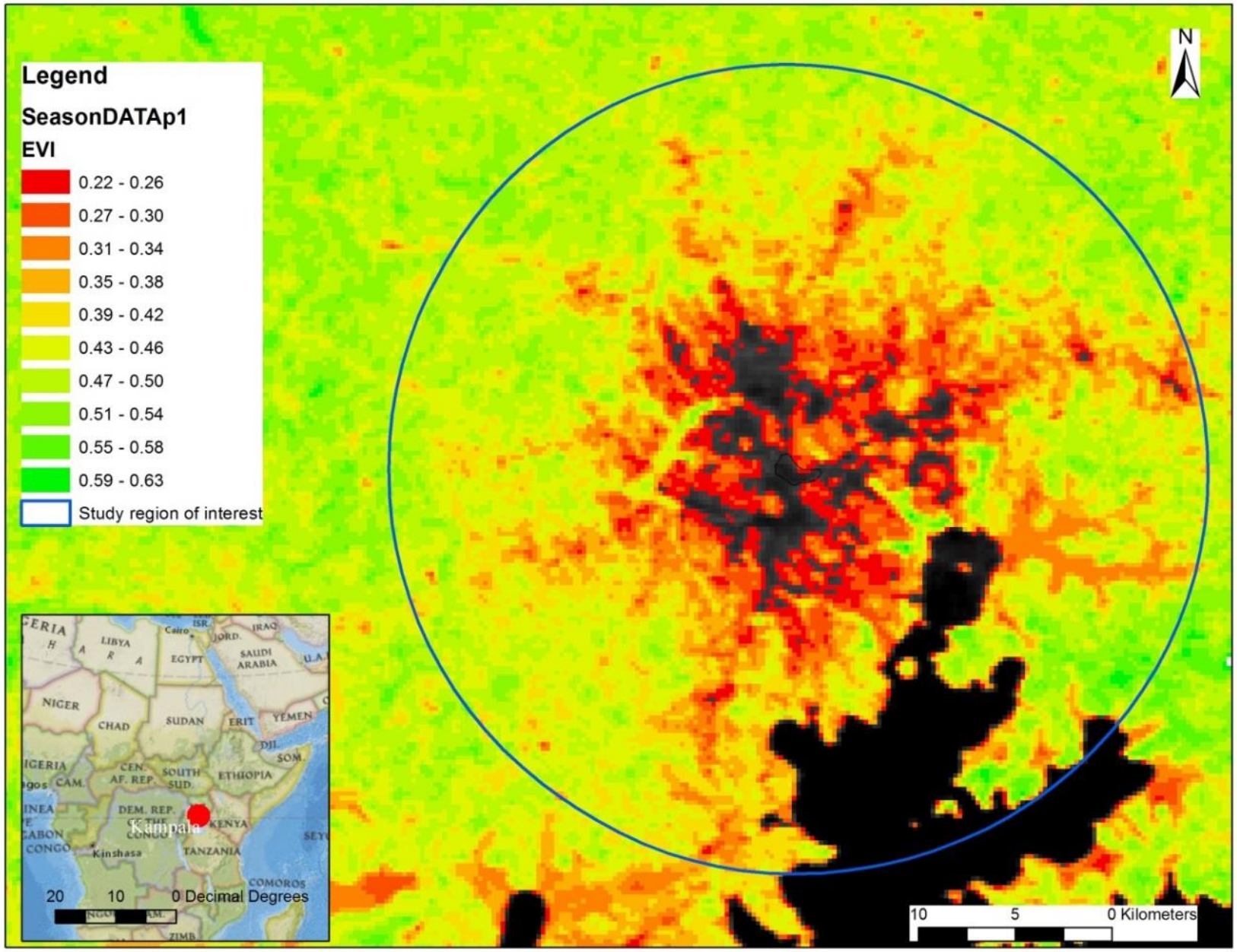

Figure 3-6: Map showing vegetation abundance from the MOD13Q1 Enhanced Vegetation Index (250 m resolution). The range of values for the EVI is -1 to 1, where values above 0.2 are indicative of increasing vegetation biomass (see APPENDIX I for more details of spatial patterns). The blue circle shows the region of interest using in the analysis

3.2.2 Landscape phenology characterisation

Landscape phenological parameters (Figure 3-7; Table 3-2) that represent the distinct stages of vegetation development or changes in photosynthetic activity are extracted using time series analysis of remotely sensed satellite data depicting vegetation reflectance (vegetation index) across a vegetation growing season (Morisette *et al.*, 2009; Reed, Schwartz and Xiao, 2009; Hanes, Liang and Morisette, 2014; Eklundh and Jönsson, 2015, 2016). Time series reconstructs the vegetation seasonal growth course from noisy satellite signals due to atmospheric conditions (e.g. cloud cover), artifacts of data resampling, geometric misregistration, anisotropic reflectance effects and electronic errors (Cai *et al*., 2017).

3.2.2.1 **Data source**

The MODIS EVI MOD13Q1 product is designed to provide consistent spatial and temporal data related to the condition of vegetation (Huete *et al.*, 2011) and was the choice of data for this study. MOD13Q1 product has a very high temporal resolution of daily image acquisition that is then averaged across 16 days. Moreover, MOD13Q1 is suitable for application in urban environments because it minimises canopy background variations and maintains sensitivity over dense vegetation (Huete *et al.*, 2011). MOD13Q1 has been used to successfully characterise spatial patterns of phenology in cities (e.g. Buyantuyev and Wu, 2012).

A three year time period (2013, 2014 & 2015) was chosen to minimise the effects of rapid changes in the built environment and vegetation cover on vegetation phenology, and achieve accurate estimates of the effects of urbanisation on landscape phenology.

3.2.2.2 **Time series analysis**

In this study, time series analysis and extraction of seasonal (Figure 3-7; Table 3-2) was performed in TIMESAT 3.2 program (Jonsson and Eklundh, 2004; Eklundh and Jönsson, 2015). TIMESAT has a choice of three methods that utilise least-squares fits to the upper envelope. An appropriate method needs to be chosen by testing the different methods with different settings in the graphical interface of the software. These methods include: Savitzky-Golay filtering; assymetric Gaussians; Double logistic functions which will often give similar results for comparatively smooth time series (Jonsson and Eklundh, 2004; Eklundh and Jönsson, 2015). The adaptive Savitsky-Golay

algorithm which uses local polynomial fitting functions was chosen for this study because of its simplicity and ability to preserve features (i.e. maximum, minimum and width) of the dataset (Yao *et al.*, 2017). Savitsky-Golay filtering uses a least squares fit to a quadratic polynomial, thus reducing the noise in the data associated with cloud cover (Han and Xu, 2013). A polynomial function is fitted to each data point in a window and for this study we used a moving window width of 2 (69 days).

Equation 3-2 where "*t*" is the time position and "*c1*", "*c2*", "*c3*" are determined by weighted least-squares fitting, and the degree of smoothing is controlled by the width of the window (Eklundh and Jönsson, 2016).

$$f(t) = c_1 + c_2 t + c_3 t^2$$

TIMESAT extracts data only for the n–1 centre-most seasons for n expected seasons in a time series (Eklundh and Jönsson, 2015). However, Eklundh and Jönsson (2015) noted that the seasonal parameters from a single year can be retrieved by duplicating the time-series from the same year twice to make an artificial time-series spanning three years. Therefore, in this study, artificial time-series were created for the candidate years (i.e. 2013, 2014 and 2015).

3.2.2.3 **Extraction of seasonal parameters**

In TIMESAT, the two approaches for determining the start and end of the season are the threshold and amplitude method (Eklundh and Jönsson, 2015, 2016). In the threshold method, start and end of season are the dates that the fitted curve rises and falls to the set threshold whereas, start and end of season in the amplitude method are the dates that the fitted curve rises and falls to the proportion of amplitude (i.e. the range in EVI in a given year). For choice of method to determine the start and end of season, the amplitude method was chosen because it is better suited than the threshold method for computing phenology metrics in urban settings where vegetation cover is lower than the surrounding rural areas. Lower vegetation cover in urban areas in comparison to rural areas makes it hard to find a threshold for determining dates for start and end of season (Zhou *et al.*, 2016; Yao *et al.*, 2017). In this study, the start and end of the vegetation growing season were, therefore, the time the fitted EVI curve increased and progressively declined 40% of the seasonal amplitude (Jonsson and Eklundh, 2004; Eklundh and Jönsson, 2015).

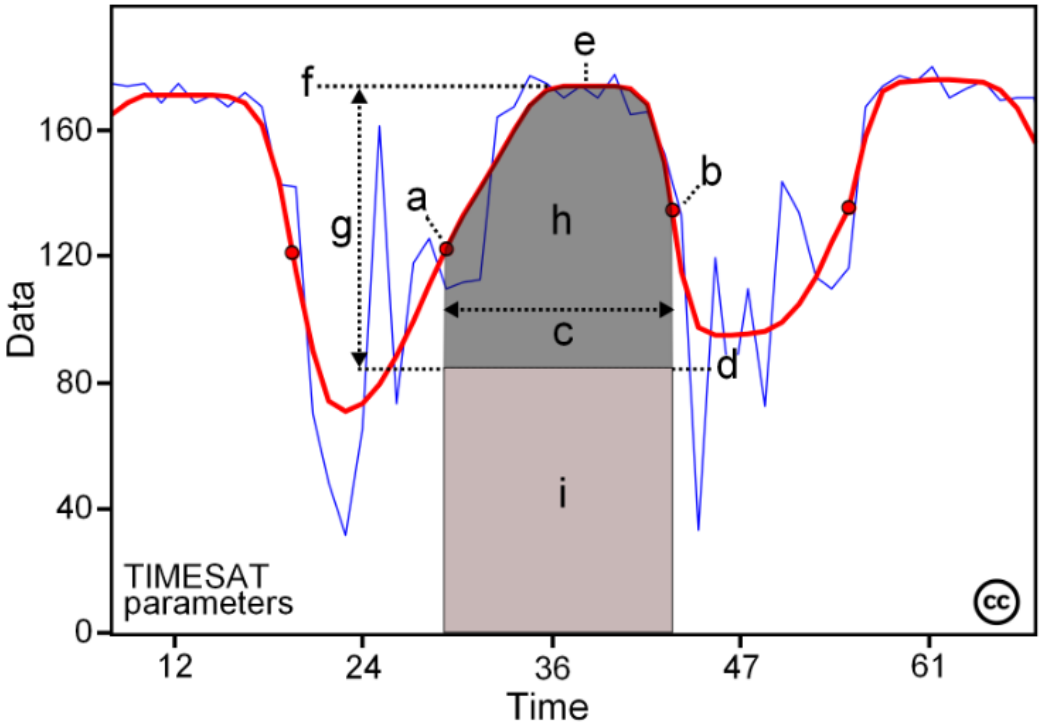

Figure 3-7: algorithm theoretic basis of for performing time series analysis and extracting seasonality parameters in TIMESAT (Source: Eklundh and Jönsson, 2015, 2016). The blue line depicts the actual vegetation index data value for a give pixel at different points in time, whereas the red line shows the fitted vegetation index data. A summary of each phenology parameter (represented by letters "a"-"i" of the alphabet) is presented in Table 3-2

Table 3-2: shows the definition of phenology metrics in land surface phenology (Source: Eklundh and Jönsson, 2015, 2016)

Figure 3-7 **code**	Seasonality parameter generated in TIMESAT
(a)	**Start of Season**: Timing (Day of year) of the start of the growing season and precedes increment in photosynthetic activity
(b)	**End of Season**: Timing (Day of year) of end of the growing season following a decline in photosynthetic activity
(c)	**Season length**: Duration of the growing season (difference between the start and the end of the vegetation growing season)
(d)	**Base value**: The average of the right and the left value
(e)	**Mid/Peak of season**: Timing (Day of year) of peak photosynthetic activity/primary production
(f)	**Maximum value**: Maximum vegetation index value for the fitted function during the season
(g)	**Amplitude**: The change in photosynthetic activity across the growing season and represents the strength of the seasonality (intra-annual variability of primary production)

(h)	**Small integrated value**: The area below the base level from the start to the end of the season
(h+i)	**Large integrated value**: The area under the smoothed curve between the start and the end of the season

Table 3-3: Summary table of settings applied in TIMESAT 3.2 for smoothing the image time series and extraction of the seasonal parameters

Short description	Input and explanation
Use of quality data. MOD13Q1 images have quality flags that assess the reliability of each pixel in each (i.e. classification of cloud cover or other image quality indicators). This forms the basis for assigning weights to the actual as measure of uncertainty in the actual EVI data.	Yes; Effect of cloud significantly reduced
Quality range 1 and weight (Lower and upper values for quality class 1 and assigned weight)	From 0.1 to 0.9; weights 0.1
Quality range 2 and weight (Lower and upper values for quality class 2 and assigned weight)	From 1 to 2.9; weights 0.5
Lower and upper values for quality class 3 and assigned weight	From 3 to 4.1; weights 1
Amplitude cut-off value	All data was processed in the series
Use land cover (1/0) – optional	No land cover data was used
Spike method	Spike method was based on median filtering
Spike value. A low value will remove more spikes	3; this high value implies that fewer spikes were removed
Seasonality parameter	Time series were fit for two seasons each year (we extracted data for the second season only)
No. of envelope interations 1,2,3	Only one iteration was set
Adaptation strength (1-10)	0 (very low); Strength of the envelope adaptation. 10 is the maximum strength
Force to minimum and value of minimum after fitting	No value were forced to a minimum
Fitting methods	Savitzky-Golay fitting method was used
Weight update method	Weight update method was not in use
Window for Savitzky-Golay. Half window for Savitzky-Golay filtering with high values resulting in high degree of smoothing	3; This value implied a conservative smoothing

Season start method	Amplitude method
Season start / end values. The values must fall between 0 and 1	0.4 (40%)

3.2.3 Land surface temperature

Land surface temperature data was derived from the MODIS MOD11A2 product for the years 2013, 2014 and 2015 to quantify the effect of variation in urban climate (temperature) on phenology. The MOD11A2 is an 8-day composite image of LST data collected by the MODIS sensor, enabling computation of seasonal differences across space and time. Moreover, the MOD11A2 has been observed to provide adequate estimates of maximum air temperature in tropical urban environments (Ayanlade, 2016). Due to the noisy satellite signals that is associated with atmospheric conditions (e.g. cloud cover), artefacts of data resampling, geometric mis-registration, anisotropic reflectance effects and electronic errors, time series was performed to reconstruct temporal patterns of temperature across the study area (Cai *et al*., 2017).

A Savitzky-Golay smoothing filter was fit to the LST time series data in TIMESAT for day and night time LST for each year separately (i.e. artificial time series spanning three years). MODIS quality assessment data was included to denoise the time series and improve the LST signal. Maximum land surface temperature was derived as the peak temperature of the fitted LST curve and this value derived for both day and night time temperature, for each year following Han and Xu (2013). The average of the day and night maximum LST was computed to represent maximum LST across each given year as a proxy of high temperature that might affect vegetation phenology (Hatfield and Prueger, 2015; Gray and Brady, 2016).

3.3 Phenological processes of individual tree species

This section describes the methods for linking phenology of individual tree to microscale climate (see 2.1.2.1). Urban form and function are critical for understanding the relationship between microscale climate effects and phenology of trees (see section 2.1.1) and an ideal approach for urban form characterisation will concede that urban features have a combined effect on climate within a given space (see section 2.1.2.3).

3.3.1 Select tree species

Deciduous trees are more sensitive than evergreen species to differences in local environmental settings (Williams *et al.*, 1997) and were chosen as the focus of this study in anticipation that they would respond strongly to local urban climate variability. Drawing on information from the Kampala Capital City Authority about the most abundant trees within Kampala CBD (the most built up part of the), *Tabebuia rosea* and *Jacaranda mimosifolia* were identified as the most abundant deciduous species. Therefore, this study was based on the leaf canopy phenology of *Jacaranda mimosifolia* and *Tabebuia rosea* (Table 3-4). More details about the two species are covered in APPENDIX III.

Table 3-4 showing the characteristics of *Tabebuia rosea* and *Jacaranda mimosifolia*

Species	General characteristics
Jacaranda mimosifolia (D. Don)	-Deciduous trees species of the family *Bignoniaceae* native to the neo-tropics (Argentina & Brazil) but has been widely elsewhere in other tropical countries (Uganda, South Africa, Australia) - The trees grow up to 20 m in height with spreading branches making a light crown with considerable leaf fall (data source: World Agroforestry) -The species has previously been observed to show shortened leaf flush after the rains and high leaf fall with transition from the wet to dry season (Huxley and Vaneck, 1974) -The species is characteristically known as a bio-indicator for air pollution (Olowoyo, van Heerden and Fischer, 2010; Barroso *et al.*, 2018)
Tabebuia rosea (Bertol.) DC.	-Deciduous trees species of the family *Bignoniaceae* native to the neo-tropics (Mexico, Venezuela & Ecuador) but extensively grown elsewhere in the tropics (e.g Uganda, Sri Lanka) - Trees grow up to 25 m with considerable flush and shoot growth during the early in the rain season (data source: World Agroforestry). - Leaf fall has been observed to be pronounced during the dry season favoured by high temperature and drought (Figueroa and Fournier,

	1996) -It has been shown to significantly reduce air temperature in comparison to other species in Penang, Malaysia because of its high Leaf Area Index (Tukiran, Ariffin and Ghani, 2016) -The species has been shown to be tolerant to acid rain (Ceron *et al.*, 2009)

3.3.2 Phenology sampling sites

A systematic survey was carried out across Kampala with the aid of the LCZ map in order to select sites with the select candidate tree species in neighbourhoods of varying urban form. Nine sites were selected that contained *Tabebuia rosea* and *Jacaranda mimosifolia* for leaf canopy phenology observations to be undertaken. An additional thirteen sites (totalling to twenty two sites) were selected for data collection to be used in the analysis of the spatiotemporal patterns of local climate. The selected sites exemplified the variety of urban surface structural differences across Kampala (Figure 3-8) and a detailed summary of the land cover characteristics of each site is presented in

Table 3-6. All sites were located within an 80 m altitudinal range to minimize the influence of elevation on urban climate (Jochner *et al.*, 2012). The nine phenology sites contained between 2 to 8 individuals of any one of the candidate tree species (Table 3-5) and all trees were located within less than 100 m of each other.

Table 3-5: Showing the number of trees at each phenology site.

Phenology sites	One	Two	Three	Four	Five	Six	Seven	Eight	Nine
Location code (all 22 sites)	1	2	13	6	8	7	16	22B	23B
Jacaranda	5	2	6	5	6		5	5 8	6
Tabebuia	4	5	0	5	0		3	0 0	7

Differences in tree size and age were minimized by selecting trees with a similar height and trunk size (i.e. diameter at breast height) as summarised in APPENDIX III. None of the trees was actively managed during the course of the study (March to September 2017).

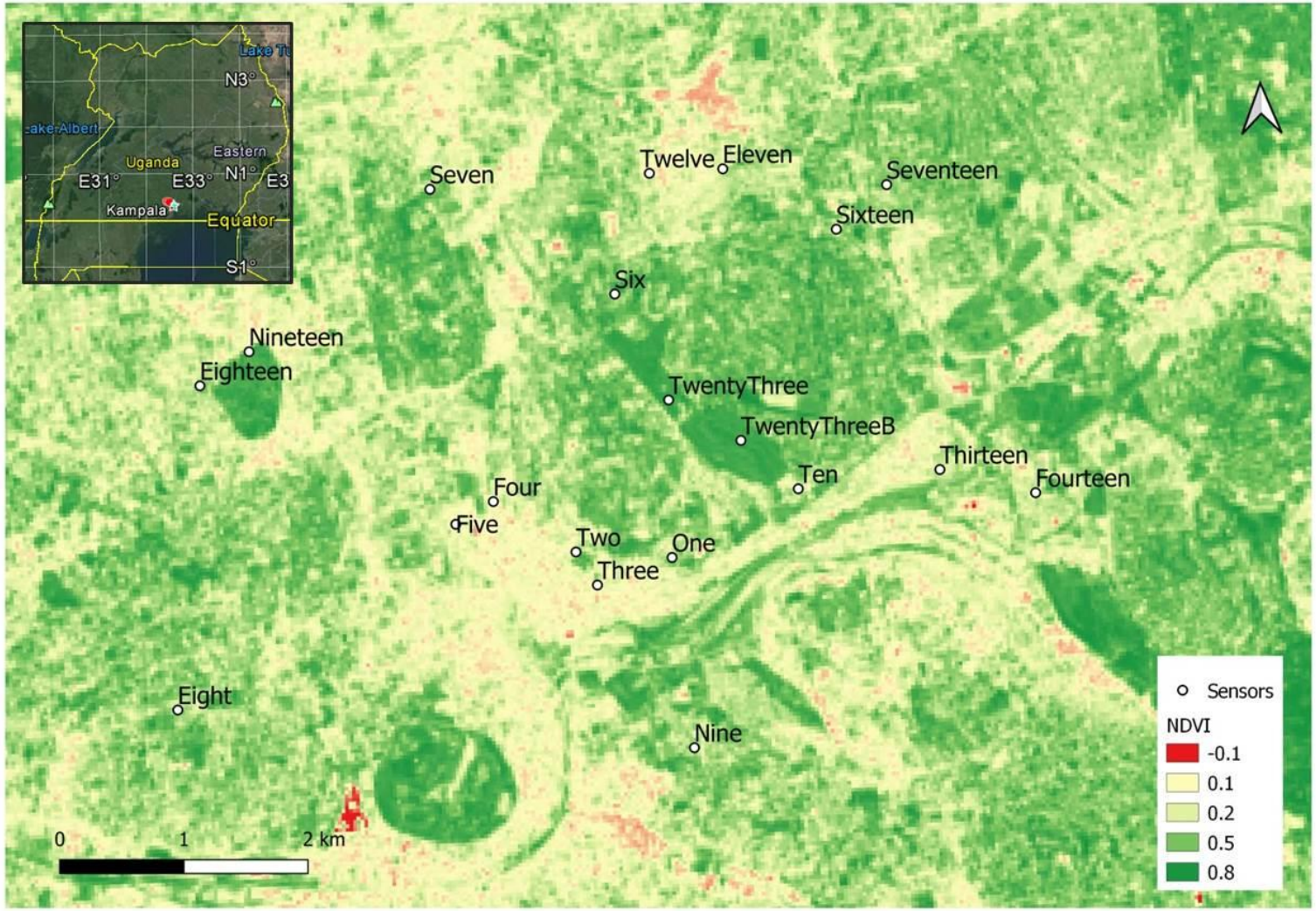

Figure 3-8 showing surface cover differences of sites used for microscale climate and phenology processes. Locations 1, 2, 6, 7, 8, 13, 16, 22B, 23B were used for phenology (see 3.4.2.2). NDVI (30 m) was scaled to show the extent of differences in vegetation cover and impervious surfaces.

3.3.3 Characterisation of surface cover and structure at each site

The classification of surface structure and cover of a given area of interest provides data on the extent of urbanisation for attribution of urban form to local climate (Mimet et al 2009; Stewart and Oke, 2012; Jochner et al 2013; Seress et al 2014). In this study, classification of surface cover and structure for attribution to local climate was achieved using Object Based Image Analysis.

Pixel based analysis draws on the spectral signature of pixels for image classification (Blaschke, 2010; Blaschke *et al.*, 2014). In coarse and moderate resolution images where features of interest are the same size (or smaller than) as the pixel, pixel-based approaches are well adept for identifying unique features of interest in the landscape as a whole. However, pixel-based analysis would be unsuitable in instances where the features of interest are larger than the pixel as is the case with very high-resolution imagery (Blaschke, 2010; Blaschke *et al.*, 2014). For example, a large water body would be represented by multiple small water bodies the size of a pixel and the 'salt and pepper' effect depicting misclassified pixels using pixel based classification. This is because pixel-based image analysis uses the spectral signal of individual pixels and does not consider spatial-autocorrelation in the classification workflow (Blaschke, 2010; Blaschke *et al.*, 2014). Object-Based Image Analysis overcomes the limitations associated with pixel-based methods by accounting for spatial autocorrelation and the creation of regions (objects) of homogeneity in one or more dimensions of feature space. Moreover, the OBIA, approach generates additional spectral information in comparison to single-pixel classification (e.g. mean, median, minimum, maximum, values per band, etc.) and the spatial information of the objects used in the image classification (Blaschke *et al.*, 2014).

A WorldView3 satellite image (spatial resolution of 0.5 m) taken on 25/10/2016 was used for classifying buildings, paved surfaces, tree cover and pervious surfaces (i.e. soil and low vegetation) using object based image analysis (OBIA) in eCognition Developer (Version 9) using the work flow summarised in Figure 3-9. A fully automated classification was hard to achieve due to the high heterogeneity within the selected sites. Therefore, a semi-automated approach was adopted that involved both automatic and manual classification to achieve accurate classifications of urban

features. Classification was undertaken within a region of 200 m at each of phenology and urban climate sites, because 200 m represents the unit of space for attribution of local land cover to local climate (i.e. meteorological station) (Stewart and Oke, 2012).

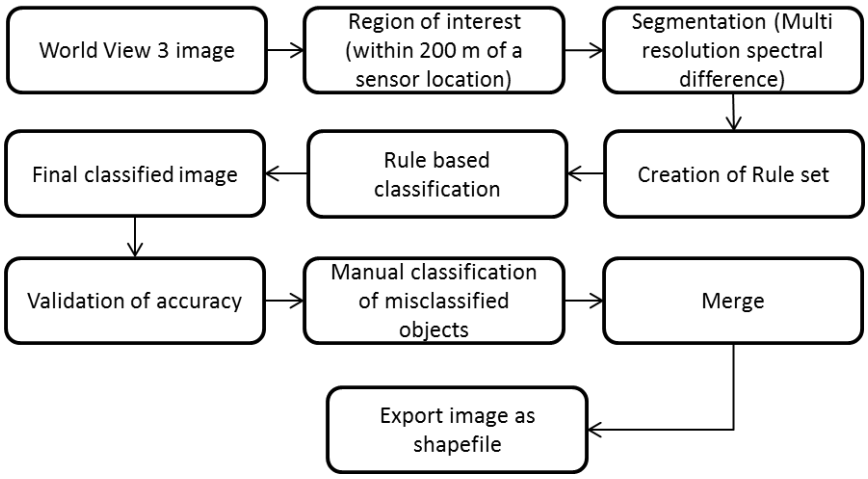

Figure 3-9: Workflow of Worldview images classification using OBIA

3.3.4 Phenology data collection

As with other studies that have focussed on the spatial variability of vegetation development within a city in a given season (e.g. Gazal *et al.*, 2008; Jochner, Alves-Eigenheer, *et al.*, 2013), this study focussed only on the dry season. Whereas previous studies on phenology of trees in tropical cities focussed on the timing (date) of budding, this study was based on the canopy development. Therefore multiple observations were made across wet and dry season (March to September) of 2017.

Visual observations are a standardised technique that is widely used for monitoring vegetation phenology (e.g. Williams *et al.*, 1997; Condit *et al.*, 2000; Morellato *et al.*, 2010; Valdez-Hernandez *et al.*, 2010; de Camargo *et al.*, 2018) and was the choice of approach in this study. In addition to identification of the timing of phenological events, visual observations enable quantification of the intensity of particular phenophases for derivation of metrics like magnitude (Morellato *et al.*, 2010; Denny *et al.*, 2014). Visual observations outperform other direct observation techniques like use of litterfall traps (Morellato *et al.*, 2010), and visual observations are commonly used for validating indirect sensor-based measures of phenology (e.g. Chuine, Cambon and Comtois, 2000; Fisher, Mustard and Vadeboncoeur, 2006; Zhang, Friedl and Schaaf,

2006; Maignan *et al.*, 2008; Reed, Schwartz and Xiao, 2009; Liang, Schwartz and Fei, 2011; Donnelly and Yu, 2017; Lim *et al.*, 2018).

To accurately characterise the phenology of a given population of tree species, Morellato *et al*., (2010) recommended a minimum of 1 observation every two weeks for a sample of fifteen trees. Therefore, each tree was observed four times every fortnight by a single observer using binoculars in a two-step process. In step 1, a score of 0 to 4 was used to depict the relative level of leaf presence (0 = absence of leaves, 1 = 1-25 %, 2 = 26-50 %, 3 = 51-75 % and 4 = 76 – 100 %). In step 2, a sub-score of 1, 2 or 3 was assigned to refine the canopy score (e.g. 3_1, 3_2 or 3_3). Either a 1 or 3 was appended if the percentage estimates in the first score was distinguishable as being within the upper half or lower half of the associated range. Otherwise a 2 (median) was appended if the estimate was indistinct. For example, a tree with a 3 in the first step would be assigned either 3_1 or 3_3 to distinguish between 51% and 75%, otherwise a 3_2 would be assigned if the estimate was indistinct. The final categorical scores were finally converted to their indicative percentage values (e.g. Williams *et al.*, 1997; Morellato *et al.*, 2010; Valdez-Hernandez *et al.*, 2010).

3.3.5 Urban climate characterisation

Data logging for spatiotemporal characterisation of urban climate was consistently undertaken from March to September 2017. This period marks the rainfall season from March to May and the dry season that follows (June to September). Representations of these seasonal transitions have been provided in APPENDIX IV and APPENDIX V.

3.3.5.1 **Air temperature and relative humidity**

Air temperature and relative humidity data were recorded every 30 minutes at all twenty-two sites using iButtons (DS1923) (Figure 3-10 a). The DS1923 iButton Hygrochron logger (MaximIntegrated, 2016) was set to collect temperature (accuracy better than ± 0.5°C) and humidity data (accuracy better than 5 %) at resolutions of 0.5°C for temperature and 0.64% for humidity. The loggers are individually calibrated in a NIST (National Institute of Standards and Technology)-Traceable chamber (MaximIntegrated, 2010) and are designed to record data in a protected memory section of the device, making it a self-sufficient system. The logger is made out of

durable stainless-steel and hydrophobic material that can withstand environmental hazards such as dirt, dust, contaminants, moisture and mechanical shock.

HOBO sensors (model HOBO U23-001 Pro v2, Onset Corporation) (Figure 3-10 b) that are costlier but with higher accuracies than i-buttons for both temperature (± 0.21°C) and relative humidity (2.5 %) were added to the phenology sites to assess the quality and stability of the i-button recordings. The HOBO sensors were factory calibrated according to NIST standards and a calibration certificate acquired for one of the sensors as a reference.

The sensors were housed in radiation shields 3 m above the ground (Figure 3-10 c). Although 1-2 m (i.e. screen height) is the recommended height for siting meteorological stations for canopy UHI studies (Stewart and Oke, 2012), the loggers in this study were placed at heights of 3 m to minimise vandalism.

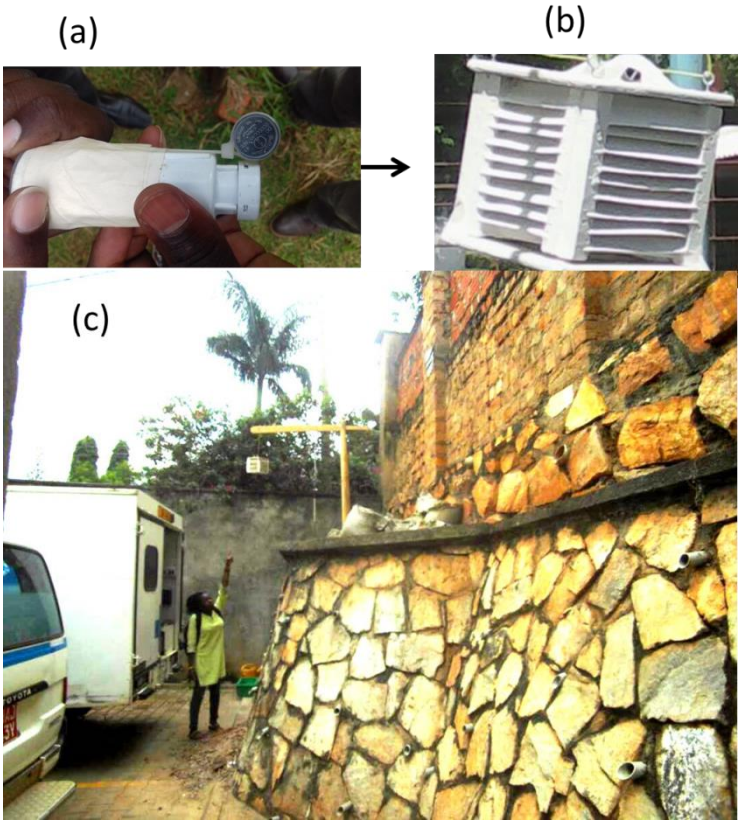

Figure 3-10: (a) An i-button (model DS1923) and HOBO (U23-001) displayed side by side; (b) Radiation shield (L: 15 cm*W: 15 cm* H: 15 cm) used to house the sensors (c) Sensor housed in a radiation shield at one of the sites

3.3.5.2 **Soil moisture**

Volumetric soil moisture content (VMC) was collected at each phenology site to characterise the temporal change in precipitation (water availability) that is known to influence UDI (see 2.1.5), tropical UHI (see 2.1.4.2) and canopy phenology (see 2.2.3.1). The VMC was collected biweekly, coincident with recording of phenology data. VMC recordings were taken for the top most soil layer (8 cm of top soil) at the same location within 3 meters from each tree trunk using a portable ThetaProbe (model ML3 ThetaProbe, Delta-T Devices).

3.4 Data Processing and Analysis

The data emanating from the direct field monitoring (i.e. urban climate and phenology) was in tabular format, necessitating converting all relevant auxiliary data sets (i.e. urban structure) into matching matching formats and creation of a 'tidy data' before any meaningful analysis could be undertaken. Tidy data are data matrices arranged in a way that each variable is a column, and each observation is a row (Wickham, 2015). Data processing in this study was undertaken in excel and R software.

3.4.1 Local scale climate and phenological processes

3.4.1.1 **Selection of candidate local climate zones**

It was anticipated that there might be a higher level of uncertainty on the representativeness of the LCZs that covered small areas (fewer pixels) than those that covered a substantially large area of the study site due to the differences in area covered by the LCZs. Therefore, the top four local climate zone types in terms of surface area and that had contrasting physical characteristics were selected for the analysis (Figure 3-11 & Figure 3-12). An area within 20 km of the city centre covering the Kampala greater metropolitan area and neighbouring rural area was selected as the region of interest for this study and the candidate LCZ classes covered roughly 87% of this area (Figure 3-5).

LCZ type	Description	Surface characteristics
LCZ 3 (Compact low-rise) + LCZ F (Bare soil or sand) 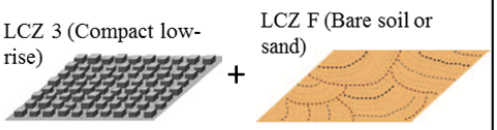	Dense mix of 1-3 storied buildings.. Concrete, stone, brick, tile structures dominated. Surface mostly covered by soil and paving	40-70 building fraction;
LCZ 6 (Open low-rise) 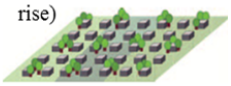	1-3 storied buildings interspersed with pervious vegetated areas. Low plants, scattered trees. Concrete, stone, brick, wood, tile structures	20-40 building fraction; <20-0% impervious surface fraction; >30-60% pervious surface fraction
LCZ 9 (Sparsely built)	Small or medium-sized buildings interspersed a natural setting with pervious surface. Low plants, scattered trees	10-20 building fraction; <20% impervious surface fraction; >60-80% pervious surface fraction
LCZ B (Scattered trees)	Mixed allotment of evergreen trees and low plants on pervious surface. Function includes: natural forest, tree cultivation and urban park	<10 building fraction; <10% impervious surface fraction; >90% pervious surface fraction

Figure 3-11: Characteristics of the candidate LCZ classes used in this study (Adapted from: Stewart and Oke, 2012)

LCZ3_F. Compact lowrise_Bare soil

LCZ6. Open lowrise

LCZ9. Sparsely Built

LCZB. Scattered trees

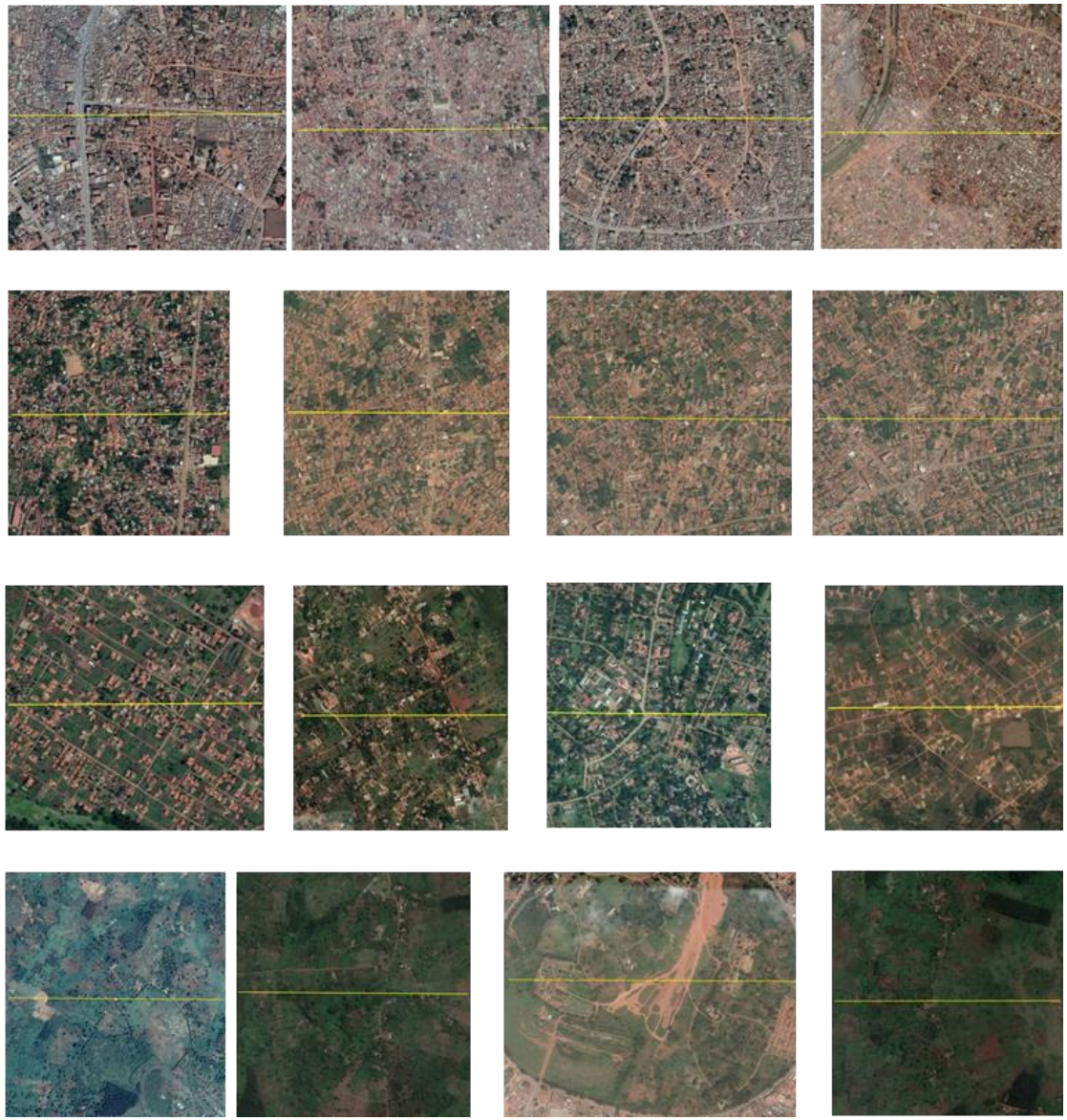

Figure 3-12 showing aerial imagery acquired from Google Earth representing the candidate LCZ classes used in the analysis. A yellow line stretching 1 km has been added as a reference for the scale

Vegetation/surface cover data for each of the candidate LCZ classes classified from the MODIS13Q was the basis for verifying that the four candidate local climate zones were inherently and statistically different before any analysis could be done. This was achieved by performing, Kruskal-Wallis H-test and paired post-hoc tests (Figure 3-13).

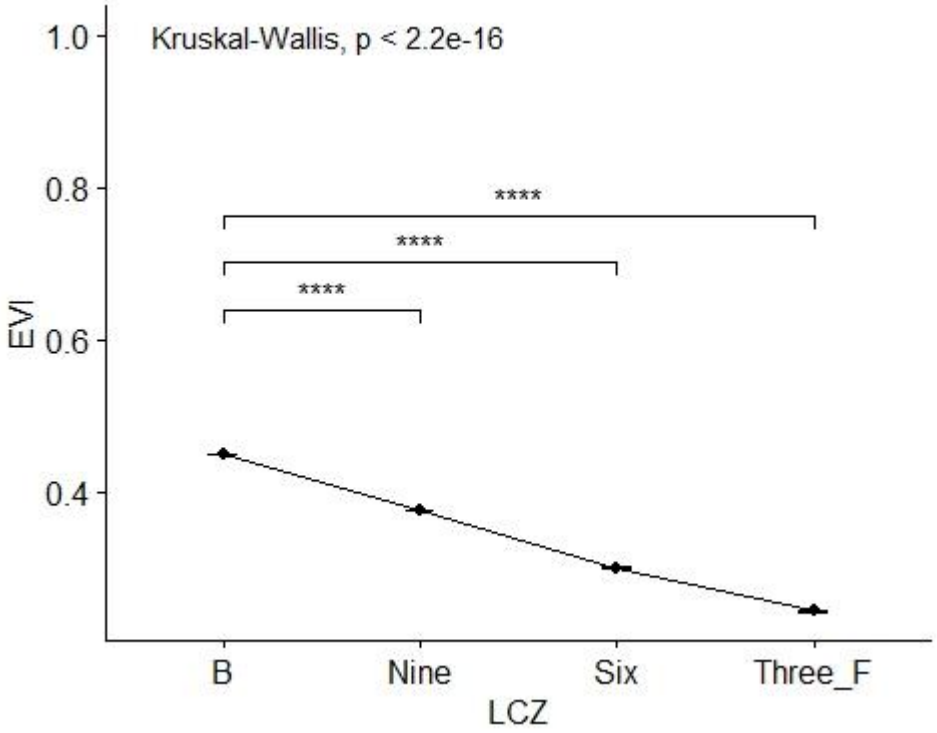

Figure 3-13 showing box plots depicting the denoting the extent and significance of differences in vegetation cover (EVI) across all LCZ types and between pairs of LCZs

3.4.1.2 Selection of unit for analysis

The MODIS13Q1 pixel was selected as the unit of analysis (i.e. observation/row) (Figure 3-14). The MODIS13Q1 was the smallest spatial unit of primary data enabling consistent comparisons to be made across different data types. Each MODIS13Q1 pixel was assigned relevant attributes (i.e variable/column) for the phenology parameters (i.e. start, end and length of season) and the maximum day and night-time LST for each year.

To account for the effect of diminishing urban climate with declining development along the urban rural gradient (McDonnell and Pickett, 1990), the linear distance of each individual pixel from the CBD (compact mid-rise; Figure 3-5) was calculated using the proximity function in Arc-GIS (10.4). The distributions of data linked to surface

temperature and phenology across the local climate zones and urban-rural distance gradient is presented under APPENDIX I.

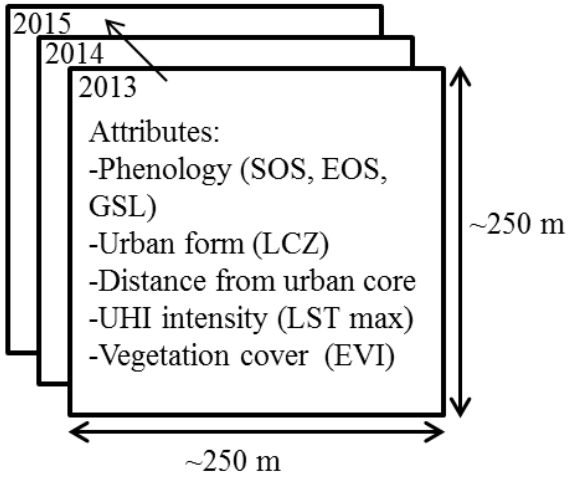

Figure 3-14: shows a summary of data attributes for each MODIS EVI pixel as a unit of the analysis

3.4.2 Micro scale climate and phenological processes

3.4.2.1 **Urban characterisation**

Due to the heterogeneous nature of the sites (i.e. uneven land cover composition), the feasibility of attributing local climate to land cover in an area of radius=200 m was compared to a smaller area of radius 100 m within which land cover was more homogenous.

The sites were grouped into three groups highlighting urbanisation intensity (i.e. high, medium and low) on the basis of similarity in land cover composition, using hierarchical cluster analysis for the 100 m and 200 m land cover data separately. Analysis of similarity (ANOSIM) (Clarke, 1993) was used to statistically test whether there was significant difference in urban climate between the groups for both the 100 m and 200 m separately. An anosim R statistic of R=0.556 (p=0.001) for the 100 m data set was higher than R=0.321 (p=0.005) for the 200 m dataset, indicating stronger differences in urban climate between groups for the 100 m dataset. Therefore subsequent analysis on the influence of land cover on urban climate and phenology was based on land cover within a radius of 100 m (Table 3-6). APPENDIX II contains imagery showing the surface cover and structural differences across all sites.

Table 3-6: Surface cover and structural characteristics (percentage of impervious surfaces, paved surfaces, buildings, trees and pervious surfaces) of the twenty two urban climate stations. The locations are grouped row-rise with relation to proportion of man-made impervious surfaces. Phenology sites are indicated in bold and underlined.

Urban intensity groups	Location number (code)	Impervious surfaces (%)	Paved surfaces (%)	Buildings (%)	Trees (%)	Pervious (%)
HIGH	05	84	49	35	5	11
	12	81	21	60	6	13
	04	80	35	44	9	11
	03	79	36	44	9	12
	11	69	37	32	11	21
	14	65	32	33	13	21
MEDIUM	**13**	**59**	**39**	**21**	**11**	**30**
	10	59	39	21	21	19
	01	**51**	**32**	**20**	**37**	**12**
	09	49	17	32	24	26
	02	**48**	**39**	**9**	**30**	**22**
	17	44	22	22	28	28
	18	37	14	23	20	43
	16	**33**	**13**	**20**	**31**	**35**
	08	**33**	**16**	**17**	**18**	**49**
LOW	**07**	**23**	**5**	**19**	**35**	**42**
	06	**19**	**10**	**9**	**15**	**65**
	19	19	11	8	31	50
	23	9	8	1	43	48
	22	5	4	2	50	45
	22B	**0**	**0**	**0**	**60**	**40**
	23B	**0**	**0**	**0**	**44**	**56**

3.4.2.2 **Classification of phenology sites**

To create a 3-level categorical data set depicting urbanisation intensity for comparison among sites, hierarchical cluster analysis of the land cover data for the phenology sites only was performed in R software (3.4.3) to group sites into 3 classes (Table 3-7). The three classes included: lightly built, moderately built and heavily built). Each level of urbanisation intensity (see APPENDIX II) thus served as a population and the trees per

species within a given level of urbanisation intensity represented the sample of a given category of urbanisation intensity (i.e. population).

Table 3-7: Characteristics of the nine phenology sites, their associated urban form (percentage cover of pervious surfaces, paved surfaces and buildings) and number of individual trees (per species) sampled at each phenology site. The last row indicates the urbanisation intensity category assigned to each phenology site

Phenology site code	One	Two	Three	Four	Five	Six	Seven	Eight	Nine
Location code (all 22 sites)	01	02	13	06	08	07	16	22B	23B
Proportion of man-made impervious features	51%	48%	59%	19%	33%	23%	33%	0%	0%
Urbanisation intensity category	Heavily built			Moderately built				Lightly built	

3.4.2.3 **Phenology data processing**

Time-series profiles of canopy cover were acquired for each tree using LOESS smoothing algorithm (see APPENDIX IV) to de-noise the data and enhance the temporal pattern of canopy cover change (Jacoby, 2000). Temporal interpolation of the time series was undertaken in R software 3.5.

Two measures of leaf phenological traits were determined from each time series to quantify canopy cover changes across the dry season (i.e. DOY 150 to 250). The area under the curve between the first and last phenological observation was computed to represent total percentage tree canopy cover, whereas the difference between the maximum and minimum percentage tree canopy cover across the observation period represented net leaf loss (Figure 3-15).

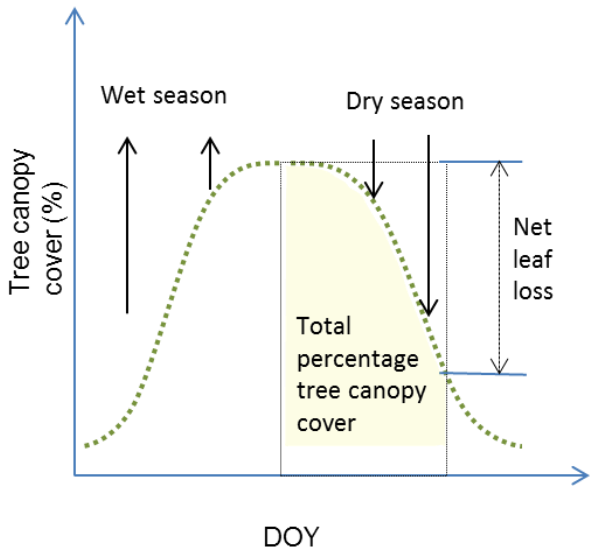

Figure 3-15: Conceptual diagram showing tree canopy change across time and traits of canopy cover change (total percentage canopy cover and net leaf loss) that were extracted from the time series as indicators of leaf production and leaf loss

3.4.2.4 Spatioemporal patterns of urban climate

The daily average of nighttime temperature (sunset 18:00 to sunrise 06:00) and daily relative humidity were calculated at each phenology site (see APPENDIX V). Additionally, volumetric soil moisture content data were temporally interpolated using locally weighted regression (loess) model to derive a daily time series of mean soil moisture (see APPENDIX V) at each phenology site. Temporal change in surface moisture across the entire study site was acquired by temporally interpolating the data from all sites to determine the end of the rain season and start of the dry season (see APPENDIX V).

3.4.3 Analysis

Regression analyses (i.e. mixed modelling, multivariate and univariate regression) and Information-Theoretic analysis were the main data analysis performed in this study. Therefore, cautious exploration of the data before analysis was undertaken to avoid violating the underlying assumptions of regression analyses that could cause Type I and Type II errors (Zuur, Ieno and Elphick, 2010; Zuur and Ieno, 2016). Graphics were crucial for data exploration because they can be applied to any data set, unlike normality and homogeneity tests that have a limited scope of application (Zuur, Ieno and Elphick, 2010 and references therein). Data quality checks undertaken in accordance with Zuur *et al.*, (2010) included: outlier detection; homogeneity of variance; normality of the data; collinearity; relationships between dependent and

independent variables; accounting for interactions; and dependence structures of response variables. Outliers were detected using box plots and queried in the main data to verify if they were actual values or error. Errors were subsequently eliminated from the dataset and data transformations implemented accordingly. Residuals were plotted against fitted values for checks on the homogeneity of variance and histograms used to check for normality of the data. Collinearity was assessed in models that had more than one variable by calculating the Variance Inflation Factors (VIF) and dropping variables accordingly where the VIF values were substantially large. Scatter plots of dependent and independent variables were used to examine the relatedness of dependent and independent variables and for evaluating the need for accounting for interactions. The appropriate mixed models (Baayen, 2008) were used where response variables showed dependence and imbalanced data structures.

The models used in this study are covered in detail under chapters 4, 5 and 6 with the appropriate steps undertaken for conducting regression analyses and presentation of results undertaken. These steps include justification of the models; presentation of the model output as graphs and tables (Zuur and Ieno, 2016).

CHAPTER 4. EVIDENCE OF URBAN HEAT ISLAND IMPACTS ON LANDSCAPE PHENOLOGY IN A TROPICAL CITY

4.1 Abstract

Knowledge about the effects of urban areas and the urban heat island intensity on vegetation phenology is vital for understanding the spatial patterns of vegetation ecosystem functions and vegetation phenological responses to the elevated temperature associated with climate change. To date, there is a general lack of knowledge and understanding about how the urban heat island (UHI) influences landscape phenological processes in the tropics despite there being sufficient evidence of these relationships in temperate cities. This study, therefore, aimed to examine vegetation phenological responses to urban form and distance from the city centre and the associated surface temperature differences in the tropical city of Kampala, Uganda. Estimates of vegetation growing season length and land surface temperature were derived from MODIS satellite imagery for the vegetation growing seasons of 2013, 2014 and 2015, and urban form was characterised using the Local Climate Zone (LCZ) classification (Stewart and Oke, 2012). This study showed that the length of the vegetation growing season increased with increasing distance along the urban-rural gradient ($p<0.001$) and was also longest in the least built-up LCZ class ($p<0.001$). Growing Season length significantly reduced with an increase in land surface temperature ($p<0.001$). These findings contrast with the traditional knowledge of phenological patterns in temperate cities, longer vegetation growing seasons are associated with higher temperatures and heavily built-up urban form types, suggesting that the UHI effect is a limiting factor to the length of the vegetation growing season in tropical cities.

4.2 Introduction

The phenomenon in which urban areas experience significantly higher temperatures than the less urbanised rural surrounding commonly termed the Urban Heat Island (UHI) results from differences in the cycling of energy and material between urban and rural areas (Landsberg, 1981; Voogt and Oke, 2003; Heisler and Brazel, 2010; Kleerekoper, Van Esch and Salcedo, 2012; Roth, 2012). The higher proportion of impervious surfaces and buildings at the expense of vegetated and pervious surfaces in urban areas promote heat capture and storage (Landsberg, 1981; Oke, 1987); minimises natural radiative cooling through evapotranspiration (Taha, 1997; Dimoudi and Nikolopoulou, 2003; Feyisa, Dons and Meilby, 2014) and impede water storage and capture (Barnes, Morgan and Roberge, 2001; Whitford, Ennos and Handley, 2001). Vegetation in urban environments lessens the UHI intensity through thermal regulation via evapotranspiration (Cavan *et al.*, 2014; Feyisa, Dons and Meilby, 2014; Norton *et al.*, 2015; Lee, Mayer and Chen, 2016) and provision of shade (Li, Ratti and Seiferling, 2018). In the tropics where climate change is expected to exacerbate the effects of high all-year-round temperatures, vegetation has the potential to buffer the urban populace and minimise the risk of exposure (Cilliers *et al.*, 2013; Lindley *et al.*, 2018).

UHI intensities are influenced by regional climate, the magnitude of seasonal changes in vegetation cover and the size and nature of urban morphology determined by differences in urban planning practices (Roth, 2007; Giridharan and Emmanuel, 2018). The tropics vary in terms of temperature and precipitation with five main tropical climate types according to the Köppen climate classification (Roth, 2007; Giridharan and Emmanuel, 2018). Equally tropical cities have inherent differences in city morphology (Cavan *et al.*, 2014; Antos *et al.*, 2016; Taubenböck, Kraff and Wurm, 2018). As of 2007, one-fifth of the UHI research focussed on tropical cities (Roth, 2007) and although the past decade has seen a significant increase in tropical urban climate research (Giridharan and Emmanuel, 2018), more exemplar UHI research is needed that depicts the differences in urban morphology and tropical climate types (Roth, 2007; Giridharan and Emmanuel, 2018). Furthermore, although there has been much research on the usefulness of vegetation on UHI mitigation in tropical cities, equivalent

understanding of the impacts of urbanisation and the associated UHI effect on vegetation phenology is very minimal in tropical cities (Jochner and Menzel, 2015).

Vegetation phenology is defined as the study of the seasonal timing of the different stages of plant growth (e.g. leaf, flower and fruit development), their magnitude and drivers (Fenner, 1998). The UHI induces early starts of the vegetation growing season in urban areas of temperate regions (Neil and Wu, 2006; Jochner and Menzel, 2015) due to the higher sensitivity of springtime vegetation development to temperature (and photoperiod) after wintertime dormancy (Menzel *et al.*, 2006; Zhang, Friedl and Schaaf, 2006). Although extensive research on urban phenological processes has been undertaken in temperate regions, equivalent understanding of the UHI effect on phenology in the tropics is limited (Jochner and Menzel, 2015) and emerges from two studies that have compared the UHI effect on the start of tree budding for select tree species between tropical and temperate cities (Gazal *et al.*, 2008; Jochner, Alves-Eigenheer, *et al.*, 2013). The effect of the UHI intensity was observed to exert a stronger influence in temperate than tropical cities (Gazal *et al.*, 2008; Jochner, Alves-Eigenheer, *et al.*, 2013) because UHI intensities are stronger in temperate than temperate cities (Roth, 2007).

Weak UHI intensities in the wet season (Roth, 2007; Giridharan and Emmanuel, 2018) season might have weak impacts on vegetation as it undergoes leaf flush during the wet season (Williams *et al.*, 1997; Clinton *et al.*, 2014; de Camargo *et al.*, 2018) as compared to much stronger UHI intensities in the dry season (Roth, 2007; Giridharan and Emmanuel, 2018). Stronger UHI intensities would result in stronger evaporation demand (Zipper *et al.*, 2017) and less soil moisture availability for vegetation use further intensifying the occurrence of leaf fall that occurs during the dry season with the increase of temperature (Williams *et al.*, 1997; Condit *et al.*, 2000; Dalmolin *et al.*, 2015; de Camargo *et al.*, 2018). However, present knowledge on tropical urban phenological processes (e.g. Gazal *et al.*, 2008; Susanne Jochner *et al.*, 2013) has focused on timing of start of leaf budding alone and overlooked the other phenological parameters such as end, duration, magnitude and intensity that represent later stages of vegetation development (Fenner, 1998; Denny *et al.*, 2014) and differ from start of season events (Guan *et al.*, 2014).

Phenology of individual species is inherently different from the combined phenological response of vegetation at the landscape scale (Badeck *et al.*, 2004; Jochner and Menzel, 2015), commonly known as landscape phenology (Liang and Schwartz, 2009; Morisette *et al.*, 2009). Landscape phenology provides an aggregate measure of the timing of start, end and duration of vegetation activity, covering a wide range of plant functional types and species (Liang and Schwartz, 2009; Morisette *et al.*, 2009). A comprehensive assessment of phenological processes at both species and landscape-scale are required to fully understand the effects of urbanisation and the UHI effect (Jochner and Menzel, 2015).

In temperate cities experiencing cool climates, heavily built-up urban areas experience extended vegetation growing seasons due to the UHI effect (White *et al.*, 2002; Zhang, Friedl, Schaaf, Strahler, *et al.*, 2004; Han and Xu, 2013; Dallimer *et al.*, 2016; Zhou *et al.*, 2016; Zipper *et al.*, 2016; Melaas *et al.*, 2016; Gervais, Buyantuev and Gao, 2017; Li *et al.*, 2017; Qiu, Song and Li, 2017; Yao *et al.*, 2017; Parece and Campbell, 2018; Ren *et al.*, 2018). The duration of the vegetation growing season has been observed to decline along the urban-rural gradient (Zhang, Friedl, Schaaf, Strahler, *et al.*, 2004; Zhou *et al.*, 2016) depicting the mesoscale UHI effect resulting from the presence of a city (Oke, 2008; Roth, 2012). Also, the duration of the vegetation growing season has been observed to be highly localised with relation to land cover composition (Melaas *et al.*, 2016; Zipper *et al.*, 2016; Parece and Campbell, 2018) depicting the local UHI effect (Oke, 2008; Roth, 2012). Equivalent understanding of landscape phenological processes in the context of tropical cities is lacking. The transferability and assumption of landscape phenological processes observed in temperate studies to tropical cities is limited due to the inherent differences in urban and regional climate between tropical and temperate regions (Roth, 2007; Giridharan and Emmanuel, 2018).

This study aims to examine the effect of the urban heat island effect on vegetation phenology in the tropical city of Kampala, Uganda. Therefore, the objectives of the study were to: (i) determine the influence of local climate climate depicted as urban form and distance from the city centre respectively on phenology (ii) determine the combined influence of the urban form and distance from the city centre on LST and how it varies between years; (iii) to assess the effect of elevated LST on phenology.

4.3 Materials and methods

4.3.1 Study area

The study focussed on Kampala the capital city of Uganda, located at 00°18′49″N 32°34′52″E (Figure 4-3) that has a population density of ~8700 inhabitants/km^2. The city's southern and northern limits are located approximately 25 km and 45 km respectively north of the equator (< 0.5°north of the equator). Kampala has a tropical rainforest (equatorial) climate (*Af*) (Köppen climate classification), characterised by two annual wet seasons (March-May & September-November). The most torrential rains per month are in the shorter rainy season (March to May) and July is the driest month.

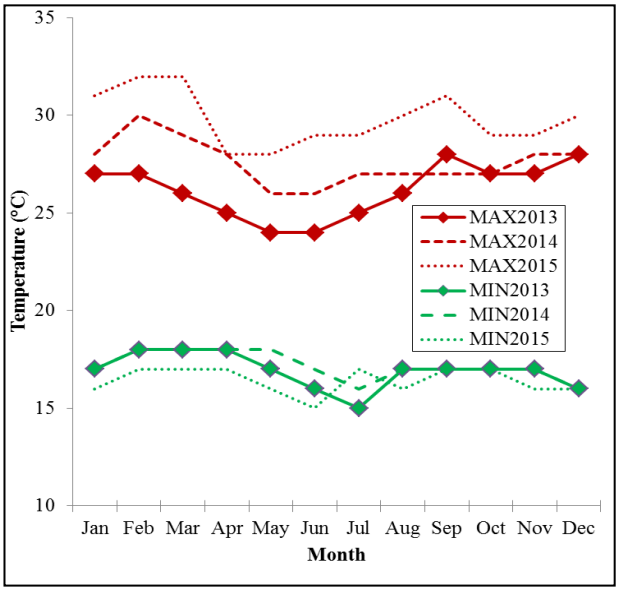

Figure 4-1: Monthly maximum and minimum air temperature across the study site in the 2013, 2015 and 2015 (Source: WorldWeatherOnline, 2019)

Also, June and July are the cooler months of the year whereas February experiences the warmest temperature throughout the entire year (see 3.1.2 and Figure 3-1). The years 2013, 2014 & 2015 that were used in this study varied in weather depicted by differences in air temperature (Figure 4-1) specifically maximum air temperature.

4.3.2 Data

The data sources used in this study were derived from satellite imagery, and data processing steps are summarised in Figure 4-2 and described in detail under the respective sections.

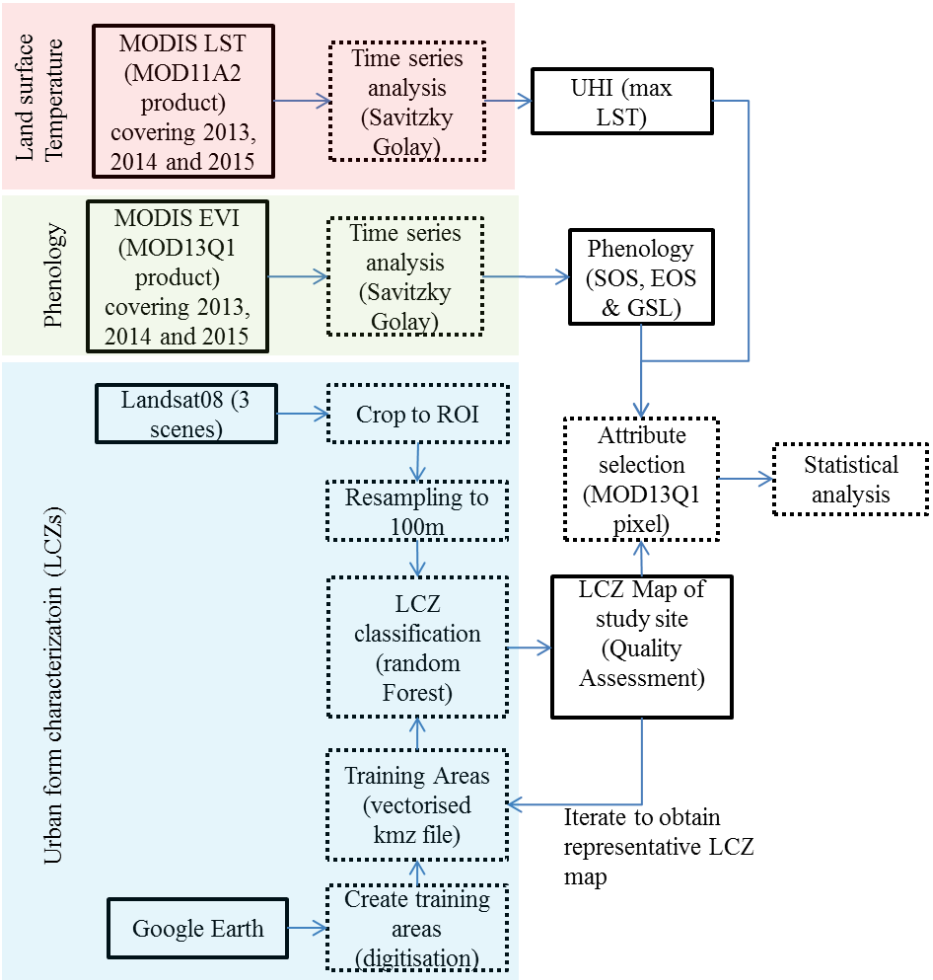

Figure 4-2 shows the workflow of the data processing steps and analysis used in this study

4.3.2.1 Urban form

We used the Local Climate Zone (LCZ) classification scheme (Stewart and Oke, 2012) to characterise urban form across the study site (Figure 4-3).

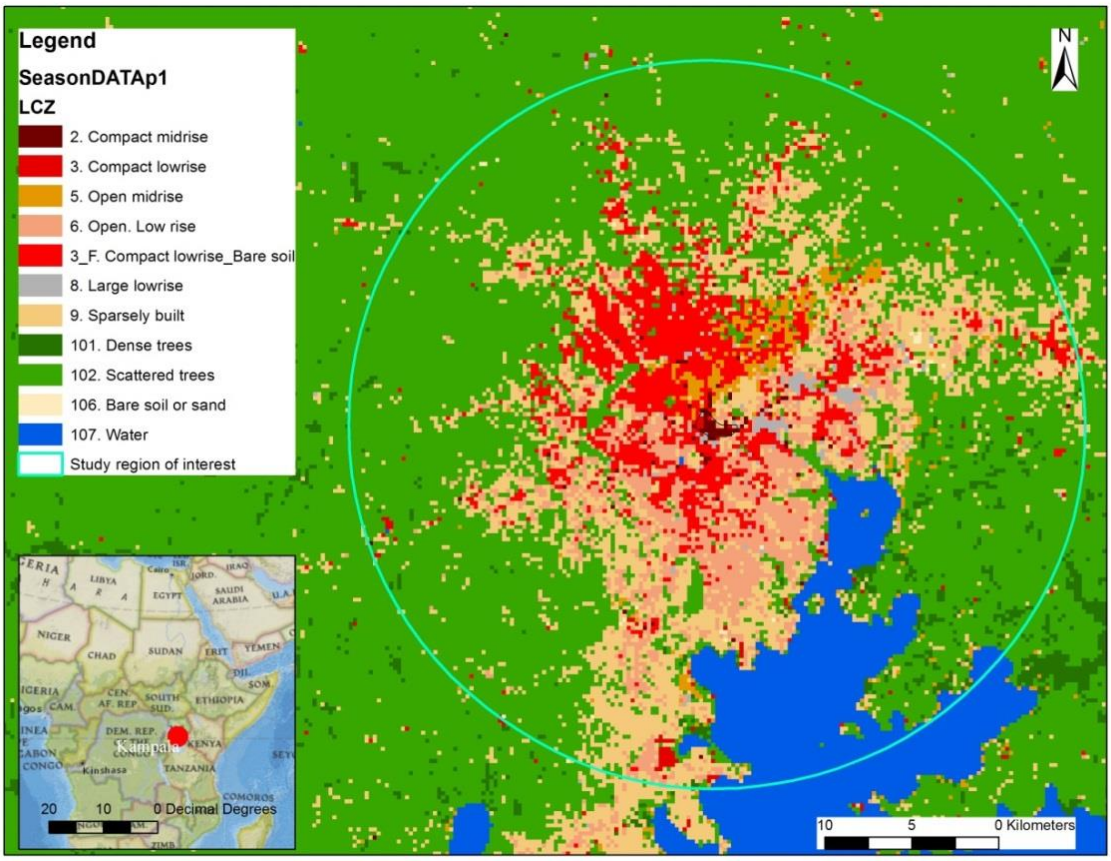

Figure 4-3: An LCZ map of Kampala showing the location of the study site and Region of Interest (within ~20 km of the city centre) that was the basis of the analysis.

LCZs are a robust, objective and universally applicable approach for characterising urban form and function of cities (Stewart and Oke, 2012; Stewart, Oke and Krayenhoff, 2014). In addition to their use and validation in urban climatology (Stewart, Oke and Krayenhoff, 2014; Geletič, Lehnert and Dobrovolný, 2016; Kotharkar and Bagade, 2018; Mushore *et al.*, 2019), LCZ usage has been extended to studying environmental processes related to the ecoclimatology of the LCZs (Perera and Emmanuel, 2018; Verdonck *et al.*, 2018; Brousse *et al.*, 2019; Franco *et al.*, 2019) validating their wider significance of application in urban ecology. The LCZ scheme contains seventeen classes, each representing unique surface cover and structural properties of the urban fabric, with provision for users to combine and create new classes, for zones that have characteristics that do not fall within the existing LCZ framework. An LCZ map was generated for the study site (Figure 4-3) using the World Urban Database and Access Portal Tools (WUDAPT) protocol for generating Level 0 data (Bechtel *et al.*, 2015, 2019). The method uses supervised machine learning to

generate a city-wide LCZ map from multispectral Landsat8 imagery in a 3-step process that involves: (i) acquisition and preprocessing of cloud-free images, (ii) creation of training areas in google earth and (iii) implementation of the classification in SAGA-GIS (Conrad *et al.*, 2015).

Two LANDSAT8 OLI-TIRS scenes obtained for the 27/02/2015 (dry) and 15/03/2015 (wet) season were selected to account for the spectral changes occurring from seasonal changes in vegetation cover. The images were radiometrically calibrated to Top of the Atmosphere reflectance and resampled from 30 to 100 m to obtain a spectral signal of urban structures at a local-scale representative of local-scale climate (Cai *et al.*, 2018). Training areas were selected using high spatial resolution imagery available within Google Earth. Subclass 3_F (Compact low rise_Bare soil) was included in the selection of LCZ-classes to highlight this type of urban form in Kampala that is absent in the standard set of LCZ classes (Stewart and Oke, 2012). The LCZ classification was implemented using Random Forest classifier in SAGA-GIS using the preprocessed LANDSAT8 images and training areas as inputs. Accuracy of the resulting LCZs was done by visual examination and reselection and reclassification of the image undertaken iteratively to improve the representativeness of the LCZ output. Four LCZ classes that covered a large proportion of the study area and that had different physical features (i.e. impervious surfaces and vegetation cover) were selected for the analysis. To derive more representative estimates of LST and the associated phenological response linked to different types of urban form, LCZs covering large areas were selected for subsequent analysis (Table 4-1 & Figure 4-4).

Table 4-1 shows the area covered by the selected LCZ types. In total this represented approximately 87% of the study area

LCZ category	Number of EVI pixels	~Area (Km^2)
LCZ B. Scattered trees	13664	854
LCZ 9. Sparsely built	4439	277
LCZ 6. Open Low rise	2186	136.7
LCZ 3_F. Compact low rise_ Bares soil	2144	134

LCZ type	Description	Surface characteristics
LCZ 3 (Compact low-rise) + LCZ F (Bare soil or sand) 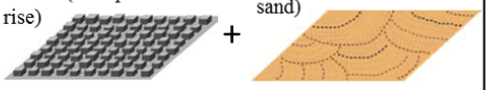	Dense mix of 1-3 storied buildings.. Concrete, stone, brick, tile structures dominated. Surface mostly covered by soil and paving	40-70 building fraction;
LCZ 6 (Open low-rise) 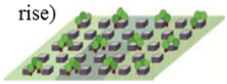	1-3 storied buildings interspersed with pervious vegetated areas. Low plants, scattered trees. Concrete, stone, brick, wood, tile structures	20-40 building fraction; <20-0% impervious surface fraction; >30-60% pervious surface fraction
LCZ 9 (Sparsely built)	Small or medium-sized buildings interspersed a natural setting with pervious surface. Low plants, scattered trees	10-20 building fraction; <20% impervious surface fraction; >60-80% pervious surface fraction
LCZ B (Scattered trees)	Mixed allotment of evergreen trees and low plants on pervious surface. Function includes: natural forest, tree cultivation and urban park	<10 building fraction; <10% impervious surface fraction; >90% pervious surface fraction

Figure 4-4: Characteristics of the candidate LCZ classes used in this study (Adapted from Stewart and Oke, 2012)

Remote sensing is useful for depicting spatial and temporal patterns of vegetation abundance in urban settings using Vegetation Indices (e.g. Weng, Lu and Schubring, 2004; Yuan and Bauer, 2007; Huete *et al.*, 2011; Senanayake, Welivitiya and Nadeeka, 2013). Vegetation Indices are proxy measures for "canopy greenness" connoting the combined properties of leaf chlorophyll, leaf area, canopy cover and structure (Huete *et al.*, 2011). In this study, estimates of vegetation abundance across 2013 derived from Enhanced Vegetation Index of MODIS satellite imagery (MODIS13Q1 EVI) were used to determine contrasts in surface cover across the candidate LCZs (Table 4-1) by performing a Kruskal-Wallis H-test and paired post-hoc tests. The MODIS13QI EVI images are 16-day composites with a spatial resolution of 250 m and are suited for urban environments because they minimise canopy background variations and maintain sensitivity over dense vegetation (Huete *et al.*, 2011). The images were acquired from the Oak Ridge National Laboratory (ORNL), Distributed Active Archive Centre (DAAC), of the National Aeronautics and Space Agency along with quality assessment images.

$$EVI=2.5(\rho_{NIR}-\rho_{RED})/(L+\rho_{NIR}+C_1\rho_{RED}-C_2\rho_{BLUE})$$

where ρ is reflectance; L is the canopy background adjustment factor, C_1 and C_2 are aerosol resistance weights. The coefficients are L=1; C_1=6 and C_2=7.5

4.3.2.2 **Vegetation Phenology**

This study was based on time series analysis of EVI images for the years 2013-2015 in TIMESAT 3.2 software. Accurate estimates of phenological responses necessitate phenological and climate data spanning multiple years to control for interannual variability of climate. This study focused on three years only to minimise the phenological response to rapid urbanisation, which is estimated to occur at a rate of 5% annually (Vermeiren *et al.*, 2012; Bidandi and Williams, 2017). The software was used to fit MODIS-EVI time series using an adaptive Savitsky-Golay algorithm which uses local polynomial fitting functions. The influence of clouds on the time-series was minimised by assigning low weights to data points with low quality using the MODIS pixel quality information (MOD13Q1 quality images). Phenology parameters (SOS, EOS and GSL) were extracted from the smoothed time series using the amplitude method (Jonsson and Eklundh, 2004; Eklundh and Jönsson, 2015). The amplitude method is better suited than the threshold method in urban settings because of low vegetation cover is making it hard to find a threshold for determining dates for start and end of season (Zhou *et al.*, 2016; Yao *et al.*, 2017).

4.3.2.3 **Land surface temperature**

To examine the effect of urban induced surface temperature on phenology, we derived land surface temperature data (LST) from the MODIS MOD11A2 product for the years 2013, 2014 and 2015. MODIS (Figure 4-2). Spatial patterns of high temperatures capable of affecting phenology across an entire season can be obtained from MOD11A2 due to the high temporal resolution of 8 days, and this product has been observed to provide adequate estimates of maximum air temperature in tropical urban environments (Ayanlade, 2016). Therefore, the peak temperature of a time series of MOD11A2 images fit in TIMESAT 3.2 software using the Savitzky-Golay fitting procedure was obtained to represent maximum temperature across the study site. MODIS quality images were included in the fitting procedure to de-noise the data and minimise the effects of could. Urban form type (LCZ class), EVI (i.e. vegetation cover),

LST and distance from the city centre were assigned to each MODIS13Q1 EVI pixel as the unit (data point) of the analysis (Figure 4-5).

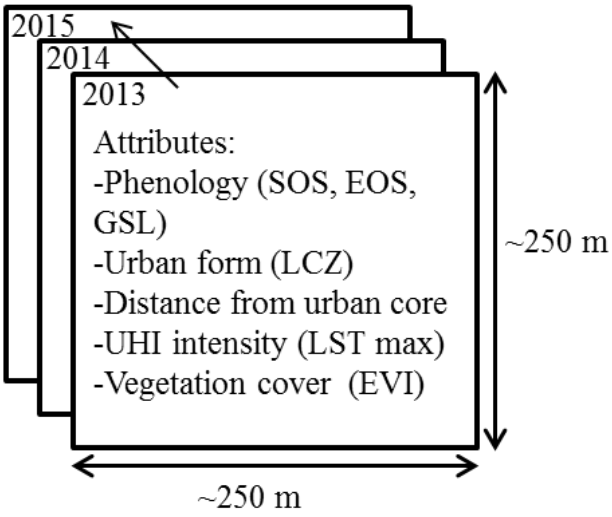

Figure 4-5 shows a summary of data attributes for each MODIS EVI pixel as a unit of the analysis

4.3.3 Data analysis

Linear mixed models were used to analyse the effect of urban form and distance from the city centre on SOS, EOS, GSL and LST. Therefore we fitted a model for each response variable into which we included local climate zone class and distance from the city centre as explanatory variables. Year was included as a fixed effect to control for differences across years in the phenology models. Interactions between year and urban form and between year and distance from the city centre were included in the LST model to account for varying effects of urban form and distance from the urban core among years on LST. Location was included as a random effect to allow for correlated error terms caused by repeated observations on the same pixel for each year. Therefore, each data point represented a given pixel location and its associated phenological and surface temperature attributes in a given year. The modelling was done using the "lmer" function of the "lme4" package in R (Bates *et al.*, 2015; R Core Team, 2018).

The significance of the final full model was tested against a null model comprising the intercept only using a likelihood ratio test. The significance of each explanatory variable was obtained by performing a likelihood ratio test comparing the full model with respective reduced models using the R function "drop1". Collinearity was

assessed by computing variance inflation factors using standard linear models that excluded random effects and interaction terms and no issues were found (Zuur, Ieno and Elphick, 2010). Normality and independence of the residuals were confirmed by inspecting qqplots and plots of residuals against fitted values.

To assess the influence of LST spatial differences on the timing of the start, end and duration of the vegetation growing season, a linear mixed model was fit with LST spatial difference and mean LST in a year as predictors and year as a random effect. This way, we were able to control for the effect of LST varying across years, while examining the influence of LST spatial differences. Within-subject centring (de Pol and Wright, 2009) allows for separation of spatial differences in LST and LST differences across years and their effect on GSL. Model diagnostics (significance of final full model and normality of residuals) were performed as described in the previous section.

4.4 Results

4.4.1 Surface and structural differences between urban form (LCZ) types

There were significant differences in vegetation abundance (i.e. mean EVI) among the LCZs and between all LCZ pairs (Figure 4-6). EVI (vegetation cover) decreased along a gradient of urbanisation intensity from the most to least built up LCZ type (i.e. Scattered trees > Sparsely Built > Open low rise > Compact low rise) (Figure 4-6).

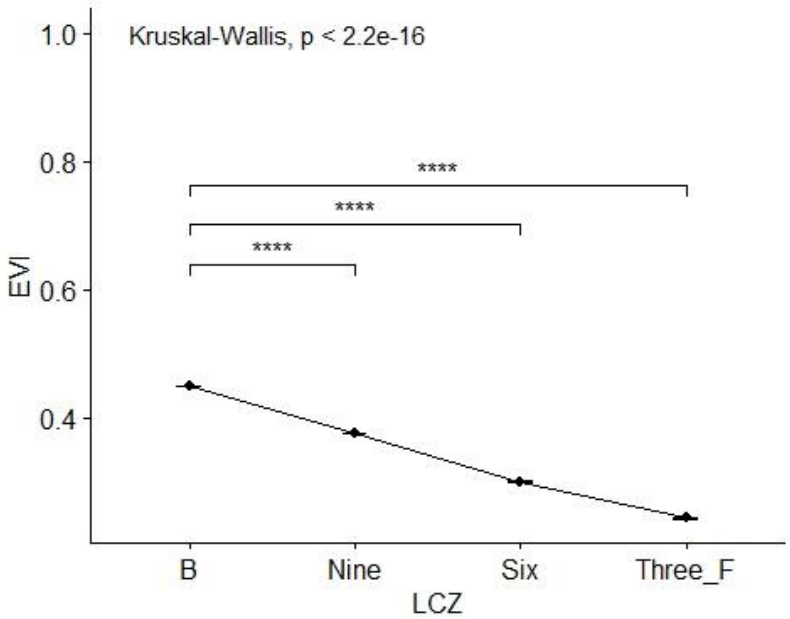

Figure 4-6 showing box plots depicting the denoting the extent and significance of differences in vegetation cover (EVI) across all LCZ types and between pairs of LCZs

4.4.2 Phenology

The predictors (i.e. LCZ, Distance and Year) had a well-defined influence on SOS (likelihood ratio test: X^2=1097, df=6, p<0.001), EOS (likelihood ratio test: X^2=7963, df=6, p<0.001) and GSL (likelihood ratio test: X^2=284.2, df=11, p<0.001). Specifically, LCZ type had a significant influence on SOS, EOS, and GSL (Table 4-2). LCZB (least built-up LCZ category) experienced the earliest SOS (Figure 4-7a) and the latest EOS (Figure 4-7c) in comparison to other built-up LCZs (Figure 4-7). As such, LCZB showed longer seasons than LCZNine (estimate=-3.3, standard error=0.5, p<0.001; Figure 4-7e), LCZSix (estimate=-8.6, standard error=0.7, p<0.001; Figure 4-7) and LCZ3_F (estimate=-13.2, standard error=0.7, p<0.001; Figure 4-7). Distance from the city centre significantly influenced Length of the season (Table 4-2) such that a 20 km increase in distance from the city increased the length of the growing season by more than two days (Figure 4-7). Although LCZ showed a significant influence on the timing of start and end season, distance from the city centre showed a negligible influence on the start and end of the growing (Table 4-2). Nonetheless, effect plots of distance from the city centre on SOS and EOS (Figure 4-7) show a general tendency towards later SOS and earlier EOS closer to the city centre than the distant rural areas.

Table 4-2 showing mixed model assessing the effect of urban form (LCZ) and distance from the city centre on Phenology

		Year	LCZ	Distance
SOS	F value	507.3	17	1.2
	NumDF	2	3	1
	DenDF	41,768	21,487	21,607
	Pr(> F)	0.0001	0.0001	0.27
EOS	F value	4,128	55.6	1.2
	NumDF	2	3	1
	DenDF	41,883	21,416	21,539
	Pr(> F)	0.0001	0.0001	0.28
GSL	F value	4,226	119	6.3
	NumDF	2	3	1
	DenDF	41,776	21,400	21,522
	Pr(> F)	0.0001	0.0001	0.012

4.4.3 Land surface temperature

Urban form, distance from the city centre and year significantly influenced LST (likelihood ratio test: X^2=37944, df=14, p<0.001). Although, LST showed pronounced differences consistently across all years in the same ascending order from the least built to most built-up LCZ category (i.e. Scattered trees < Sparsely Built < Open low rise < Compact low rise; Figure 4-7g), these LST differences among LCZ significantly varied among years (interaction between Year and LCZ: $F_{6, 43739}$ = 6.7, P < 0.001).

LST declined with increased distance from the city centre across all years (Figure 4-7h), but the magnitude of change significantly varied across years (interaction between Year and squared distance: $F_{2, 43819}$ = 1247.7, P < 0.001). The magnitude of LST differences between the urban and rural areas was higher in 2013 than 2014 and 2015 (Figure 4-7h). All years showed the comparably high temperature of ~28°C around the city centre, but rural areas in 2014 and 2015 experienced LST that was 2°C more than in 2013 (Figure 4-7h).

4.4.4 Relationship between LST and Phenology

The combined effect of spatial differences in LST representing the UHI effect and differences in LST across years had a significant effect on SOS (likelihood ratio test: X^2=21.5, df=2, p<0.001), EOS (likelihood ratio test: X^2=104.4, df=2, p<0.001), and GSL (comparison of full with null model: X^2=31.5, df=2, p<0.001).

There was a significant positive relationship between spatial differences in LST representing the UHI and SOS such that increase in LST resulted in later SOS (estimate=-0.5, standard error=0.1, p< 0.0001). However, was no effect of LST across years on SOS (estimate=-4, standard error=5, p=0.46).

EOS showed a negative relationship and statistically significant relationship with spatial differences in LST depicting the UHI effect (estimate=-1, standard error=0.1, p<0.0001) and LST differences across years (estimate=-24, standard error=2.3, p=0.002). In both cases, higher LST was associated with earlier ends of seasons.

There was a significant negative relationship between LST spatial differences depicting the UHI effect and spatial patterns of GSL such that increased temperature resulted in shorter seasons (estimate=-0.5, standard error=0.08, p< 0.0001). However, LST

differences among years were not significantly related to spatial patterns in growing season length (estimate=-20, standard error=7.2, p=0.07).

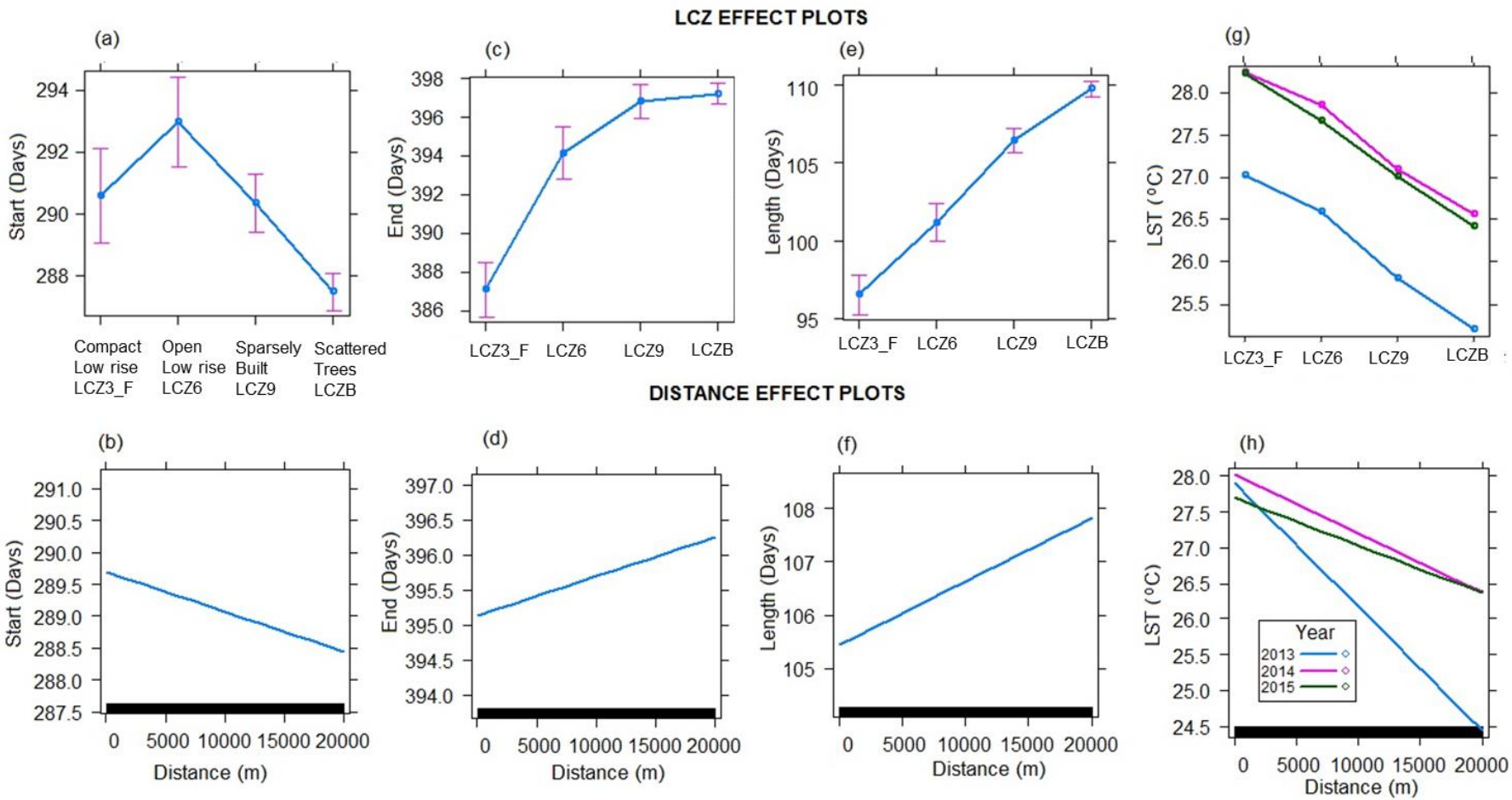

Figure 4-7: Effect plots showing the influence of urban form and distance from the city centre on Start (a & b), End (c & d) and Length (e & f) of season and day (g & h). LCZ classification: B-Scattered trees; Nine-sparsely Built, Six-Open lowrise; Three_F-Compact low rise_Bare soil

4.5 Discussion

Our results show that landscape phenological processes in the context of tropical urban areas are influenced by the Surface UHI intensity, such that higher Surface UHI intensities result in late SOS, early EOS and shorter GSL. LST which was used to characterise the Surface UHI in Kampala declined from the most to least built-up urban form types and along the urban-rural gradient (i.e. Compact low rise > Open low rise > Sparsely built > Scattered trees). The start of the season was observed to differ significantly across LCZ types with the least built (and highly vegetated) urban form type, LCZB (scattered trees) accounting for earlier SOS than heavily built-up urban form types. End of season occurred later in the lightly built LCZ types than heavily built-up LCZ types (i.e. Compact low rise < Open low rise < Sparsely built < Scattered trees). The GSL increased from the most to least built (and most vegetated) urban form type (i.e. Compact low rise < Open low rise < Sparsely built < Scattered trees). The distance gradient from the city to rural areas showed shorter GSL and higher LST in urban than rural areas. Moreover, LST differences along the distance gradient were observed to differ across years.

The select urban form types (LCZ classes) used in this study had contrasting surface characteristics, in terms of vegetation abundance and impervious surface as highlighted by differences in EVI. The LST differences across different LCZ classes highlight the influence of vegetation cover and impervious surfaces which is consistent with studies that have observed similar patterns in LST with relation to urbanisation intensity (Senanayake, Welivitiya and Nadeeka, 2013; Fonseka *et al.*, 2019; Mushore *et al.*, 2019). High latent heat flux through evapotranspiration associated with vegetated surfaces results in cooler temperatures in highly vegetated areas in comparison to areas of low vegetation cover (Roth, 2007; Cavan *et al.*, 2014; Giridharan and Emmanuel, 2018). Conversely, areas of high impervious surface are and building density is associated with higher thermal admittance, high heat storage and slow rates of cooling and resulting in high UHI intensities (Landsberg, 1981; Oke, 1987). However, LST differences along the urban-rural gradient differed across years. Specifically, LST differences across years occurred most strongly in the distant rural areas whereas the city centre recorded consistently high temperatures across all years.

The differences in annual weather conditions account for Inter-annual differences in spatial patterns of LST. The years 2013-2015 varied in terms of air temperature with 2014 and 2015 recording substantially higher air temperature than 2013 (Figure 4-1) as a result of the 2014 drought and 2015 el Niño (Bastos *et al.*, 2018; Zhang *et al.*, 2019). The year 2013 exhibited weather conditions depicting a typical year according to long-term climate records of Kampala (comparison between Figure 4-1 and Figure 3-1) with specific regard to maximum air temperature. Locations within and close to the city centre where vegetation cover is generally low and temperature is high did not exhibit substantial differences in LST between years, whereas rural areas in 2014 and 2015 experienced higher temperatures in 2013. This might suggest that the temperature associated with the regional climate anomaly was lower than the temperature associated with a great proportion of impervious surfaces and buildings within cities. However, the temperature associated with the regional climate anomaly was higher than the temperature in rural areas in 2013.

Although soil moisture was not accounted for in this study, the years 2014 and 2015 in comparison to 2013, might have experienced significant reduction in soil water resources because of the high evapotranspiration associated with high temperatures (Zipper *et al.*, 2017). This, in turn, resulted in shorter vegetation growing seasons and low vegetation cover in 2014 and 2015 in comparison to 2013. As with high LST across years limiting the length of vegetation growing seasons, high LST associated with heavily built-up urban form resulted in shorter vegetation growing seasons. In addition to low water availability resulting from high evaporation due to high temperature in heavily built-up areas, impede soil water capture and storage (Whitford, Ennos and Handley, 2001) might further limit water availability leading to shorter vegetation growing season. Moreover, vegetation management practice as through watering might explain the observation on early SOS in the most built-up urban form types (LCZ3_F; compact low rise) given the tendency for vegetation in heavily built up areas to have shorter growing seasons. On the other hand, longer growing seasons were observed in highly vegetated locations which agree with the findings of Guan *et al.*, (2014) natural tropical environments. Highly vegetated areas are often pervious and in this way could enable higher water capture and storage for plant use than heavily built

locations. Equally, highly vegetated areas have lower temperature and less water would be lost through evaporative demand resulting in higher water availability for vegetation use.

Our findings on the effect of urban form and distance from the city centre and the UHI intensity contrast with established phenological patterns in temperate cities (White *et al.*, 2002; Zhang, Friedl, Schaaf, Strahler, *et al.*, 2004; Han and Xu, 2013; Dallimer *et al.*, 2016; Zhou *et al.*, 2016; Zipper *et al.*, 2016; Melaas *et al.*, 2016; Gervais, Buyantuev and Gao, 2017; Li *et al.*, 2017; Qiu, Song and Li, 2017; Yao *et al.*, 2017; Parece and Campbell, 2018; Ren *et al.*, 2018), where heavily built-up areas show earlier SOS, later EOS and longer GSL.

4.6 Conclusion

In this study, we showed that GSL declines with an increase in temperature associated with the UHI effect. In tropical climates where water availability is so often considered the main driver of phenological activity, we provide important new evidence about the role temperature plays as a limiting factor to growing seasons length in the context of urban environments. The effect of low vegetation linked with shorter vegetation growing season might feedback into the local climate resulting in higher temperatures in areas that experience shorter growing season. As to whether shorter growing seasons resulting from elevated temperature were a consequence of low water availability through increased evapotranspiration was not covered under the scope of this study but is represented in chapter 5 of the thesis. Therefore, future studies on the influence of the UHI on phenology in tropical cities ought to account for the spatial and temporal variability of soil moisture.

This study demonstrates the usefulness of the LCZ scheme in the growing field of urban phenology and urban ecology. The evaluation of EVI at each LCZ level (a proxy for vegetation cover) was useful for understanding the intrinsic attributes of the LCZs and how they might be associated with local climate and phenology. This additional step of quantifying surface cover vis-à-vis vegetation abundance highlights the importance of using vegetation indices in order to corroborate our understanding of

the ecoclimatological characteristics of LCZs. This is particularly important in remote sensing studies that focus on the 2-dimensional feature space in cities.

The findings of this study are useful for understanding the impacts of different land-use decisions on vegetation seasonality and resulting impacts on vegetation ecosystem functions like climate regulation vegetation provision services. With this, policy changes aimed at improving urban ecosystem functions can be reached more so in developing cities that are rapidly urbanising and experiencing high de-vegetation, yet little information exists on the consequences of ongoing urbanisation practices. Moreover, urban planning policies for the management of green spaces and urban agriculture in cities would benefit from knowledge about the patterns and dynamics of vegetation seasonality.

CHAPTER 5. SPATIOTEMPORAL DYNAMICS OF URBAN CLIMATE DURING THE WET-DRY SEASON TRANSITION IN A TROPICAL AFRICAN CITY

5.1 Abstract

In the tropics, soil moisture drives the onset of vegetation activity and plays a significant role in the partitioning of energy in urban environments, such that the intensity of the urban-rural temperature differences is weaker in the wet than the dry season. However, an understanding as to how the influence of land cover composition varies between the wet and the dry season is very limited because of differences in urban morphology and tropical climate types among cities. Furthermore, the wet-dry season dichotomy overlooks the continuum of gradual temporal change in soil moisture and the resulting outcome for intra-urban climatic differences. Here investigate the spatiotemporal dynamics of urban climate during the wet-dry season transition in the tropical African city of Kampala, Uganda by: (1) examining spatial differences in urban climate (air temperature and relative humidity) with relation to daily changes in soil moisture; (2) and determining the variations in the influence of land cover composition on urban climate between the wet and dry season. We gathered soil moisture, air temperature and relative humidity from 22 locations that typify the wide range of surface and structural cover differences in Kampala (0% to 84% human-made impervious surfaces) across 50 days marking the transition from the wet to dry season in 2017. Our findings showed significant differences in the rate of increase in nighttime temperature during the dry-down period ($F_{1,22}$ =23.61, $p<0.0001$), with the most built-up locations showing the fastest rates of increase in nighttime temperature and less built-up locations the lowest. Similarly, rate of decline in relative humidity during the dry-down period strongly varied among locations with the most built-up locations undergoing a more rapid decline in relative humidity than densely vegetated and pervious areas ($F_{1,22}$=16.48, $p=0.0005$). However, the wet period preceding dry-down was marked by insignificant differences among locations in

the gradual decline and increase of nighttime temperature ($F_{1,22}$ =1.85, p=0.190) and relative humidity ($F_{1,22}$ =1.501, p=0.235) respectively. Landcover (i.e. paved surfaces, buildings and pervious surfaces) influenced spatial differences in nighttime temperature during both seasons, with paved surfaces accounting for 62.1% and 61.5% of the temperature differences during the wet and dry season respectively. Although tree cover was observed to have no significant effect on night time temperature during the wet season, during the dry season tree cover and pervious surfaces had a combined effect accounting for 61.7% of the night time temperature differences. The combined effect of the proportion of trees and pervious surfaces accounted for 77.6% of the differences in relative humidity during the wet season and 80.2% during the dry season. These findings are significant for understanding the effect of Urban Heat Island Intensity (UHI) on evapotranspirative demand and plant-water requirements within urban areas.

5.2 Introduction

Urbanisation alters the cycling of materials and energy in the atmosphere and near-surface through the replacement of natural vegetation and pervious land cover with buildings and impervious surface layers and intensified human activity such as heavy traffic (Grimm *et al.*, 2008; McCarthy, Best and Betts, 2010; Pataki *et al.*, 2011; Pickett *et al.*, 2011; Wu, 2014). Paved surfaces impede the uptake of water (Barnes, Morgan and Roberge, 2001; Whitford, Ennos and Handley, 2001) whereas artificial surfaces (e.g. concrete, asphalt and metal) and compactness of cities (i.e. high building density, tall buildings, narrow streets) promote the transformation of short wave radiation into heat and its retention (Landsberg, 1981; Oke, 1987). In contrast, highly pervious and vegetated areas within cities and neighbouring rural areas, have higher fluxes of latent heat than sensible heat through evapotranspiration (Taha, 1997; Dimoudi and Nikolopoulou, 2003; Weng, Lu and Schubring, 2004; Pataki *et al.*, 2011; Kleerekoper, Van Esch and Salcedo, 2012; Cavan *et al.*, 2014; Feyisa, Dons and Meilby, 2014; Duarte *et al.*, 2015; Lindley *et al.*, 2015). As a result, cities experience a distinct climate from their neighbouring rural surroundings which includes an elevated temperature in what is commonly known as the urban heat island effect (Landsberg, 1981; Voogt and Oke, 2003; Heisler and Brazel, 2010; Kleerekoper, Van Esch and Salcedo, 2012). The urban

heat island effect increases evapotranspirative demand and water requirements in urban areas (Zipper *et al.*, 2017) which might in turn affect canopy cover and the provision of regulatory functions of vegetation.

Urban climates differ from regional climate as a result of urbanisation. To date, there are fewer empirical studies and less knowledge about the urban climate in tropical than temperate cities. Although the UHI phenomena and the urban climate theory apply virtually to all cities, differences in baseline regional climates imply that the vast body of literature and theory about urban climate in temperate cities may not be transferable to tropical cities. For example, UHI intensities have been observed to be weaker in tropical than temperate cities due to differences in surface energy balance and anthropogenic heat release (Roth, 2007). Consequently, there is a need for further research on the urban climates of the tropics that exemplify the wide range of tropical urban climate types (Giridharan and Emmanuel, 2018). Moreover, tropical developing cities represent ~90% of the forecasted global growth in urban size and population (Schneider, Friedl and Potere, 2010) and are expected to be most affected by the impacts of climate change (Heisler and Brazel, 2010; Pauleit *et al.*, 2015).

Although the last decade has seen a rise in the number of tropical urban climate studies (Giridharan and Emmanuel, 2018), a significant proportion of these studies have emerged from Asia and far fewer studies are reported from Africa. African cities also represent a very small proportion (~1%) of studies on urban green space and densification (Haaland and van den Bosch, 2015). Rapid growth in urban populations of several countries in tropical Africa, and insubstantial coping strategies of urban planning structures to pressures and demand for infrastructural changes have led to polarised developments (Bidandi and Williams, 2017; Lindley *et al.*, 2018). As such, many such cities in Africa are characterised by heterogeneous urban morphology consisting of extensive areas of informal developments and this complexity in urban morphology varies between cities (Cavan *et al.*, 2014; Antos *et al.*, 2016).

In the context of tropical African cities, UHI intensities have been observed to be highest at night (Ojeh, Balogun and Okhimamhe, 2016) and to increase as a result of high building density (Cavan *et al.*, 2014; Ayanlade, 2016; Mushore *et al.*, 2019) and

development of informal settlements (Scott *et al.*, 2017). In contrast, vegetation cover has been observed to decrease the intensity of the UHI effect (Cavan *et al.*, 2014; Feyisa, Dons and Meilby, 2014; Ayanlade, 2016). Urban climate is increasingly being analysed with relation to land cover composition wholly as opposed to a single aspect of land cover such as vegetation in acknowledgement of the connectivity of urban features at a local scale (Stewart and Oke, 2012). Although some studies have done so in Africa (e.g. Cavan *et al.*, 2014; Mushore *et al.*, 2019), the differences in urban morphology between cities (Cavan *et al.*, 2014; Antos *et al.*, 2016; Taubenböck, Kraff and Wurm, 2018) necessitates further research that exemplifies the wide variety of urban morphologies in African cities.

Soil moisture partitions incoming solar and longwave radiation into outgoing longwave radiation, latent, sensible and ground heat flux (Lakshmi, Jackson and Zehrfuhs, 2003). Soil moisture considerably influences energy partitioning in cities alongside land cover such that the weaker season experiences weaker UHI intensities than the dry season (Roth, 2007; Giridharan and Emmanuel, 2018). Stronger UHI intensities have been observed in several tropical African cities (Balogun and Balogun, 2014; Ayanlade, 2016; Ojeh, Balogun and Okhimamhe, 2016), and tropical cities elsewhere in the world (Roth, 2007; Giridharan and Emmanuel, 2018). However, there are no studies to date that have examined the seasonality of urban climate within African cities which have a tropical rainforest climate, where precipitation levels are often higher than other tropical climate types. The wet and dry season transition is an important phase for leaf flush in trees (de Camargo *et al.*, 2018). Differences in how the UHI effect influences evapotranspirative demand, and the associated differences in plant water requirements (Zipper *et al.*, 2017), as a consequence of the transition from wet to dry, may have a subsequent influence upon the extent of leaf flush and canopy establishment and thus climate regulation (Feyisa, Dons and Meilby, 2014). However, there is a lack of understanding to date of intra-urban differences in the wet-dry season transition.

The UHI effect has dominated tropical urban climate research (Roth, 2007; Giridharan and Emmanuel, 2018) because of its relevance to human health (Heaviside, Macintyre and Vardoulakis, 2017). Relative humidity which is an essential predictor of:

spatiotemporal dynamics of soil moisture (e.g. Archibald and Scholes, 2007; Roth, 2007; Yang, Ren and Hou, 2017; Cai *et al.*, 2019); and phenological processes (Do *et al.*, 2005; Archibald and Scholes, 2007; Jochner, Alves-Eigenheer, *et al.*, 2013) remains overlooked in tropical urban climate ecology.

In this paper, we aim to investigate the spatiotemporal dynamics of urban climate during the wet-dry season transition in the tropical city of Kampala, Uganda. Our main objectives are as follows:

- To determine the relationship between spatial differences in urban climate (air temperature and relative humidity) and daily changes in soil moisture from the wet season through to dry down.
- To determine the differences in the influence of land cover composition on urban climate between the wet and dry season

5.3 Methods

5.3.1 Study area

The study was carried out in Kampala (located at 00°18’49”N 32°34’52”E), the capital city of Uganda (Figure 5-1), which has a population density of ~8700 inhabitants/Km2. Kampala has a tropical rainforest (equatorial) climate (Köppen climate classification) and experiences two rainy seasons per year, during March-May and September-November. March-May is the shorter of the two rain season, although it experiences the most torrential rains (~169 mm) whereas July receives the least rainfall (~ 63 mm). In 2017, the dry season started in May and continued through September (Figure 5-2). This study focused on 50 days spanning the wet-dry transition (i.e. Julian day DOY: 100-150).

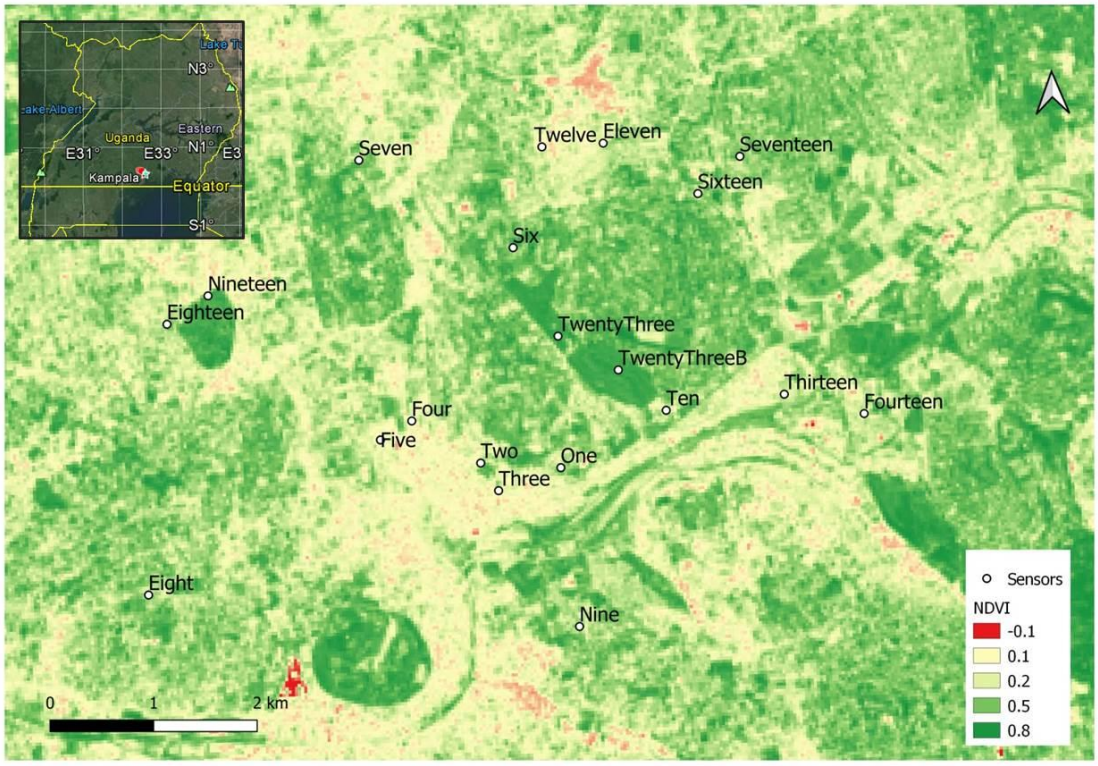

Figure 5-1: Location (numbered) of the urban climate monitoring sites and volumetric soil moisture content (crossed) with relation to proportion of man-made features (and vegetation cover, as indicated by higher values of the NDVI (normalised difference vegetation index))

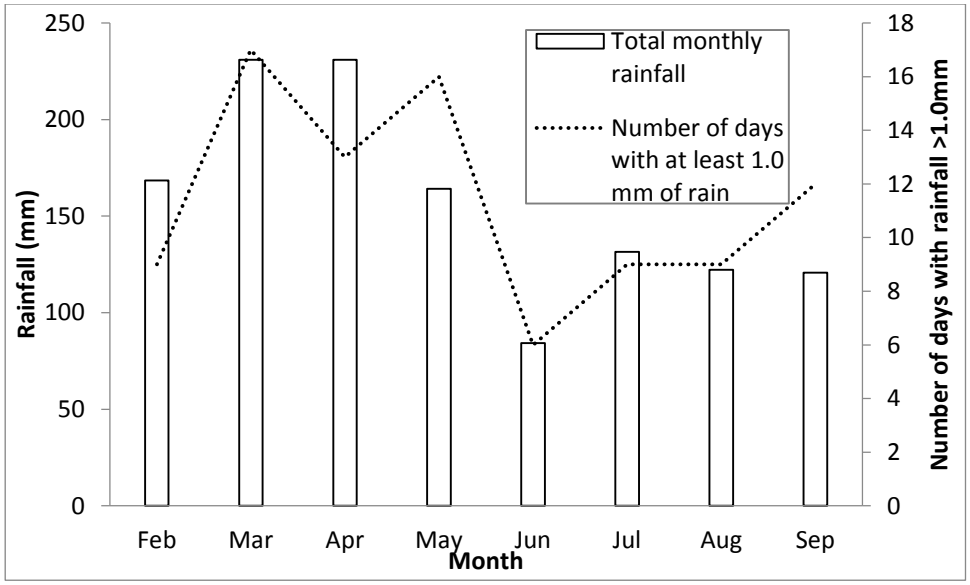

Figure 5-2: Kampala's climate between February and September 2017, depicting monthly rainfall and number of days with more than 1mm of rain

5.3.1.1 **Meteorological sites and data**

Twenty two sites were selected across Kampala Figure 5-1 that represented the wide range in surface cover and structure (Table 5-1) that are known to influence local climate (Stewart and Oke, 2012) and in turn influence urban ecological processes (Grimm *et al.*, 2008; McCarthy, Best and Betts, 2010; Pataki *et al.*, 2011; Pickett *et al.*, 2011; Wu, 2014). Air temperature and relative humidity data were acquired at each site using i-button sensors (model DS1923, Maxim Integrated) housed in a radiation shield positioned at the height of 3 m above the ground. The loggers were individually factory calibrated in a NIST (National Institute of Standards and Technology)-Traceable chamber (MaximIntegrated, 2010) before deployment in the field and assessed for drift during data collection. Each sensor collected temperature and relative humidity data at 30-minute intervals, and we calculated the daily average of nighttime temperature (sunset 18:00 to sunrise 06:00) and daily relative humidity at each location. The daily standard deviation of nighttime temperature and relative humidity across all allude was computed to determine spatiotemporal variation.

5.3.1.2 **Characterization of meteorological sites**

The urban environment was characterized via an Object-Based image Analysis classification of a WorldView3 satellite image (spatial resolution of 0.5 m) taken on 25/10/2016. Buildings, paved surface cover and pervious surfaces were classified and their proportion (percentage) at each site quantified within 200 m. Although a radius of 200 m for homogenous continuous urban form has been recommended as the zone of influence for local urban climate related to surface cover and surface structure (Stewart and Oke, 2012), the land cover around our candidate sites was heterogeneous. Therefore, the representativeness of an area of a 200 m radius for attributing local climate to land cover was compared to the effectiveness of a smaller area (radius of 100 m) with less land cover heterogeneity.

Each site was assigned to one of three urban intensity groups (i.e. high, medium and low), on the basis of similarity in land cover composition, using hierarchical cluster analysis for the 100 m and 200 m land cover data separately. Analysis of similarity (ANOSIM) (Clarke, 1993) was used to statistically test whether urban climate significantly differed between the urban intensity groups for both the 100 m and 200

m separately The ANOSIM indicated that the 100 m data set showed more significant differences in urban climate between the intensity groupings than the commonly used 200 m radius approach (R=0.556 (p=0.001) and n R=0.321 (p=0.005); respectively). Therefore subsequent analysis on the influence of landcover on urban climate and was based on land cover within a radius of 100 m of each meteorological site (Table 5-1).

Table 5-1 showing the urban intensity groups and propotion of different land cover types (impervious surfaces, paved surfaces, buildings, trees and pervious surfaces) at each location. Location used for observation on volumetric soil moisture content are in bold and underlined

Urban intensity groups	Location number (code)	Impervious surfaces (%)	Paved surfaces (%)	Buildings (%)	Trees (%)	Pervious (%)
HIGH	05	84	49	35	5	11
	12	81	21	60	6	13
	04	80	35	44	9	11
	03	79	36	44	9	12
	11	69	37	32	11	21
	14	65	32	33	13	21
MEDIUM	**13**	**59**	**39**	**21**	**11**	**30**
	10	59	39	21	21	19
	01	**51**	**32**	**20**	**37**	**12**
	09	49	17	32	24	26
	02	**48**	**39**	**9**	**30**	**22**
	17	44	22	22	28	28
	18	37	14	23	20	43
	16	**33**	**13**	**20**	**31**	**35**
	08	**33**	**16**	**17**	**18**	**49**
LOW	**07**	**23**	**5**	**19**	**35**	**42**
	06	**19**	**10**	**9**	**15**	**65**
	19	19	11	8	31	50
	23	9	8	1	43	48
	22	5	4	2	50	45
	22B	**0**	**0**	**0**	**60**	**40**
	23B	**0**	**0**	**0**	**44**	**56**

5.3.1.3 **Data on soil moisture changes**

To relate spatial differences in urban climate to daily changes in soil moisture from the wet period through to dry down, soil volumetric moisture content (VMC; Table 5-1) was measured in nine of the twenty-two sites. These nine sites represent a wide range of surface covers and structures within Kampala. Soil VMC (expressed as a percentage) was measured twice a week using a ThetaProbe (model ML3 ThetaProbe , Delta-T Devices), at five points at each site. The VMC data were temporally interpolated using locally weighted regression (loess) model to derive a daily time series of mean soil moisture across the entire study site and determine the end of the wet season and beginning of dry down (Figure 5-3). The day of year when VMC was greatest marked the end of the wet season and was used to demarcate the wet and dry seasons. Mean soil moisture from the nine sites across Kampala gradually increased and reached its peak at DOY~130 which was in the first week of May 2017. (Figure 5-2 & Figure 5-3). This period was marked as the end of the wet season and beginning of the dry down period.

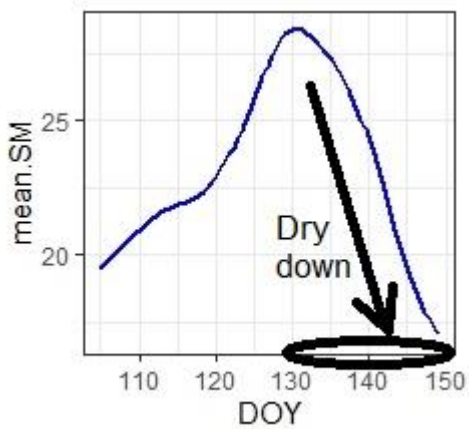

Figure 5-3: Temporal change in Volumetric moisture content that was used to demarcate the dry down period from the rainy season. Dry indicate the transition for the wet season show the transition time of the end of the rains and start of the dry down period (DOY=130)

5.3.2 Data analysis

5.3.2.1 **Temporal change in urban climate**

Linear mixed models (Baayen, 2008) were used to determine the effect of urbanisation represented as the proportion of human-made features on rate of change of urban climate. The proportion of impervious surfaces (i.e. proportion of building and paved surfaces) and Julian day (DOY) and their interaction were used as fixed effects

(predictor variables), and a separate model generated for each of the two urban climate variables for the wet and the dry season separately. Therefore, each data point in each model represented the urban climatic data on a given day at a given location. As such, individual location was included as a random effect for correlated error terms caused by repeated measures taken at the same location. The significance of the full model was determined using a likelihood ratio test comparing the full model to a null model (lacking the temporal autocorrelation structure). Visual inspection of residuals plotted against fitted values revealed normally distributed and homogeneous residuals. For better interpretation of model coefficients, we centred DOY around zero. The modelling was done in R using the "nlme" package (Pinheiro *et al.*, 2018; R Core Team, 2018).

Additionally, linear regression was used to compare daily changes in spatial differences in urban climate between the wet and the dry season. The significance of time (DOY) for the daily standard deviation across all sites of nighttime temperature and relative humidity was analysed and compared between the wet and the dry season. To determine the relationship between soil moisture and spatial difference in urban climate, we used analysed the relationship between daily mean soil moisture and daily spatial differences in relative humidity and nighttime air temperature using linear regression.

5.3.2.2 **Influence of land cover composition**

The relative influence of land cover composition on nighttime temperature and relative humidity during the dry and wet season was assessed using an Information-Theoretic approach (Burnham, Anderson and Huyvaert, 2011). Regression models were derived using combinations of indicators of land cover types (i.e. proportion of paved surfaces; pervious surface; buildings, tree cover) as predictors of relative humidity and night time temperature for the wet and dry season separately. Collinearity between predictor variables was assessed by calculating variance inflation factors ("vif" function of the R package *car*) for each model, with variables with VIF>3 removed from the models. The explanatory effect of other variables not covered under the scope of this study was accounted for by including a null model in each set of models. Model selection was undertaken using the MuMIn package in R [R version

3.5.0 (Barton, 2018; R Core Team, 2018)] to identify models with the simplest structure that best predicted relative humidity and nighttime temperature. Ranking of models was undertaken using the Akaike Information Criterion (AICc) corrected for small samples. The significance of predictor variables investigated under the scope of this study was considered to be weak if the null model (intercept only) had a ΔAICc =0. Models with ΔAIC <2 were considered as potentially suitable models. Variables that best predicted urban climate were identified from the relative importance values (RIV) derived from the sum of Akaike weights (Burnham and Anderson, 2003).

5.4 Results

5.4.1 Temporal change in urban climate with relation to proportion of man-made surface

All locations experienced a decrease in nighttime temperature with the advancement of the wet season depicted by an increase in soil moisture whereas advancement of the dry season was associated with increases in nighttime temperature (Figure 5-3 and Figure 5-4 (c & d)). Whereas, the increase in soil moisture during the wet season was associated with increase in relative humidity, the decline in soil moisture during the dry down period was associated with a decline in relative humidity across all locations (Figure 5-3 and Figure 5-4 (a & b)).

5.4.1.1 **Nighttime temperature**

The proportion of man-made surfaces and time (DOY) significantly influenced night time temperature during both the wet (likelihood ratio test: $p<0.0001$) and dry season (likelihood ratio test: $p<0.0001$). The built-up locations recorded the highest levels of nighttime temperature whereas the least built-up locations recorded the lowest nighttime temperature at any one point in time during the dry and the wet season (Figure 5-4 (a) & (b)). Although temperature differences significantly increased among locations with the advancement of the dry season (interaction between DOY and built-up area: $P =0.03$), the preceding period marking the wet season showed insignificant changes in the magnitude nighttime temperature differences among locations (interaction between DOY and built-up area: $P = 0.45$. The variation in the temporal change of spatial differences in nighttime temperature between the wet and the dry season was shown in the evolution of the standard deviation of night time temperate.

Spatial differences in nighttime temperature were relatively static during the wet season (significance of the effect of time: $F_{1,22}$ =1.85, p=0.190), but significantly increased with dry down ($F_{1,22}$ =23.61, p<0.0001; Figure 5-5 (a)). Spatial differences in nighttime temperature during the dry season had a strong positive relationship with mean soil moisture (R^2=0.503; $F_{1,22}$ =24.28, estimate ± SE: -0.023 ±0.005, t_{22}=-4.972, p<0.0001; Figure 5-5(b)).

5.4.1.2 **Relative humidity**

Spatial differences in relative humidity were significantly influenced by the proportion of human-made surfaces and time during the wet (likelihood ratio test: p=0.0374) and the dry season (likelihood ratio test: p<0.0001). The most built-up locations consistently recorded the lowest relative humidity whereas the least built-up locations recorded the highest levels of relative humidity throughout the observation period (Figure 5-4 (c) & (d)). As with nighttime temperature, the advancement of the dry season showed significant increase in spatial differences in relative humidity (significance of the effect of time: $F_{1,22}$ =16.48, p=0.0005; Figure 5-5(c)), whereas the day to day variation in relative humidity was insignificant during the wet season ($F_{1,22}$ =1.501, p=0.235). Spatial differences in relative humidity (i.e. standard deviation) had a significant negative relationship with mean soil moisture (R^2=0.493; $F_{1,22}$ =23.33, estimate ± SE: -0.074 ±0.015, t_{22}=-4.83; p<0.0001; Figure 5-5(d)).

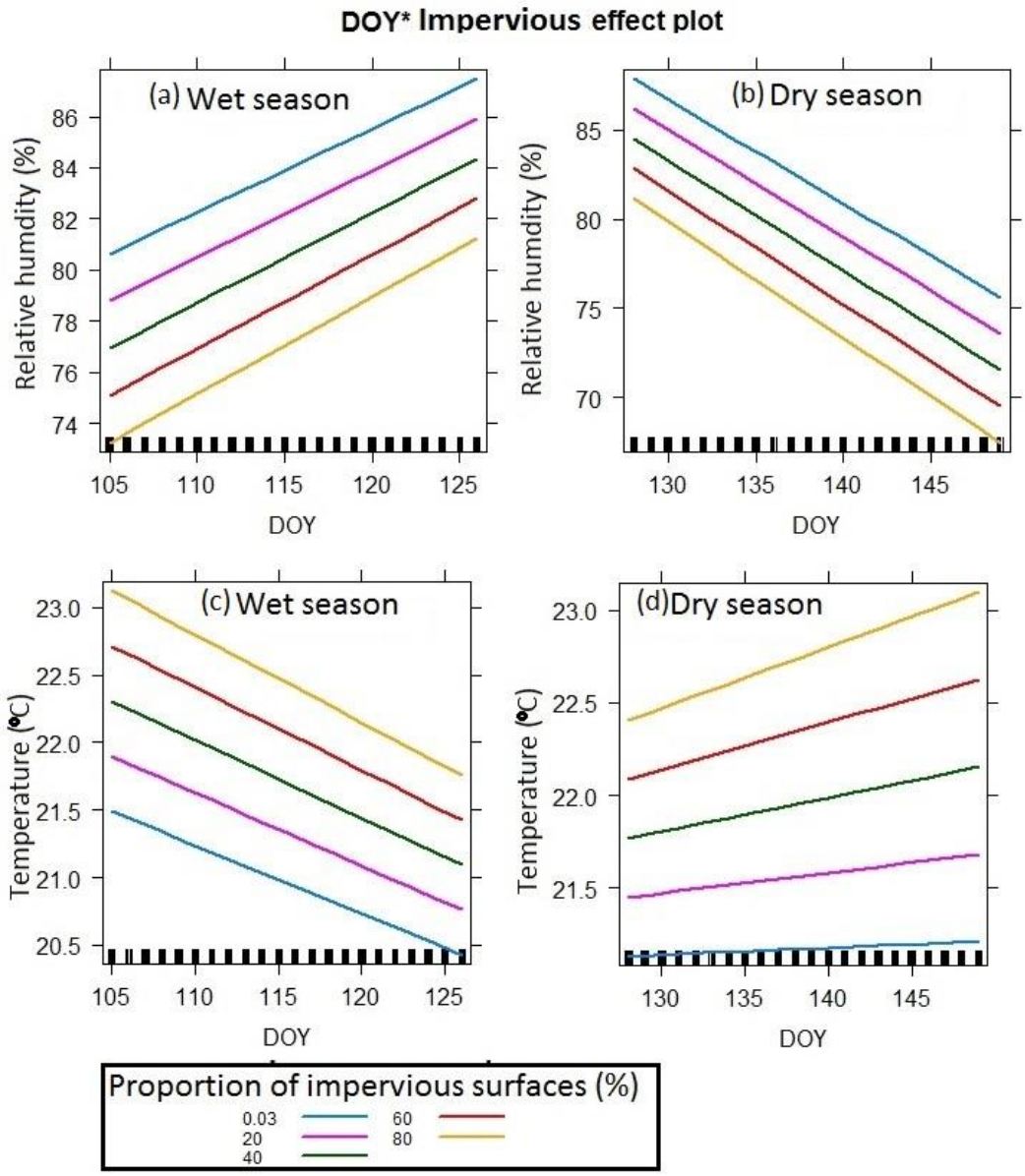

Figure 5-4: Spatiotemporal differences in night time air temperature and relative humidity with relation to proportion of man-made features

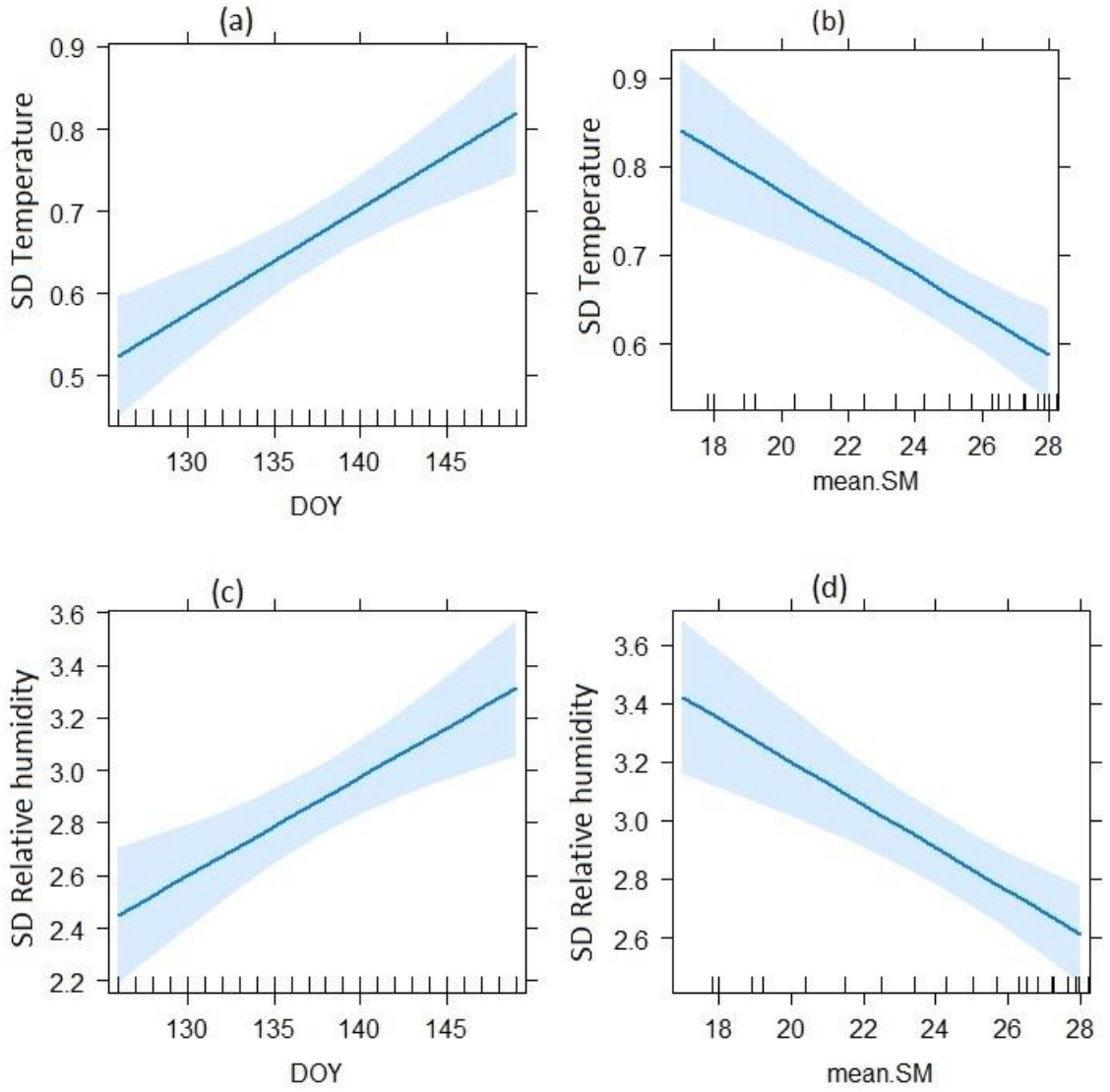

Figure 5-5: Spatiotemporal differences in temperature (a) and relative humidity (c) during the dry season. (b) Relationship between spatial differences in temperature and mean soil moisture. (c) Relationship between spatial differences in relative humidity and mean soil moisture

5.4.2 Influence of land cover on urban climate

5.4.2.1 **Temperature**

Three candidate models (of the 16 models) explaining the variation in nighttime temperature during the wet season had a ΔAIC<2 (Table 5-2). The proportion of paved surfaces, impervious surface and buildings were in the three top models, but the Relative Importance Value (RIV) of paved surfaces was more than twice as high as all other variables. Paved surfaces significantly influenced night time temperature during the wet season (R^2=0.621, $F_{1,22}$ =33.77, p<0.0001). Specifically, nighttime temperature increased with increasing paved surface area (estimate ± SE: 0.034 ± 0.006, t_{22}=5.811,

p=0.0001). Low temperature was also associated with high proportion of pervious surfaces (Table 5-2).

There were four top models with ΔAICc < 2 predicting night time temperature spatial differences during the dry season (Table 5-2). All land cover types covered under the scope of this study were observed to influence spatial patterns of nighttime temperature, including the proportion of trees that was insignificant during the wet season. However paved surface had a high RIV that was almost double the next land cover variable (pervious surfaces; Table 5-3) indicating the strong importance of paved surfaces in both seasons.

5.4.2.2 **Humidity**

The proportion of trees, buildings, pervious surfaces and impervious surfaces featured in the top candidate models predicting relative humidity (ΔAIC<2). Proportions of pervious surfaces and trees had the highest RIV scores (Table 5-3) and significantly influenced spatial differences in relative humidity during both the wet (R^2=0.776, $F_{2,22}$ =35.67, p<0.0001) and dry (R^2=0.8, $F_{2,22}$ =41.53, p<0.0001) seasons. Increase in relative humidity during the dry season was related with both high pervious surface area (estimate ± SE: 0.115 ± 0.025, t_{22}=4.645, p=0.0002) and increases in tree cover (estimate ± SE: 0.057 ± 0.023, t_{22}=2.390, p=0.028). Similarly, relative humidity during the dry season had a positive relationship with pervious surface area (estimate ± SE: 0.130 ± 0.024, t_{22}=5.332, p<0.0001) and tree cover (estimate ± SE: 0.052 ± 0.023, t_{22}=2.203, p=0.041).

Table 5-2: AICc statistics for models for relative humidity and nighttime temperature with relation to land cover for the wet and dry season. AICc = AIC corrected for small sample size, df = degrees of freedom, R^2 = adjusted regression coefficient, p = p-value, ΔAICc = difference between the top model and given model AICc, wi = model weight. Only models with ΔAICc < 2 are shown.

Period	Urban climate	Model variables	AICc	logLik	df	Adjusted R^2	p	delta	weight
Wet	Temperature	Paved surfaces	25.64	-9.11	3	0.621	0.00001	0	0.472
Wet	Temperature	Buildings, paved surfaces	26.21	-7.85	4	0.645	0.00003	0.568	0.355

Wet	Temperature	Pervious surfaces	27.64	-10.113	0.583	0.00003	2	0.173
Wet	Humidity	Pervious surfaces, Trees	76.38	-32.944	0.776	0.00000	0	0.678
Wet	Humidity	Buildings, Paved surfaces	77.87	-33.684	0.760	0.00000	1.488	0.322
Dry	Temperature	Paved surfaces	26.91	-9.75	0.615	0.00002	0	0.374
Dry	Temperature	Buildings, Paved surfaces	27.53	-8.51	0.638	0.00004	0.616	0.275
Dry	Temperature	Pervious surfaces	28.13	-10.363	0.592	0.00002	1.214	0.204
Dry	Temperature	Pervious surfaces, Trees	28.77	-9.13	0.617	0.00006	1.854	0.148
Dry	Humidity	Pervious surfaces, Trees	75.61	-32.564	0.802	0.00000	0	0.724
Dry	Humidity	Pervious surfaces	77.54	-35.063	0.762	0.00000	1.926	0.276

Table 5-3: Relative importance values (RIV) of predictor variables for models relating land cover with temperature and relative humidity during both the wet and dry season

Period	Urban climate	Paved surface	Pervious surface	Buildings	Trees
Wet	Temperature	0.72	0.28	0.29	0.22
Wet	Humidity	0.26	0.74	0.33	0.53
Dry	Temperature	0.65	0.34	0.28	0.22
Dry	Humidity	0.13	0.87	0.23	0.55

5.5 Discussion

This study demonstrated the synergistic effect of soil moisture and land cover composition on intra-urban climatic variability. The effect of land cover composition varied according to water availability such that gradual increases in soil moisture were matched by a gradual decline in relative differences in both nighttime temperature and relative humidity. On the other hand, diminishing soil moisture gradually intensified urban climatic differences among sites. The proportion of buildings, paved and pervious surfaces accounted for spatial differences in nighttime temperature during both seasons. Whereas trees had no significant effect on spatial differences in air temperature during the wet season, their influence was more pronounced during the dry season. The combined effect of proportion of trees and pervious surface accounted for 77.6% of the differences in relative humidity during the wet season and 80.2% during the dry season in the dry season. Higher coefficient of determination for the relationship between land cover composition and urban climate were generally observed for relative humidity than nighttime air temperature.

Spatial differences in urban climate with relation to proportion of human-made features were observed at all points in time. Heavily built-up areas consistently experienced the highest nighttime temperatures and lowest relative humidity, whereas the least built-up locations experienced the lowest temperatures and highest relative humidity at any given point in time. This finding is consistent with other studies that have shown that heavily built-up areas experience high temperature (Cavan *et al.*, 2014; Feyisa, Dons and Meilby, 2014; Scott *et al.*, 2017) and low relative humidity (Hass *et al.*, 2016; Yang, Ren and Hou, 2017) in comparison to less built-up and highly vegetated locations. Materials such as concrete, asphalt and the 3-dimensionality of buildings promote the transformation of short wave radiation into heat and its retention (Landsberg, 1981; Oke, 1987) whereas vegetation increases latent heat flux from greater evapotranspiration, resulting in less heat storage (Chow and Roth, 2006; Cavan *et al.*, 2014; Feyisa, Dons and Meilby, 2014; Duarte *et al.*, 2015). The novelty in the current study is the multitemporal assessment of intra-urban climatic differences.

The tendency towards weaker intra-urban climatic differences among sites as soil moisture increases (i.e. during the wet season) as compared to when soil moisture decreases allude to a higher UHI intensity in the dry than the wet season. This finding is consistent with other studies in tropical urban environments (Chow and Roth, 2006; Balogun and Balogun, 2014; Ojeh, Balogun and Okhimamhe, 2016; Amorim and Dubreuil, 2017; Acero and Gonzalez-Asensio, 2018). The novelty in this study is that it establishes these seasonal climatic differences within the city (intra-urban). Here, we see an increasing tendency towards cooler conditions across all land covers with the advancement of the rainy season. Although heavily built-up urban areas are generally associated with high water loss through runoff (Whitford, Ennos and Handley, 2001), the declines in nighttime temperature regardless of proportion of man-made features suggest that increased soil moisture at all sites results in cooler temperatures through increased latent heat flux (Lakshmi, Jackson and Zehrfuhs, 2003; Weng, Lu and Schubring, 2004).

Although soil moisture derived from the top-most soil layer was useful for depicting temporal changes in soil moisture across the entire study site, the high heterogeneity in soil type and depth of urban environments limited the use of this data for characterisation of spatiotemporal patterns of soil moisture. Nonetheless, the positive relationship between soil moisture and relative humidity (e.g. Archibald and Scholes, 2007; Cai *et al.*, 2019) formed the basis for inferring spatiotemporal patterns of soil moisture from the relative humidity, such that the increase in relative humidity during the wet season across all sites highlighted increase in soil moisture. Moreover, highest levels of relative humidity in lightly built locations at any given point in time indicated high levels of water capture and storage and less evapotranspiration demand. Moreover the combined effect of proportion of paved surfaces and buildings (i.e. impervious surfaces) accounted for 77% of the differences in relative humidity during the rainy season, highlighting the significance of impervious surface in impeding rainwater capture and storage as previous studies have shown (e.g. Whitford, Ennos and Handley, 2001). We also note that paved surfaces and buildings accounted for 64.5% of the differences in nighttime temperature during the wet season. It is conceivable from these differences that the effect of impervious surfaces, in general,

was much stronger on relative humidity than night-time temperature. Although stronger precedence has been given to temperature over relative humidity because of the correlation of the two variables, the current study shows strong inherent differences.

During the dry season, in the heavily built-up locations, the presence of low soil moisture might result in a weak cooling effect resulting in stronger UHI intensity. A stronger UHI, in turn, exerts higher evapotranspiration demand in heavily built-up locations as previous studies have shown (Zipper *et al.*, 2017), resulting in much greater decreases in soil moisture. The reverse can be said about the lightly built locations as having a stronger cooling effect and a weaker evaporative demand in comparison to heavily built-up locations. This phenomenon was shown to occur in a temperate city (Zipper *et al.*, 2017), but there was very little previous evidence for its occurrence in a tropical city context, which this study achieves.

A stronger relationship between the proportion of tree cover and nighttime temperature in the dry season might result from a much stronger UHI intensity and spatial differences in soil moisture. During the wet season as vegetation undergoes leaf flush (Williams *et al.*, 1997; Dalmolin *et al.*, 2015; Singh and Kushwaha, 2016; de Camargo *et al.*, 2018) UHI intensities are low and would, in turn, result in weak spatial differences in leaf flush. However, in the dry season as vegetation undergoes leaf fall, with the decline in soil moisture and increase in temperature (Williams *et al.*, 1997; Dalmolin *et al.*, 2015; Singh and Kushwaha, 2016; de Camargo *et al.*, 2018), stronger spatial differences in leaf fall would result from stronger UHI intensities through evapotranspiration demand and increased plant water requirements (Zipper *et al.*, 2017). Spatial differences in canopy and associated spatial differences in evaporative cooling (Li, Ratti and Seiferling, 2018) further intensify the UHI. Although this phenomenon of differences in tree canopy cover resulting from differences in local environmental settings is well established in natural environments in tropics (Williams *et al.*, 1997; Dalmolin *et al.*, 2015; Singh and Kushwaha, 2016; de Camargo *et al.*, 2018), there is little to no evidences about these processes in tropical urban environments. These changes in the relationship between land cover composition and

urban climate showcase the complex non-static relationship between land cover and urban climate.

5.6 Conclusions

Using a network of 22 locations that represent the wide range of surface and structural cover characteristic in the tropical city of Kampala, we empirically examined the spatiotemporal dynamics of urban climate during 50 days marking the transition from the wet to dry season. This study showed that the magnitude of spatial differences in urban climate varied in relation to temporal changes in soil moisture content and that the influence of land cover composition varied between the wet and the dry season. The findings are important for understanding the spatiotemporal patterns of urban climate and reflect on how they might influence vegetation seasonality, and vegetation's provisioning and regulatory functions. This study provides important evidence about the seasonality of intra-urban climatic differences in the context of a tropical African city with a tropical rain forest climate. The current study also provides relevant information related to the characterisation of urban structure for urban climate studies in the context of cities that have a complex and heterogeneous urban morphology. Such knowledge is very useful for developing standard procedures and protocols for characterising urban form and function which often necessitate a wide range of exemplary studies for different urbanisation practices.

CHAPTER 6. SENSITIVITY OF CANOPY PHENOLOGY TO LOCAL URBAN ENVIRONMENTAL CHARACTERISTICS IN A TROPICAL CITY

6.1 Abstract

Canopy phenology is sensitive to variability in local environmental settings. In temperate climates, urban phenological processes and their determinants are relatively well understood. Equivalent understanding of processes in tropical urban settings is, however, less resolved. In this paper, we explore the influence of urbanisation intensity, land cover and urban climate on canopy phenology of two deciduous tree species (*Jacaranda mimosifolia* and *Tabebuia rosea*) in a tropical city (Kampala, Uganda). Our study design involved ground monitoring and field sampling in 2017, with a focus on the dry season. We found that both species experienced significantly higher rates of canopy cover decline in the heavily built neighbourhood category ($p<0.05$ for both species). Moreover, *Jacaranda* was more sensitive to differences in urbanisation intensity than *Tabebuia*, both in terms of total percentage tree canopy cover ($p<0.01$) and net leaf loss ($p<0.05$). Total percentage tree canopy cover for *Jacaranda*, declined with increasing paved surface area and was positively related to relative humidity ($R^2=0.21$, $p<0.01$). Net leaf loss in *Jacaranda* increased with decreasing pervious surface areas and as night time air temperature increased ($R^2=0.25$, $p<0.01$). In contrast, land cover and urban climate had no significant influence on either measure of phenological traits for *Tabebuia*. These results provide new evidence on the relationship between urbanisation and canopy phenology of different tree species in the tropics. Such knowledge offers new insights on the spatial and temporal differences in the regulatory functions of trees and also serves as a proxy for possible species responses under future climate change.

6.2 Introduction

Urbanisation characterised by increased human habitation, intensive modification of the landscape and increased per capita energy consumption (McDonnell and Pickett, 1990) results in environmental change (Grimm *et al.*, 2008; McCarthy, Best and Betts, 2010; Pickett *et al.*, 2011; Wu, 2014). The urban heat island (UHI) effect, where urban areas experience elevated temperatures relative to neighbouring rural areas (Voogt and Oke, 2003; Zhou *et al.*, 2015; Melaas *et al.*, 2016), is one of the most well documented environmental consequences of urbanisation. The UHI effect is often greatest at night and exponentially decays along the urban-rural gradient (Zhang, Friedl, Schaaf, Strahler, *et al.*, 2004; Zhou *et al.*, 2015), effectively amplifying the effects of climate change (McCarthy, Best and Betts, 2010). The potential implications of these urban characteristics on the quality of life and public health have resulted in the growing interest in research on the impacts of urbanisation (Grimm *et al.*, 2008; Pickett *et al.*, 2011; Wu, 2014). This is particularly important because the world's global population living in urban areas is predicted to reach six billion by 2050. Most of this growth is expected to take place in developing countries (McCarthy, Best and Betts, 2010), where urban residents rely most strongly on urban ecosystem functions for health and wellbeing (Lindley *et al.*, 2018).

Vegetation phenology is the study of the timing and duration of plant development phases as determined by changes in the environment (Lieth, 1974). Due to its sensitivity to climate variability, phenology has been used for quantifying the effects of urbanization, which traditionally has involved comparing phenological differences between urban and rural areas (e.g. Roetzer *et al.*, 2000; White *et al.*, 2002; Zhang, Friedl, Schaaf, Strahler, *et al.*, 2004; Gazal *et al.*, 2008). Evidence suggests that urban areas in temperate climates experience early start and longer growing seasons than rural areas (e.g. Neil and Wu, 2006; Jochner and Menzel, 2015). Although these phenological differences have been largely attributable to the UHI effect, some studies (Jochner *et al.*, 2011; e.g. Buyantuyev and Wu, 2012; Walker, de Beurs and Henebry, 2015) have demonstrated that variability of other abiotic factors such as soil moisture is equally important. Far fewer studies have been undertaken in tropical urban settings (e.g. Gazal *et al.*, 2008; Jochner, Alves-Eigenheer, *et al.*, 2013) where soil moisture is a

primary driver of phenology (e.g. Huxley and Vaneck, 1974; Borchert, 1983; Williams *et al.*, 1997; Zhang *et al.*, 2005; Clinton *et al.*, 2014; de Camargo *et al.*, 2018). Most tropical urban phenological studies (e.g. Gazal *et al.*, 2008; Jochner, Alves-Eigenheer, *et al.*, 2013) make comparisons between tropical and temperate cities, yet the influence of soil moisture variability is as yet, unexplored. The UHI plays a more limited role over the timing of the start of the growing season in the tropics, as compared to temperate settings (Gazal *et al.*, 2008; Jochner, Alves-Eigenheer, *et al.*, 2013), possibly as a consequence of milder seasonal temperature changes in the tropics as compared to temperate regions. However, relative humidity has been shown to strongly correlate with season onset dates of some tropical trees (Jochner, Alves-Eigenheer, *et al.*, 2013). Consequently, the variability of temperature, soil moisture and relative humidity ought to be considered for accurate characterisation of phenology in tropical cities.

The degree of heterogeneity in urban form, land cover and land use within a city can also have a significant impact on urban phenology (Jochner *et al.*, 2012; Jochner, Alves-Eigenheer, *et al.*, 2013; Zhang *et al.*, 2014; Melaas *et al.*, 2016; Zipper *et al.*, 2016). As with the research of UHI effects, most studies that relate urban form, land cover and land use to phenology have been undertaken in temperate cities and there remains very little scientific understanding of their influence on phenology in tropical urban environments. Moreover, many tropical cities are experiencing rapid rates of urbanisation that take on different urban forms, land cover and types of land use in comparison to urbanisation in temperate cities (Lindley *et al.*, 2018). Therefore, studies that examine the phenology of tropical trees in response to urban form, land cover and land use advance our understanding of the drivers of leaf phenology in tropical environments with implications for policy and planning.

Existing vegetation phenological knowledge in tropical urban settings emanates almost exclusively from studies that have focused upon the timing of the start of the growing season (e.g. Gazal *et al.*, 2008; Jochner, Alves-Eigenheer, *et al.*, 2013). Canopy cover changes of trees in response to the dry season in the tropics are not well established in the urban context, although some studies have been undertaken in natural habitats (e.g. Williams *et al.*, 1997; Condit *et al.*, 2000; Valdez-Hernandez *et al.*, 2010; Dalmolin *et al.*, 2015; de Camargo *et al.*, 2018). Conclusions from such studies suggest that soil

moisture reduction in the dry season will result in considerable amounts of leaf loss, although the level of leaf loss may differ between species and depend upon local environmental conditions. Unusually high levels of leaf loss may impact upon the productivity of vegetation in successive growing seasons with implications for ecosystem function (Singh and Kushwaha, 2016) and the extent of shading offered from tree stands. Consequently, understanding how tropical tree canopy cover may change during the dry season, is important for understanding the ecological impacts of climate change (Singh and Kushwaha, 2016). Whether changes in canopy cover follow similar patterns in tropical cities is currently unknown.

In this paper, we study tree canopy cover change of two deciduous tree species (*Jacaranda mimosifolia* and *Tabebuia rosea*) with relation to intra-urban variability in urbanisation intensity, land cover and climate in Kampala, Uganda in 2017. We test three key hypotheses: (i) Urbanization intensity influences rate of change of canopy cover. We expect that heavily built neighbourhoods would experience higher rates of decline in tree canopy cover in comparison to less built neighbourhoods. (ii) We anticipate that tree canopy cover change represented by total percentage tree canopy cover and net leaf loss between heavily and lightly or moderately built neighbourhoods will differ between the species. (iii) Variations in total percentage tree canopy cover and net leaf loss for each individual species are accounted for by differences in land cover and urban climate.

6.3 Methods

6.3.1 Study area

The study was undertaken in Kampala, the capital city of Uganda (East Africa) between February and September 2017. Kampala is located at 00°18’49”N 32°34’52”E (Figure 6-1) and has a population density of ~8700 inhabitants/km^2. Kampala has a tropical rainforest (equatorial) climate (Af) according to the Köppen climate classification. Climate records over thirty years show that Kampala has two wet seasons annually (March-May and September-November) and annual precipitation of ~ 1, 200 mm (data source: WMO, World Meteorological Organization). The heaviest monthly rains are in the shorter rain season (generally March to May) with April typically recording the heaviest rains (~169 mm), while July is the driest month (~ 63 mm). In 2017, the dry

season started in May and continued through September (Figure 6-2(a)), and nighttime temperature and relative humidity varied across the city (Figure 6-2(b)).

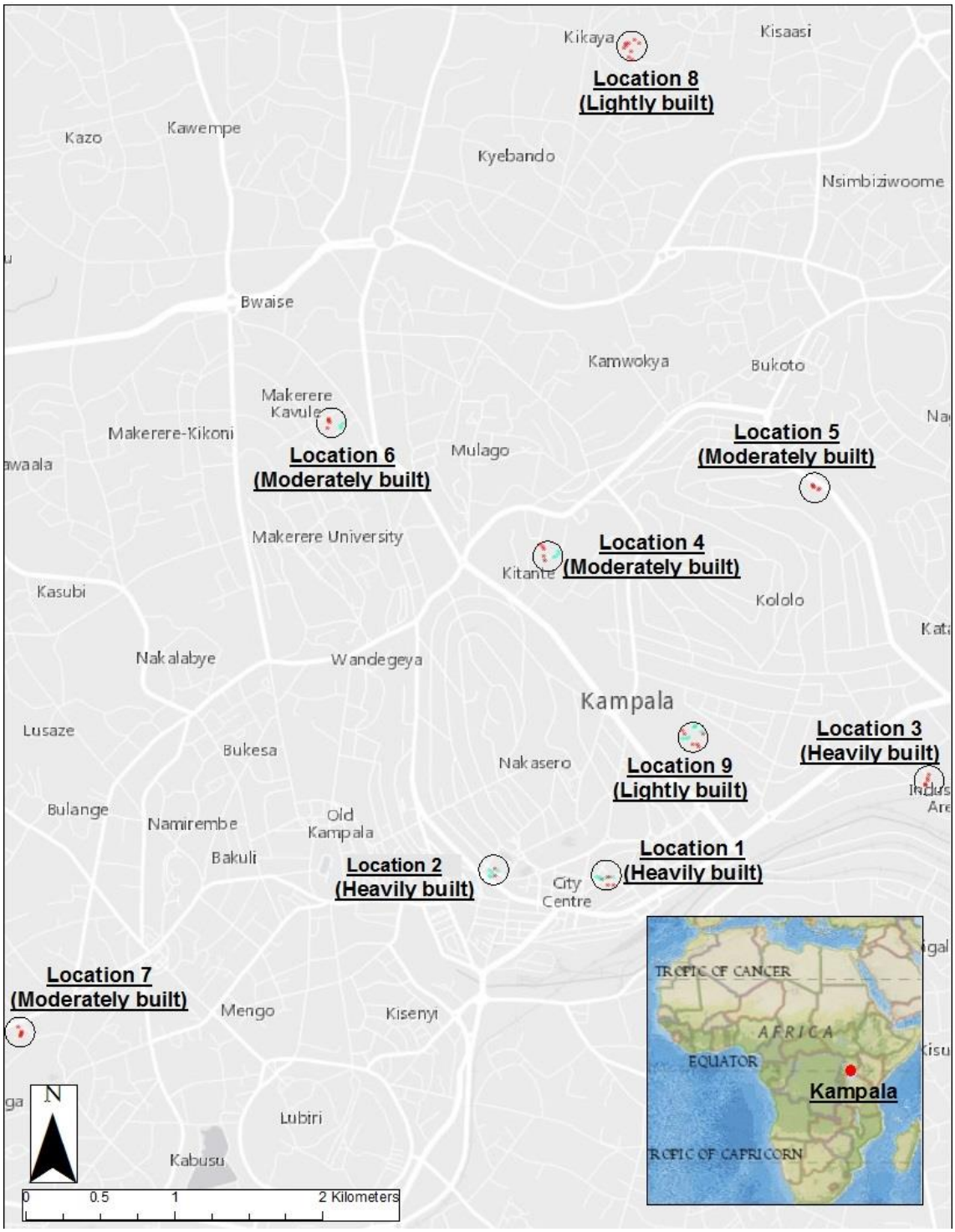

Figure 6-1: Locations of *Jacaranda* (red) and *Tabebuia* (turquoise) trees within each phenology site (black ring). Each phenology site (radius=100 m) represents the coverage of the sensor measurements (air temperature and relative humidity). Tree sample sizes, land cover, and urban form characteristics are summarised in Table 6-1

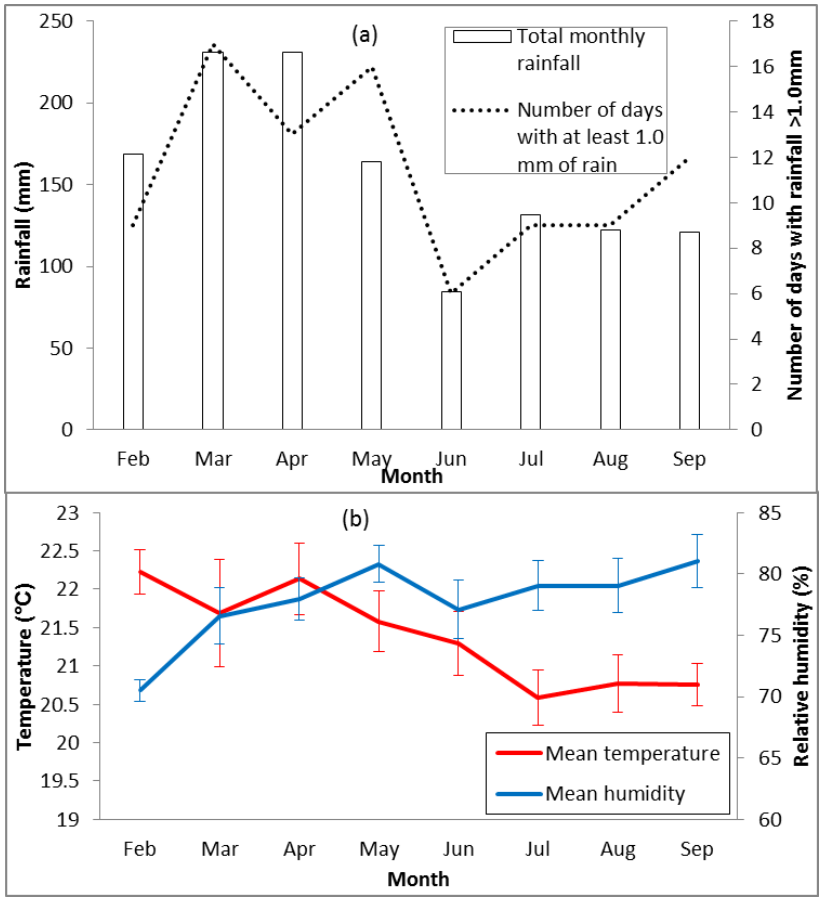

Figure 6-2: Kampala's climate between February and September 2017, (a) monthly rainfall and number of days with more than 1mm of rain and (b) Monthly night time air temperature and relative humidity. Error bars represent the standard deviation and show the monthly variation of nighttime temperature and relative humidity across the phenology sites.

6.3.2 Selected tree species

Two deciduous tree species (*Jacaranda mimosifolia* and *Tabebuia rosea*) were selected for the analysis of canopy cover change. Both species are commonly found throughout Kampala (Figure 6-3). *Jacaranda mimosifolia* (D. Don) and *Tabebuia rosea* (Bertol.) DC both belong to the family *Bignoniaceae* and are native to the neo-tropics (e.g. Argentina, Brazil, Mexico, Venezuela and Ecuador) but are widely grown in other tropical countries (e.g. Uganda, Sri Lanka, South Africa and Australia). *Jacaranda* trees grow up to 20 m in height with spreading branches making a light crown (data source: World Agroforestry). The species has previously been observed to show extended leaf flush coincidental with the onset of the rain season and high leaf fall at the start of leaf flush and throughout the dry season (Huxley and Vaneck, 1974). *Tabebuia* trees grow up to 25 m high and exhibit considerable shoot growth and leaf flushing during the rain

season (data source: World Agroforestry), whilst leaf fall is pronounced during the dry season in response to increasing air temperature (Figueroa and Fournier, 1996).

6.3.3 Individual tree and phenology site selection

Nine phenology sites were selected for the analysis (Figure 6-1). The sites were distributed across Kampala so as to represent the wide range in surface cover and structure that can be observed across the city (Table 6-1) and that are known to influence temperature and local climate (Stewart and Oke, 2012) and in turn influence phenology (Jochner and Menzel, 2015). Each phenology site contained between 3 and 8 individual trees of one of the candidate species and a total of 48 *Jacaranda* trees and 24 Tabebuia trees were selected for the study (Table 6-1).

To minimise the potential phenological influence of elevation, each phenology site was located within an 80 m altitudinal range of one another, (Jochner *et al.*, 2012). Differences in tree size and age were minimised by selecting trees with a similar height and trunk size (i.e. diameter at breast height). We also ensured that the selected trees were not actively managed.

Figure 6-3: (a) *Jacaranda* and (b) *Tabebuia* are ornamental trees commonly found throughout Kampala

The urban environment was characterized via an Object-Based image Analysis classification of a WorldView3 satellite image (spatial resolution of 0.5 m) taken on 25/10/2016. Buildings, paved surface cover and pervious surfaces were classified and their proportion (percentage) at each site quantified within 100 m (Table 6-1). Although a radius of 200 m for homogenous continuous urban form has been

recommended as the zone of influence for local urban climate-related to surface cover and surface structure (Stewart and Oke, 2012), the land cover of the phenology sites was heterogeneous, which warranted a smaller radius over which surface structure and surface cover could be considered as more uniform. Hierarchical cluster analysis was used to generate a generic qualifier of urbanisation intensity for each phenology site. Clustering was based on the proportional coverage of buildings, paved and pervious surfaces within each site. The clustering resulted in the generation of three categories of urbanisation intensity, namely: lightly built, moderately built and heavily built (Table 6-1). Urbanisation intensity was used to simplify the urban environment in such a way that individual trees located in the same category of urbanisation intensity could be treated as a population.

Table 6-1: Characteristics of the nine phenology sites, their associated urban form (percentage cover of pervious surfaces, paved surfaces and buildings) and the number of individual trees (per species) sampled at each phenology site. The last row indicates the urbanization intensity category assigned to each phenology site.

Phenology sites	One	Two	Three	Four	Five	Six	Seven	Eight	Nine
Pervious	49%	52%	41%	81%	67%	77%	67%	95%	100%
Paved Surface	32%	39%	39%	10%	13%	5%	16%	4%	0%
Building	20%	9%	21%	9%	20%	19%	17%	2%	0%
Jacaranda	5	2	6	5	6	5	5	8	6
Tabebuia	4	5	0	5	0	3	0	0	7
Urbanisation intensity category	Heavily built			Moderately built				Lightly built	

6.3.4 Phenology data

As with other studies that have focussed on the spatial variability of vegetation development within a city in a given season (e.g. Gazal *et al.*, 2008; Jochner, Alves-Eigenheer, *et al.*, 2013), this study focussed only on the dry season. Phenological observations were undertaken between March and September 2017 and each tree observed twice a week to increase the accuracy of characterising tree canopy change. Moreover, unlike other studies (e.g. Gazal *et al.*, 2008; Jochner, Alves-Eigenheer, *et al.*, 2013) where phenology has focussed on the timing of bud burst which is a single day's event, in this study we track temporal change of trees canopies across an entire season.

Visual estimation of canopy cover was undertaken by a single observer using a two-step process to generate a measure of leaf abundance. In step 1, the canopy cover was assigned a cover score relating to the relative level of leaf presence (0 = absence of leaves, 1 = 1-25 %, 2 = 26-50 %, 3 = 51-75 % and 4 = 76 – 100 %). In step 2, each canopy score was refined by assigning a sub-score of 1, 2 or 3. A 1 or 3 was appended if the percentage estimates in the first score was distinguishable as being within the upper half or lower half of the associated range, otherwise a 2 (median) was appended. For example, a tree with a 3 in the first step would be assigned either 3.1 or 3.3 to distinguish between 51% and 75%, or a 3.2 would be assigned if the estimate was indistinct. The final categorical scores were subsequently converted to their indicative percentage values for use in further analysis (e.g. Williams *et al.*, 1997; Morellato *et al.*, 2010; Valdez-Hernandez *et al.*, 2010).

6.3.5 Phenology data processing

Time-series profiles of percentage canopy cover were generated for each individual tree sampled (n= 72). A LOESS smoothing algorithm was applied to each time series to minimize the noise in the temporal profile (Figure 6-4). To quantify canopy cover changes across the entire dry season (i.e. DOY 150 to 250), two measures of leaf phenological traits were determined from each time series. Total percentage tree canopy cover was calculated as the area under the curve between the first and last phenological observation and net leaf loss was calculated as the difference between the maximum and minimum percentage tree canopy cover over the period of observation (Figure 6-4). Measures of leaf production and leaf loss are able to explain the canopy cover change in response to intra-urban differences in urbanisation intensity, land cover and urban climate.

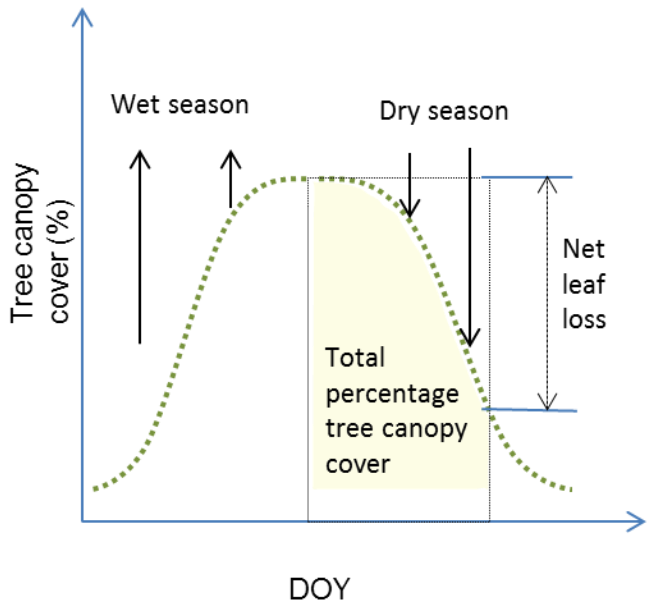

Figure 6-4: Conceptual diagram showing tree canopy change across time and traits of canopy cover change (total percentage canopy cover and net leaf loss) that were extracted from the time series as indicators of leaf production and leaf loss

6.3.6 Urban climate

Volumetric soil moisture content (VMC) was collected at each phenology to depict temporal change in precipitation (water availability) that is known to influence UDI (see 2.1.5), tropical UHI (see 2.1.4.2) and canopy phenology (see 2.2.3.1). The VMC was collected biweekly coincident with recording of phenology data. VMC recordings were taken for the top most soil layer (within 5cm) at the same location each time within 3 meters from each tree trunk using a portable ThetaProbe (model ML3 ThetaProbe, Delta-T Devices).

Air temperature and relative humidity were acquired from HOBO sensors (model HOBO U23-001 Pro v2, Onset Corporation) housed in a radiation shield at a height of 3 m, which was located less than 100 metres from the sampled trees (Figure 6-1). Each sensor collected data at 30-minute intervals and was calibrated every three months against a factory-calibrated sensor. We calculated the dry season average of each urban climate variable (i.e. night time temperature (sunset 18:00 to sunrise 06:00), volumetric soil moisture content and relative humidity) for comparison with differences in total percentage tree canopy cover and net leaf loss.

6.3.7 Data analysis

For each tree species, a linear mixed model was used to determine whether urbanisation intensity influenced rates of decline in tree canopy cover over the duration of the observation period. Each data point represented observed canopy cover for an individual tree on a given day ($n_{Jacaranda\ model}$ = 672; $n_{Tabebuia\ model}$=336) and was used as the response variable. The fixed effects were Julian day (DOY) and urbanization intensity (categorical with three levels: high, moderate or low) and their interaction. The individual tree was included as a random effect to allow for correlated error terms caused by repeated observations on the same tree. The significance of the full model was compared to a corresponding null model (a model that did not account for temporal autocorrelation) using a likelihood ratio test. Visual inspection of qqplots and plots of residuals plotted against fitted values for the significant models revealed normally distributed and homogeneous residuals. DOY was centred around zero for interpretation of model coefficients. The modelling was implemented using the "lme" function of the "nlme" package in R (Pinheiro *et al.*, 2018; R Core Team, 2018).

General linear models were used to determine whether the effect of urbanisation on total percentage tree canopy cover and net leaf loss varied between species. We used only locations where both species occurred and each data point represented an individual tree ($n_{Jacaranda}$ = 23; $n_{Tabebuia}$ =24). Total percentage tree canopy cover and net leaf loss were modelled separately. Species, urbanisation intensity and their interaction, were explanatory variables in both models. The significance of the full models was tested against a reduced model with a single explanatory variable of urban intensity, using a likelihood ratio test to assess the effect of species. Prior to modelling, total percentage canopy cover and net leaf loss were log-transformed. An exact Mann-Whitney U test was used to determine whether total percentage tree canopy cover and net leaf loss differed between the species. Again, a visual inspection of qqplots and plots of residuals plotted against fitted values for the significant models revealed normally distributed and homogeneous residuals.

We used an information-theoretic approach (Burnham, Anderson and Huyvaert, 2011) to explore the relative influence of different urban climate variables and land cover composition on each of the measured phenological traits. This was undertaken to

identify the explanatory effect of individual elements of urban climate and land cover. We derived linear models for each response variable (total percentage tree canopy cover and net leaf loss) into which land cover (percentage cover of buildings, trees, paved and pervious surfaces) or urban climate (night time temperature, relative humidity and volumetric soil moisture) were included as explanatory variables. This resulted in two sets of models; one for land cover and the other for urban climate, with each model set comprising all combinations of their input variables. Variance inflation factors (VIFs) were calculated ("vif" function of the R package *car*) for each model to assess collinearity between continuous explanatory variables, resulting in the sequential exclusion of models in which explanatory variables had a VIF>3. We also formulated a null model with the intercept only to represent the explanatory nature of other variables not covered in this study. Model selection approaches were used to determine the structure of the simplest model explaining the phenology-land cover-urban climate relationships using the MuMIn package in R [R version 3.5.0 (Barton, 2018; R Core Team, 2018)]. The Akaike information criterion corrected for small sample size (AICc) was used to rank and assess individual model performance. The correlative relationship between land cover, urban climate and phenology was considered to be weak if the null model (intercept only) had a ΔAICc =0. Models with ΔAICc < 2 when comparing models with the top-ranked model, were considered as potentially suitable models. For all remaining models, the relative influence of land cover and urban climate (separately) on total percentage tree canopy cover and net leaf loss was assessed. The sum of Akaike weights for each model was used to obtain the relative importance value (RIV) for a given explanatory variable (Burnham and Anderson, 2003), in order to identify variables that were most closely associated with total canopy cover and net leaf loss.

6.4 Results

6.4.1 Temporal changes in canopy cover

Both species showed a general pattern of increasing canopy cover during the wet season, followed by canopy cover decline with the onset of the dry season. Furthermore, the temporal pattern in soil moisture and canopy cover where relatively similar (Figure 6-5).

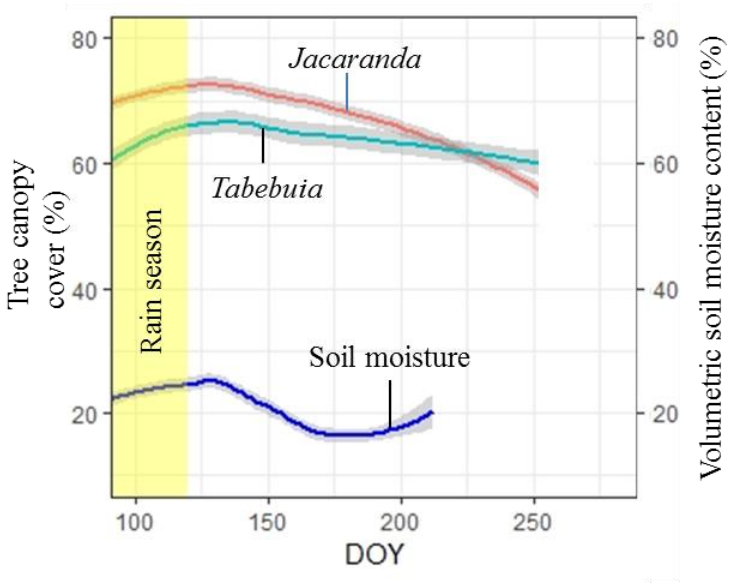

Figure 6-5: Temporal changes in canopy cover for all trees for each species of trees with relation to changes in volumetric soil moisture content. Soil moisture data after DOY=212 were removed prior to analysis due to equipment malfunction

6.4.2 Rate of change of tree canopy cover under varying urbanisation intensity

The combined effect of time (DOY) and urbanisation intensity significantly influenced canopy cover for both tree species (likelihood ratio test: $p<0.0001$). Both species experienced significantly higher rates of tree canopy cover decline in heavily built neighbourhoods in comparison to less built neighbourhoods ($p<0.05$ in both models). The change in slope (i.e. rate of change in canopy cover) from lightly built to heavily built neighbourhoods was significant for both *Jacaranda* (estimate=0.16, standard error=0.02, $p<0.01$; Table 6-2) and *Tabebuia* (estimate=0.03, standard error=0.01, $p<0.01$; Table 6-2). Similarly, the change in slope from moderately built to heavily built neighbourhoods was highly significant for *Jacaranda* (estimate=0.11, standard error=0.01, $p<0.01$; Table 6-2) and *Tabebuia* (estimate=0.02, standard error=0.01, $p<0.05$; Table 6-2).

6.4.3 Species Influence on total percentage of tree canopy cover

Species had an effect on the relationship between urbanization intensity and total percentage cover (comparison of full with reduced model: χ^2=-0.18, df=3, $p<0.01$). In comparison to *Jacaranda*, *Tabebuia* showed negligible differences in total percentage canopy cover between lightly and heavily built neighborhoods (estimate = -0.257, standard error =0.087, $p<0.01$) and between moderately built and heavily

neighborhoods (estimate = -0.22, standard error =0.08, p<0.01) as shown in Table 6-3 and Figure 6-6.

6.4.4 Species Influence on net leaf loss

The relationship between urbanisation intensity and net leaf loss was influenced by species (likelihood ratio test: χ^2=13.583, df=3, p=0.0000). Overall, mean net leaf loss across all neighbourhood categories differed between *Jacaranda* and *Tabebuia* (Mann-Whitney U-test: U=430, p=0.002805). *Tabebuia* showed negligible differences in mean net leaf loss between lightly and heavily built neighbourhoods in comparison to *Jacaranda* (estimate = 1.266, standard error =0.591, p<0.05; Table 6-3; Figure 6-6). However, differences in net leaf loss between moderately built and heavily built neighbourhoods were relatively the same for *Tabebuia* and *Jacaranda* (estimate = 0.420, standard error =0.545, p>0.05; Table 6-3; Figure 6-6).

Table 6-2: Estimated regression parameters, standard errors (in brackets) and significance levels for the relationship between urbanisation intensity and canopy cover decline. NB: *p<0.1; **p<0.05; ***p<0.01

	Dependent variable:	
	Leaves (%)	
	Tabebuia	*Jacaranda*
	(1)	(2)
DOY	-0.216***	-0.047***
	(0.011)	(0.006)
Lightly built	11.539***	0.648
	(3.537)	(3.474)
Moderately built	9.963***	-0.250
	(3.241)	(3.349)
DOY:Lightly built	0.160***	0.027***
	(0.015)	(0.009)
DOY:Moderately built	0.105***	0.022**
	(0.014)	(0.009)
Intercept	57.966***	64.224***
	(2.547)	(2.298)

Observations	672	336

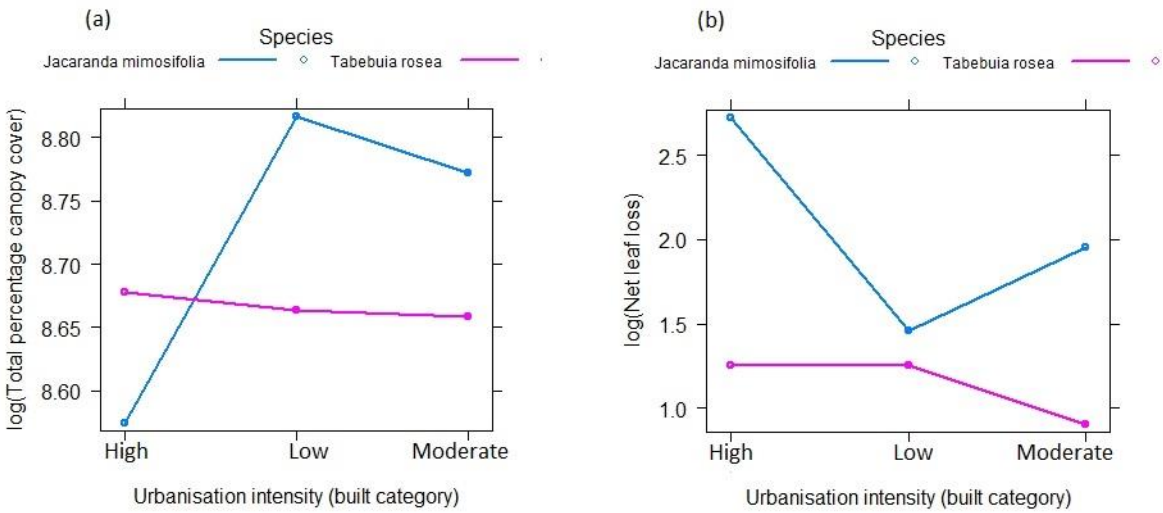

Figure 6-6: Interaction effect of species and urbanisation intensity on (a) Total percentage canopy cover and (b) Net leaf loss.

Table 6-3: Estimated regression parameters, standard errors (in brackets) and significance levels for the effects of species on the relationship between urbanisation intensity and (1) Net leaf loss (2) Total percentage canopy cover. NB: *p<0.1; **p<0.05; ***p<0.01

	Dependent variable:	
	log(Net leaf loss)	log(Total percentage canopy cover
	(1)	(2)
Tabebuia	-1.472***	0.103*
	(0.397)	(0.058)
Lightly built	-1.265***	0.242***
	(0.438)	(0.064)
Moderately built	-0.767*	0.197***
	(0.388)	(0.057)
Tabebuia:Lightly built	1.266**	-0.257***
	(0.591)	(0.087)
Tabebuia:Moderately built	0.420	-0.217***
	(0.545)	(0.080)
Intercept	2.723***	8.575***
	(0.297)	(0.044)
Observations	47	47

6.4.5 Influence of land cover

Paved surfaces and pervious surface area significantly influenced total percentage canopy ($F_{1,46}$ =16.6, p<0.01) and net leaf loss ($F_{1,46}$ =12.37, p<0.01) respectively for *Jacaranda*, and this is supported by the high RIV scores (Table 6-5). Specifically, total percentage canopy cover decreased with increase in paved surface area (R^2=0.25, estimate ± SE: -0.005 ± 0.001, t_{46}=-4.07; Table 6-4; Figure 6-7) while increase in pervious surface area resulted in decrease in net leaf loss (R^2=0.2, estimate ± SE: -0.21 ± 0.006, t_{46}=-3.517; Table 6-4; Figure 6-7). However, there was no significant model for total percentage canopy cover and net leaf loss in *Tabebuia* (Table 6-4).

6.4.6 Influence of urban climate

Total percentage canopy cover and net leaf loss for *Jacaranda* were significantly influenced by differences in relative humidity ($F_{1,46}$ =14.47, p=0.0004; Table 6-4) and nighttime temperature ($F_{1,46}$ =16.24, p=0.0002; Table 6-4) respectively. Total percentage canopy cover increased with increase in relative humidity (R^2=0.222, estimate ± SE: 0.04 ± 0.01, t_{46}=3.804; Table 6-4; Figure 6-7) while increase in pervious surface area resulted in decrease in net leaf loss (R^2=0.245, estimate ± SE: 1.425 ± 0.354, t_{46}=4.03; Table 6-4; Figure 6-7). There was no significant model explaining the relationship between urban climate and phenological traits in *Tabebuia* (Table 6-4; Table 6-5).

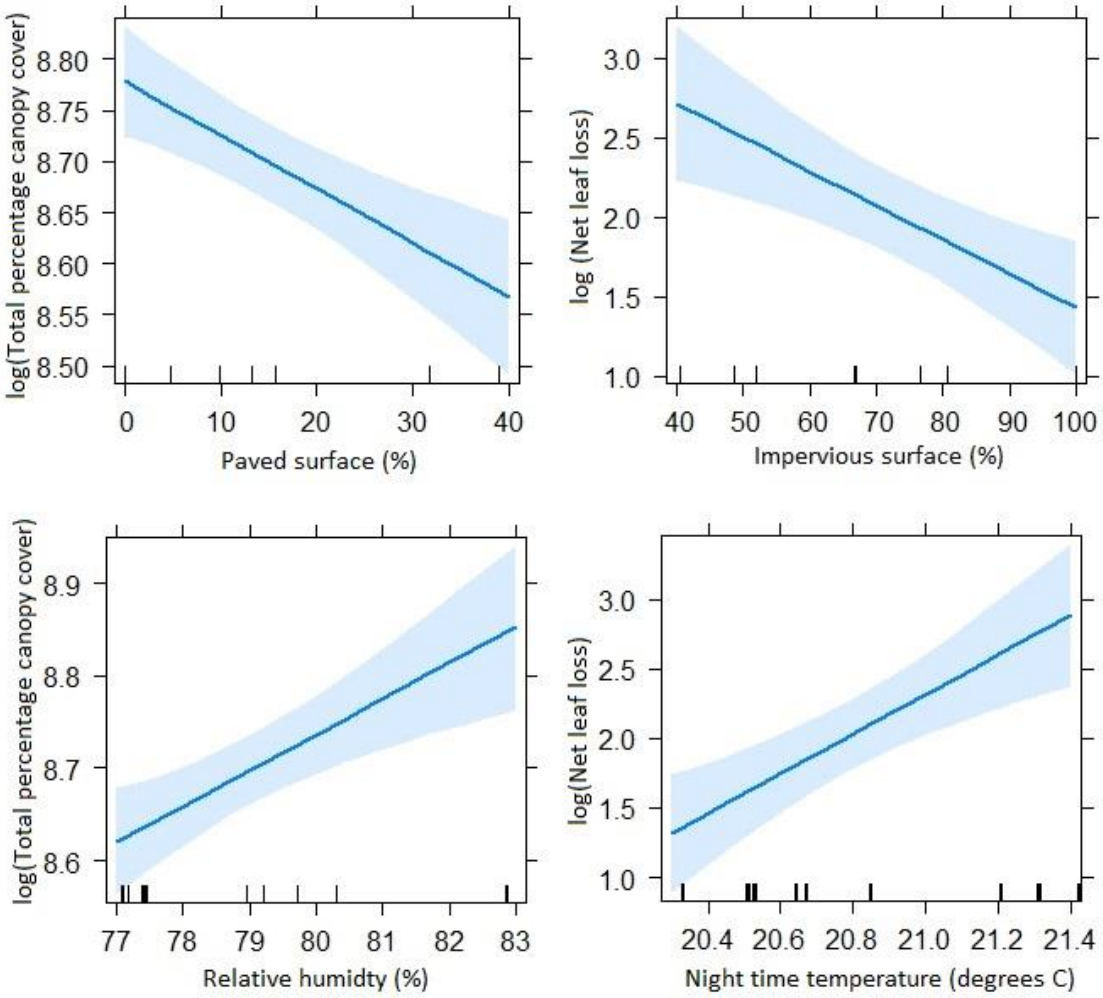

Figure 6-7: Effect plots showing the influence of land cover and urban climate on total percentage canopy cover and net leaf loss

Table 6-4: AICc statistics for models for total percentage canopy cover and net leaf loss relationships with land cover and urban climate for each species separately. AICc = AIC corrected for small sample size, df = degrees of freedom, R^2 = adjusted regression coefficient, p = model p-value, ΔAICc = difference between the top model and given model AICc, wi = model weight. Only models with ΔAICc < 2 are shown.

Metric	Species	Model class	Model variables	AICc	logLik	df	Adjusted R^2	p	delta	weight
Total percentage	*Jacaranda*	Land cover	Paved surfaces	-56.6	31.6	3	0.25	0.0002	0	0.46
			Pervious surfaces, Trees	-56	32.4	4	0.26	0.0004	0.69	0.33
			Buildings, Paved surface, Trees	-55	33.2	5	0.27	0.0008	1.60	0.21
		Urban climate	Relative humidity	-55	-30.8	3	0.21	0.0004	0	0.65

canopy cover										
			Night temp	-53.7	30.14	3	0.20	0.0007	1.25	0.35
	Tabebuia	Land cover	Intercept only	-32.8	18.7	2			0	1
		Urban climate	Intercept only	-32.8	18.7	2			0	0.7
			Night temp	-31.1	19.2	3	-0.01	0.356	1.68	0.3
Net leaf loss	*Jacaranda*	Land cover	Pervious surface	129.14	-61.3	3	0.2	0.001	0	0.45
			Pervious surface, trees	129.57	-60.3	4	0.2	0.0019	0.43	0.36
			Paved surface	130.78	-62.1	3	0.17	0.0023	1.64	0.2
		Urban climate	Night temp	126.05	-59.8	3	0.25	0.0002	0	0.67
			Night temp, soil moisture	127.5	-59.3	4	0.24	0.0007	1.44	0.33
	Tabebuia	Land cover	Intercept only	53.79	-24.6	2			0	1
		Urban climate	Intercept only	53.79	-24.6	2			0	1

Table 6-5: Relative importance values (RIV) of predictor variables for models predicting total percentage canopy cover and net leaf loss for each species separately based on land cover and urban climate

		Model category						
		Land cover				Urban climate		
Metric	Species	Paved surface	Trees	Pervious surface	Buildings	Night temp	Soil moisture	Relative humidity
Total percentage canopy cover	*Jacaranda*	0.64	0.42	0.36	0.28	0.36	0.26	0.63
	Tabebuia	0.16	0.18	0.19	0.18	0.29	0.26	0.15
Net leaf loss	*Jacaranda*	0.33	0.35	0.58	0.27	0.83	0.33	0.16
	Tabebuia	0.151	0.18	0.183	0.181	0.21	0.22	0.168

6.5 Discussion

The current study found that tree canopy cover decline during the dry season varied with urbanisation intensity for two deciduous tree species *Jacaranda mimosifolia* and *Tabebuia rosea* in a tropical city. Specifically, heavily built neighbourhoods experienced the highest rates of tree canopy cover decline. However, the relationship between urbanisation intensity and phenological traits relating to tree canopy cover change (total percentage canopy cover and net leaf loss) differed between the species. *Jacaranda* showed stronger differences in total percentage of tree canopy cover and net leaf loss between heavily built and less built neighbourhoods than *Tabebuia*. Total percentage canopy cover and net leaf loss in *Jacaranda* increased with decreasing paved and pervious surface area respectively. Equally, increases in relative humidity (positively correlated with volumetric soil water content) and nighttime temperature increased total percentage canopy cover and net leaf loss respectively for *Jacaranda*. However, there was no evidence to suggest that land cover composition or the measured urban climate variables influenced the phenology of *Tabebuia*.

Relatively similar patterns of canopy cover decline with decreasing soil moisture content during the dry season, and species differences have been observed in natural habitats (e.g. Williams *et al.*, 1997; Condit *et al.*, 2000; de Camargo *et al.*, 2018). This study, however, provides important new evidence of these processes in tropical urban environments. Differences between tree species have been linked with species-specific endogenous mechanisms (e.g. Borchert, 1983; Williams *et al.*, 1997). *Jacaranda* and *Tabebuia* have been observed to show different mechanisms for the timing of leaf loss in relation to leaf production. For example, Huxley and Vaneck (1974) observed that *Jacaranda* exhibited extended periods of leaf production that coincided with the rain season and that leaf loss occurred simultaneously with leaf production. Start of leaf loss in *Tabebuia*, however, has been observed to occur much later after leaf production during the dry season (Borchert, 1983). Moreover, *Tabebuia* has been observed to exhibit weak tree canopy cover change under moderate seasonal climatic conditions (Reich, 1995) and to show subtle leaf loss in some dry seasons (Condit *et al.*, 2000).

The intra-urban differences in canopy cover change (total percentage canopy cover and net leaf loss) between the two species showed that *Jacaranda* is more sensitive to the combined effect of urbanisation and the dry season than *Tabebuia*. Relatively similar species differences in phenology have been observed in urban phenological studies in the tropics, though these studies focused on the timing of the start of season (e.g. Gazal *et al.*, 2008; Jochner, Alves-Eigenheer, *et al.*, 2013). The measures of canopy cover change used in this study (i.e. rates of change in canopy cover decline, total percentage canopy cover and net leaf loss) are indicative of the net effect of canopy dynamics across an extended time period/season and offer a novel approach for characterising phenology in tropical urban environments. Similar approaches can be used alongside traditional phenological observations (e.g. timing of start, end and length of season) to deepen our understanding of phenological processes.

Our analysis showed that *Jacaranda* trees in sites that had low paved surface area and high relative humidity, (positively correlated with soil moisture; Pearson's r=0.63) were related to high total percentage canopy cover. In turn, *Jacaranda* trees in sites of low pervious surface area and high nighttime air temperature experienced high net leaf loss. Leaf flush peak and Leaf fall peak which are indicators of total percentage canopy cover and net leaf loss respectively have been observed to be strongly affected by relative humidity and air temperature respectively (Do *et al.*, 2005). Although we were not able to identify a strong relationship between soil moisture and total percentage cover as expected (Huxley and Vaneck, 1974; Borchert, 1983), the positive correlation between soil moisture and humidity that has been established in other studies (e.g. Archibald and Scholes, 2007; Cai *et al.*, 2019) might be indicative of the effect of soil moisture. Whilst the measurements taken for volumetric soil moisture content at the topmost soil layer (within ~8cm) were indicators of relative differences in volumetric soil moisture content among locations, these measures would not suffice to accurately represent relative differences in volumetric soil moisture content at deeper soil depths (Lakshmi, Jackson and Zehrfuhs, 2003). Moreover, some studies suggest that trees in tropical environments have complex water use mechanisms that rely on groundwater (Do *et al.*, 2005; Guan *et al.*, 2014) which might explain the lack of a direct relationship between total percentage canopy cover and soil moisture observed in this study. Soil

moisture plays a significant role even in temperate climate (Melaas *et al.*, 2016; Zipper *et al.*, 2016) and future urban phenological studies ought to account for its variability along a gradient of depth in relation to vegetation phenology.

Although *Tabebuia* showed variations in decline in canopy cover along a gradient of urbanisation intensity, there was little to no evidence to show that land cover and urban climate influenced total percentage canopy cover and net leaf loss. This is in agreement with some studies (e.g. Jochner, Alves-Eigenheer, *et al.*, 2013) that have observed weak differences in phenology as a result of intra-urban climatic differences.

The differences in the rate of change in canopy cover decline for *Tabebuia* might be attributable to intensified land use (e.g. heavier traffic) in heavily built neighbourhoods. Jochner et al. (2015) observed that ozone, NO_2, NOx and PM levels were significantly related to delays in phenology. Additionally, high foliar concentrations of potassium, boron, zinc, and calcium have been linked to earlier onset dates (leaf flushing) by enabling cell extension, membrane function and stability (Jochner, Hofler, *et al.*, 2013). Consequently, the observed spatial differences in phenology for *Tabebuia* along an urbanisation intensity gradient (that highlight land-use intensity) could be linked to measures other than temperature, soil moisture and relative humidity.

6.5.1 Conclusion

This study provides new evidence that shows that urbanisation affects the rate of change of canopy cover of different trees in tropical urban environments during the dry season, but the dynamics of these processes vary among species. Moreover, the differences in sensitivity of species to urbanisation intensity, land cover and urban climate might imply that some species are better adapted than others to urban environments. Therefore, the direction for future research that assesses the regulatory services of trees ought to account for locational differences in urbanisation intensity, land cover, and temporal changes in canopy cover at individual species level. Equally, future studies on vegetation phenology in tropical urban environments ought to explore the effect of different factors (e.g. nutrients and pollution) in addition to urbanisation intensity, land cover and urban climate.

The findings in this study have direct implications for the understanding of the provision of vital regulatory functions of vegetation. Suppressed tree canopy cover in the heavily built neighbourhoods might limit mitigation of the UHI through shading and evaporative cooling. Furthermore, the amplified effect of the dry season as a result of intensified urbanisation is indicative of potential impacts of climate change which is expected to result in extremely dry seasons. The observations made on both species in the heavily built neighbourhoods in comparison to the less built neighbourhoods might offer insights on how the species and other taxonomically related species would respond in their natural habitats to extreme events like drought that are expected to increase under predicted climate change. The findings from this study form the baseline for further studies to be undertaken on the phenomenon relating urbanisation intensity, land cover and urban climate to tree canopy cover change in tropical environments. Such studies are important because they improve our understanding of temporal changes in primary production and their effects on nutrient cycling, water and energy fluxes and resource availability at the ecosystem level.

CHAPTER 7. **CONCLUSIONS**

7.1 Introduction

This chapter summarises the key findings of this study regarding the research aims highlighted in the introductory chapter. A discussion of these findings and their significance for climate and phenology in the context of tropical cities then follows. The final discussion focuses on the rigour and limitations of the study and recommendations for future work.

7.2 Summary of research findings

The thesis has three main aims, each related to understanding urban climate and its significance to canopy phenological processes using the case study of Kampala, Uganda. The research aims were as follows:

- To examine the influence of the urban heat island effect on landscape phenology
- To investigate the spatiotemporal dynamics of urban climate during the wet-dry season transition
- To investigate the sensitivity of canopy phenology to local environmental settings

Therefore, an evaluation of the attainment of the overarching goal of this study is achieved by reflecting upon the outcomes of each one of the three research aims. There then follows an ensemble interpretation and discussion of the relevance of these findings.

7.2.1 Effect of the urban heat island on landscape phenological processes

The literature review revealed a lack of published studies which empirically investigated the influence of urban form and urban climate (UHI) on landscape phenological patterns in the tropics. Cities in cooler climates, on the other hand, have had a large number of studies on landscape phenological processes (e.g. Zhang, Friedl,

Schaaf, Strahler, *et al.*, 2004; Dallimer *et al.*, 2016; Melaas *et al.*, 2016; Zhou *et al.*, 2016; Zipper *et al.*, 2016).

In this study, spatial patterns of vegetation seasonality (i.e. start, end and length of the vegetation growing season), maximum land surface temperature (LST) and urban form were derived from remotely sensed satellite imagery covering Kampala. Spatial patterns in landscape phenology were analysed with relation to differences in urban form using the local climate zone (LCZ) framework and associated surface temperature differences.

Land surface temperature was observed to increase along a distance gradient from urban to rural areas and to be greatest in locations that typified densely built-up and lightly vegetated areas (i.e. ~3.5°C higher than the least built-up location). The magnitude of the decline in LST along the urban-rural gradient varied across years such that smaller differences in LST between urban and rural areas were observed in 2014 (~1.5°C) and 2015 (~1°C) than 2013 (~3.5°C). The Start of season was earlier in rural than urban areas, and earlier in highly vegetated urban form types (less built) in comparison to densely built-up urban form types (i.e. two days difference) across all three years. Land surface temperature had a positive relationship with start of season such that 2°C increase in temperature was associated with a one day delay in the start of the vegetation growing season. The end of season occurred later in rural areas and areas that typified lightly built urban form types in comparison to densely built urban form types (i.e. seven days differences). More specifically, higher LST was associated with earlier end of the growing season, such that a 2°C increase in temperature shortened the timing of the end of season by two days. The duration of the vegetation growing season was longer in rural than urban areas (2 days difference) and in locations that were lightly built (highly vegetated) in comparison to the most built-up urban form type (15 days). Increases in LST by 2°C resulted in a reduction of duration of the growing season by one day. These findings are in contrast to the traditional knowledge of landscape phenological processes in cities located in cooler climates where the heavily built-up locations experience earlier start of season and longer vegetation growing seasons than rural areas due to the UHI effect.

7.2.2 Spatiotemporal dynamics of urban climate during the wet-dry season transiton

Surface moisture influences canopy phenology through leaf flush in tropical natural environments (Williams *et al.*, 1997; Clinton *et al.*, 2014; de Camargo *et al.*, 2018). Consequently, an understanding of the influence of the UHI on canopy phenology in tropical cities can be better gained my controlling for the effect of surface moisture. In the current study, spatiotemporal analysis of urban climate was undertaken to reveal: the temporal change of spatial differences in urban climate that drive spatial differences in phenology; and to investigate the influence of land cover composition on urban climate. This involved spatiotemporal analysis of relative humidity (UDI effect) and nighttime air temperature (UHI effect) with relation to temporal changes in surface moisture that represented the wet-dry season transition. Also the influence of land cover composition on spatial variability in urban climate was assessed during the wet and dry season separately. Twenty-one locations representing the wide range of urban structural differences within the city were selected for acquisition of urban climate data.

The vast majority of urban climate studies in tropical cities have focused on the UHI effect (Roth, 2007; Roth and Chow, 2012; Giridharan and Emmanuel, 2018) because of its relevance to human health (Heaviside, Macintyre and Vardoulakis, 2017). Relative humidity used for characterising the UDI effect and an indicator of phenological processes (Do *et al.*, 2005; Archibald and Scholes, 2007; Jochner, Alves-Eigenheer, *et al.*, 2013) and spatiotemporal dynamics of surface moisture (e.g. Archibald and Scholes, 2007; Roth, 2007; Yang, Ren and Hou, 2017; Cai *et al.*, 2019) has often been overlooked. This study revealed the inherent differences between temperature and relative humidity demonstrated by differences in key determinants of their spatial variability. The proportion of paved surfaces and buildings accounted for 64.5% and 63.8% of the differences in nighttime air temperature in the wet and the dry season respectively. Increase in temperature was associated with a high proportion of buildings and paved surfaces. The proportion of trees and pervious surfaces accounted for 77.6% and 80.2% of the differences in relative humidity during the wet and dry season respectively. High pervious surface cover and proportion of trees cover was

associated with higher relative humidity. Although the proportion of tree cover had a significant influence on relative humidity during both the wet and dry season, tree cover influenced temperature in the dry season only, such that higher proportion of trees was associated with lower temperature.

The gradual increase in soil moisture during the wet season resulted in a decrease in nighttime temperature and an increase in relative humidity across all locations. During the dry season, a decline in surface moisture resulted in an increase in air temperature and a decrease in relative humidity across all locations.

The spatial differences in air temperature and relative humidity were observed to decline with a gradual increase in surface moisture. However, the dry down period increased spatial differences in both nighttime air temperature and relative humidity. During the dry season, the fastest rates of changes in nighttime air temperature and relative humidity were observed in the most built-up locations, whereas locations that had the least proportion of human-made features underwent the slowest rates of change in air temperature and relative humidity.

7.2.3 The sensitivity of canopy phenology to local environmental settings

A review of the literature showed a lack of published studies which quantitatively investigated the influence of urbanisation and the UHI on canopy cover change in urban environments despite there being an extensive number of studies in tropical natural environments (e.g. Williams *et al.*, 1997; Condit *et al.*, 2000; Valdez-Hernandez *et al.*, 2010; Dalmolin *et al.*, 2015; de Camargo *et al.*, 2018). *Jacaranda* and *Tabebuia* trees of similar sizes in nine locations highlighting the wide range of differences in urban form across Kampala were monitored from March to September 2017. Canopy phenology of the two deciduous species was analysed with relation to differences in urbanisation intensity, land cover and urban climate in the dry season that is associated with leaf senescence (Williams *et al.*, 1997; Condit *et al.*, 2000; Valdez-Hernandez *et al.*, 2010; Dalmolin *et al.*, 2015; de Camargo *et al.*, 2018). The rate of decline of canopy cover during the dry season for both *Jacaranda* and *Tabebuia* increased along a gradient of increasing urbanisation intensity. However, *Jacaranda*

was more sensitive to differences in urbanisation intensity than *Tabebuia*, both in terms of the total percentage of tree canopy cover and net leaf loss. Total percentage tree canopy cover for *Jacaranda* decreased as the proportion of paved surfaces increased and with a decline in relative humidity. The decline in the proportion of pervious surfaces and an increase in nighttime temperature were associated with increased Net leaf loss in *Jacaranda*. In contrast, land cover and urban climate had no significant influence on total percentage canopy cover and net leaf loss in *Tabebuia*.

7.3 Significance of the findings of the research

7.3.1 Tropical urban climate

The gradual decline in nighttime temperature across all locations with the increase in soil moisture during the wet season could be explained by higher radiative cooling due to high latent heat flux (Lakshmi, Jackson and Zehrfuhs, 2003; Weng, Lu and Schubring, 2004). The decline in spatial differences in nighttime temperature with increased soil moisture highlights the fact that the effect of high radiative cooling associated with an increase in soil moisture superseded UHI-induced evaporation (Zipper *et al.*, 2017). Conversely, the radiative cooling effect was lessened due to the declining soil moisture in the dry down period explaining the increase in temperature across all locations. The ever increasing spatial differences in nighttime temperature were associated with contrasts in radiative cooling and evaporation, whereby heavily built-up locations experienced higher evaporative demand and weaker radiative cooling than the highly vegetated areas. Therefore densely built-up locations experienced a more rapid increase in air temperature during dry down than the highly pervious and vegetated areas.

Soil moisture measurements derived from the top-most soil layer were used in this study to characterise soil moisture temporal changes across the entire study area. However, the high level of heterogeneity in soil types and depth depicted in urban environments rendered the data of soil moisture from the top layer impractical for representing spatiotemporal variations in soil moisture. However, the positive relationship between soil moisture and relative humidity (Archibald and Scholes, 2007; Roth, 2007; Yang, Ren and Hou, 2017; Cai *et al.*, 2019) was used to deduce spatial differences in soil moisture from relative humidity. Consequently, the gradual increase

in soil moisture during the wet season explains the gradual increase in relative humidity across all locations. However, at any given point in time, lightly built-up areas consistently recorded higher relative humidity (i.e. high soil moisture) than the heavily built-up locations highlighting higher water capture and storage in lightly built-up areas. Lower water content in heavily built-up locations can be explained by stronger evaporation through the UHI effect (Zipper *et al.*, 2017) and higher proportion of impervious surfaces that restrict water capture and storage (Barnes, Morgan and Roberge, 2001; Whitford, Ennos and Handley, 2001). With the end of the wet season and reduction in the cooling effect through soil moisture-induced latent heat flux (Lakshmi, Jackson and Zehrfuhs, 2003; Weng, Lu and Schubring, 2004), UHI-induced water loss via evaporation (Zipper *et al.*, 2017) significantly increased in the heavily built-up locations. Consequently, densely built-up locations experienced a more rapid decline in soil moisture exhibited by a more rapid decline in relative humidity than highly pervious and vegetated areas.

The tendency towards stronger UHI intensity in the dry than wet season observed in this study agrees with findings from other tropical UHI studies (e.g. Roth, 2007; Cui and De Foy, 2012; Balogun and Balogun, 2014; Ayanlade, 2016; Ojeh, Balogun and Okhimamhe, 2016; Amorim and Dubreuil, 2017; Giridharan and Emmanuel, 2018). However, the determination of the magnitude of intra-city differences in UHI intensity and relative humidity with relation to subtle changes in soil moisture as opposed to the urban-rural and wet-dry season dichotomies are novel features of this study.

7.3.2 Phenology in tropical cities

In this study, both remote sensing and field monitoring approaches revealed strong UHI intensity in the most built-up locations of the study site which is in agreement with a vast number of UHI studies in the tropics (Roth, 2007; Roth and Chow, 2012; Giridharan and Emmanuel, 2018 and references therein). This study, however, revealed inter-annual differences in the magnitude of LST between urban and rural areas, such that LST in rural areas in 2014 and 2015 were considerably higher than in 2013. The years 2014 and 2015 were associated with drought and El Niño episodes respectively and experienced higher air temperature than 2013 throughout the entire year as described in Chapter 4. Moreover, inter-annual climatic anomalies such as the

drought and El Niño associated with elevated temperatures negatively affect vegetation productivity in tropical regions (Kogan and Guo, 2017; Bastos *et al.*, 2018; Rifai *et al.*, 2018; Zhang *et al.*, 2019).

Within the city, shorter growing seasons associated with high LST as derived from remote sensing show strong parallels with high canopy cover decline resulting from high air temperature observed using field monitoring approaches. On the flip side, the observed longer growing seasons using remote sensing that is associated with low LST reflect the higher leaf production associated with high soil moisture depicted by the field monitoring approach. These findings show a strong agreement between the remote sensing and visual observations of canopy phenology used in this study because both methods focus on changes in canopy structure. Furthermore, these findings agree with previous tropical phenology studies that have shown that the wet season and increased relative humidity are predictors of leaf flush (Do *et al.*, 2005; Archibald and Scholes, 2007; de Camargo *et al.*, 2018), whereas leaf fall is accelerated by temperature increase during the dry season (Williams *et al.*, 1997; Condit *et al.*, 2000; Dalmolin *et al.*, 2015; de Camargo *et al.*, 2018). The novelty of this study is the determination of canopy cover changes to local environmental settings in a tropical urban environment and that the UHI is a limiting factor to vegetation growth.

The stronger UHI intensity and strong spatial differences in the relative humidity during the dry season might result in stronger effects on leaf fall and spatial differences in the occurrence of leaf fall. Consequently, stronger differences in tree canopy cover in the dry than wet season might account for the stronger relationship between air temperature and proportion of tree cover in the dry season in comparison to the wet season. Equally greater magnitude of canopy cover in the dry season might result in strong differences thermal cooling via evapotranspiration (Li, Ratti and Seiferling, 2018) as a feedback response and intensify the UHI. Although the temporal changes in vegetation cover and their spatial variability have been overlooked to a greater extent in tropical urban climate studies, this study provides substantial evidence related to the role of phenology on local climate regulation in tropical cities.

7.3.3 Climate change science

Cities are microcosms of global-scale environmental change processes making them informative test cases for understanding dynamics of ecological systems and their responses to change (Ziska *et al.*, 2003; Grimm *et al.*, 2008). The relative differences in urban climate and the resulting variations in ecological processes form a framework for learning about global-scale ecological processes in response to relative differences in a given climatic variable. For example, the UHI effect on vegetation phenology is considered useful for advancing the understanding of vegetation phenological responses due to climate change (Neil and Wu, 2006; Jochner and Menzel, 2015).

In the context of tropical climates, the observed differences in phenology due to the UHI effect might be indicative of phenological responses to increased temperature under predicted climate change. Consequently, earlier ends of vegetation growing seasons, shorter vegetation growing seasons and lower vegetation productivity might be expected to occur with increasing temperatures in water-limited tropical environments. Such changes in climate might negatively impact on both natural and agricultural systems which might, in turn, affect water, nutrient and energy cycling and ecosystem balance. There is evidence to show that substantial reductions in rainfall (Ssentongo *et al.*, 2018) and increases in temperature (Mubiru *et al.*, 2018), are already adversely affecting agricultural production systems in some regions of tropical Africa.

In tropical cities, elevated temperatures due to climate change might amplify the effect of the UHI and further shorten the GSL. The effect of smaller and poorly established canopies would limit the provision of shade and thermal cooling through evapotranspiration and result in a further decline in thermal comfort in cities. Therefore, there is need for long term monitoring of urbanisation processes and urban climate monitoring in order to separate legacy climate change from urbanisation induced climate phenomena and the associated impacts on ecological processes.

7.3.4 Implications for urban development

The findings of the study provide invaluable evidence about urban-induced climatic and phenological processes and discourse into the feedback of these processes on

local climatic conditions. These findings are, therefore, not only relevant for the planning process in Kampala but apply to other tropical cities that are experiencing similar patterns of urbanisation and are faced by similar challenges to sustainable urbanisation.

Kampala is rapidly urbanising at an estimated rate of c.5% per annum (Vermeiren *et al.*, 2012; Bidandi and Williams, 2017), which is prototypical of the rapid urbanisation taking place in sub-Saharan Africa (Pérez-Molina *et al.*, 2017). The city has expanded beyond its administrative boundary to incorporate former satellite towns and surrounding rural areas and create an urban surface (c.800 km^2) referred to as the Kampala greater metropolitan area (Vermeiren *et al.*, 2012). Kampala's commercial and industrial activities contribute significantly to national gross domestic product. This was highlighted by a national average economic growth rate of 7.4% between 2009 and 2017. In addition to being the central hub for financial transaction, Kampala is the chief administrative, political and educational centre of the country (Lwasa, 2017). Therefore the findings of this research are critical for the advancement of knowledge related to the liveability of cities that form a core part of the economies of developing countries and could benefit policy making for the attainment of sustainable development.

One key feature of the landscape changes across Kampala is the emergence of informal developments and settlements (Bidandi and Williams, 2017; Richmond, Myers and Namuli, 2018; Nastar *et al.*, 2019) at the expense of vegetation cover (Kiggundu *et al.*, 2018) represented by LCZ3_F (compact low rise with bare soil surfaces) in this study. Informal settlements cover one-quarter of the city (Richmond, Myers and Namuli, 2018) and are home to c.70% of Kampala's population (Nastar *et al.*, 2019). Informal settlements in Kampala exhibit high levels of poverty, inequality and vulnerability, in terms of sanitation and water access (Richmond, Myers and Namuli, 2018). Whilst water and sanitation are critical indicators of vulnerability in Kampala (Richmond, Myers and Namuli, 2018), our findings on the climate regulatory role of vegetated areas strongly suggest that proximity and access to green-infrastructure are equally vital for evaluating vulnerability in African cities as previous studies have suggested (Pauleit *et al.*, 2015). Moreover, vegetation in cities has

multifunctional benefits in addition to climate regulation that include: provision of shade (Li, Ratti and Seiferling, 2018), control of storm water flow (Berland *et al.*, 2017), air quality enhancement (Soares *et al.*, 2011) and aesthetic attributes related to stress reduction (Jiang, Chang and Sullivan, 2014; Carrus *et al.*, 2015; Triguero-Mas *et al.*, 2015). The profound potential of vegetation for improving urban ecosystem functions in developing cities where other forms of infrastructure are underperforming (Lindley *et al.*, 2015) justifies initiatives aimed at provision of green-infrastructure and revegetation. Such undertakings should most focus in densely populated informal settlements that have low vegetation cover and high levels of vulnerability.

Given that the physical extent of the area used for the analysis (c. 1260 km^2) covered Kampala greater metropolitan area and stretched to the unurbanised areas, the findings of this study are beneficial for urban planning related to future developments and safeguard the provision of ecosystem services. The horizontal growth of Kampala in recent decades is expected to continue under current projections of up to 13 million inhabitants by 2040 (World Bank, 2016). The most vegetated urban form types that cover the periphery of present-day Kampala (Sparsely built and scattered tree LCZ types) will most likely house the growing population in a way similar to the observed patterns of urban growth in the past decades (World Bank, 2016). Given that the recent increase in the extent of informal settlements that constitute the compact low rise (low vegetation cover) LCZ3_F category has typified recent urban growth in Kampala, anticipated growth of the city might take on a similar pattern. The projected loss in vegetation cover and significant reduction in the provision of ecosystem functions might further intensify the UHI intensity within Kampala. Therefore, urban planning aimed at provision of ecosystem services in light of the growing population is much needed.

The application of the LCZ framework for integrating climate-sensitive urban design into local planning is a promising approach for rapidly urbanising cities in SSA as has been explored for Colombo, Sri Lanka (Perera and Emmanuel, 2018). For example, a development scenario towards more open low rise (LCZ 6) than compact low rise with bare soil (LCZ3_F) would ensure the provision of ecosystem services associated with a higher vegetation cover. Finally, while planning practices to date have often been

undertaken independently by the different administrative units constituting Kampala greater metropolitan area, the impetus for an integrated landscape and urban planning strategy covering greater Kampala is essential for sustainable urbanisation.

7.4 Strength and limitations

7.4.1 Strengths

The main strength of this study was the ability to use both remote sensing and in-situ field observations and monitoring to complement one another in the understating of urban climatic and phenological processes in a tropical city.

A vital feature of this study was the empirical approach used that generated a considerably large data set. The nature of the study involving in-situ measurements as opposed to laboratory experiments strengthens the relevance and generalisation of these findings in the real world. Moreover, the selection of a wide of range of sites within the city highlighting the heterogeneous nature of cities as opposed to using an urban-rural dichotomy depicts the continuum of urban climate and phenological processes. Moreover, the uniqueness of this study as the first one of its kind to employ the LCZ framework for examining phenology in urban environments gives a robust methodological foundation for future studies. Equally, the application of statistical modelling to examine urban climate and phenology at high temporal scales and determination of quantitative attributes of predictor and response variable form a strong foundation for the application of these findings in the real world by policymakers and urban planners.

The study provides significant new findings in the field of phenology related to tropical urban environments which more generally have been under-researched in comparison to temperate climates. The findings are relevant for the formulation of policies for sustainable urbanisation in tropical developing countries where urbanisation is taking on forms that are different from classic urbanisation in the global North. Moreover, the consequences of the current urbanisation practices in tropical developing countries are still understudied and poorly known.

7.4.2 Limitations

Inevitably, this research had some limitations. This study examined the phenological processes of only four out of ten other LCZs. Therefore, the nature of the phenological processes inherent to other local climate zones of the study site is yet to be determined. However, given that the candidate local climate zones used in this study highlighted a continuum of urbanisation intensity with some of the most and least built examples, the findings are meaningful for inferring the phenological patterns of LCZs not covered under the scope of this study. This study focused on the surface characters of cities and therefore ignored the potential influence of other variables such as sky-view factor associated with the 3-dimensions of cities or the building materials that affect albedo. Equally, the Influence of wind and precipitation were undetermined in this study.

7.5 Research recommendations

This study has provided evidence for the occurrence of urban-induced climate and phenological differences in a tropical city with a tropical rainforest climate type. There remains a need for further empirical enquiries into the phenological processes in different tropical climate types and cities that take on different morphologies in comparison to Kampala. Based on the findings of this study, some recommendations for future research can be made.

Urbanisation across the African continent is associated with very high rates of de-vegetation (Lindley *et al.*, 2015; Yao *et al.*, 2019), yet the urban population is expected to grow three-fold from c.400 million presently to 1.26 billion by 2050 (United Nations, 2014). The combined effect of rapid urbanisation and high de-vegetation is an increased risk and exposure to the hazards associated with urbanisation and climate change. However, present-day knowledge on urban ecology is very limited in Africa as evidenced by a small number of studies on urban climate (Roth, 2007), green spaces and densification (Haaland and van den Bosch, 2015) and ecosystem services of vegetation cover (Cilliers *et al.*, 2013; du Toit *et al.*, 2018). A more extensive range of exemplar studies on urban climate, green spaces and phenology that cover the scope of differences in tropical climate types and urbanisation practices in African cities is needed to strengthen the existing knowledge and scientific foundation for policy

transformations that aim for sustainable urbanisation. Moreover, long term studies in tropical African cities ought to be undertaken to track climate through time and separate the effects of urbanisation from climate change on local climate and the consequences for ecological processes associated and ecosystem functions.

The influence of vegetation cover on tropical urban climate often assumes that vegetation cover is static through time. Based on the findings of this study, however, tree canopy cover evolves as a result of local climate, and this might feedback on the local climate. Future research, therefore, ought to examine the influence of temporal changes in canopy cover on local urban climate, and the feedback responses of phenology on urban climate.

A lot of the attention of urban climate studies in tropical urban environments has focused on temperature and UHI phenomena. Relative humidity which determines human thermal comfort (Hass *et al.*, 2016; Yang, Ren and Hou, 2017), pollutant load (Lou *et al.*, 2017; Zalakeviciute, López-Villada and Rybarczyk, 2018), spatial patterns of soil moisture and phenology remains understudied. Future research in tropical environments ought to examine the spatiotemporal patterns of relative humidity and their relationship with other urban climatic variables and phenology in different tropical cities and tropical climate types.

Considering the vital role water availability plays in the determination of spatial differences in urban climate, future research seeking to understand the effect of the UHI on ecological processes in cities ought to account for the differences in soil moisture. To achieve this would require sampling and monitoring strategies that overcome the challenges posed by urban environments concerning heterogeneity in soil types, soil compaction and soil depth and the depth of the water table and the associated seasonal changes. Linked to the temporal changes in water availability is the surface energy balance for which there is minimal knowledge in the context of tropical cities.

Surface Energy Balance (SEB) in urban environments incorporate aspects of direct solar radiation, latent heat, sensible heat, energy flux storage, anthropogenic heat and the horizontal advective flux (Oke, 1988). In tropical urban environments, however, there

are only two longterm (> 1 year) SEB studies, indicating a general lack of information about the dynamics of SEB, anthropogenic heat release and the relationship between UHI and energy flux storage (Giridharan and Emmanuel, 2018). This knowledge gap has mainly been attributable to instrumentation difficulties, cost and long-term commitment for undertaking monitoring (Giridharan and Emmanuel, 2018). As such, future research ought to investigate SEB to fully understand tropical UHI and urban climate phenomena in different climate types and cities.

The LCZ framework is increasingly being adopted for urban climate research because of its numerous advantages, including universal applicability across cities with different urbanisation practices. However, designation of an LCZ class to a given zone with homogeneous land cover composition requires that the zone has a minimum radius of 200 m. The usage of the LCZ framework is thus challenging in highly heterogeneous areas within cities where considerable differences in landcover composition occur in areas of a radius less than 200 m. The intrinsic land cover and structural characteristics of each unit zone smaller than the recommended minimum unit size of an LCZ can be used for attribution to local climate to overcome this challenge as was approached in this study. Future research into the characterisation of urban form using the LCZ framework ought to explore the feasibility of adjusting the LCZ classification for cities or areas within cities that have heterogeneous urban form.

Although this study focused on only four local climate zones, there was sufficient evidence of phenological differences linked to the structural differences of the LCZs and the associated Surface UHI differences. Future research ought to investigate the phenological patterns of other LCZs not covered under the scope of this study in tropical cities. Equally, LCZs might be meaningful for phenological characterisation in temperate regions, where no phenological studies have thus far been undertaken using LCZs. Furthermore, although the current usage of LCZs was mainly for landscape phenological processes, the LCZ classification could be adopted for phenology of individual species.

Herbaceous plants are more sensitive to microclimatic variations than trees (Mimet *et al.*, 2009) and trees equally vary in their sensitivity to local environmental settings

(Williams *et al.*, 1997) as was observed for the two deciduous species in this study. Furthermore, landscape phenological patterns that encompass the wider phenological signal of all vegetation types combined irrespective of species and plant functional type were observed along a gradient of urbanisation. A strong case is made for future research into the sensitivity of the phenology of individual plant functional types (including grasses, herbs and shrubs) and evergreen trees species to urban environments. Furthermore, the sensitivity of other pheno-events such as flower and fruit development in tropical cities is an area for future research.

Other than the UHI intensity, phenology has been observed to be affected by non-climatic aspects of urban environments that vary along an urbanisation intensity gradient such as air pollutants (Jochner *et al.*, 2015) and nutrient availability (Jochner, Hofler, *et al.*, 2013). However, this phenomena has so far only been investigated temperate cities, and there is limited knowledge about the influence of non-climatic aspects of urban environments on phenology in tropical cities.

Near-surface remote sensing phenology through the use of optical and radiometric sensors above the ground (50 m or less) to quantify changes in the land surface (Richardson, Klosterman and Toomey, 2013; Brown *et al.*, 2016; Alberton *et al.*, 2017) characterises landscape phenology in a way similar to satellite remote sensors. Near-surface remote sensing is a novel and promising technique that bridges visual observations (organism scale) and satellite-based phenology (landscape scale) with numerous advantages that overcome the limitations associated with visual observations and satellite remote sensing. These include quantification of both seasonal greening and other pheno-events like flowering and fruiting; ease of separation of properties of canopy structure (Leaf Area Index) and canopy function (photosynthetic activity); and a reasonably high spatial and temporal resolution. However, the application of near-surface remote sensing is mostly limited to natural environments, and no studies have thus far used near-surface remote sensing in tropical urban environments. Future research ought to integrate all three approaches for a full appreciation of the effects of urbanisation on phenology in tropical cities.

BIBLIOGRAPHY

Abernethy, K. *et al.* (2018) 'Current issues in tropical phenology: a synthesis', *Biotropica*, 50(3), pp. 477–482. doi: 10.1111/btp.12558.

de Abreu-Harbicha, L. V, Labakia, L. C. and Matzarakis, A. (2015) 'Effect of tree planting design and tree species on human thermal comfort in the tropics', *Landscape and Urban Planning*, 138, pp. 99–109. doi: 10.1016/j.landurbplan.2015.02.008.

Acero, J. A. and Gonzalez-Asensio, B. (2018) 'Influence of vegetation on the morning land surface temperature in a tropical humid urban area', *URBAN CLIMATE*, 26, pp. 231–243. doi: 10.1016/j.uclim.2018.09.004.

Ackerman, B., Changnon, S. and Dzurisin, G. (1978) 'Summary of METROMEX, volume 2: Causes of precipitation anomalies', *Urbana*.

Adole, T., Dash, J. and Atkinson, P. M. (2016) 'A systematic review of vegetation phenology in Africa', *Ecological Informatics*, 34, pp. 117–128. doi: 10.1016/j.ecoinf.2016.05.004.

Akbari, H. and Hashem (2005) 'Energy Saving Potentials and Air Quality Benefits of Urban HeatIslandMitigation', *First International Conference on Passive and Low Energy Cooling for the Built Environment*.

Akbari, H., Pomerantz, M. and Taha, H., 2001. Cool surfaces and shade trees to reduce energy use and improve air quality in urban areas. *Solar energy*, *70*(3), pp.295-310.

Alberton, B. *et al.* (2017) 'Introducing digital cameras to monitor plant phenology in the tropics: applications for conservation', *Perspectives in Ecology and Conservation*, 15(2), pp. 82–90. doi: 10.1016/j.pecon.2017.06.004.

Amorim, M. C. de C. T. and Dubreuil, V. (2017) 'Intensity of urban heat islands in tropical and temperate climates', *Climate*. doi: 10.3390/cli5040091.

Antos, S. E. *et al.* (2016) 'The Morphology of African Cities', *World Bank Policy Research Working Paper*.

Archibald, S. and Scholes, R. J. (2007) 'Leaf green-up in a semi-arid African savanna - separating tree and grass responses to environmental cues', *Journal of Vegetation Science*, 18(4), pp. 583–594. doi: 10.1658/1100-9233(2007)18[583:lgiasa]2.0.co;2.

Arnfield, A. J. (2020) 'Köppen climate classification', *Encyclopedia Britannica*. Encyclopedia Britannica, inc. Available at: https://www.britannica.com/science/Koppen-climate-classification.

Asner, G. P., Townsend, A. R. and Braswell, B. H. (2000) 'Satellite observation of El Nino effects on Amazon forest phenology and productivity', *Geophysical Research Letters*, 27(7), pp. 981–984. doi: 10.1029/1999gl011113.

Ayanlade, A. (2016) 'Variation in diurnal and seasonal urban land surface temperature:

landuse change impacts assessment over Lagos metropolitan city', *Modeling Earth Systems and Environment*. doi: 10.1007/s40808-016-0238-z.

Baayen, R. H. (2008) *Analyzing Linguistic Data: A Practical Introduction to Statistics using R*. Cambridge: Cambridge University Press. doi: DOI: 10.1017/CBO9780511801686.

Balchin, W. G. V. and Pye, N. (1947) 'A micro-climatological investigation of bath and the surrounding district', *Quarterly Journal of the Royal Meteorological Society*. doi: 10.1002/qj.49707331706.

Badeck, F. W. *et al.* (2004) 'Responses of spring phenology to climate change', *New Phytologist*, 162(2), pp. 295–309. doi: 10.1111/j.1469-8137.2004.01059.x.

Balogun, I. A. and Balogun, A. A. (2014) 'Urban heat island and bioclimatological conditions in a hot-humid tropical city: The example of Akure, Nigeria', *Erde*. doi: 10.12854/erde-145-2.

Barnes, K. B., Morgan, J. and Roberge, M. (2001) 'Impervious surfaces and the quality of natural and built environments', *Baltimore: Department of Geography and Environmental Planning, Towson University*.

Barton, K. (2018) 'MuMIn: Multi-Model Inference'. Available at: https://cran.r-project.org/package=MuMIn.

Bastos, A. *et al.* (2018) 'Impact of the 2015/2016 El Nino on the terrestrial carbon cycle constrained by bottom-up and top-down approaches', *Philosophical Transactions of the Royal Society B: Biological Sciences*, 373(1760), p. 20170304. doi: 10.1098/rstb.2017.0304.

Bates, D. *et al.* (2015) 'Fitting Linear Mixed-Effects Models Using {lme4}', *Journal of Statistical Software*, 67(1), pp. 1–48. doi: 10.18637/jss.v067.i01.

Bechtel, B. *et al.* (2015) 'Mapping Local Climate Zones for a Worldwide Database of the Form and Function of Cities', *Isprs International Journal of Geo-Information*, 4(1), pp. 199–219. doi: 10.3390/ijgi4010199.

Bechtel, B. *et al.* (2019) 'Generating WUDAPT Level 0 data – Current status of production and evaluation', *Urban Climate*, 27, pp. 24–45. doi: https://doi.org/10.1016/j.uclim.2018.10.001.

Berland, A. *et al.* (2017) 'The role of trees in urban stormwater management', *Landscape and Urban Planning*, 162, pp. 167–177. doi: 10.1016/j.landurbplan.2017.02.017.

Bidandi, F. and Williams, J. J. (2017) 'The terrain of urbanisation process and policy frameworks: A critical analysis of the Kampala experience', *Cogent Social Sciences*, 3, p. 13. doi: 10.1080/23311886.2016.1275949.

Blaschke, T. (2010) 'Object based image analysis for remote sensing', *ISPRS journal of photogrammetry and remote sensing*. New York, NY :, 65(1), pp. 2–16. doi:

10.1016/j.isprsjprs.2009.06.004.

Blaschke, T. *et al.* (2014) 'Geographic Object-Based Image Analysis – Towards a new paradigm', *ISPRS Journal of Photogrammetry and Remote Sensing*. Elsevier, 87, pp. 180–191. doi: 10.1016/J.ISPRSJPRS.2013.09.014.

Borchert, R. (1983) 'PHENOLOGY AND CONTROL OF FLOWERING IN TROPICAL TREES', *Biotropica*, 15(2), pp. 81–89. doi: 10.2307/2387949.

Borchert, R., Rivera, G. and Hagnauer, W. (2002) 'Modification of vegetative phenology in a tropical semi-deciduous forest by abnormal drought and rain', *Biotropica*, 34(1), pp. 27–39. doi: 10.1111/j.1744-7429.2002.tb00239.x.

Brinkhoff, T. (2019) '(City, Uganda) - Population Statistics, Charts, Map and Location', *(City, Uganda) - Population Statistics, Charts, Map and Location*. Available at: http://www.citypopulation.de/php/uganda-admin.php?adm2id=012.

Brooks, D. S. and Eronen, M. I. (2018) 'The significance of levels of organization for scientific research: A heuristic approach', *Studies in History and Philosophy of Science Part C: Studies in History and Philosophy of Biological and Biomedical Sciences*. Pergamon, 68–69, pp. 34–41. doi: 10.1016/J.SHPSC.2018.04.003.

Brousse, O. *et al.* (2019) 'Using Local Climate Zones in Sub-Saharan Africa to tackle urban health issues', *Urban Climate*, 27, pp. 227–242. doi: 10.1016/j.uclim.2018.12.004.

Brown, M. E., de Beurs, K. and Vrieling, A. (2010) 'The response of African land surface phenology to large scale climate oscillations', *Remote Sensing of Environment*, 114(10), pp. 2286–2296. doi: 10.1016/j.rse.2010.05.005.

Brown, T. B. *et al.* (2016) 'Using phenocams to monitor our changing Earth: toward a global phenocam network', *Frontiers in Ecology and the Environment*, 14(2), pp. 84–93. doi: 10.1002/fee.1222.

Burnham, K. P. and Anderson, D. R. (2003) *Model selection and multimodel inference: a practical information-theoretic approach*. Springer Science & Business Media.

Burnham, K. P., Anderson, D. R. and Huyvaert, K. P. (2011) 'AIC model selection and multimodel inference in behavioral ecology: some background, observations, and comparisons', *Behavioral Ecology and Sociobiology*, 65(1), pp. 23–35. doi: 10.1007/s00265-010-1029-6.

Buyantuyev, A. *et al.* (2012) 'A Space-For-Time (SFT) Substitution Approach to Studying Historical Phenological Changes in Urban Environment', *Plos One*, 7(12), p. 13. doi: 10.1371/journal.pone.0051260.

Buyantuyev, A. and Wu, J. (2012) 'Urbanization diversifies land surface phenology in arid environments: Interactions among vegetation, climatic variation, and land use pattern in the Phoenix metropolitan region, USA', *Landscape and Urban Planning*, 105(1–2), pp. 149–159. doi: 10.1016/j.landurbplan.2011.12.013.

Cai, M. *et al.* (2018) 'Investigating the relationship between local climate zone and land surface temperature using an improved WUDAPT methodology - A case study of Yangtze River Delta, China', *Urban Climate*, 24, pp. 485–502. doi: 10.1016/j.uclim.2017.05.010.

Cai, Y. *et al.* (2019) 'Research on soil moisture prediction model based on deep learning', *PLOS ONE*. Public Library of Science, 14(4), pp. 1–19. doi: 10.1371/journal.pone.0214508.

Cai, Z. *et al.* (2017) 'Performance of smoothing methods for reconstructing NDVI time-series and estimating vegetation phenology from MODIS data', *Remote Sensing*, 9(12). doi: 10.3390/rs9121271.

de Camargo, M. G. G. *et al.* (2018) 'Leafing patterns and leaf exchange strategies of a cerrado woody community', *Biotropica*, 50(3), pp. 442–454. doi: 10.1111/btp.12552.

Cao, C., Lee, X., Liu, S., Schultz, N., Xiao, W., Zhang, M. and Zhao, L., 2016. Urban heat islands in China enhanced by haze pollution. *Nature Communications*, *7*(1), pp.1-7.

Carrus, G. *et al.* (2015) 'Go greener, feel better? The positive effects of biodiversity on the well-being of individuals visiting, urban and peri-urban green areas', *Landscape and Urban Planning*, 134, pp. 221–228. doi: 10.1016/j.landurbplan.2014.10.022.

Cavan, G. *et al.* (2014) 'Urban morphological determinants of temperature regulating ecosystem services in two African cities', *Ecological indicators.* Amsterdam :, 42, pp. 43–57. doi: 10.1016/j.ecolind.2014.01.025.

Chapman, S. *et al.* (2018) 'The Effect of Urban Density and Vegetation Cover on the Heat Island of a Subtropical City', *JOURNAL OF APPLIED METEOROLOGY AND CLIMATOLOGY*, 57(11), pp. 2531–2550. doi: 10.1175/JAMC-D-17-0316.1.

Charabi, Y. and Bakhit, A. (2011) 'Assessment of the canopy urban heat island of a coastal arid tropical city: The case of Muscat, Oman', *ATMOSPHERIC RESEARCH*, 101(1–2), pp. 215–227. doi: 10.1016/j.atmosres.2011.02.010.

Cheesman, A. W. and Winter, K. (2013a) 'Elevated night-time temperatures increase growth in seedlings of two tropical pioneer tree species', *New Phytologist*, 197(4), pp. 1185–1192. doi: 10.1111/nph.12098.

Cheesman, A. W. and Winter, K. (2013b) 'Growth response and acclimation of CO2 exchange characteristics to elevated temperatures in tropical tree seedlings', *Journal of Experimental Botany*, 64(12), pp. 3817–3828. doi: 10.1093/jxb/ert211.

Cheung, H.K.W., 2011. *An urban heat island study for building and urban design* (Doctoral dissertation, University of Manchester).

Chibuike, E. M. *et al.* (2018) 'Assessment of green parks cooling effect on Abuja urban microclimate using geospatial techniques', *Remote Sensing Applications: Society and Environment*. Elsevier, 11, pp. 11–21. doi: 10.1016/J.RSASE.2018.04.006.

Chotchaiwong, P. and Wijitkosum, S. (2019) 'Relationship between Land Surface

Temperature and Land Use in Nakhon Ratchasima City, Thailand', *Engineering Journal*, 23(4), pp. 1–14.

Chow, W. T. L. *et al.* (2016) 'Assessment of measured and perceived microclimates within a tropical urban forest', *URBAN FORESTRY & URBAN GREENING*, 16, pp. 62–75. doi: 10.1016/j.ufug.2016.01.010.

Chow, W. T. L. and Roth, M. (2006) 'Temporal dynamics of the urban heat island of Singapore', *International Journal of Climatology*, 26(15), pp. 2243–2260. doi: 10.1002/joc.1364.

Cilliers, S. *et al.* (2013) 'Ecosystem services of urban green spaces in African countries-perspectives and challenges', *Urban Ecosystems*, 16(4), pp. 681–702. doi: 10.1007/s11252-012-0254-3.

Clarke, K. R. (1993) 'Non-parametric multivariate analyses of changes in community structure', *Australian Journal of Ecology*. doi: 10.1111/j.1442-9993.1993.tb00438.x.

Clinton, N. *et al.* (2014) 'Global-Scale Associations of Vegetation Phenology with Rainfall and Temperature at a High Spatio-Temporal Resolution', *Remote Sensing*, 6(8), pp. 7320–7338. doi: 10.3390/rs6087320.

Clinton, N. and Gong, P., 2013. MODIS detected surface urban heat islands and sinks: Global locations and controls. *Remote Sensing of Environment*, *134*, pp.294-304.

Collier, C.G., 2006. The impact of urban areas on weather. *Quarterly Journal of the Royal Meteorological Society: A journal of the atmospheric sciences, applied meteorology and physical oceanography*, *132*(614), pp.1-25.

Comber, A. and Brunsdon, C. (2015) 'A spatial analysis of plant phenophase changes and the impact of increases in urban land use', *International Journal of Climatology*, 35(6), pp. 972–980. doi: 10.1002/joc.4030.

Condit, R. *et al.* (2000) 'Quantifying the deciduousness of tropical forest canopies under varying climates', *Journal of Vegetation Science*, 11(5), pp. 649–658. doi: 10.2307/3236572.

Conrad, O. *et al.* (2015) 'System for automated geoscientific analyses (SAGA) v. 2.1. 4', *Geoscientific Model Development*. Copernicus GmbH, 8(7), pp. 1991–2007.

Cui, Y. Y. and De Foy, B. (2012) 'Seasonal variations of the urban heat island at the surface and the near-surface and reductions due to urban vegetation in Mexico City', *Journal of Applied Meteorology and Climatology*. doi: 10.1175/JAMC-D-11-0104.1.

Cunningham, S. C. and Read, J. (2002) 'Comparison of temperate and tropical rainforest tree species: photosynthetic responses to growth temperature', *Oecologia*, 133(2), pp. 112–119. doi: 10.1007/s00442-002-1034-1.

Daac.ornl.gov (2016) 'Global Subsets Tool: MODIS/VIIRS Land Products', *MODIS/VIIRS Subsets*. Available at: https://modis.ornl.gov/cgi-bin/MODIS/global/subset.pl.

Dallimer, M. *et al.* (2016) 'The extent of shifts in vegetation phenology between rural and urban areas within a human-dominated region', *Ecology and Evolution*, 6(7), pp.

1942–1953. doi: 10.1002/ece3.1990.

Dalmolin, A. C. *et al.* (2015) 'Is the dry season an important driver of phenology and growth for two Brazilian savanna tree species with contrasting leaf habits?', *Plant Ecology*, 216(3), pp. 407–417. doi: 10.1007/s11258-014-0445-5.

Demuzere, M. *et al.* (2017) 'Impact of urban canopy models and external parameters on the modelled urban energy balance in a tropical city', *QUARTERLY JOURNAL OF THE ROYAL METEOROLOGICAL SOCIETY*, 143(704, A), pp. 1581–1596. doi: 10.1002/qj.3028.

Denny, E. G. *et al.* (2014) 'Standardized phenology monitoring methods to track plant and animal activity for science and resource management applications', *International Journal of Biometeorology*, 58(4), pp. 591–601. doi: 10.1007/s00484-014-0789-5.

Dimoudi, A. and Nikolopoulou, M. (2003) 'Vegetation in the urban environment: microclimatic analysis and benefits', *Energy and buildings*, 35(1), pp. 69–76. doi: 10.1016/s0378-7788(02)00081-6.

Dj, D. (1996) 'Increased activity of northern vegetation inferred from atmospheric C0, measurements', *Nature*. [London] :, 382, p. 11.

Do, F. C. *et al.* (2005) 'Environmental influence on canopy phenology in the dry tropics', *Forest Ecology and Management*, 215(1), pp. 319–328. doi: https://doi.org/10.1016/j.foreco.2005.05.022.

Donnelly, A. and Yu, R. (2017) 'The rise of phenology with climate change: an evaluation of IJB publications', *International Journal of Biometeorology*, 61, pp. S29–S50. doi: 10.1007/s00484-017-1371-8.

Doughty, C. E. and Goulden, M. L. (2008) 'Are tropical forests near a high temperature threshold?', *Journal of Geophysical Research-Biogeosciences*, 113, p. 12. doi: 10.1029/2007jg000632.

Duarte, D. H. S. *et al.* (2015) 'The impact of vegetation on urban microclimate to counterbalance built density in a subtropical changing climate', *URBAN CLIMATE*, 14(2, SI), pp. 224–239. doi: 10.1016/j.uclim.2015.09.006.

Eklundh, L. and Jönsson, P. (2015) *TIMESAT 3.2 with parallel processing Software Manual*. ed. S. Lund and Malmö University.

Eklundh, L. and Jönsson, P. (2016) 'TIMESAT for Processing Time-Series Data from Satellite Sensors for Land Surface Monitoring', in Ban, Y. (ed.) *Multitemporal Remote Sensing: Methods and Applications*. Cham: Springer International Publishing, pp. 177–194. doi: 10.1007/978-3-319-47037-5_9.

EPA, R. U. H. I. (2015) 'Compendium of strategies urban heat island basics, 2009', *Available on line at: http://www. epa. gov/hiri/resources/compendium. htm*.Voogt, J. A. (2000) 'Image representations of complete urban surface temperatures', *Geocarto International*, 15(3), pp. 21–32. doi: 10.1080/10106040008542160.

FAO (1981) 'Part IICOUNTRY BRIEFS - UGANDA', *Tropical forest resources assessment*

project - Forest resource of Tropical Africa Vol. II. Available at: http://www.fao.org/3/ad910e/AD910E30.htm.

Fenner, D. *et al.* (2014) 'Spatial and temporal air temperature variability in Berlin, Germany, during the years 2001–2010', *Urban Climate*, 10, pp. 308–331. doi: 10.1016/j.uclim.2014.02.004.

Fenner, M. (1998) 'The phenology of growth and reproduction in plants', *Perspectives in Plant Ecology, Evolution and Systematics*, 1(1), pp. 78–91.

Feyisa, G. L., Dons, K. and Meilby, H. (2014) 'Efficiency of parks in mitigating urban heat island effect: An example from Addis Ababa', *Landscape and Urban Planning*. Amsterdam :, 123, pp. 87–95. doi: 10.1016/j.landurbplan.2013.12.008.

Figueroa, P. G. and Fournier, L. A. (1996) 'Phenology and physiology in two populations of Tabebuia rosea in Costa Rica (Scrophulariales: Bignoniaceae)', *Revista De Biologia Tropical*, 44(1), pp. 61–70.

Fitchett, J. M., Grab, S. W. and Thompson, D. I. (2015) 'Plant phenology and climate change: Progress in methodological approaches and application', *Progress in Physical Geography*, 39(4), pp. 460–482. doi: 10.1177/0309133315578940.

Flores, J. L. R., Pereira Filho, A. J. and Karam, H. A. (2016) 'Estimation of long term low resolution surface urban heat island intensities for tropical cities using MODIS remote sensing data', *URBAN CLIMATE*, 17, pp. 32–66. doi: 10.1016/j.uclim.2016.04.002.

Foley, J. A. *et al.* (2005) 'Global consequences of land use', *Science*. doi: 10.1126/science.1111772.

Fonseka, H. P. U. *et al.* (2019) 'Urbanization and its impacts on land surface temperature in Colombo Metropolitan Area, Sri Lanka, from 1988 to 2016', *Remote Sensing*. doi: 10.3390/rs11080926.

Franco, D. M. P. *et al.* (2019) 'Effect of Local Climate Zone (LCZ) classification on ozone chemical transport model simulations in Sao Paulo, Brazil', *Urban Climate*, 27, pp. 293–313. doi: 10.1016/j.uclim.2018.12.007.

Gazal, R. *et al.* (2008) 'GLOBE students, teachers, and scientists demonstrate variable differences between urban and rural leaf phenology', *Global Change Biology*, 14(7), pp. 1568–1580. doi: 10.1111/j.1365-2486.2008.01602.x.

Geletič, J., Lehnert, M. and Dobrovolný, P. (2016) 'Land surface temperature differences within local climate zones, Based on two central European cities', *Remote Sensing*, 8(10). doi: 10.3390/rs8100788.

Gervais, N., Buyantuev, A. and Gao, F. (2017) 'Modeling the Effects of the Urban Built-Up Environment on Plant Phenology Using Fused Satellite Data', *Remote Sensing*, 9(1). doi: 10.3390/rs9010099.

Gill, S. E. *et al.* (2008) 'Characterising the urban environment of UK cities and towns: A template for landscape planning', *Landscape and Urban Planning*. Amsterdam :, 87(3),

pp. 210–222. doi: 10.1016/j.landurbplan.2008.06.008.

Gioia, A., Paolini, L., Malizia, A., Oltra-Carrió, R. and Sobrino, J.A., 2014. Size matters: vegetation patch size and surface temperature relationship in foothills cities of northwestern Argentina. *Urban ecosystems*, *17*(4), pp.1161-1174.

Giridharan, R. and Emmanuel, R. (2018) 'The impact of urban compactness, comfort strategies and energy consumption on tropical urban heat island intensity: A review', *Sustainable Cities and Society*, 40, pp. 677–687. doi: 10.1016/j.scs.2018.01.024.

Gorse, C. *et al.* (2019) 'The Planning and Design of Buildings: Urban Heat Islands---Mitigation', in Dastbaz, M. and Cochrane, P. (eds) *Industry 4.0 and Engineering for a Sustainable Future*. Cham: Springer International Publishing, pp. 211–225. doi: 10.1007/978-3-030-12953-8_13.

Gray, S. B. and Brady, S. M. (2016) 'Plant developmental responses to climate change', *Developmental Biology*, 419(1), pp. 64–77. doi: https://doi.org/10.1016/j.ydbio.2016.07.023.

Grimm, N. B. *et al.* (2008) 'Global change and the ecology of cities', *Science*, 319(5864), pp. 756–760. doi: 10.1126/science.1150195.

Grimmond, C. S. B. and Oke, T. R. (2002) 'Turbulent heat fluxes in urban areas: Observations and a local-scale urban meteorological parameterization scheme (LUMPS)', *Journal of Applied Meteorology*. doi: 10.1175/1520-0450(2002)041<0792:THFIUA>2.0.CO;2.

Guan, K. *et al.* (2014) 'Continental-scale impacts of intra-seasonal rainfall variability on simulated ecosystem responses in Africa', *Biogeosciences*, 11(23), pp. 6939–6954. doi: 10.5194/bg-11-6939-2014.

Guan, K. Y. *et al.* (2013) 'Seasonal coupling of canopy structure and function in African tropical forests and its environmental controls', *Ecosphere*, 4(3), p. 21. doi: 10.1890/es12-00232.1.

Guan, K. Y. *et al.* (2014) 'Terrestrial hydrological controls on land surface phenology of African savannas and woodlands', *Journal of Geophysical Research-Biogeosciences*, 119(8), pp. 1652–1669. doi: 10.1002/2013jg002572.

Haaland, C. and van den Bosch, C. K. (2015) 'Challenges and strategies for urban green-space planning in cities undergoing densification: A review', *Urban Forestry & Urban Greening*, 14(4), pp. 760–771. doi: 10.1016/j.ufug.2015.07.009.

Hage, K. D. (1975) 'Urban-Rural Humidity Differences', *Journal of Applied Meteorology*. doi: 10.1175/1520-0450(1975)014<1277:urhd>2.0.co;2.

Han, G. and Xu, J. (2013) 'Land Surface Phenology and Land Surface Temperature Changes Along an Urban-Rural Gradient in Yangtze River Delta, China', *Environmental Management*, 52(1), pp. 234–249. doi: 10.1007/s00267-013-0097-6.

Hanes, Jonathan M, Liang, L. and Morisette, J. T. (2014) 'Land Surface Phenology', in

Hanes, J M (ed.) *Biophysical Applications of Satellite Remote Sensing*, pp. 99–125. doi: 10.1007/978-3-642-25047-7_4.

Hass, A. L. *et al.* (2016) 'Heat and Humidity in the City: Neighborhood Heat Index Variability in a Mid-Sized City in the Southeastern United States', *International Journal of Environmental Research and Public Health*, 13(1). doi: 10.3390/ijerph13010117.

Hatfield, J. L. and Prueger, J. H. (2015) 'Temperature extremes: Effect on plant growth and development', *Weather and Climate Extremes*, 10, pp. 4–10. doi: https://doi.org/10.1016/j.wace.2015.08.001.

Heaviside, C., Macintyre, H. and Vardoulakis, S. (2017) 'The Urban Heat Island: Implications for Health in a Changing Environment', *Current environmental health reports*. doi: 10.1007/s40572-017-0150-3.

Heisler, G. M. and Brazel, A. J. (2010) 'The urban physical environment: Temperature and urban heat islands', *Urban ecosystem ecology*, (urbanecosysteme), pp. 29–56.

Hudson, I. L. and Keatley, M. R. (2009) *Phenological research: methods for environmental and climate change analysis*. Springer Science & Business Media.

Huete, A. *et al.* (2011) *MODIS Vegetation Indices*, *Land Remote Sensing and Global Environmental Change: Nasa's Earth Observing System and the Science of Aster and Modis*. Edited by B. Ramachandran, C. O. Justice, and M. J. Abrams. doi: 10.1007/978-1-4419-6749-7_26.

Hufkens, K. *et al.* (2012) 'Linking near-surface and satellite remote sensing measurements of deciduous broadleaf forest phenology', *Remote Sensing of Environment*, 117, pp. 307–321. doi: 10.1016/j.rse.2011.10.006.

Huxley, P. A. and Vaneck, W. A. (1974) 'SEASONAL-CHANGES IN GROWTH AND DEVELOPMENT OF SOME WOODY PERENNIALS NEAR KAMPALA, UGANDA', *Journal of Ecology*, 62(2), pp. 579-. doi: 10.2307/2259000.

IPCC (2014) 'Part A: Global and Sectoral Aspects. (Contribution of Working Group II to the Fifth Assessment Report of the Intergovernmental Panel on Climate Change)', *Climate Change 2014: Impacts, Adaptation, and Vulnerability.*

Jacoby, W. G. (2000) 'Loess: a nonparametric, graphical tool for depicting relationships between variables', *Electoral Studies*, 19(4), pp. 577–613. doi: 10.1016/s0261-3794(99)00028-1.

Jåuregui, E. and Tejeda, A. (1997) 'Urban-rural humidity contrasts in Mexico city', *International Journal of Climatology*. doi: 10.1002/(SICI)1097-0088(199702)17:2<187::AID-JOC114>3.0.CO;2-P.

Jiang, B., Chang, C. Y. and Sullivan, W. C. (2014) 'A dose of nature: Tree cover, stress reduction, and gender differences', *Landscape and Urban Planning*, 132, pp. 26–36. doi: 10.1016/j.landurbplan.2014.08.005.

Jin, H. *et al.* (2018) 'Assessing the effects of urban morphology parameters on

microclimate in Singapore to control the urban heat island effect', *Sustainability*. Multidisciplinary Digital Publishing Institute, 10(1), p. 206.

Jochner, S, Hofler, J., *et al.* (2013) 'Nutrient status: a missing factor in phenological and pollen research?', *Journal of Experimental Botany*, 64(7), pp. 2081–2092. doi: 10.1093/jxb/ert061.

Jochner, S, Alves-Eigenheer, M., *et al.* (2013) 'Using phenology to assess urban heat islands in tropical and temperate regions', *International Journal of Climatology*, 33(15), pp. 3141–3151. doi: 10.1002/joc.3651.

Jochner, Susanne *et al.* (2013) 'Using phenology to assess urban heat islands in tropical and temperate regions', *INTERNATIONAL JOURNAL OF CLIMATOLOGY*, 33(15), pp. 3141–3151. doi: 10.1002/joc.3651.

Jochner, S. *et al.* (2015) 'The effects of short- and long-term air pollutants on plant phenology and leaf characteristics', *Environmental Pollution*, 206, pp. 382–389. doi: 10.1016/j.envpol.2015.07.040.

Jochner, S. C. *et al.* (2011) 'Effects of extreme spring temperatures on urban phenology and pollen production: a case study in Munich and Ingolstadt', *Climate Research*, 49(2), pp. 101–112. doi: 10.3354/cr01022.

Jochner, S. C. *et al.* (2012) 'The influence of altitude and urbanisation on trends and mean dates in phenology (1980-2009)', *International Journal of Biometeorology*, 56(2), pp. 387–394. doi: 10.1007/s00484-011-0444-3.

Jochner, S., Caffarra, A. and Menzel, A. (2013) 'Can spatial data substitute temporal data in phenological modelling? A survey using birch flowering', *Tree Physiology*, 33(12), pp. 1256–1268. doi: 10.1093/treephys/tpt079.

Jochner, S. and Menzel, A. (2015) 'Urban phenological studies - Past, present, future', *Environmental Pollution*, 203, pp. 250–261. doi: 10.1016/j.envpol.2015.01.003.

Jonsson, P. and Eklundh, L. (2004) 'TIMESAT - a program for analyzing time-series of satellite sensor data', *Computers & Geosciences*, 30(8), pp. 833–845. doi: 10.1016/j.cageo.2004.05.006.

Kabisch, N. *et al.* (2017) 'Nature-Based Solutions to Climate Change Adaptation in Urban Areas', *Theory and Practice of Urban Sustainability Transitions*.

Ketterer, C. and Matzarakis, A. (2015) 'Comparison of different methods for the assessment of the urban heat island in Stuttgart, Germany', *International Journal of Biometeorology*, 59(9), pp. 1299–1309. doi: 10.1007/s00484-014-0940-3.

Kiggundu, N. *et al.* (2018) 'Assessing Land Use and Land Cover Changes in the Murchison Bay Catchment of Lake Victoria Basin in Uganda', *Journal of Sustainable Development*, 11, p. 44. doi: 10.5539/jsd.v11n1p44.

Kikon, N. *et al.* (2016) 'Assessment of urban heat islands (UHI) of Noida City, India using multi-temporal satellite data', *Sustainable Cities and Society*. Elsevier, 22, pp. 19–

28. doi: 10.1016/J.SCS.2016.01.005.

King, John (2011) 'Growth: the long and the short of it', in *Reaching for the Sun: How Plants Work*. 2nd edn. Cambridge University Press, p. 101-117. doi: 10.1017/CBO9780511973895.012.

King, J (2011) *Reaching for the Sun: How Plants Work*. Cambridge University Press. Available at: https://books.google.co.uk/books?id=wh9sW9QII6kC.

Kleerekoper, L., Van Esch, M. and Salcedo, T. B. (2012) 'How to make a city climate-proof, addressing the urban heat island effect', *Resources, Conservation and Recycling*. Elsevier, 64, pp. 30–38.

Kogan, F. and Guo, W. (2017) 'Strong 2015-2016 El Nino and implication to global ecosystems from space data', *International Journal of Remote Sensing*, 38(1), pp. 161–178. doi: 10.1080/01431161.2016.1259679.

Kolokotroni, M., Ren, X., Davies, M. and Mavrogianni, A., 2012. London's urban heat island: Impact on current and future energy consumption in office buildings. *Energy and buildings*, *47*, pp.302-311.

Kondo, H. and Kikegawa, Y., 2003. Temperature variation in the urban canopy with anthropogenic energy use. In *Air Quality* (pp. 317-324). Birkhäuser, Basel.

Kotharkar, R. and Bagade, A. (2018) 'Evaluating urban heat island in the critical local climate zones of an Indian city', *Landscape and Urban Planning*, 169, pp. 92–104. doi: 10.1016/j.landurbplan.2017.08.009.

Kottek, M., Grieser, J., Beck, C., Rudolf, B. and Rubel, F., 2006. World map of the Köppen-Geiger climate classification updated. *Meteorologische Zeitschrift*, *15*(3), pp.259-263.

Kotharkar, R. and Surawar, M. (2016) 'Land use, land cover, and population density impact on the formation of canopy urban heat islands through traverse survey in the Nagpur urban area, India', *Journal of Urban Planning and Development*. doi: 10.1061/(ASCE)UP.1943-5444.0000277.

Krehbiel, C., Zhang, X. and Henebry, G. M. (2017) 'Impacts of Thermal Time on Land Surface Phenology in Urban Areas', *Remote Sensing*, 9(5). doi: 10.3390/rs9050499.

Kurniati, A. C. and Nitivattananon, V. (2016) 'Factors influencing urban heat island in Surabaya, Indonesia', *Sustainable Cities and Society*. Elsevier, 27, pp. 99–105. doi: 10.1016/J.SCS.2016.07.006.

Kuttler, W. (2008) 'The urban climate--basic and applied aspects', in *Urban ecology*. Springer, pp. 233–248.

Lakshmi, V., Jackson, T. J. and Zehrfuhs, D. (2003) 'Soil moisture--temperature relationships: results from two field experiments', *Hydrological processes*. Wiley Online Library, 17(15), pp. 3041–3057.

Lamsal, L.N., Martin, R.V., Parrish, D.D. and Krotkov, N.A., 2013. Scaling relationship for NO2 pollution and urban population size: a satellite perspective. *Environmental science & technology*, *47*(14), pp.7855-7861.

Landsberg, H. E. (1981) *The Urban Climate*. Elsevier Science. Available at: https://books.google.co.uk/books?id=zkKHiEXZGBIC.

Lee, H., Mayer, H. and Chen, L. (2016) 'Contribution of trees and grasslands to the mitigation of human heat stress in a residential district of Freiburg, Southwest Germany', *Landscape and Urban Planning*, 148, pp. 37–50. doi: 10.1016/j.landurbplan.2015.12.004.

Li, X.-X. *et al.* (2013) 'A multi-resolution ensemble study of a tropical urban environment and its interactions with the background regional atmosphere', *JOURNAL OF GEOPHYSICAL RESEARCH-ATMOSPHERES*, 118(17), pp. 9804–9818. doi: 10.1002/jgrd.50795.

Li, X. C. *et al.* (2017) 'Response of vegetation phenology to urbanization in the conterminous United States', *Global Change Biology*, 23(7), pp. 2818–2830. doi: 10.1111/gcb.13562.

Li, X. J., Ratti, C. and Seiferling, I. (2018) 'Quantifying the shade provision of street trees in urban landscape: A case study in Boston, USA, using Google Street View', *Landscape and Urban Planning*, 169, pp. 81–91. doi: 10.1016/j.landurbplan.2017.08.011.

Li, H., Meier, F., Lee, X., Chakraborty, T., Liu, J., Schaap, M. and Sodoudi, S., 2018. Interaction between urban heat island and urban pollution island during summer in Berlin. *Science of the total environment*, *636*, pp.818-828.

Li, X. *et al.* (2019) 'Urban heat island impacts on building energy consumption: A review of approaches and findings', *Energy*. Pergamon, 174, pp. 407–419. doi: 10.1016/J.ENERGY.2019.02.183.

Liang, L. and Schwartz, M. (2009) 'Landscape phenology: an integrative approach to seasonal vegetation dynamics', *Landscape Ecology*, 24(4), pp. 465–472. doi: 10.1007/s10980-009-9328-x.

Liang, L., Schwartz, M. D. and Fei, S. (2011) 'Validating satellite phenology through intensive ground observation and landscape scaling in a mixed seasonal forest', *Remote Sensing of Environment*, 115(1), pp. 143–157. doi: 10.1016/j.rse.2010.08.013.

Lieth, H. (1974) 'Phenology and seasonality modeling Springer-Verlag-Berlin', *Heidelberg, New York*, 444.

Lim, C. H. *et al.* (2018) 'Ecological consideration for several methodologies to diagnose vegetation phenology', *Ecological Research*, 33(2), pp. 363–377. doi: 10.1007/s11284-017-1551-3.

Lindley, S. *et al.* (2018) 'Rethinking urban green infrastructure and ecosystem services from the perspective of sub-Saharan African cities', *Landscape and Urban Planning*, 180, pp. 328–338. doi: 10.1016/j.landurbplan.2018.08.016.

Lindley, S. J. *et al.* (2015) 'Green Infrastructure for Climate Adaptation in African Cities', *Urban vulnerability and climate change in Africa :* Cham :, 4, pp. 107–152. doi: 10.1007/978-3-319-03982-4.

Loridan, T. and Grimmond, T. (2012) 'Characterization of energy flux partitioning in urban environments: Links with surface seasonal properties', *Journal of Applied Meteorology and Climatology*, 51(2), pp. 219–241. doi: 10.1175/JAMC-D-11-038.1.

Lou, C. *et al.* (2017) 'Relationships of relative humidity with PM2.5 and PM10 in the Yangtze River Delta, China', *Environmental Monitoring and Assessment*. doi: 10.1007/s10661-017-6281-z.

Lu, P. *et al.* (2006) 'Advance of tree-flowering dates in response to urban climate change', *Agricultural and Forest Meteorology*, 138(1–4), pp. 120–131. doi: 10.1016/j.agrformet.2006.04.002.

Lwasa, S. (2017) 'Options for reduction of greenhouse gas emissions in the low-emitting city and metropolitan region of Kampala', *Carbon Management*. Taylor & Francis, 8(3), pp. 263–276. doi: 10.1080/17583004.2017.1330592.

Mathew, A., Khandelwal, S. and Kaul, N. (2016) 'Spatial and temporal variations of urban heat island effect and the effect of percentage impervious surface area and elevation on land surface temperature: Study of Chandigarh city, India', *Sustainable Cities and Society*. Elsevier, 26, pp. 264–277. doi: 10.1016/J.SCS.2016.06.018.

MaximIntegrated (2010) 'iButton Data-Logger Calibration and NIST Certificate FAQs', *Maxim integrated*. Available at: https://www.maximintegrated.com/en/app-notes/index.mvp/id/4629.

MaximIntegrated (2016) 'DS1923 iButton Hygrochron Temperature/Humidity Logger with 8KB Data-Log Memory', *Maxim integrated*. Available at: https://www.maximintegrated.com/en/products/ibutton/data-loggers/DS1923.html/tb_tab0.

McCarthy, M. P., Best, M. J. and Betts, R. A. (2010) 'Climate change in cities due to global warming and urban effects', *Geophysical Research Letters*, 37. doi: 10.1029/2010gl042845.

McGrane, S. J. (2016) 'Impacts of urbanisation on hydrological and water quality dynamics, and urban water management: a review', *Hydrological Sciences Journal*. doi: 10.1080/02626667.2015.1128084.

McDonnell, M. J. and Pickett, S. T. A. (1990) 'ECOSYSTEM STRUCTURE AND FUNCTION ALONG URBAN RURAL GRADIENTS - AN UNEXPLOITED OPPORTUNITY FOR ECOLOGY', *Ecology*, 71(4), pp. 1232–1237. doi: 10.2307/1938259.

McPhearson, T. *et al.* (2016) 'Advancing Urban Ecology toward a Science of Cities', *Bioscience*, 66(3), pp. 198–212. doi: 10.1093/biosci/biw002.

Melaas, E. K. *et al.* (2016) 'Interactions between urban vegetation and surface urban heat islands: a case study in the Boston metropolitan region', *Environmental Research Letters*, 11(5), p. 11. doi: 10.1088/1748-9326/11/5/054020.

Menzel, A. *et al.* (2006) 'European phenological response to climate change matches the warming pattern', *Global Change Biology*, 12(10), pp. 1969–1976. doi:

10.1111/j.1365-2486.2006.01193.x.

Menzel, A. and Fabian, P. (1999) 'Growing season extended in Europe', *Nature*, 397(6721), p. 659. doi: 10.1038/17709.

Mimet, A. *et al.* (2009) 'Urbanisation induces early flowering: evidence from Platanus acerifolia and Prunus cerasus', *International Journal of Biometeorology*, 53(3), pp. 287–298. doi: 10.1007/s00484-009-0214-7.

Morellato, L. P. C. *et al.* (2010) 'The Influence of Sampling Method, Sample Size, and Frequency of Observations on Plant Phenological Patterns and Interpretation in Tropical Forest Trees', *Phenological Research: Methods for Environmental and Climate Change Analysis*, pp. 99–121. doi: 10.1007/978-90-481-3335-2_5.

Morisette, J. T. *et al.* (2009) 'Tracking the rhythm of the seasons in the face of global change: phenological research in the 21st century', *Frontiers in Ecology and the Environment*, 7(5), pp. 253–260. doi: 10.1890/070217.

Mubiru, D. N. *et al.* (2018) 'Climate trends, risks and coping strategies in smallholder farming systems in Uganda', *Climate Risk Management*. Elsevier, 22, pp. 4–21. doi: 10.1016/J.CRM.2018.08.004.

Mushore, T. D. *et al.* (2019) 'Remotely sensed retrieval of Local Climate Zones and their linkages to land surface temperature in Harare metropolitan city, Zimbabwe', *Urban Climate*, 27, pp. 259–271. doi: 10.1016/j.uclim.2018.12.006.

Nastar, M. *et al.* (2019) 'A case for urban liveability from below: exploring the politics of water and land access for greater liveability in Kampala, Uganda', *Local Environment*. Routledge, 24(4), pp. 358–373. doi: 10.1080/13549839.2019.1572728.

Neil, K. L., Landrum, L. and Wu, J. G. (2010) 'Effects of urbanization on flowering phenology in the metropolitan phoenix region of USA: Findings from herbarium records', *Journal of Arid Environments*, 74(4), pp. 440–444. doi: 10.1016/j.jaridenv.2009.10.010.

Neil, K. and Wu, J. (2006) 'Effects of urbanization on plant flowering phenology: A review', *Urban Ecosystems*, 9(3), pp. 243–257. doi: 10.1007/s11252-006-9354-2.

Norton, B. A. *et al.* (2015) 'Planning for cooler cities: A framework to prioritise green infrastructure to mitigate high temperatures in urban landscapes', *Landscape and Urban Planning*, 134, pp. 127–138. doi: 10.1016/j.landurbplan.2014.10.018.

Ojeh, V. N., Balogun, A. A. and Okhimamhe, A. A. (2016) 'Urban-rural temperature differences in Lagos', *Climate*. doi: 10.3390/cli4020029.

Oke, T.R., 1973. City size and the urban heat island. *Atmospheric Environment (1967)*, *7*(8), pp.769-779.

Oke, T.R., 1982. The energetic basis of the urban heat island. *Quarterly Journal of the Royal Meteorological Society*, *108*(455), pp.1-24.

Oke, T. R. (1987) *Boundary Layer Climates*. Routledge. Available at: https://books.google.co.uk/books?id=K_2dW7crfVIC.

Oke, T. R. (1988) 'The urban energy balance', *Progress in Physical Geography*. doi: 10.1177/030913338801200401.

Oke, T. R. (1997) 'Urban environments', *The surface climates of Canada*. McGill—Queen's University Press, pp. 303–327.

Oke, T. R. (2008) 'Urban observations. Guide to meteorological instruments and methods of observation, Part II of Observing Systems, WMO-No. 8', *World Meteorological Organization, II-11-1--II-11-25*.

Ooi, M. C. G. *et al.* (2017) 'Interaction of Urban Heating and Local Winds During the Calm Intermonsoon Seasons in the Tropics', *JOURNAL OF GEOPHYSICAL RESEARCH-ATMOSPHERES*, 122(21), pp. 11499–11523. doi: 10.1002/2017JD026690.

Pablos, M. *et al.* (2016) 'Multi-temporal evaluation of Soil Moisture and land surface temperature dynamics using in situ and satellite observations', *Remote Sensing*. doi: 10.3390/rs8070587.

Parece, T. E. and Campbell, J. B. (2018) 'Intra-Urban Microclimate Effects on Phenology', *Urban Science*, 2(1). doi: 10.3390/urbansci2010026.

Pataki, D. E. *et al.* (2011) 'Coupling biogeochemical cycles in urban environments: ecosystem services, green solutions, and misconceptions', *Frontiers in Ecology and the Environment*, 9(1), pp. 27–36. doi: 10.1890/090220.

Pauleit, S. *et al.* (2015) 'Urban vulnerability and climate change in Africa', *Future City*. Springer, 4.

Peel, M. C., Finlayson, B. L. and McMahon, T. A. (2007) 'Updated world map of the Köppen-Geiger climate classification', *Hydrology and Earth System Sciences*. doi: 10.5194/hess-11-1633-2007.

Perera, N. G. R. and Emmanuel, R. (2018) 'A "Local Climate Zone" based approach to urban planning in Colombo, Sri Lanka', *Urban Climate*, 23, pp. 188–203. doi: 10.1016/j.uclim.2016.11.006.

Pérez-Molina, E. *et al.* (2017) 'Developing a cellular automata model of urban growth to inform spatial policy for flood mitigation: A case study in Kampala, Uganda', *Computers, Environment and Urban Systems*. Pergamon, 65, pp. 53–65. doi: 10.1016/J.COMPENVURBSYS.2017.04.013.

Pickett, S. T. A. *et al.* (2011) 'Urban ecological systems: Scientific foundations and a decade of progress', *Journal of Environmental Management*, 92(3), pp. 331–362. doi: 10.1016/j.jenvman.2010.08.022.

Pidwirny, M. (2006) 'Earth-Sun relationships and insolation', *Fundamentals of physical geography*. (2nd Ed.). Okanagan, Canada: University of British Columbia, 2.

Pinheiro, J. *et al.* (2018) '{nlme}: Linear and Nonlinear Mixed Effects Models'. Available

at: https://cran.r-project.org/package=nlme.

de Pol, M. and Wright, J. (2009) 'A simple method for distinguishing within-versus between-subject effects using mixed models', *Animal behaviour*. Citeseer, 77(3), p. 753.

Primack, D. *et al.* (2004) 'Herbarium specimens demonstrate earlier flowering times in response to warming in Boston', *American Journal of Botany*, 91(8), pp. 1260–1264. doi: 10.3732/ajb.91.8.1260.

Qiu, T., Song, C. H. and Li, J. X. (2017) 'Impacts of Urbanization on Vegetation Phenology over the Past Three Decades in Shanghai, China', *Remote Sensing*, 9(9), p. 16. doi: 10.3390/rs9090970.

R Core Team (2018) 'R: A Language and Environment for Statistical Computing'. Vienna, Austria. Available at: https://www.r-project.org/.

Rathcke, B. and Lacey, E. P. (1985) 'PHENOLOGICAL PATTERNS OF TERRESTRIAL PLANTS', *Annual Review of Ecology and Systematics*, 16, pp. 179–214. doi: 10.1146/annurev.es.16.110185.001143.

Reed, B. C., Schwartz, M. D. and Xiao, X. (2009) 'Remote Sensing Phenology: Status and the Way Forward', *Phenology of Ecosystem Processes: Applications in Global Change Research*, pp. 231–246. doi: 10.1007/978-1-4419-0026-5_10.

Reich, P. B. (1995) 'Phenology of tropical forests: patterns, causes, and consequences', *Canadian Journal of Botany*, 73(2), pp. 164–174. doi: 10.1139/b95-020.

Ren, Q. *et al.* (2018) 'Urbanization Impacts on Vegetation Phenology in China', *Remote Sensing*, 10(12), p. 16. doi: 10.3390/rs10121905.

Richardson, A. D., Klosterman, S. and Toomey, M. (2013) 'Near-Surface Sensor-Derived Phenology', in Schwartz, M. D. (ed.) *Phenology: An Integrative Environmental Science*. Dordrecht: Springer Netherlands, pp. 413–430. doi: 10.1007/978-94-007-6925-0_22.

Richardson, A. D. *et al.* (2018) 'Intercomparison of phenological transition dates derived from the PhenoCam Dataset V1.0 and MODIS satellite remote sensing', *Scientific Reports*, 8, p. 12. doi: 10.1038/s41598-018-23804-6.

Richmond, A., Myers, I. and Namuli, H. (2018) 'Urban informality and vulnerability: A case study in Kampala, Uganda', *Urban Science*. Multidisciplinary Digital Publishing Institute, 2(1), p. 22.

Rifai, S. W. *et al.* (2018) 'ENSO Drives interannual variation of forest woody growth across the tropics', *Philosophical Transactions of the Royal Society B: Biological Sciences*, 373(1760), p. 20170410. doi: 10.1098/rstb.2017.0410.

Roetzer, T. *et al.* (2000) 'Phenology in central Europe - differences and trends of spring phenophases in urban and rural areas', *International Journal of Biometeorology*. Heidelberg :, 44(2), pp. 60–66. doi: 10.1007/s004840000062.

Rosenzweig, C. *et al.* (2007) 'Assessment of observed changes and responses in natural

and managed systems'.

Roth, M. (2007) 'Review of urban climate research in (sub)tropical regions', *International Journal of Climatology*, 27(14), pp. 1859–1873. doi: 10.1002/joc.1591.

Roth, M. (2012) 'Urban Heat Islands', in *Handbook of Environmental Fluid Dynamics, Volume Two*. CRC, p. 1-587.

Roth, M. and Chow, W. T. L. (2012) 'A historical review and assessment of urban heat island research in Singapore', *SINGAPORE JOURNAL OF TROPICAL GEOGRAPHY*, 33(3), pp. 381–397. doi: 10.1111/sjtg.12003.

Sabiiti, E. *et al.* (2014) 'Assessing Urban and Peri-urban Agriculture in Kampala, Uganda', in.

Sailor, D. J. (1995) 'Simulated Urban Climate Response to Modifications in Surface Albedo and Vegetative Cover', *Journal of Applied Meteorology*. Boston, MA :, 34(7), pp. 1694–1704. doi: 10.1175/1520-0450-34.7.1694.

Sailor, D. J. (2011) 'A review of methods for estimating anthropogenic heat and moisture emissions in the urban environment', *International Journal of Climatology*, 31(2), pp. 189–199. doi: 10.1002/joc.2106.

Schaber, J. and Badeck, F. W. (2003) 'Physiology-based phenology models for forest tree species in Germany', *International Journal of Biometeorology*, 47(4), pp. 193–201. doi: 10.1007/s00484-003-0171-5.

Skelhorn, C. P., Levermore, G. and Lindley, S. J. (2016) 'Impacts on cooling energy consumption due to the UHI and vegetation changes in Manchester, UK', *Energy and Buildings*. Elsevier, 122, pp. 150–159. doi: 10.1016/J.ENBUILD.2016.01.035.

van Schaik, C. P., Terborgh, J. W. and Wright, S. J. (1993) 'The phenology of tropical forests: adaptive significance and consequences for primary consumers', *Annual Review of Ecology and Systematics*, pp. 353–377.

Schneider, A., Friedl, M. A. and Potere, D. (2010) 'Mapping global urban areas using MODIS 500-m data: New methods and datasets based on "urban ecoregions"', *Remote Sensing of Environment*, 114(8), pp. 1733–1746. doi: 10.1016/j.rse.2010.03.003.

Schuyt, K. D. (2005) 'Economic consequences of wetland degradation for local populations in Africa', *Ecological Economics*. Elsevier, 53(2), pp. 177–190. doi: 10.1016/J.ECOLECON.2004.08.003.

Schwartz, M. D. (1998) 'Green-wave phenology', *Nature*, 394(6696), pp. 839–840. doi: 10.1038/29670.

Schwartz, M. D. (2002) 'Examining the onset of spring in China', *Climate Research*. Amelinghausen, Germany :, 21(2), p. 157.

Schwartz, M. D. (2003) 'PHENOLOGY: An integrative environmental science', *Phenology: an Integrative Environmental Science*, pp. 3–7. doi: 10.1007/978-94-007-6925-0.

Scott, A. A. *et al.* (2017) 'Temperature and heat in informal settlements in Nairobi', *PloS one*. Public Library of Science, 12(11), p. e0187300.

Senanayake, I. P., Welivitiya, W. D. D. P. and Nadeeka, P. M. (2013) 'Remote sensing based analysis of urban heat islands with vegetation cover in Colombo city, Sri Lanka using Landsat-7 ETM+ data', *Urban Climate*. Elsevier, 5, pp. 19–35. doi: 10.1016/J.UCLIM.2013.07.004.

Shivanna, K. R. and Tandon, R. (2014) 'Phenology', in *Reproductive Ecology of Flowering Plants: A Manual*. New Delhi: Springer India, pp. 19–23. doi: 10.1007/978-81-322-2003-9_3.

Singh, K. P. and Kushwaha, C. P. (2016) 'Deciduousness in tropical trees and its potential as indicator of climate change: A review', *Ecological Indicators*, 69, pp. 699–706. doi: 10.1016/j.ecolind.2016.04.011.

Singh, P., Kikon, N. and Verma, P. (2017) 'Impact of land use change and urbanization on urban heat island in Lucknow city, Central India. A remote sensing based estimate', *Sustainable Cities and Society*. Elsevier, 32, pp. 100–114. doi: 10.1016/J.SCS.2017.02.018.

Soares, A. L. *et al.* (2011) 'Benefits and costs of street trees in Lisbon, Portugal', *Urban Forestry & Urban Greening*, 10(2), pp. 69–78. doi: 10.1016/j.ufug.2010.12.001.

Ssentongo, P. *et al.* (2018) 'Changes in Ugandan Climate Rainfall at the Village and Forest Level', *Scientific Reports*. doi: 10.1038/s41598-018-21427-5.

Stewart, I. D. (2011) 'A systematic review and scientific critique of methodology in modern urban heat island literature', *International Journal of Climatology*. Chichester :, 31(2), pp. 200–217. doi: 10.1002/joc.2141.

Stewart, I. D., Oke, T. R. and Krayenhoff, E. S. (2014) 'Evaluation of the "local climate zone" scheme using temperature observations and model simulations', *International Journal of Climatology*, 34(4), pp. 1062–1080. doi: 10.1002/joc.3746.

Stewart, I. and Oke, T. (2012) 'LOCAL CLIMATE ZONES FOR URBAN TEMPERATURE STUDIES', *Bulletin of the American Meteorological Society*. Boston, 93(12), pp. 1879–1900.

Suni, T. *et al.* (2015) 'The significance of land-atmosphere interactions in the Earth system—iLEAPS achievements and perspectives', *Anthropocene*. Elsevier, 12, pp. 69–84. doi: 10.1016/J.ANCENE.2015.12.001.

Taha, H. (1997) 'Urban climates and heat islands: albedo, evapotranspiration, and anthropogenic heat', *Energy and buildings*. Lausanne :, 25(2), pp. 99–103. doi: 10.1016/S0378-7788(96)00999-1.

Taubenböck, H., Kraff, N. J. and Wurm, M. (2018) 'The morphology of the Arrival City - A global categorization based on literature surveys and remotely sensed data', *Applied Geography*. Pergamon, 92, pp. 150–167. doi: 10.1016/J.APGEOG.2018.02.002.

Thapa Chhetri, D. B., Fujimori, Y. and Moriwaki, R. (2017) 'LOCAL CLIMATE CLASSIFICATION AND URBAN HEAT/DRY ISLAND IN MATSUYAMA PLAIN', *Annual Journal of Hydraulic Engineering*, 73, pp. 487–492. doi: 10.2208/jscejhe.73.I_487.

Thomas, G. *et al.* (2014) 'Analysis of Urban Heat Island in Kochi, India, Using a Modified Local Climate Zone Classification', *Procedia Environmental Sciences*. Elsevier, 21, pp. 3–13. doi: 10.1016/J.PROENV.2014.09.002.

du Toit, M. J. *et al.* (2018) 'Urban green infrastructure and ecosystem services in sub-Saharan Africa', *Landscape and Urban Planning*, 180, pp. 249–261. doi: 10.1016/j.landurbplan.2018.06.001.

Triguero-Mas, M. *et al.* (2015) 'Natural outdoor environments and mental and physical health: Relationships and mechanisms', *Environment International*, 77, pp. 35–41. doi: 10.1016/j.envint.2015.01.012.

Tukiran, J. M., Ariffin, J. and Ghani, A. N. A. (2016) 'COOLING EFFECTS OF TWO TYPES OF TREE CANOPY SHAPE IN PENANG, MALAYSIA', *International Journal of Geomate*, 11(24), pp. 2275–2283.

United Nations (2018) 'The World 's Cities in 2018', *The World's Cities in 2018 - Data Booklet (ST/ESA/ SER.A/417)*.

United Nations (2014) *World Urbanization Prospects: 2014 Revision*, *New York, United*. doi: 10.4054/DemRes.2005.12.9.

USGS (2016) 'USGS Earth Explorer', *EarthExplorer*. Available at: https://earthexplorer.usgs.gov/.

Valdez-Hernandez, M. *et al.* (2010) 'Phenology of five tree species of a tropical dry forest in Yucatan, Mexico: effects of environmental and physiological factors', *Plant and Soil*, 329(1–2), pp. 155–171. doi: 10.1007/s11104-009-0142-7.

Vancutsem, C. *et al.* (2010) 'Evaluation of MODIS land surface temperature data to estimate air temperature in different ecosystems over Africa', *Remote Sensing of Environment*, 114(2), pp. 449–465. doi: 10.1016/j.rse.2009.10.002.

Varhammar, A. *et al.* (2015) 'Photosynthetic temperature responses of tree species in Rwanda: evidence of pronounced negative effects of high temperature in montane rainforest climax species', *New Phytologist*, 206(3), pp. 1000–1012. doi: 10.1111/nph.13291.

Verdonck, M. L. *et al.* (2018) 'The potential of local climate zones maps as a heat stress assessment tool, supported by simulated air temperature data', *Landscape and Urban Planning*, 178, pp. 183–197. doi: 10.1016/j.landurbplan.2018.06.004.

Vermeiren, K. *et al.* (2012) 'Urban growth of Kampala, Uganda: Pattern analysis and scenario development', *Landscape and Urban Planning*. Elsevier, 106(2), pp. 199–206. doi: 10.1016/J.LANDURBPLAN.2012.03.006.

Vermeiren, K. *et al.* (2013) 'Will urban farming survive the growth of African cities: A

case-study in Kampala (Uganda)?', *Land Use Policy*. Pergamon, 35, pp. 40–49. doi: 10.1016/J.LANDUSEPOL.2013.04.012.

Vitousek, P. M. *et al.* (1997) 'Human domination of Earth's ecosystems', *Science*, 277(5325), pp. 494–499. doi: 10.1126/science.277.5325.494.

Vizzari, M. and Sigura, M. (2015) 'Landscape sequences along the urban-rural-natural gradient: A novel geospatial approach for identification and analysis', *Landscape and Urban Planning*, 140, pp. 42–55. doi: 10.1016/j.landurbplan.2015.04.001.

Voogt, J. A. and Oke, T. R. (2003) 'Thermal remote sensing of urban climates', *Remote Sensing of Environment*, 86(3), pp. 370–384. doi: 10.1016/s0034-4257(03)00079-8.

Voogt, J. (2007) 'How researchers measure urban heat islands', in *United States Environmental Protection Agency (EPA), State and Local Climate and Energy Program, Heat Island Effect, Urban Heat Island Webcasts and Conference Calls*.

Voogt, J. A. (2000) 'Image representations of complete urban surface temperatures', *Geocarto International*, 15(3), pp. 21–32. doi: 10.1080/10106040008542160.

Voogt, J.A. and Oke, T.R., 1997. Complete urban surface temperatures. *Journal of applied meteorology*, *36*(9), pp.1117-1132.

Walker, J. J., de Beurs, K. M. and Henebry, G. M. (2015) 'Land surface phenology along urban to rural gradients in the US Great Plains', *Remote Sensing of Environment*, 165, pp. 42–52. doi: 10.1016/j.rse.2015.04.019.

Wang, K. *et al.* (2019) 'Urban heat island modelling of a tropical city: case of Kuala Lumpur', *GEOSCIENCE LETTERS*, 6. doi: 10.1186/s40562-019-0134-2.

Wang, Y. *et al.* (2018) 'Local variation of outdoor thermal comfort in different urban green spaces in Guangzhou, a subtropical city in South China', *URBAN FORESTRY & URBAN GREENING*, 32, pp. 99–112. doi: 10.1016/j.ufug.2018.04.005.

Weng, Q., Lu, D. and Schubring, J. (2004) 'Estimation of land surface temperature–vegetation abundance relationship for urban heat island studies', *Remote Sensing of Environment*, 89(4), pp. 467–483. doi: https://doi.org/10.1016/j.rse.2003.11.005.

White, M. A. *et al.* (2002) 'Satellite evidence of phenological differences between urbanized and rural areas of the eastern United States deciduous broadleaf forest', *Ecosystems*, 5(3), pp. 260–273. doi: 10.1007/s10021-001-0070-8.

White, M. A., Thornton, P. E. and Running, S. W. (1997) 'A continental phenology model for monitoring vegetation responses to interannual climatic variability', *Global Biogeochemical Cycles*, 11(2), pp. 217–234. doi: 10.1029/97gb00330.

Whitford, V., Ennos, A. R. and Handley, J. F. (2001) '"City form and natural process" - indicators for the ecological performance of urban areas and their application to Merseyside, UK', *Landscape and Urban Planning*, 57(2), pp. 91–103. doi: 10.1016/s0169-2046(01)00192-x.

Wickham, H. (2015) 'Tidy Data', *Journal of Statistical Software*. doi:

10.18637/jss.v059.i10.

Wiesner, S. *et al.* (2016) 'Spatial and temporal variability of urban soil water dynamics observed by a soil monitoring network', *Journal of Soils and Sediments*, 16(11), pp. 2523–2537. doi: 10.1007/s11368-016-1385-6.

Williams, R. J. *et al.* (1997) 'Leaf phenology of woody species in a North Australian tropical savanna', *Ecology*, 78(8), pp. 2542–2558.

WMO (2016) 'WMO - Kampala UGANDA', *World Weather Information Service*. Available at: http://worldweather.wmo.int/en/city.html?cityId=1328.

Wolkovich, E. M. *et al.* (2012) 'Warming experiments underpredict plant phenological responses to climate change', *Nature*, 485(7399), pp. 494–497. doi: 10.1038/nature11014.

World Bank (2016) *Promoting Green Urban Development in African Cities*, *Promoting Green Urban Development in African Cities*. doi: 10.1596/26676.

WorldWeatherOnline (2019) 'Kampala Monthly Climate Averages', *WorldWeatherOnline.com*. Available at: https://www.worldweatheronline.com/kampala-weather-averages/kampala/ug.aspx.

Wu, J. G. (2014) 'Urban ecology and sustainability: The state-of-the-science and future directions', *Landscape and Urban Planning*, 125, pp. 209–221. doi: 10.1016/j.landurbplan.2014.01.018.

Wu, H., Wang, T., Riemer, N., Chen, P., Li, M. and Li, S., 2017. Urban heat island impacted by fine particles in Nanjing, China. *Scientific reports*, *7*(1), pp.1-11.

Xu, H., Lin, D. and Tang, F. (2013) 'The impact of impervious surface development on land surface temperature in a subtropical city: Xiamen, China', *International Journal of Climatology*. doi: 10.1002/joc.3554.

Yan, D. *et al.* (2019) 'Understanding the relationship between vegetation greenness and productivity across dryland ecosystems through the integration of PhenoCam, satellite, and eddy covariance data', *Remote Sensing of Environment*. Elsevier, 223, pp. 50–62. doi: 10.1016/J.RSE.2018.12.029.

Yang, P., Ren, G. and Hou, W. (2017) 'Temporal–Spatial Patterns of Relative Humidity and the Urban Dryness Island Effect in Beijing City', *Journal of Applied Meteorology and Climatology*, 56(8), pp. 2221–2237. doi: 10.1175/JAMC-D-16-0338.1.

Yang, L. *et al.* (2016) 'Research on Urban Heat-Island Effect', *Procedia Engineering*. Elsevier, 169, pp. 11–18. doi: 10.1016/J.PROENG.2016.10.002.

Yao, R. *et al.* (2017) 'Investigation of Urbanization Effects on Land Surface Phenology in Northeast China during 2001-2015', *Remote Sensing*, 9(1), p. 16. doi: 10.3390/rs9010066.

Yao, R. *et al.* (2019) 'Urbanization effects on vegetation cover in major African cities during 2001-2017', *International Journal of Applied Earth Observation and*

Geoinformation, 75, pp. 44–53. doi: 10.1016/j.jag.2018.10.011.

Youngsteadt, E. *et al.* (2015) 'Do cities simulate climate change? A comparison of herbivore response to urban and global warming', *Global Change Biology*. doi: 10.1111/gcb.12692.

Yuan, F. and Bauer, M. E. (2007) 'Comparison of impervious surface area and normalized difference vegetation index as indicators of surface urban heat island effects in Landsat imagery', *Remote Sensing of Environment*, 106(3), pp. 375–386. doi: https://doi.org/10.1016/j.rse.2006.09.003.

Zalakeviciute, R., López-Villada, J. and Rybarczyk, Y. (2018) 'Contrasted effects of relative humidity and precipitation on urban PM 2.5 pollution in high elevation urban areas', *Sustainability (Switzerland)*. doi: 10.3390/su10062064.

Zhang, L. *et al.* (2019) 'The use of classification and regression algorithms using the random forests method with presence-only data to model species' distribution', *MethodsX*. Elsevier, 6, pp. 2281–2292. doi: 10.1016/J.MEX.2019.09.035.

Zhang, H. *et al.* (2014) 'An improved satellite-based approach for estimating vapor pressure deficit from MODIS data', *Journal of Geophysical Research-Atmospheres*, 119(21), pp. 12256–12271. doi: 10.1002/2014jd022118.

Zhang, X., Estoque, R. C. and Murayama, Y. (2017) 'An urban heat island study in Nanchang City, China based on land surface temperature and social-ecological variables', *Sustainable Cities and Society*. Elsevier, 32, pp. 557–568. doi: 10.1016/J.SCS.2017.05.005.

Zhang, X. Y., Friedl, M. A., Schaaf, C. B. and Strahler, A. H. (2004) 'Climate controls on vegetation phenological patterns in northern mid- and high latitudes inferred from MODIS data', *Global Change Biology*, 10(7), pp. 1133–1145. doi: 10.1111/j.1529-8817.2003.00784.x.

Zhang, X. Y., Friedl, M. A., Schaaf, C. B., Strahler, A. H., *et al.* (2004) 'The footprint of urban climates on vegetation phenology', *Geophysical Research Letters*, 31(12). doi: 10.1029/2004gl020137.

Zhang, X. Y. *et al.* (2005) 'Monitoring the response of vegetation phenology to precipitation in Africa by coupling MODIS and TRMM instruments', *Journal of Geophysical Research-Atmospheres*, 110(D12), p. 14. doi: 10.1029/2004jd005263.

Zhang, X. Y., Friedl, M. A. and Schaaf, C. B. (2006) 'Global vegetation phenology from Moderate Resolution Imaging Spectroradiometer (MODIS): Evaluation of global patterns and comparison with in situ measurements', *Journal of Geophysical Research-Biogeosciences*, 111(G4), p. 14. doi: 10.1029/2006jg000217.

Zhang, Y. *et al.* (2019) 'El Niño-Southern Oscillation-Induced Variability of Terrestrial Gross Primary Production During the Satellite Era', *Journal of Geophysical Research: Biogeosciences*. American Geophysical Union (AGU). doi: 10.1029/2019jg005117.

Zhou, D. *et al.* (2015) 'The footprint of urban heat island effect in China', *Scientific*

Reports, 5. doi: 10.1038/srep11160.

Zhou, D. C. *et al.* (2016) 'Remotely sensed assessment of urbanization effects on vegetation phenology in China's 32 major cities', *Remote Sensing of Environment*, 176, pp. 272–281. doi: 10.1016/j.rse.2016.02.010.

Zipper, S. C. *et al.* (2016) 'Urban heat island impacts on plant phenology: intra-urban variability and response to land cover', *Environmental Research Letters*, 11(5). doi: 10.1088/1748-9326/11/5/054023.

Zhou, B., Rybski, D. and Kropp, J. P. (2017) 'The role of city size and urban form in the surface urban heat island', *Scientific Reports*. doi: 10.1038/s41598-017-04242-2.

Zipper, S. C. *et al.* (2017) 'Urban heat island-induced increases in evapotranspirative demand', *Geophysical Research Letters*, 44(2), pp. 873–881. doi: 10.1002/2016gl072190.

Ziska, L. H. *et al.* (2003) 'Cities as harbingers of climate change: Common ragweed, urbanization, and public health', *Journal of Allergy and Clinical Immunology*, 111(2), pp. 290–295. doi: 10.1067/mai.2003.53.

Zuur, A. F. and Ieno, E. N. (2016) 'A protocol for conducting and presenting results of regression-type analyses', *Methods in Ecology and Evolution*, 7(6), pp. 636–645. doi: 10.1111/2041-210x.12577.

Zuur, A. F., Ieno, E. N. and Elphick, C. S. (2010) 'A protocol for data exploration to avoid common statistical problems', *Methods in Ecology and Evolution*, 1(1), pp. 3–14. doi: 10.1111/j.2041-210X.2009.00001.x.

APPENDIX I

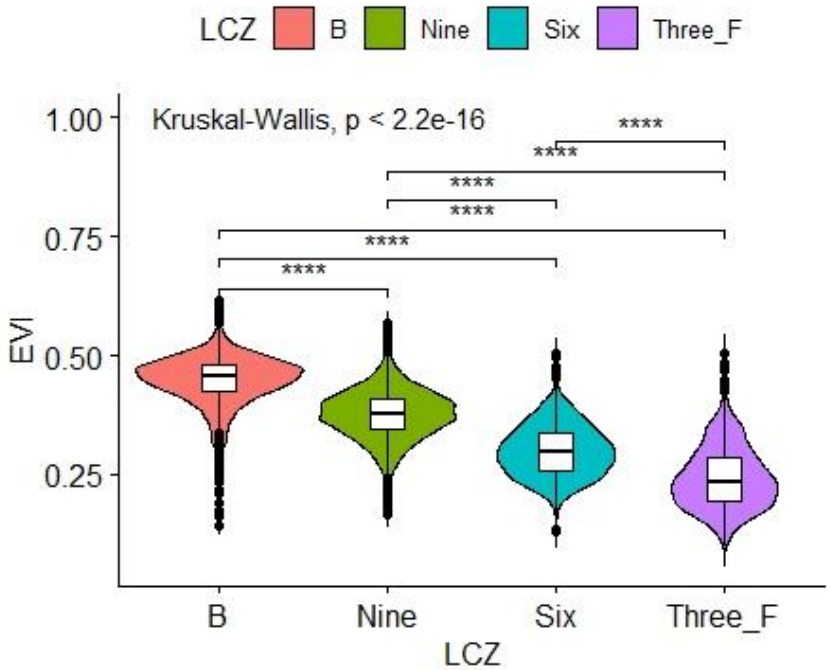

Figure AI 1: EVI scores in the select LCZ types used for the analysis depicting surface cover differences across LCZs (EVI> 0.2 depicts vegetation cover and EVI<0.2 represents vegetated surfaces.

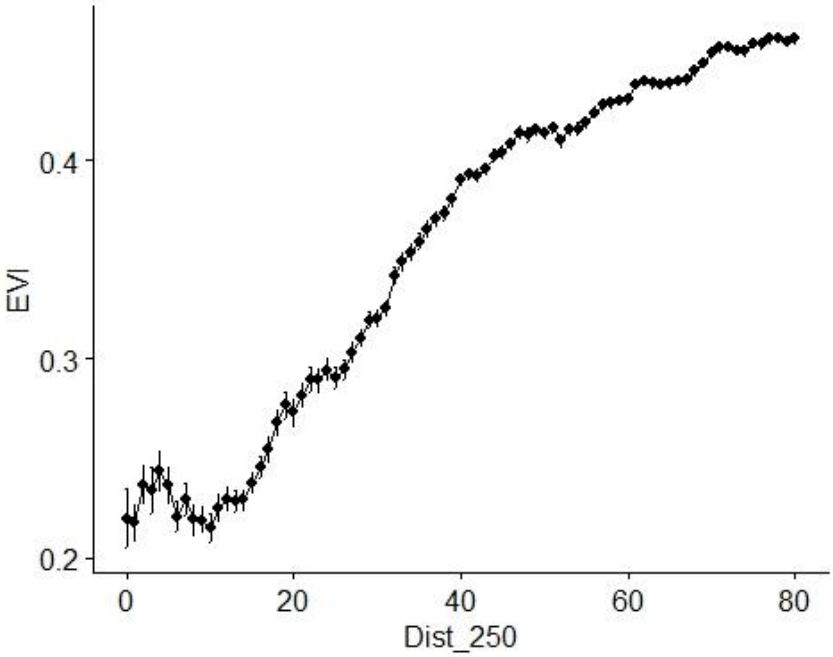

Figure AI 2 shows surface cover differences along the urban rural gradient depicted by EVI. Each unit of Distance (Dist_250) is equivalent to 250 m with mean SE bars

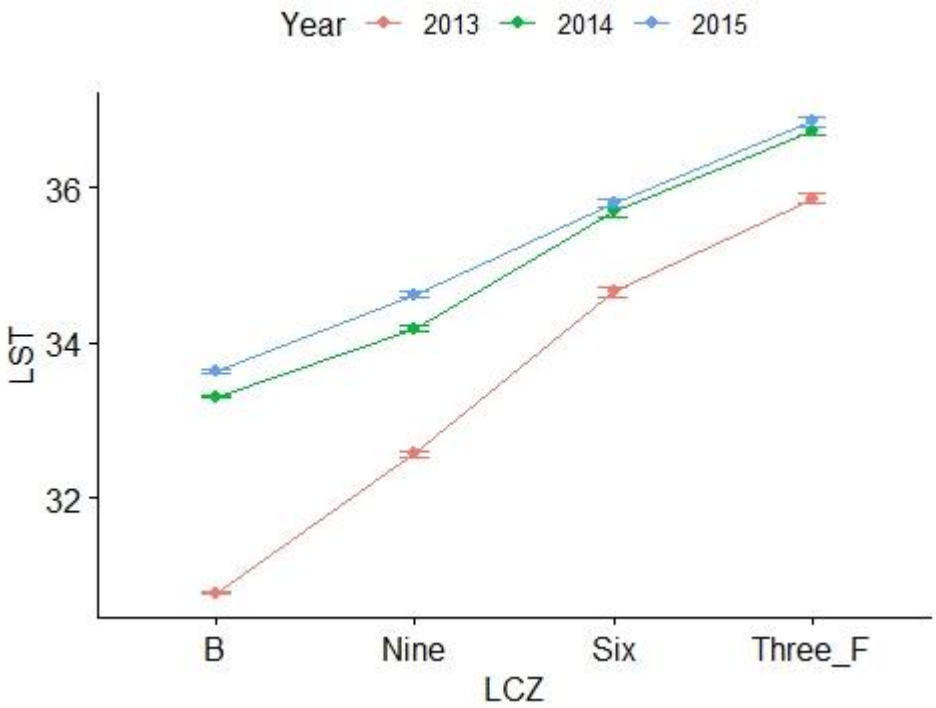

Figure AI 3: Land Surface Temperature differences (°C) between LCZ across different years with mean SE bars

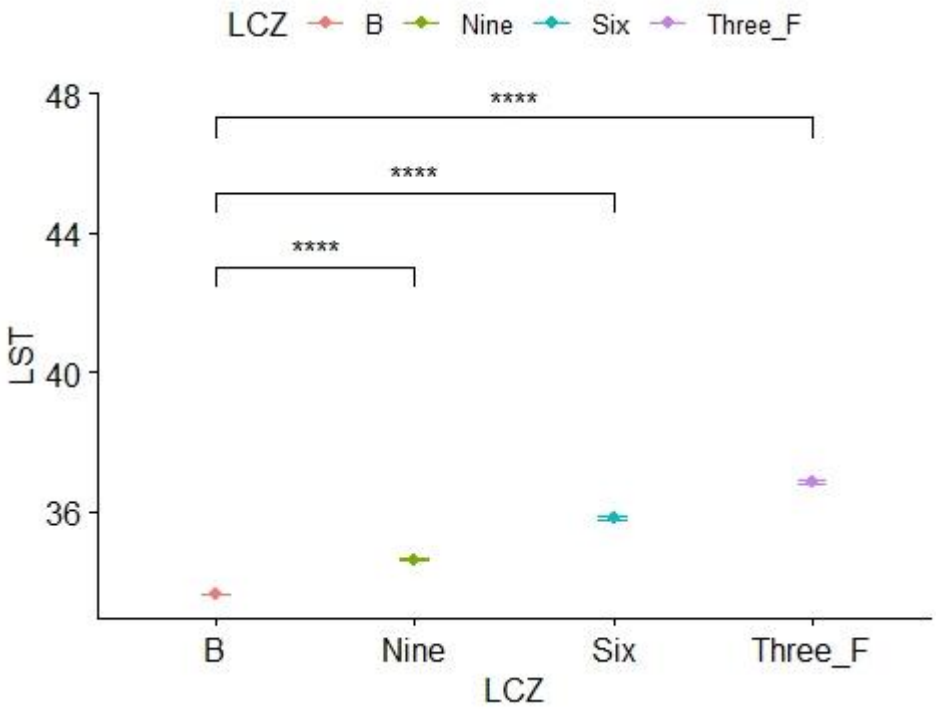

Figure AI 4: Land Surface Temperature differences (°C) between LCZ in 2015 that had the weakest differences between years with SE bars

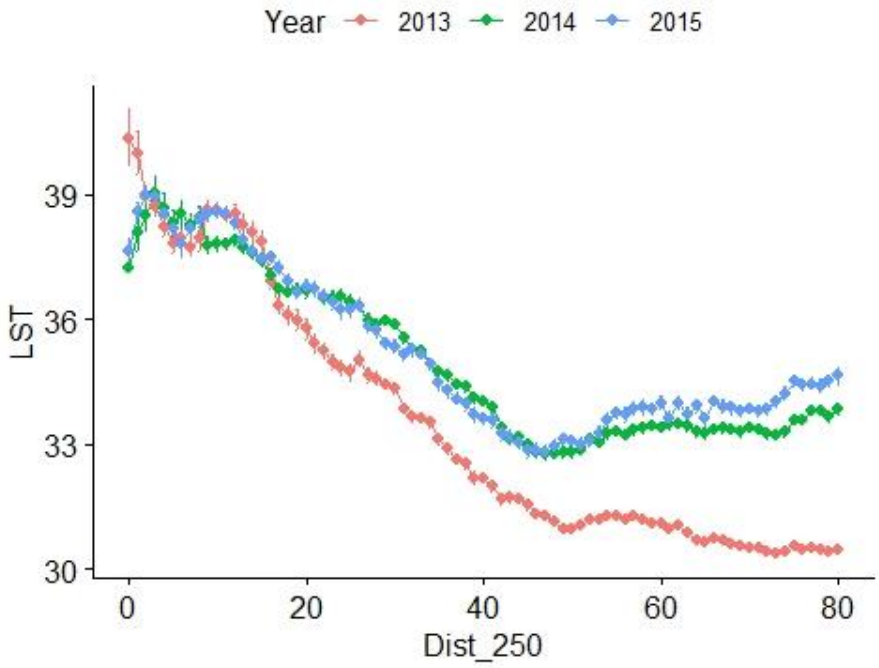

Figure AI 5 shows Land Surface Temperature differences (°C) along the urban rural gradient across three years used in the analysis. Each unit of Distance (Dist_250) is equivalent to 250 m with mean SE bars

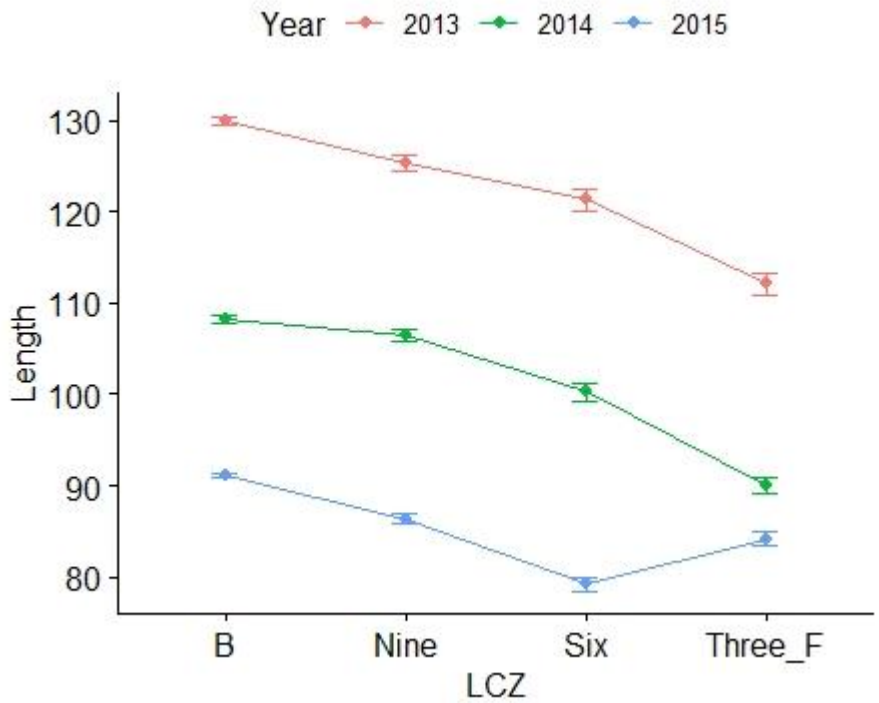

Figure AI 6 shows differences in the Length of season between the LCZ across different years with mean SE bars

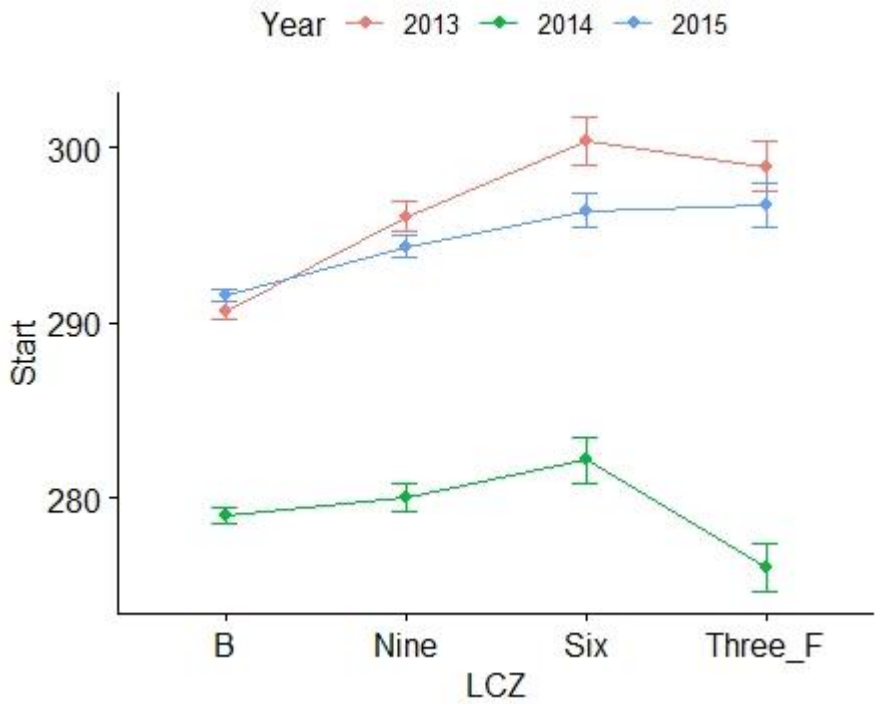

Figure AI 7 shows differences in the timing of start of season between the LCZ across different years with mean SE bars

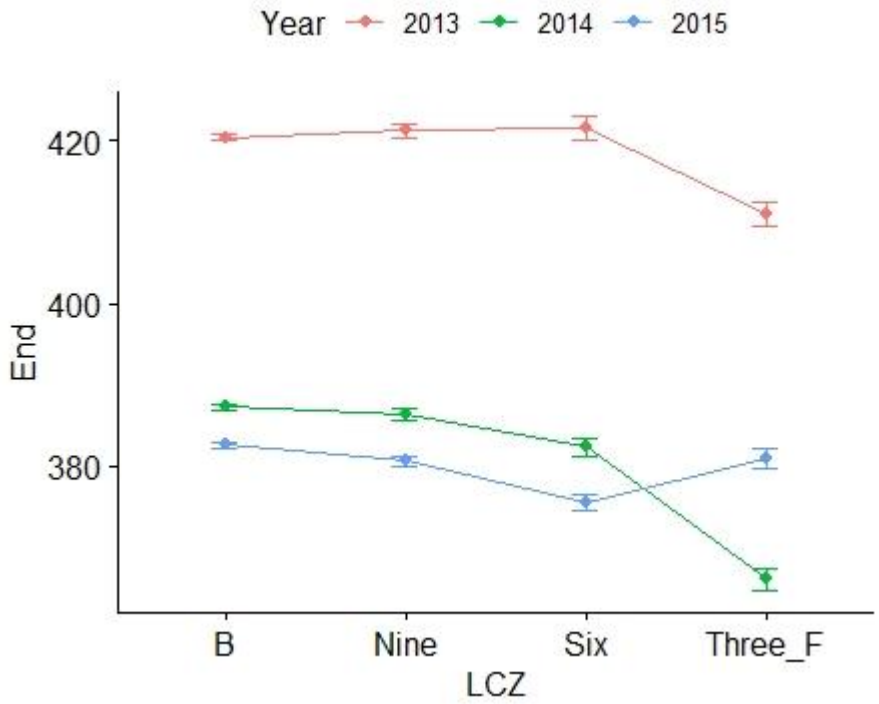

Figure AI 8 shows differences in the timing of end of season between the LCZ across different years with mean SE bars

APPENDIX II

Figure AII 1: Approach used in the classification of urban form around all 22 sites (including 9 sites for phenology) used for spatial temporal characterisation of urban climate at a microscale

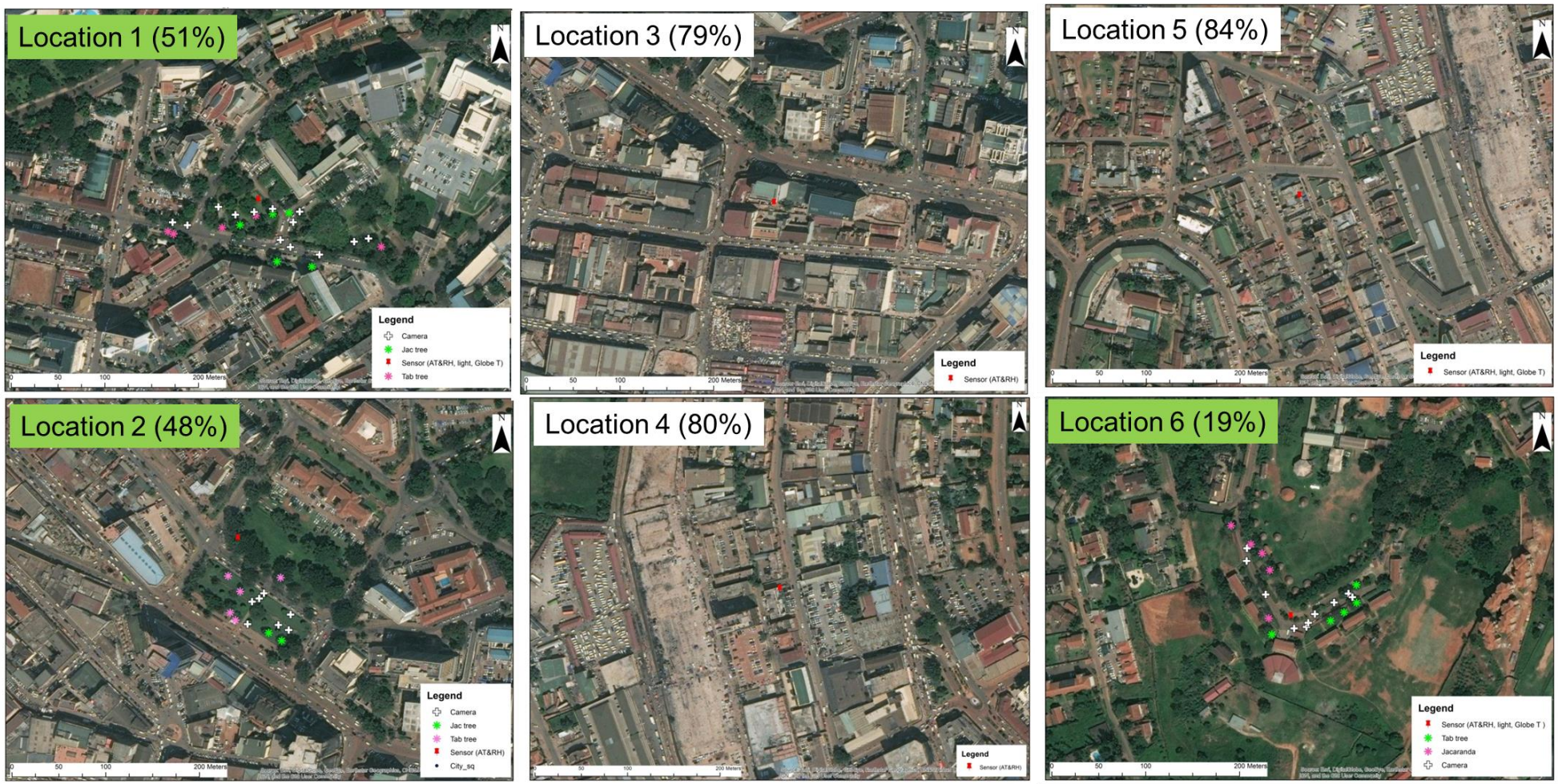

Figure AII 2: Proportion of man-made features (Buildings and paved surface) at Locations 1-6. The sensors location is represented by a red place mark. The locations with a green background (on the location name) were used for phenology of trees. *Jacaranda* and *Tabebuia* tree locations are represented by green and pink points on the map

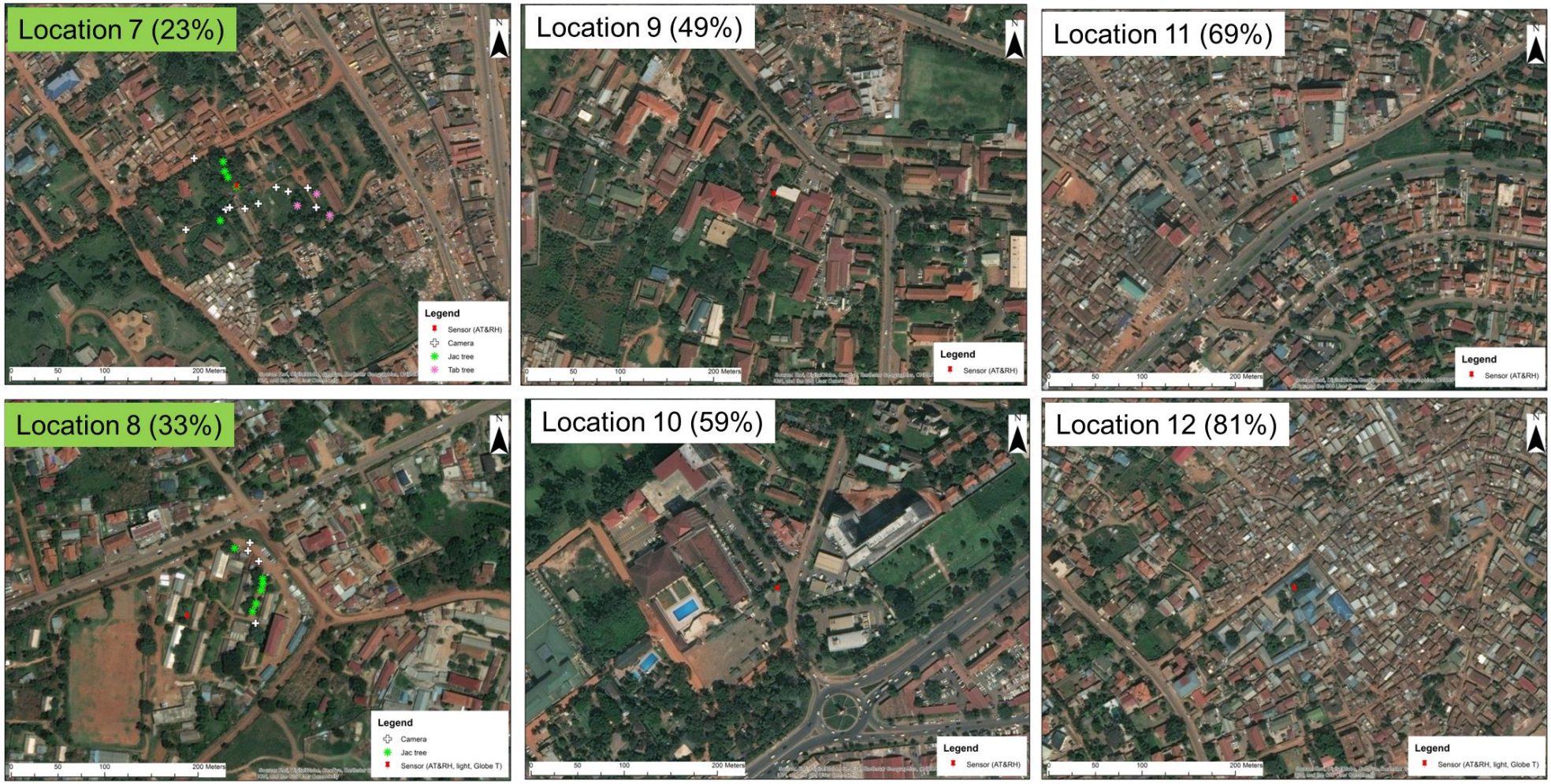

Figure AII 3: Proportion of man-made features (Buildings and paved surface) at Locations 7-12. The sensors location is represented by a red place mark. The locations with a green background (on the location name) were used for phenology of trees. *Jacaranda* and *Tabebuia* tree locations are represented by green and pink points on the map

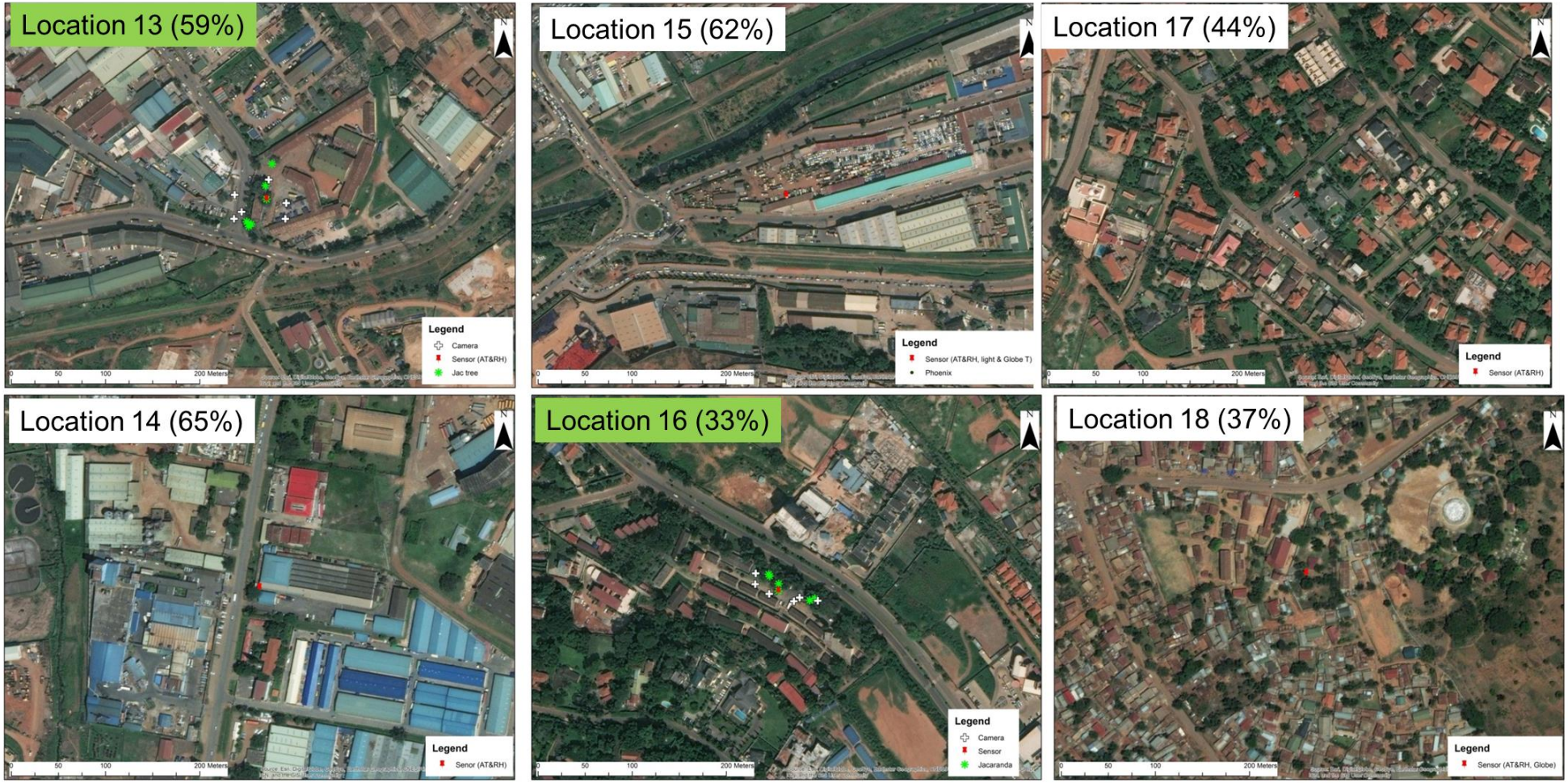

Figure AII 4: Proportion of man-made features (Buildings and paved surface) at Locations 13-18. The sensors location is represented by a red place mark. The locations with a green background (on the location name) were used for phenology of trees. *Jacaranda* locations are represented by green points on the map

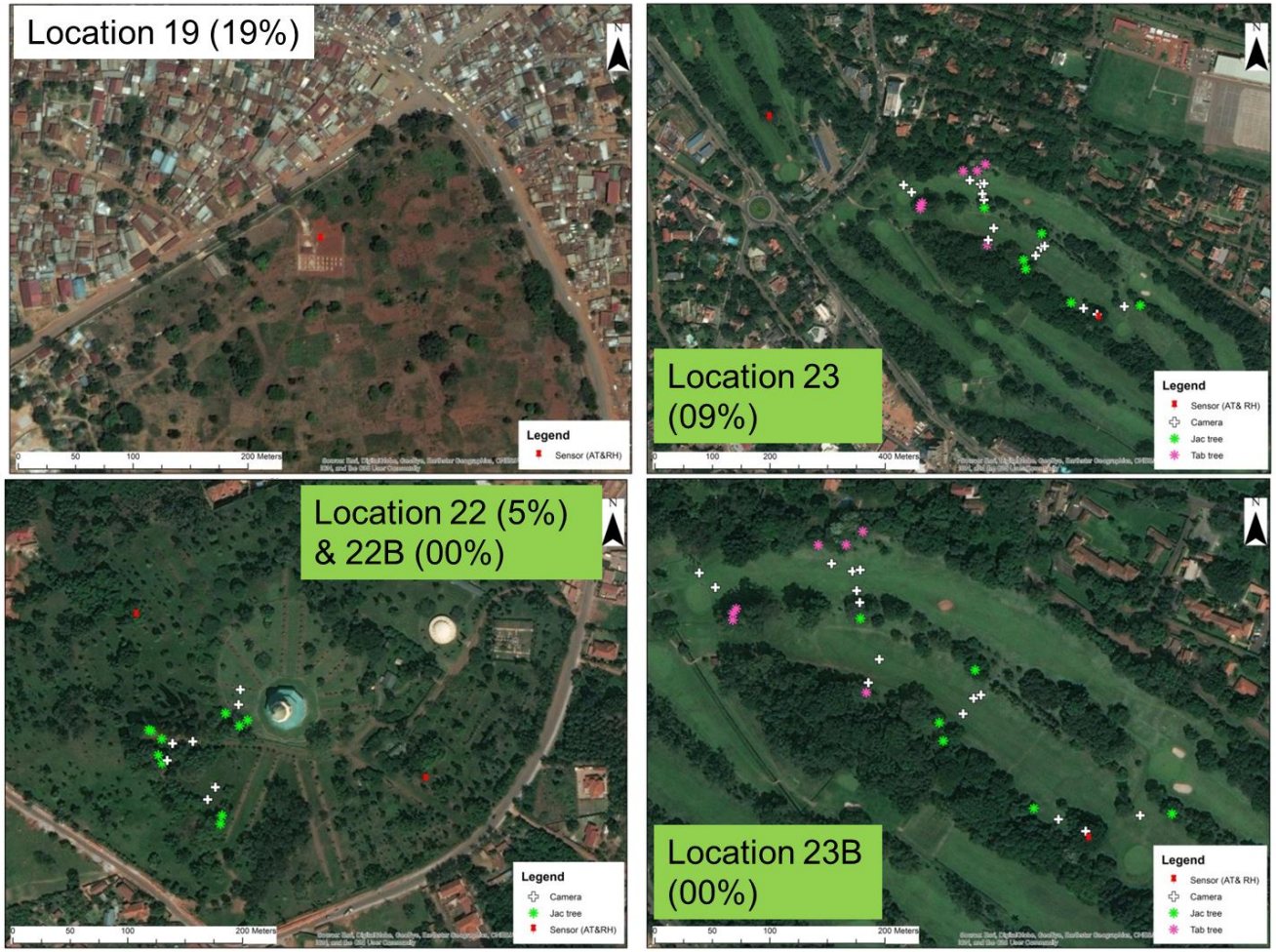

Figure AII 5: Proportion of man-made features (Buildings and paved surface) at Locations 19, 22, 22B, 23 & 23B. The sensors location is represented by a red place mark. The locations with a green background (on the location name) were used for phenology of trees. *Jacaranda* and *Tabebuia* tree locations are represented by green and pink points on the map

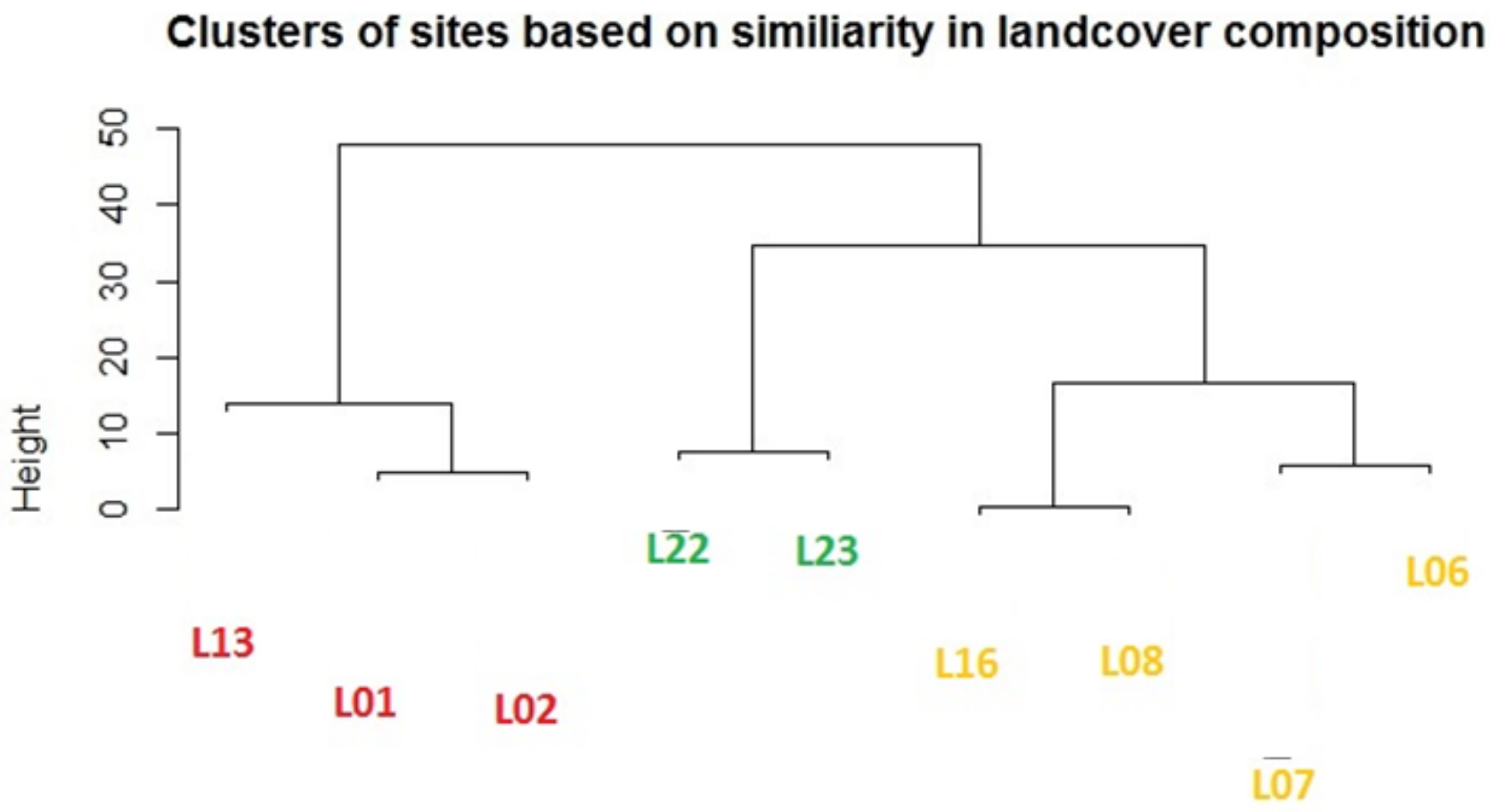

Figure AII 6: Dendogram showing clustering of the phenology sites based on urban form data. The location names have a prefix ("L"). Local Climate Zones were assigned to the

APPENDIX III

Figure AIII 1: Images of *Jacaranda mimosifolia*. The tree has compound bi-pinnate leaves, purple flowers and green seen that explodes and turns brown as it matures

Figure AIII 2: Images of *Tabebuia rosea* (common name: Pink Trumpet tree). The tree has got digitate leaves and pink "tumpet-like" flowers

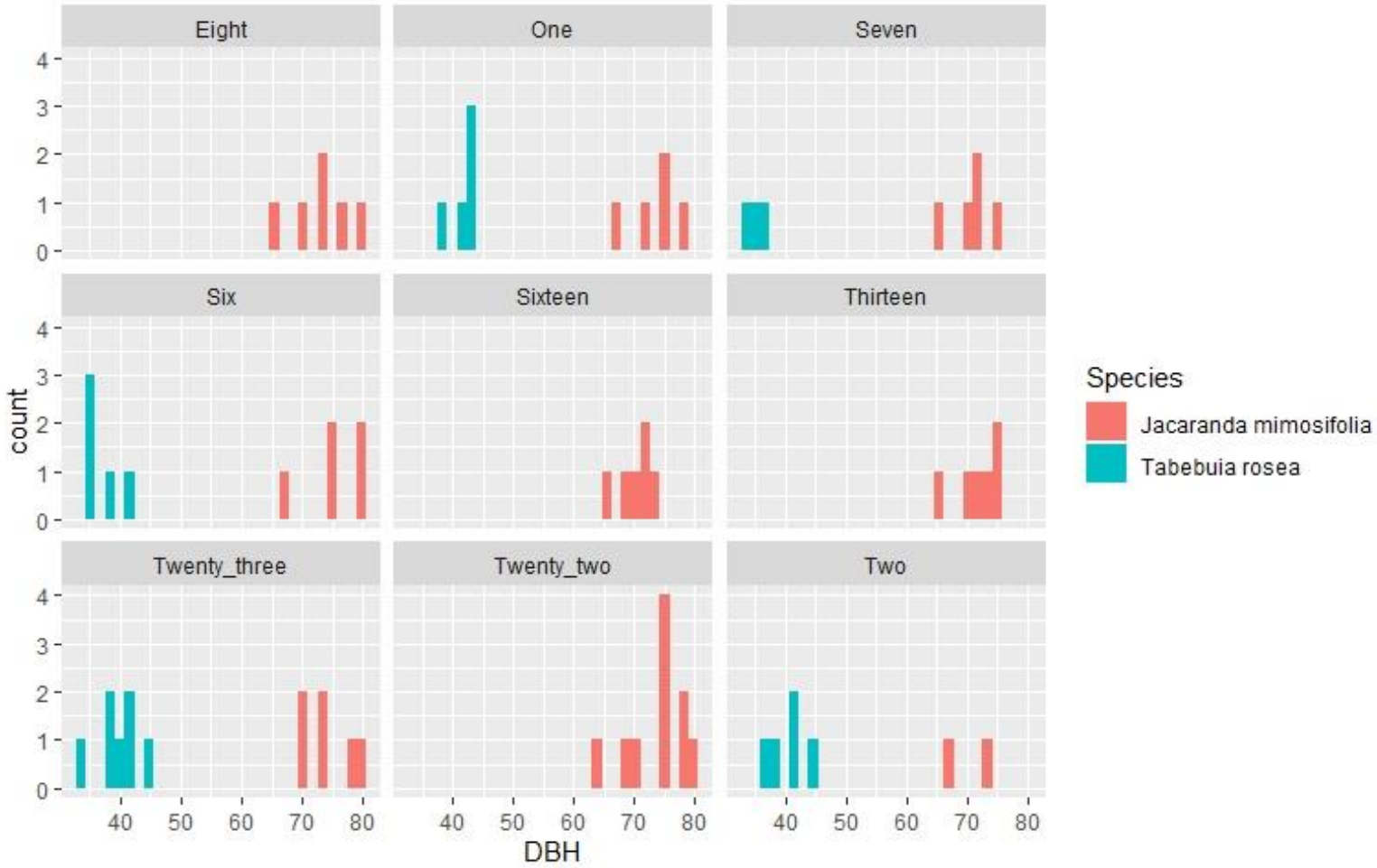

Figure AIII 3: Histograms showing Diameter at Breast Height (cm) of trees at each of the nine locations.

APPENDIX IV

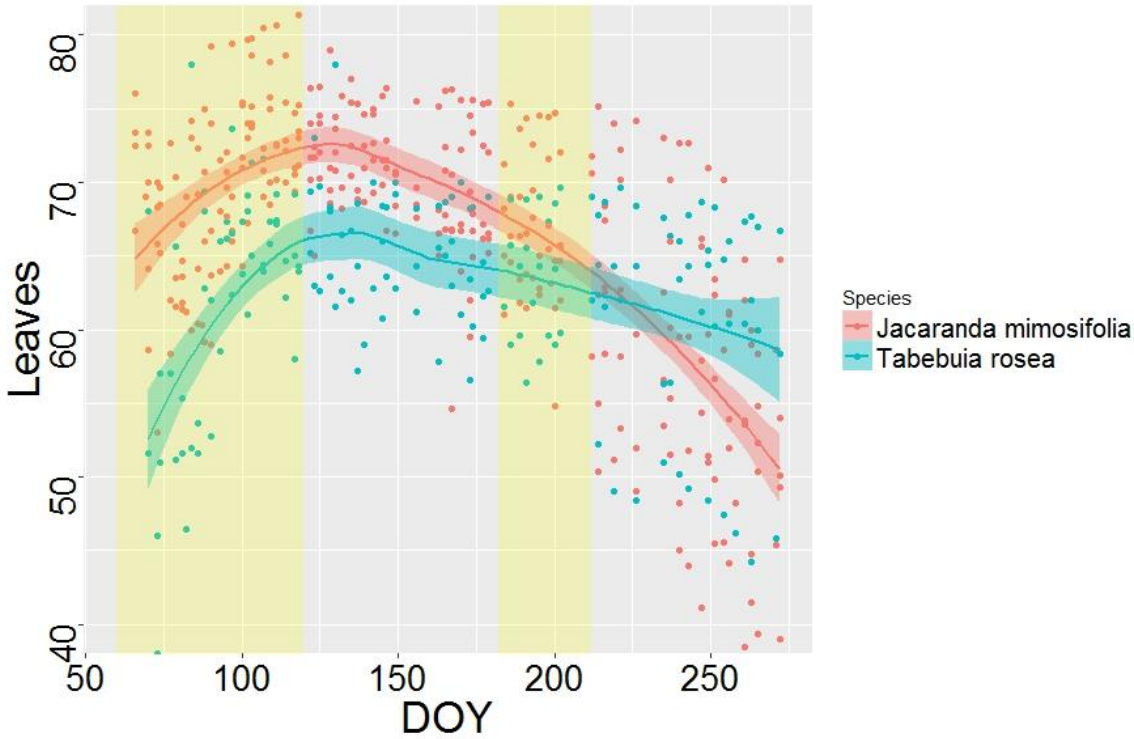

Figure AIV 1: Temporal change (March to September 2017) of canopy cover (%) of *Tabebuia* and *Jacaranda* trees pooled across all phenology locations in Kampala using a loess model. The yellow band to the left shows the main rain season (March-May), whereas the second band (to the right) highlights a mild rain season. See 221 for a detailed image of rainfall ditribution

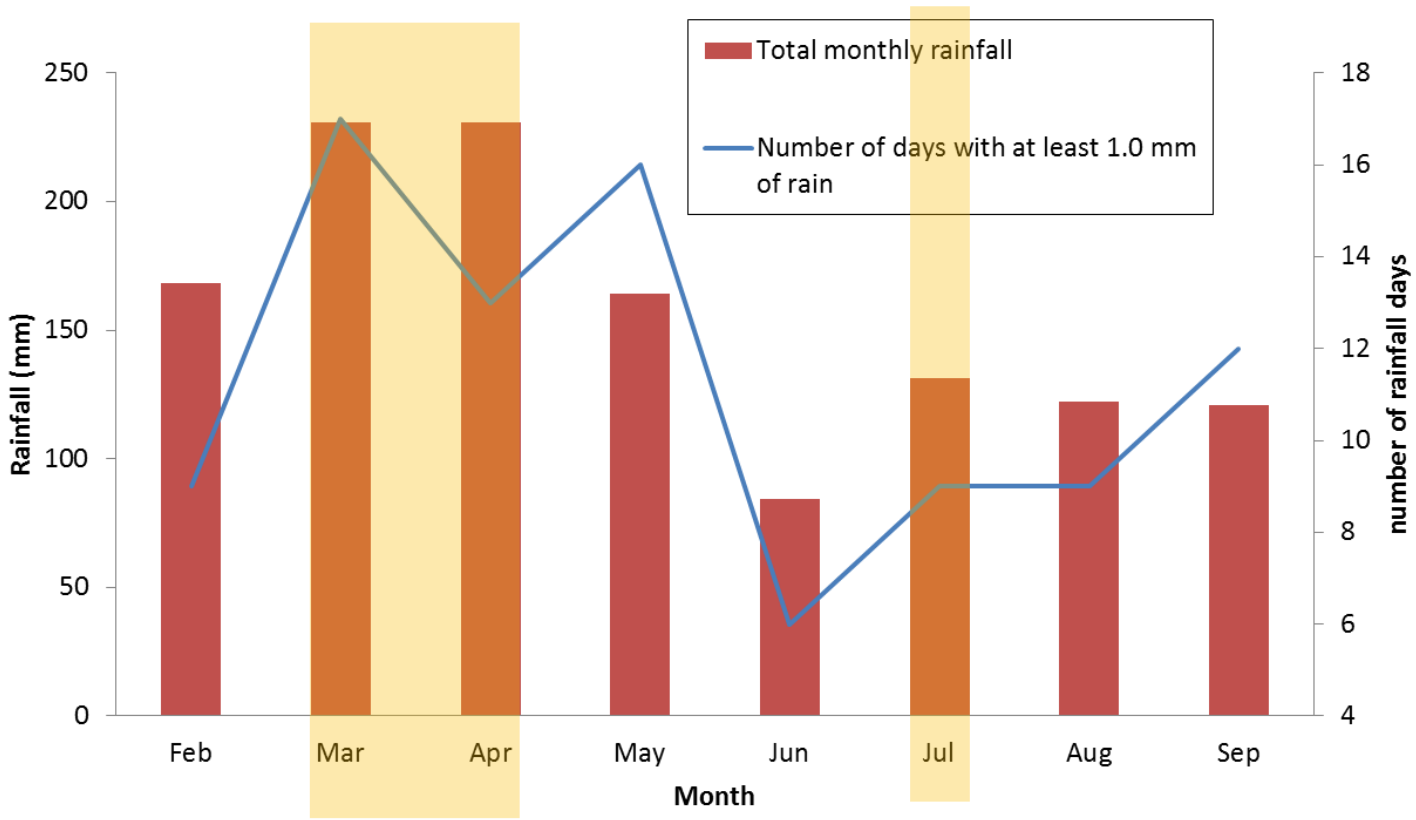

Figure AIV 2: Rainfall distribution and number of rainfall days in each month in Kampala. The yellow band represent the rain seasons

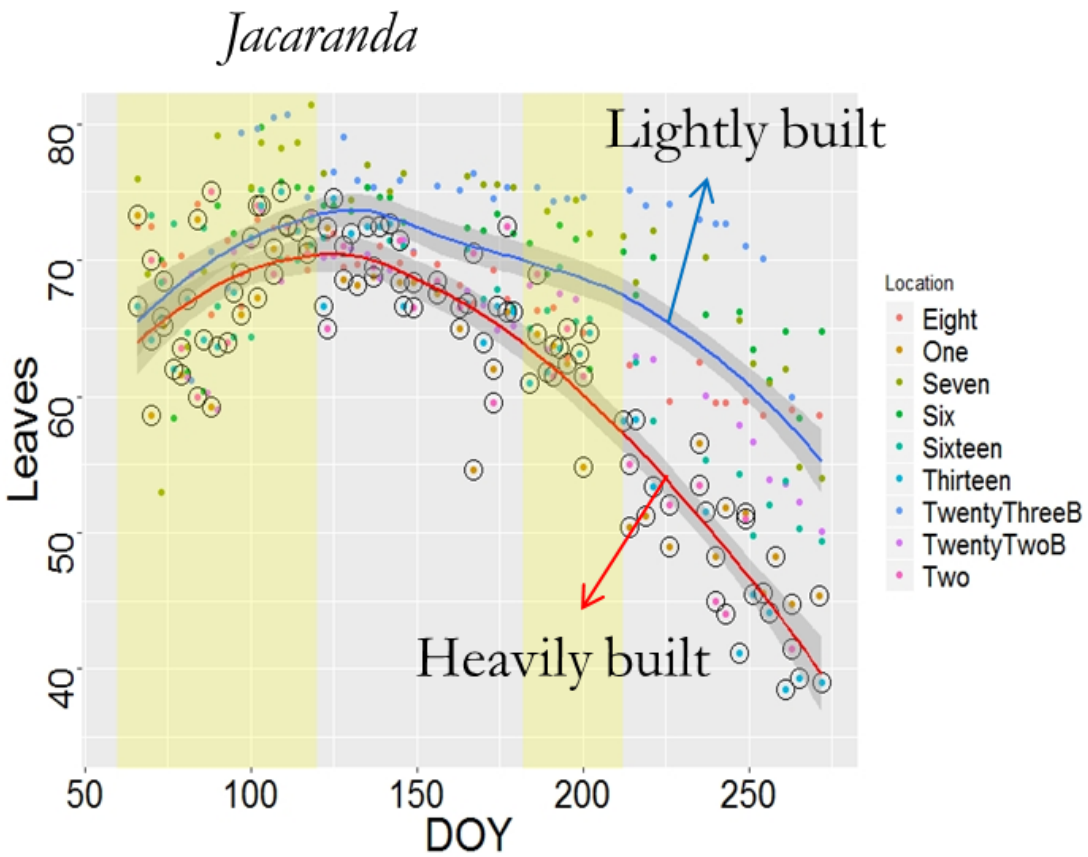

Pearson's correlation

	Building%	Paved surface%	Building + paved surface%
Area under smoothed curve	-0.4	-0.8	-0.7
Area under linear fit	-0.5	-0.8	-0.8

Figure AIV 3: Differences in temporal change of *Jacaranda* trees between heavily built and lightly built locations using a loess model. The AUCs (Area Under the Curve - indicator of leaf loss) of individual trees had a negative and significant correlation (green) with impervious surfaces, suggesting that trees in heavily built neighbourhoods experienced high leaf loss.

Tabebuia

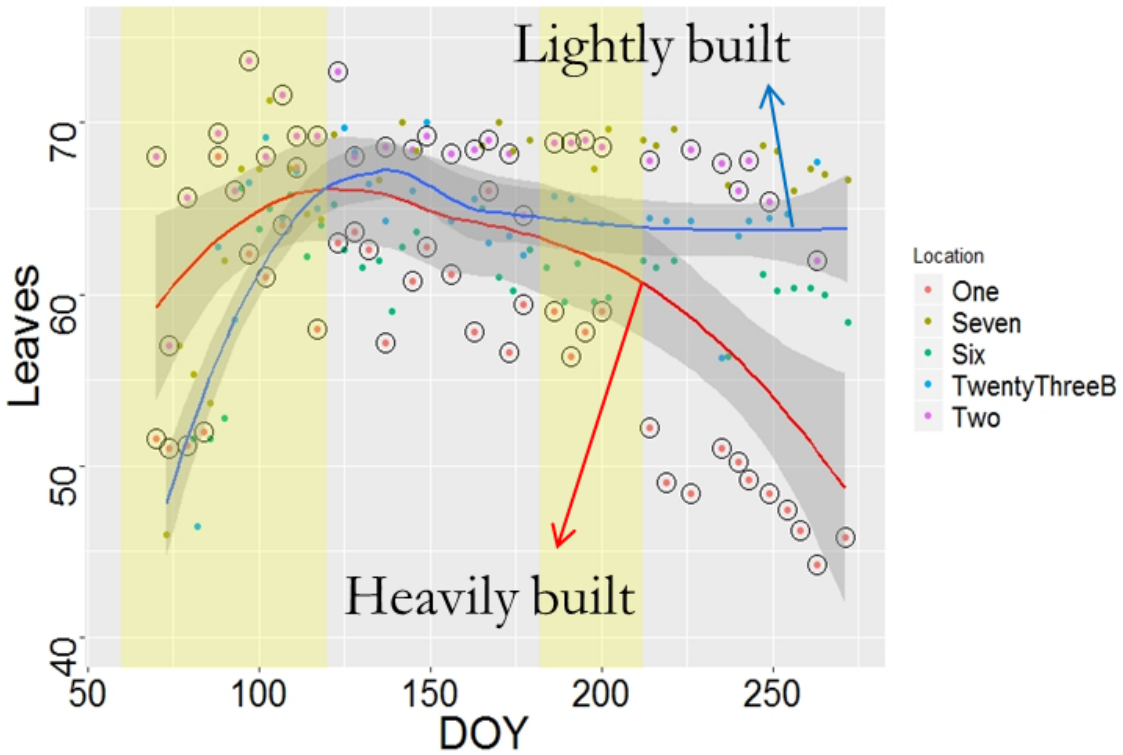

Pearson's correlation

	Buildings%	Paved surface%	Building + paved surface%
Area under smoothed curve	-0.3	-0.1	-0.2
Area under linear fit	-0.3	-0.1	-0.2

Figure AIV 4: Differences in temporal change of *Tabebuia* trees between heavily built and lightly built locations using a loess model. The AUCs (Area Under the Curve - indicator of leaf loss) of individual trees had a negative correlation with impervious surfaces, suggesting that trees in heavily built neighbourhoods experienced high leaf loss.

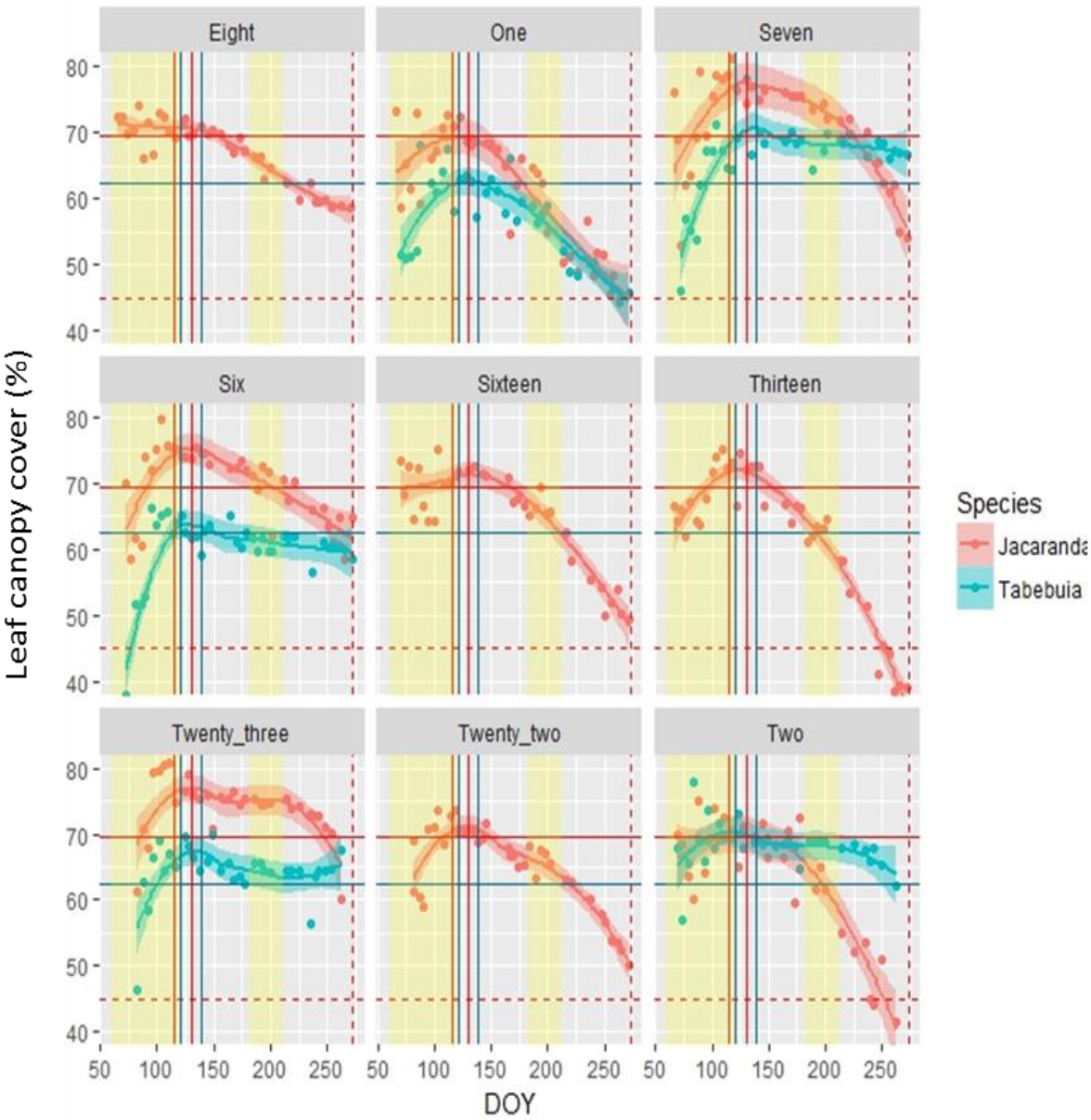

	Number of monitored individuals of a given tree species per site									
	One	Two	Six	Seven	Eight	Thirteen	Sixteen	Twenty two	Twenty three	TOTAL
J. mimosifolia	5	2	5	5	6	6	6	10	6	51
T. rosea	5	5	5	3	0	0	0	0	7	25

Figure AIV 5: Temporal change of canopy cover at each one of the phenology locations

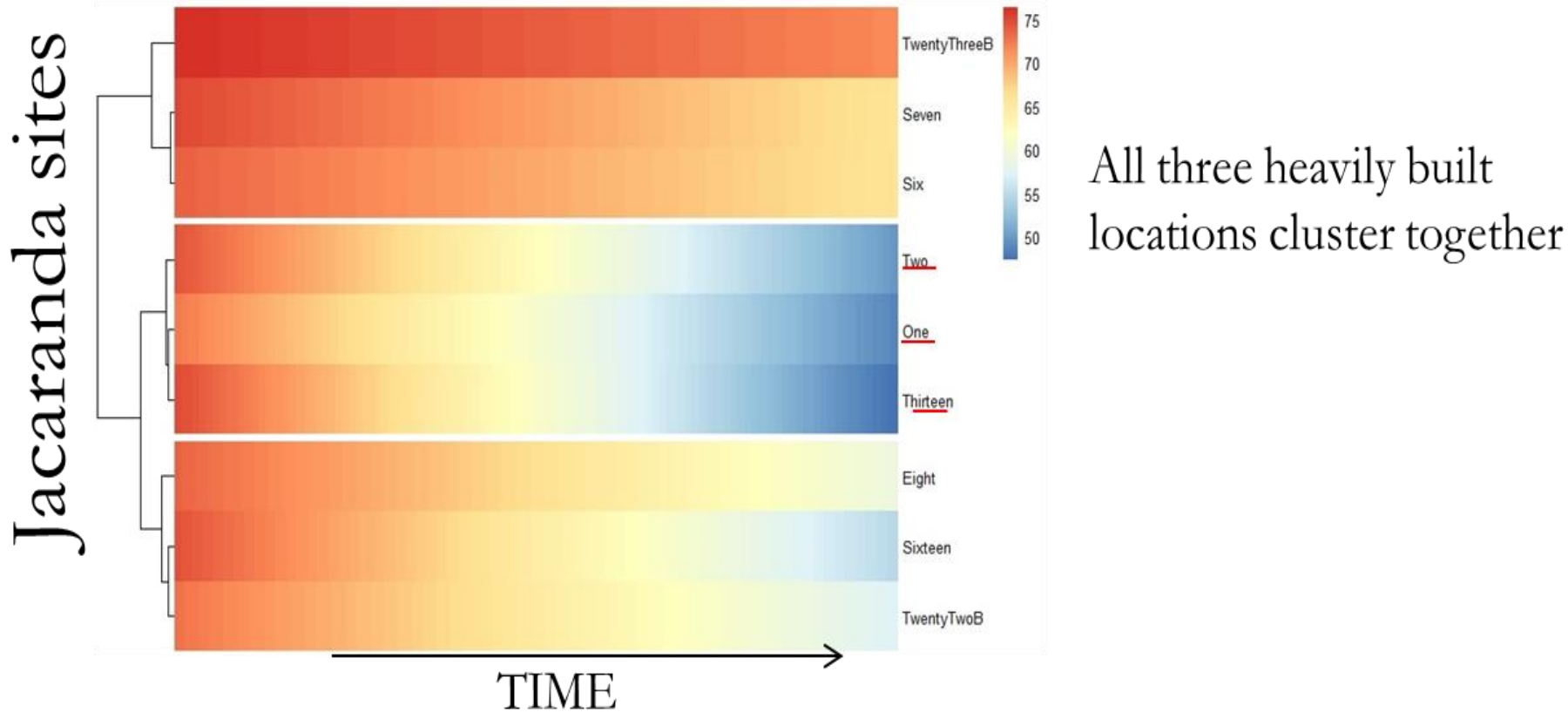

Figure AIV 6: Cluster analysis of temporal change of canopy cover of *Jacaranda* trees showed that the most built up locations (One, Two and Thirteen) had relatively similar time series

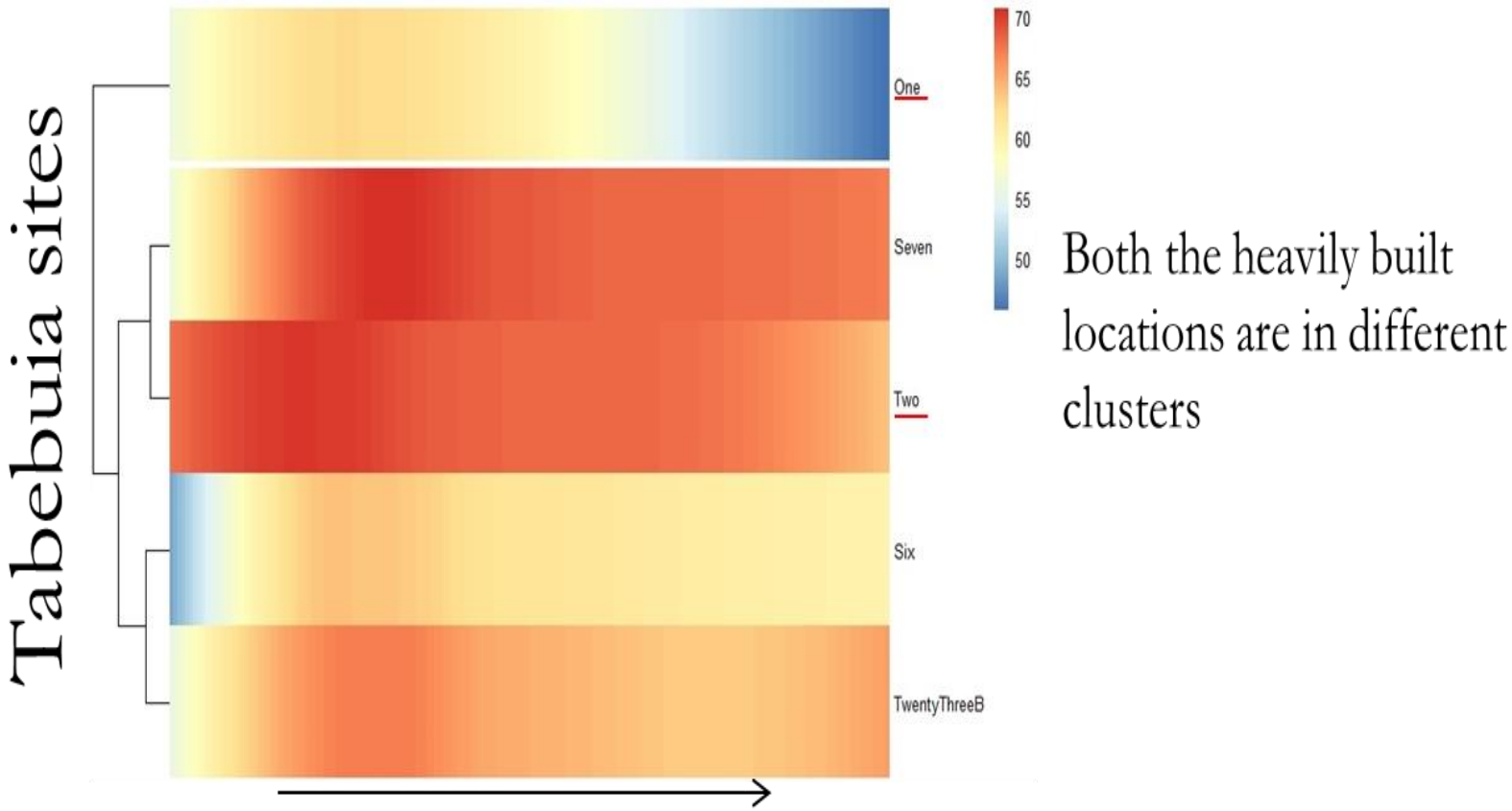

Figure AIV 7: Cluster analysis of temporal change of canopy cover of *Tabebuia* tree showed that the most built up locations (One, Two and Thirteen) had relatively similar time series

APPENDIX V

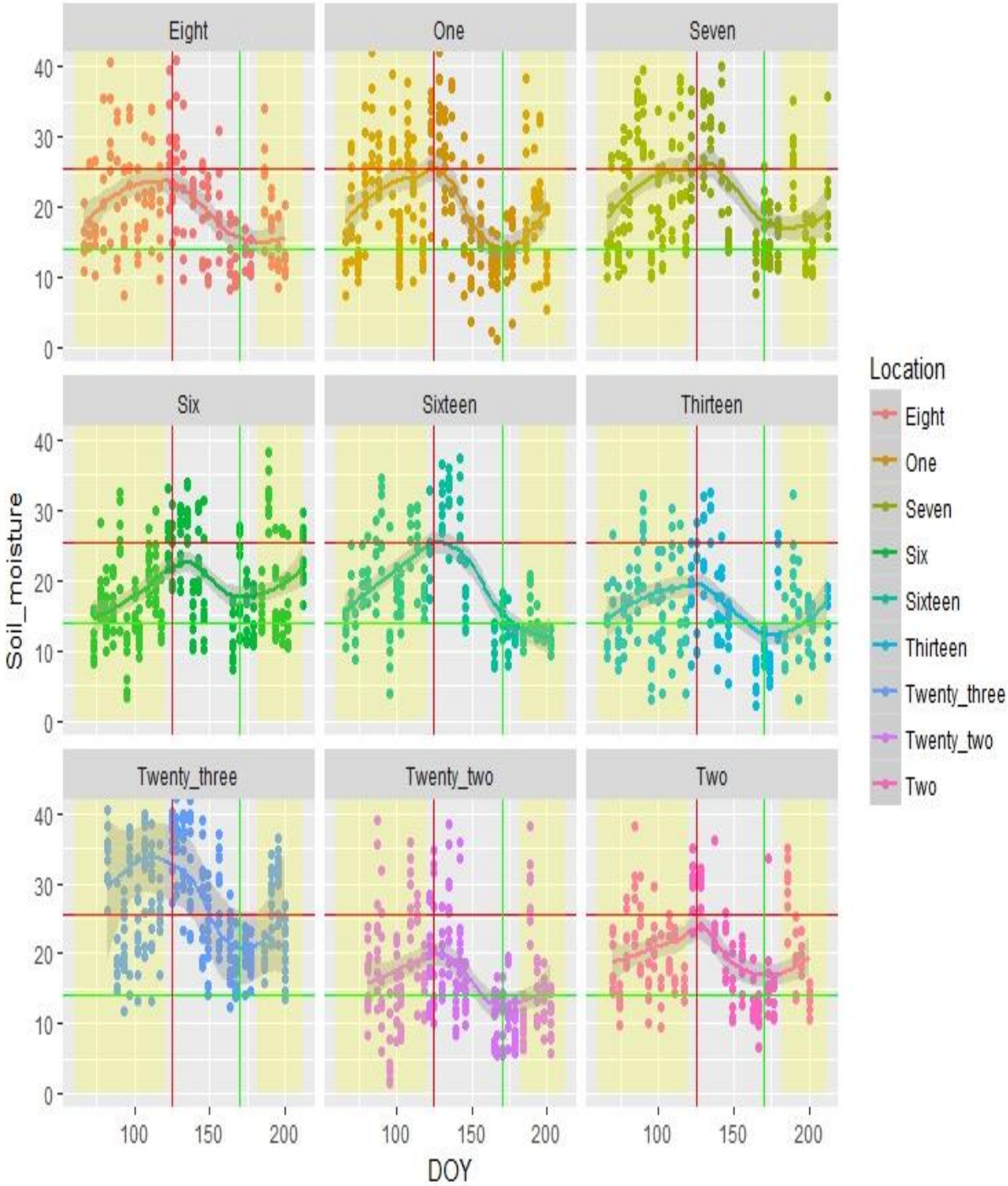

Figure AV 1: Temporal change of surface moisture at the phenology sites. Red and green lines have been added for reference to points indicating maximum and minimum surface moisture

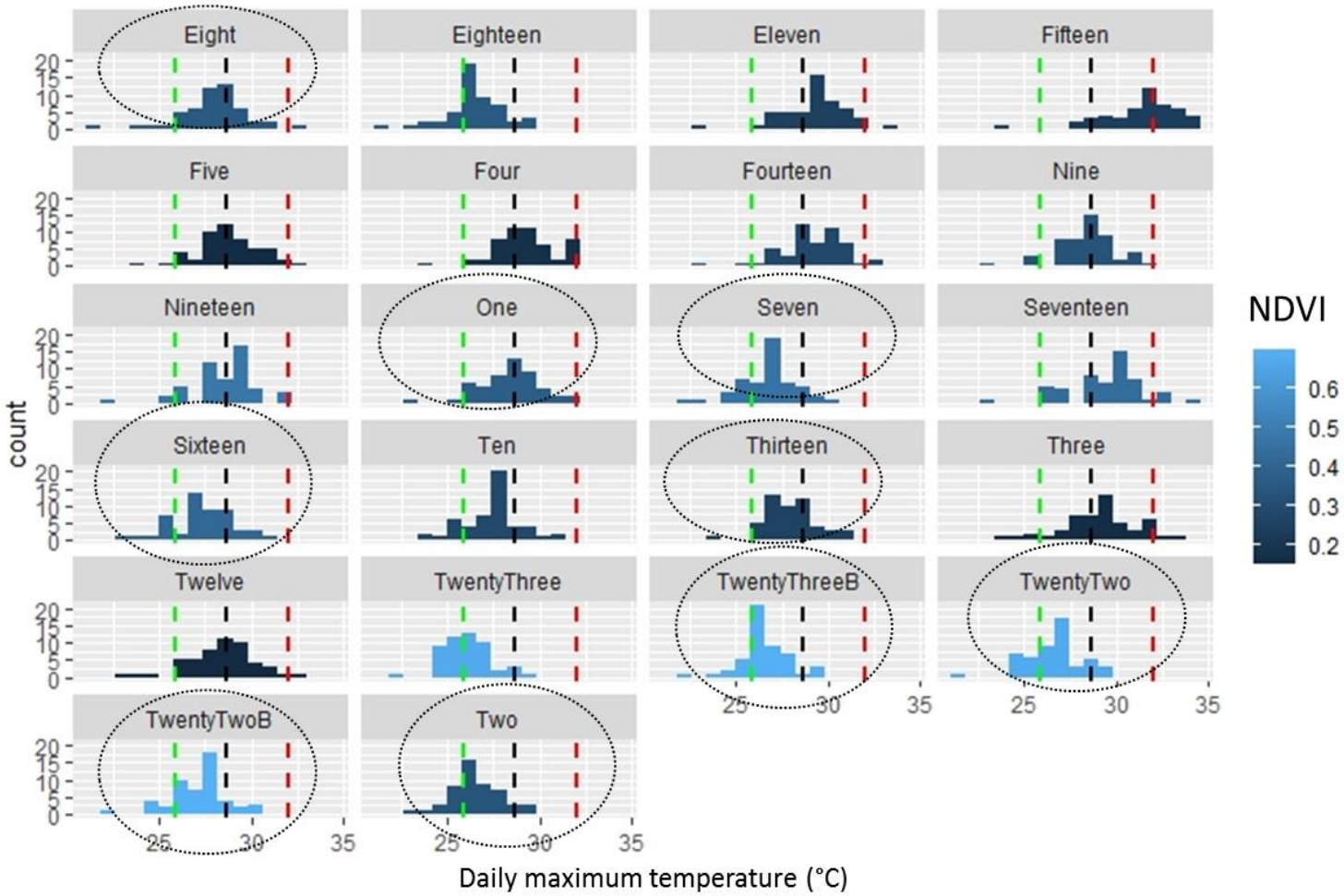

Figure AV 2: Daily maximum night time temperature at 22 urban climates sites across a 50 day period. NDVI score is used to represent the site characteristics, with the highest NDVI scores indicating high vegetation cover in a given location. Green and red vertical lines represent the highest (32°C) and lowest (18°C) mode temperatures at locations fifteen and Eighteen respectively. The black line is the mode across all sites. The nine phenology sites are encircled

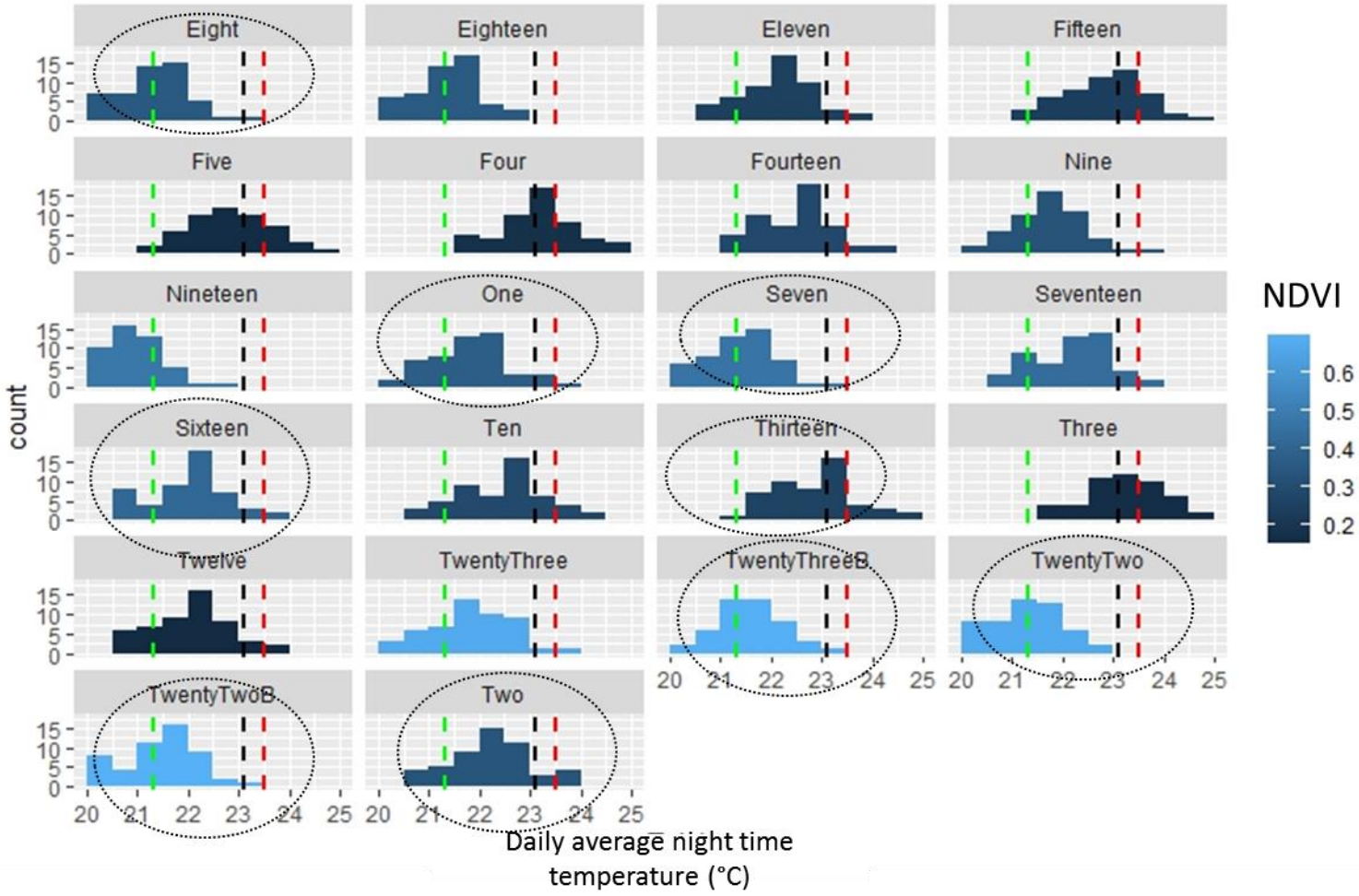

Figure AV 3: Daily average night time temperature at 22 urban climates sites across a 50 day period. NDVI score is used to represent the site characteristics, with the highest NDVI scores indicating high vegetation cover in a given location. Green and red vertical lines represent the highest (23°C) and lowest (21°C) mode temperatures at locations fifteen and nineteen respectively. The blackline is mode across all sites. The nine phenology sites are encircled

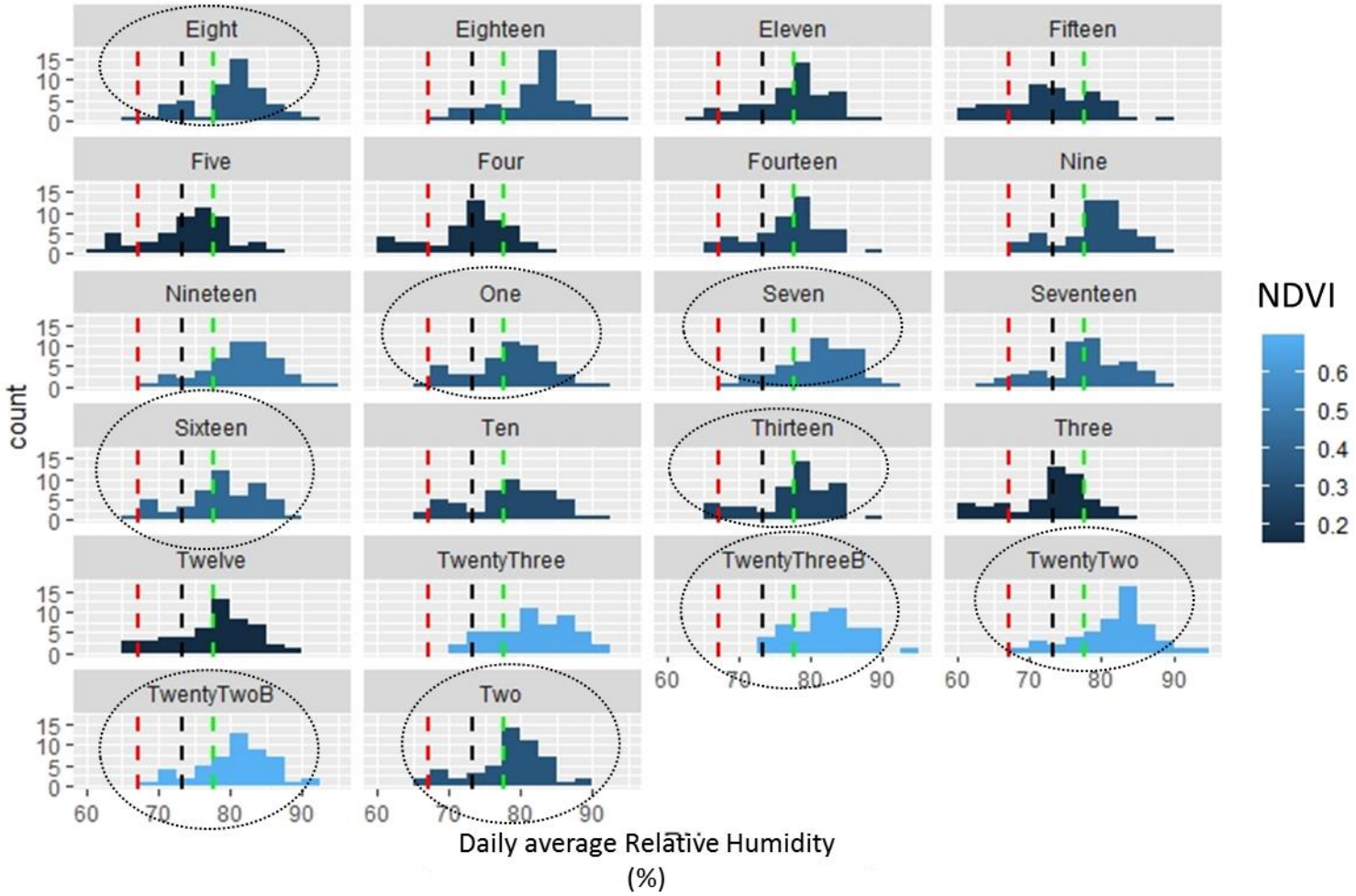

Figure AV 4: Daily average relative humidity at 22 urban climates sites across a 50 day period. NDVI score is used to represent the site characteristics, with the highest NDVI scores indicating high vegetation cover in a given location. Green and red vertical lines represent the highest (77%) and lowest (67%) mode relative humidity at locations Nineteen and Four respectively. The black line represents the mode across all sites. The nine phenology sites are encircled.